

**Universidade de Lisboa
Faculdade de Farmácia**



**TERPENOIDS AS EFFECTIVE COMPOUNDS FOR
OVERCOMING MULTIDRUG RESISTANCE IN CANCER CELLS**

Mariana Alves Reis

Orientadores: Professora Doutora Maria José Umbelino Ferreira
Professor Doutor Hermann Lage

Tese especialmente elaborada para obtenção do grau de Doutor em Farmácia,
especialidade de Química Farmacêutica e Terapêutica.

2015

**Universidade de Lisboa
Faculdade de Farmácia**



**TERPENOIDS AS EFFECTIVE COMPOUNDS FOR OVERCOMING MULTIDRUG
RESISTANCE IN CANCER CELLS**

Mariana Alves Reis

Orientadores: Professora Doutora Maria José Umbelino Ferreira
Professor Doutor Hermann Lage

Tese especialmente elaborada para obtenção do grau de Doutor em Farmácia, especialidade de Química Farmacêutica e Terapêutica.

Júri:

Presidente

Doutora Matilde da Luz dos Santos Duque da Fonseca e Castro, Professora Catedrática e Diretora da Faculdade de Farmácia da Universidade de Lisboa.

Vogais

- Doctor Hermann Lage. Principal Researcher, Campus Charité Mitte. Institute of Pathology, Germany;
- Doctor Gabriella Spengler, Researcher, Department of Medical Microbiology and Immunology, Faculty of Medicine of University of Szeged, Hungary;
- Doutora Lígia Maria Ribeiro Pires Salgueiro Silva Couto, Professora Catedrática, Faculdade de Farmácia da Universidade de Coimbra;
- Doutora Maria Emília da Silva Pereira de Sousa, Professora Auxiliar, Faculdade de Farmácia da Universidade do Porto;
- Doutora Maria José Umbelino Ferreira, Professora Associada com Agregação, Faculdade de Farmácia da Universidade de Lisboa;
- Doutora Ana Margarida Monteiro Madureira Fernandes, Professora Auxiliar, Faculdade de Farmácia da Universidade de Lisboa;
- Doutora Noélia Maria Silva Dias Duarte, Professora Auxiliar, Faculdade de Farmácia da Universidade de Lisboa.

2015

This thesis was conducted at:

*Natural Products Chemistry group, Research Institute for Medicines
(iMed.Ulisboa), Faculty of Pharmacy, Universidade de Lisboa*

*Experimental Pathology group, Institute of Pathology, Charité
Campus Mitte, Universitätsmedizin Berlin*

*The financial support was provided by Fundação para a Ciência e a
Tecnologia (FTC), Portugal (PhD grant SFRH/BD/72915/2010;
project PTDC/QEQ-MED/0905/2012)*

*Aos meus pais
Maria Romana e José*

*Para
Pedro,
Santiago
e
Miguel*

Lisboa, Berlin e Szeged

Abstract

Circumventing multidrug resistance (MDR) in cancer is a cornerstone to chemotherapy success. Modulation of P-glycoprotein (P-gp) and evaluation of the collateral sensitivity effect are among the most promising approaches to overcome MDR. The main goal of this work was to explore these two approaches in order to find and optimize new MDR reversers derived from *Euphorbia* species.

The phytochemical study of *E. piscatoria* yielded four new diterpenes, two with the *ent*-abietane skeleton (**1-2**) and two macrocyclic lathyranes (**3-4**). From *E. welwitschii* four new jatrophanes (**19-22**) were obtained. Welwitschines A (**19**) and B (**20**) present a unique combination of structural features: a 5/8/8 fused-ring system and an 12,15-ether bridge. Several known terpenoids (**5-10** and **23**) and flavonoids (**11-14**, **24** and **25**) were also isolated from these plants. Moreover, a small library of 27 macrocyclic lathyrene diterpenes (**6.1-6.27**), targeted for P-gp efflux modulation, was achieved by molecular derivatization of jolkinol D (**6**), isolated from *E. piscatoria*. This process was accomplished mainly by using several alkanoyl and aroyl anhydrides/chlorides as acylating agents. The chemical structures of the compounds were deduced from their physical and spectroscopic data (IR, MS, 1D and 2D NMR experiments). Additionally, the stereochemistry of compounds **19** and **20** was confirmed through X-ray crystallography. Piscatoric acid (**2**) was a key compound to give insights into the biogenetic pathway of *ent*-abietane lactones. In the same way, the isolation of compounds **19-22** allowed to propose the 12,17-cyclojatrophanes biogenesis.

The MDR reversal activity of compounds **6**, **6.1-6.27** and **19-23** was evaluated through combination of transport and chemosensitivity assays, using the mouse lymphoma *MDR1*-transfected cell model. The most relevant structure-activity relationships for derivatives **6.1-6.27** highlighted the importance of the aroyl moiety and its pattern of substitution for P-gp efflux modulation. Most of the derivatives revealed to interact synergistically with doxorubicin, by increasing its cytotoxic activity. The effects on P-gp ATPase were evaluated for the most potent derivative, jolkinolate P (**6.15**). This compound showed to interact with P-gp, exhibiting a profile related to compounds that inhibit its ATPase activity. In regard to the jatrophanes **19-23**, the results indicated that high conformational flexibility of the twelve-membered ring of compounds **21-23** favored P-gp modulation, in contrast to the tetracyclic scaffold of compounds **19** and **20**. Epoxiwelwitschene (**22**) displayed the highest modulatory effect and may act as a competitive modulator, as indicated by the ATPase activity assay. Drug combination experiments also corroborated the anti-MDR potential of these diterpenes due to their synergistic interaction with doxorubicin.

The potential collateral sensitivity effect of compounds **1-6**, **8**, **19-24** and **6.1-6.27** was evaluated against gastric (EPG85-257), pancreatic (EPP85-181) and colon (HT-29) human cancer cells and their drug-selected counterparts, resistant to novantrone (RN) and to daunorubicin (RDB), using a proliferation assay. Compounds **6.11**, **6.22**, **22** and **23** were able to decrease approximately 85% of the level of resistance of EPG85-257RDB cells, in comparison to parental cells. Compounds **6.11**, **6.20**, **22** and **23** also showed promising results in pancreatic cells, being able to reduce the levels of resistance in about 32 - 65%. The mechanisms of cell death were analyzed, using the annexin V/PI and active caspase-3 assays. It was verified that cell death occurred through caspase-dependent apoptosis.

The structural optimization of the compounds with the lathyrene scaffold and isolation of the jatrophanes from *E. welwitschii*, provided the identification of some important structural requirements, leading to a more effective reversion of MDR. Thus, compounds **6.11**, **6.15**, **6.20**, **6.22**, **22** and **23** can be proposed as new lead candidates for the development of MDR reversal agents.

Keywords: Collateral sensitivity effect; *ent*-abietanes; Euphorbiaceae; *Euphorbia piscatoria*; *Euphorbia welwitschii*; jatrophanes; lathyranes; macrocyclic diterpenes; MDR reversal; P - glycoprotein.

Resumo

A reversão da resistência a múltiplos fármacos (MDR) é um ponto fulcral para o sucesso do tratamento do cancro. Os mecanismos celulares associados à MDR incluem: evasão da apoptose, alterações nos alvos farmacológicos, inativação dos fármacos e aumento do efluxo de citotóxicos, entre outros. Destes, o mecanismo com maior importância na MDR envolve a sobre-expressão de transportadores da família ABC, nos quais se inclui a glicoproteína-P (P-gp). Esta proteína está envolvida no transporte de fármacos anticancerígenos para o espaço extracelular, conduzindo à ineficácia do tratamento. O desenvolvimento de moduladores da P-gp, capazes de impedir o efluxo de fármacos, aumentando por conseguinte a sua concentração nas células, representa uma abordagem promissora para a reversão da MDR. No entanto, apesar de terem sido desenvolvidas várias gerações de moduladores, não existe atualmente nenhum, que esteja em uso na prática clínica. Os conhecimentos sobre as interações modulador-transportador têm sido limitados, em parte, devido à ausência de informações estruturais sobre a P-gp humana. Em 2009, surgiu a primeira estrutura cristalográfica da P-gp de murino (87% de identidade com a P-gp humana), mostrando pela primeira vez esta proteína complexada com um ligando. Este avanço representa um novo impulso para o desenvolvimento de moduladores baseados na estrutura deste transportador.

As células cancerígenas MDR são frequentemente resistentes a diferentes classes de agentes antitumorais, mas, ao mesmo tempo, podem também ser hipersensíveis a outros compostos. Este fenómeno é denominado por efeito de sensibilidade colateral, permanecendo ainda desconhecido o mecanismo, pelo qual, este acontece. Explorar o efeito de sensibilidade colateral está entre as abordagens mais promissoras para reverter a MDR, a par do desenvolvimento de moduladores da P-gp. Deste modo, o objetivo principal deste trabalho foi explorar as duas abordagens, para encontrar e otimizar novos moduladores da MDR, obtidos a partir de plantas do género *Euphorbia*.

Através do estudo fitoquímico de *E. piscatoria* foi possível isolar quatro novos diterpenos, dois com o esqueleto do *ent*-abietano (**1-2**) e dois com o esqueleto do latirano (**3-4**). Da planta *E. welwitschii* foram obtidos quatro novos jatrofanos (**19-22**). Os compostos designados por welwitschines A (**19**) e B (**20**) apresentam a conjugação única das seguintes características estruturais: um sistema 5/8/8 de anéis fundidos e uma função éter, entre os carbonos 12 e 15. Para além destes compostos foram também isolados destas plantas outros já conhecidos, nomeadamente latiranos (**5 e 6**), um jatrofano (**23**) e diterpenos policíclicos (**7-9**). Também foram isolados, um triterpeno com o esqueleto do cicloartano (**10**), seis flavonoides (**11-14, 24 e 25**) e, ainda, quatro outros fenóis simples (**15-18**). As estruturas químicas dos compostos foram deduzidas a partir dos seus dados físicos e espectroscópicos (IV, MS, RMN 1D e 2D). A estereoquímica dos compostos welwitschines A (**19**) e B (**20**) foi confirmada por cristalografia de raios-X.

O isolamento do composto designado por ácido piscatorico (**2**) foi crucial para o desenvolvimento de uma nova proposta de via biogenética para as lactonas do tipo *ent*-abietano, moléculas geralmente presentes em plantas do género *Euphorbia*. Do mesmo modo, o isolamento dos compostos **19-22** permitiu sugerir a biogénese de diterpenos com o esqueleto do tipo 12,17-ciclojatrofano. Esta classe de compostos é considerada rara, só se conhecendo, até à data, uma molécula com este tipo de estrutura.

A partir de *E. piscatoria* foi isolado, em grande quantidade, um diterpeno macrocíclico com o esqueleto do latirano, denominado jolkinol D (**6**). Tirando partido das funções químicas deste

composto, foi possível desenvolver uma pequena biblioteca de 27 compostos (**6.1-6.27**), que permitiu estabelecer estudos de relação estrutura-atividade. Para a preparação destes derivados usaram-se principalmente reações de acilação, com vários anidridos/cloretos de ácido aromáticos e alifáticos.

A atividade anti-MDR, para os compostos **6**, **6.1-6.27** e **19-23**, foi avaliada através da combinação de ensaios funcionais com ensaios de quimiossensibilidade, usando como modelo, uma linha celular de linfoma de rato transfetada com o gene *MDR1*. Os dados obtidos pela relação estrutura atividade apontam para a importância do anel benzênico e do seu padrão de substituição, na modulação da P-gp. A maioria dos derivados revelou uma interação sinérgica com a doxorubicina, aumentando o seu efeito citotóxico. A natureza das interações com a atividade ATPásica da P-gp foi estudada usando o modulador mais potente deste grupo de derivados, o jolquinoato P (**6.15**). Este composto demonstrou inibir a hidrólise de ATP mediada pela P-gp. O perfil obtido aproxima-se ao perfil de compostos classificados como inibidores deste transportador membranar. Em relação aos jatrofanos **19-23**, a comparação dos seus efeitos modulatórios, indicou que a flexibilidade conformacional, conferida pelo anel de doze membros presente nos compostos **21-23**, favoreceu a modulação da P-gp. A estrutura tetracíclica dos compostos **19** e **20** confere-lhes uma natureza mais rígida, que parece não favorecer a sua atividade. Deste conjunto de compostos, o epoxiwelwitscheno (**22**) foi aquele que apresentou a maior atividade como modulador a 2 μM e, por esse motivo, foi selecionado para investigar o seu efeito na atividade ATPásica da P-gp. Os resultados obtidos sugeriram que poderá tratar-se de um modulador competitivo. Por outro lado, os ensaios de combinação com a doxorubicina mostraram uma interação de natureza sinérgica, entre estes jatrofanos e o agente citotóxico, reforçando o seu potencial anti-MDR.

O efeito de sensibilidade colateral foi avaliado para os compostos **1-6**, **8**, **19-24** e **6.1-6.27**, usando as seguintes linhas celulares cancerígenas humanas: gástrica (EPG85-257), pancreática (EPP85-181) e do cólon (HT-29) e suas respectivas estirpes MDR, selecionadas com novantrona (RN) e daunorrubicina (RDB). Os compostos **6.11**, **6.22**, **22** e **23** reduziram aproximadamente 85% do nível de resistência das células EPG85-257RDB, em comparação com as células parentais. Os compostos **6.11**, **6.20**, **22** e **23** também apresentaram resultados promissores nas células pancreáticas, reduzindo os níveis de resistência em cerca de 32 - 65%. Os possíveis mecanismos de morte celular foram analisados, utilizando os ensaios de anexina V/iodeto de propídeo e caspase-3 ativa. Verificou-se que a morte celular ocorreu por apoptose, dependente de caspase.

A otimização estrutural dos compostos com o esqueleto do latirano e o isolamento de jatrofanos, da planta *E. welwitschii*, proporcionou a identificação de alguns requisitos estruturais conducentes a uma modulação mais eficaz da P-gp. Por conseguinte, os compostos **6.11**, **6.15**, **6.20**, **6.22**, **22** e **23** podem ser propostos como novos candidatos a protótipos no desenvolvimento de agentes reversores da MDR. Os estudos fitoquímicos desenvolvidos neste trabalho contribuem ainda para o conhecimento da diversidade química existente nas espécies do género *Euphorbia*, tendo ainda dado azo à proposta de novas vias biogénicas para alguns dos compostos isolados.

Palavras-chave: Diterpenos macrocíclicos; efeito de sensibilidade colateral; *ent*-abietano; Euphorbiaceae; *Euphorbia piscatoria*; *Euphorbia welwitschii*; glicoproteína-P; jatrofano; latirano; moduladores da MDR.

Related publications

On the scope of this thesis, several publications and presentations in scientific meetings have been produced.

Papers

Reis MA, André V, Duarte MT, Lage H, Ferreira, MJU (2015) Welwitschines A and B: unusual jatrophone-type diterpenes from *Euphorbia welwitschii*, *submitted*.

Reis MA, Paterna A, Mónico A, Molnar J, Lage H, Ferreira MJU (2014) Diterpenes from *Euphorbia piscatoria*: Synergistic Interaction of Lathyranes with Doxorubicin on Resistant Cancer Cells. *Planta Med.*, **80**(18): 1739-45 (DOI: 10.1055/s-0034-1383244).

Reis MA, Paterna A, Ferreira RJ, Lage H, Ferreira MJU (2014) Macrocyclic diterpenes resensitizing multidrug resistant phenotypes. *Bioorg Med Chem*, **22**: 3696-3702 (DOI: 10.1016/j.bmc.2014.05.006).

Ferreira MJU, Duarte N, **Reis MA**, Madureira AM, Molnár J (2014) *Euphorbia* and *Momordica* metabolites for overcoming multidrug resistance. *Phytochem Rev*, **13**(4): 915-935 (DOI: 10.1007/s11101-014-9342-8).

Reis M, Ferreira RJ; Santos M, Santos D, Molnár J, Ferreira MJU (2013) Enhancing Macrocyclic Diterpenes As Multidrug-Resistance Reversers: Structure-Activity Studies On Jolkinol D Derivatives. *J Med Chem*, **56**(3): 748–760 (DOI: 10.1021/jm301441w).

Oral communications

Reis MA, Spengler G, Molnár J, Lage H, Ferreira MJU (2015) Tackling Multidrug Resistance in Cancer. I International Summer School on Natural Products, 6th-10th July, Naples, Italy

Reis MA, Paterna A, Ferreira RJ, Lage H, Ferreira MJU (2014) Jolkinol D and its derivatives: anti-proliferative selectivity towards multi-drug resistant cancer cells. Flash poster presentation. 1st EFMC Young Medicinal Chemist Symposium, September 2014, Lisboa, Portugal

Reis MA, Paterna A, Ferreira RJ, Lage H, Ferreira MJU (2014) Diterpenic compounds with selective antiproliferative activity in multidrug resistant cancer cells. *Planta Med*, **80**(16), SL34. 62nd International Congress and Annual Meeting of the Society for Medicinal Plant and Natural Product Research, September 2014, Guimarães, Portugal

Reis MA, Paterna A, Ferreira RJ, Lage H, Ferreira MJU (2014) Diterpenic compounds: tackling multidrug resistant cancer phenotypes. 6th iMed.UL Post-Graduate Students Meeting, Lisbon, Portugal, 2nd July 2014

Reis MA (2012) Terpenoids as effective compounds for overcoming multidrug resistance in cancer cells. iMed.UL, Lisbon, Portugal

Reis MA, Ferreira RJ, Santos MMM, Molnar J and Ferreira MJU (2011) Macrocyclic lathyrane diterpenoids from *Euphorbia piscatoria* - Their potential as MDR reversal agents in cancer cells- 3rd iMed.UL Post-Graduate Students Meeting , Lisbon, Portugal

Poster communications

Reis MA, Ahmed O, Spengler G, André V, Duarte T, Molnár J, Lage H, Ferreira MJU (2015) P-glycoprotein efflux modulation and selective apoptosis induction by jatrophone diterpenes. 7th iMed.UL Post-Graduate Students Meeting, 15th July 2014, Lisbon, Portugal– Best Poster Prize.

Reis MA, Paterna A, Ferreira RJ, Lage H, Ferreira MJU (2014) Jolkinol D and its derivatives: anti-proliferative selectivity towards multi-drug resistant cancer cells. XXIII International Symposium on Medicinal Chemistry, September 2014, Lisboa, Portugal

Neto S, Vieira C, Matos AM, Mónico A, Ferreira R, **Reis MA**, Pedro C, Madureira AM, Spengler G, Molnár J, Duarte N, Ferreira MJU (2014) Lathyrane diterpenes from *Euphorbia boetica* and *Euphorbia pedroi*: Promising ABCB1 modulators for overcoming multidrug resistance. *Planta Med*, **80**(16), P1L5. 62nd International Congress and Annual Meeting of the Society for Medicinal Plant and Natural Product Research, September 2014, Guimarães, Portugal – Best Poster Prize.

Reis MA, Lage H, Ferreira MJU (2013) Bioactive diterpenoids: from structural elucidation to antiproliferative activity. Portuguese National Meeting of Organic Chemistry and the 1st Portuguese-Brazilian Organic Chemistry Symposium, September 2013, Lisboa, Portugal.

Reis MA, Ferreira RJ, Santos MMM, Santos DJVA dos, Molnár J, Ferreira MJU (2012) Structure activity-relationships of P-Glycoprotein modulation using a small library of macrocyclic lathyrane diterpenes. *Planta Med*, **78** (DOI: 10.1055/s-0032-1320394). 8th International Congress on Natural Products Research, August 2012, New York, USA.

Reis MA, Paterna A, Ferreira MJU. Phytochemical investigations of *Euphorbia piscatoria* (2012) *Planta Med*, **78** (DOI: 10.1055/s-0032-1321070). 8th International Congress on Natural Products Research, August 2012, New York, USA.

Ferreira RJ, **Reis MA**, Santos MMM, Molnár J, Santos DJVA dos, Ferreira MJU (2012) Modulation of P-Glycoprotein activity: Insights from docking studies. (DOI: 10.1055/s-0032-1320395). 8th International Congress on Natural Products Research, August 2012, New York, USA.

Reis MA, Serly J, Madureira AM, Duarte N, Molnar J, Ferreira MJU (2011) Evaluation of diterpenic compounds as inhibitors of multidrug resistance on human colon adenocarcinoma cells. 59th International Congress and Annual Meeting of the Society for Medicinal Plant and Natural Product Research. September 2011, Antalya, Turkey

Reis MA, Ferreira RJ, Santos MM, Ferreira MJU (2011) Alkanoyl and aroyl derivatives of a lathyrane-type macrocyclic diterpene. 59th International Congress and Annual Meeting of the Society for Medicinal Plant and Natural Product Research. September 2011, Antalya, Turkey.

Acknowledgments

I would like to express my sincere gratefulness to my supervisors Professors Maria José Umbelino Ferreira and Hermann Lage for their continuous support throughout my work, for their patience, motivation and teachings. Their guidance helped me open up new horizons that allowed this work to go forward. For the indispensable help in the nebulous times and for the timely criticism, always towards a better progress. Finally, I want to thank Prof. Maria José for seeding the enthusiasm for NMR and Prof Hermann for the Wednesday's insightful meetings, as well as, the warm welcoming in Berlin.

My sincere acknowledgements also go to Professor Joseph Molnár and to Dr. Gabriella Spengler from the department of Medical Microbiology, University of Szeged, Hungary for their encouragement and for providing me an opportunity to join their team, giving me access to the research facilities. Without their precious support it would not be possible to conduct part of this research.

I would like to thank Dr. Teresa Vasconcelos from Instituto Superior de Agronomia de Lisboa, for the identification and collection of plant material. Dr. Olívia Furtado from Laboratório Nacional de Energia e Geologia, for providing access to the polarimeter for the optical rotation measurements. I also acknowledge Dr. Carlos Cordeiro for providing data from the FTICR-MS at Faculdade de Ciências da Universidade de Lisboa and João Ferreira for the ESI-MS data at Faculdade de Farmácia da Universidade de Lisboa.

To all my fellow lab mates at Lisboa I acknowledge the times we had together that fortunately crossed the frontier of the lab. In particular, but in no particular order, my islandic friends Angela Paterna, Roberta Paterna and Sofia Mendes, the inspiring João Rosa, the dance partner Carlos Ribeiro, the gym comrades Daniela Miranda and Ana Ressurreição, the singers Sara Neto e Ângelo Monteiro, the smart aleck Ricardo Ferreira and the rookie Andreia Mónico. For answering my organic chemistry qualms also João Lavrado, Susana Lucas, Marta Carrasco and Rudi Oliveira. To Profs Noélia Duarte and Margarida Madureira, and Cátia Ramallete for their teachings, support, counseling and chit-chat moments. And finally, to all, present and past, Drug Design group members, for the good working environment.

To my colleagues in Szeged a big thanks for the warm welcoming in the city and in the lab, namely to Gabi, Juli and Anikó. To Ana and Attila a special hug for their companionship. To Szeged and to all the inhabitants I have met.

To my colleagues in Berlin, a big toast to Erika and Nadine, thanking for the great times in the city as well as in the lab. And to the wise Omar, a special roommate and lab mate, for all the company and work together. My thanks to Dr. Denise Treue and the technicians Barbara Meyer-Bartell and Birgit Schaefer for their teachings and help. To Berlin, and to all wonderful moments I have come across.

A todos os meus companheiros e amigos espalhados pelo mundo agradeço pelos pequenos nada.

Aos meus queridos pais, irmão, meus queridinhos Pedro e Santiago e família por tudo.

Table of Contents

Abstract	i
Resumo	iii
Related publications	v
Acknowledgments	vii
Table of Contents	ix
Tables Index	xiii
Schemes Index	xv
Figures Index	xv
Abbreviations	xxi

Chapter 1

Introduction	1
1.1. Multidrug resistance in cancer	3
1.1.1. Mechanisms of drug resistance.....	4
1.1.2. Strategies to overcome cancer MDR.....	9
1.2. P-glycoprotein and multidrug resistance	11
1.2.1. Structure and function of P-glycoprotein.....	12
1.2.2. Current status of P-glycoprotein modulators.....	15
1.2.3. Ligand-based and structure-based studies for P-gp modulators.....	17
1.3. Targeting MDR cancer cells by collateral sensitivity effect	20
1.4. Natural products as a source of bioactive molecules for cancer MDR reversion	24
1.4.1. Diterpenoids from <i>Euphorbia</i> species.....	25
1.4.1.1. Biosynthesis of diterpenes.....	27
1.4.2. Bioactive diterpenes from <i>Euphorbia</i> species.....	30
1.4.2.1. MDR reversal activity.....	31
1.4.2.2. Cytotoxic and anti-viral activity.....	35

Chapter 2

Objectives	39
2.1 Objectives	41

Chapter 3

Phytochemical investigations of <i>Euphorbia piscatoria</i>. Results and Discussion.....	43
3.1 Structure elucidation of isolated compounds.....	46
3.1.1. Diterpenes with polycyclic scaffold.....	46
3.1.1.1. Piscatolide - 3 α ,14 β -dihydroxy-ent-abieta-8,13(15)-dien-16,12-olide (1).....	46
3.1.1.2. Piscatoric acid - 3-oxo-ent-abieta-8(14),13(15)-dien-16-oic acid (2).....	49
3.1.1.3. Helioscopinolide E (7).....	51
3.1.1.4. Proposed biogenetic pathway for ent-abietane α,β -unsaturated γ -lactones.....	52
3.1.1.5. ent-13[R]-hydroxy-3,14-dioxo-16-atiseene (8).....	52
3.1.1.6. Portlanquinol - 16-hydroxy-abieta-8,12-diene-11,14-dione (9).....	53
3.1.2. Diterpenes with lathyrane-type scaffold.....	55
3.1.2.1. Piscatoriol A - 15 β -acetoxy-lathyrane-6,12-diene-3 β ,5 α -diol-14-one (3).....	55
3.1.2.2. Piscatoriol B - 15 β -acetoxy-lathyrane-6(17),12-diene-3 β ,5 α -diol-14-one (4).....	57
3.1.2.3. 15-acetoxy-5,6-epoxylathyr-12-en-3-ol-14-one (5).....	58
3.1.2.4. Jolkinol D (6).....	60
3.1.2.5. Biogenic relationships of lathyranes 3-6.....	60
3.1.3. Cycloartane-type triterpene.....	61
3.1.3.1. Cycloart-23-ene-3 β ,25-diol (10).....	61
3.1.4. Phenolic compounds.....	63
3.1.4.1. Naringenin (11), aromadendrin (12), taxifolin (13) and quercetin (14).....	63
3.1.4.2. Ferulic acid (15), scopoletin (16), vanillin (17) and p-hydroxybenzaldehyde (18).....	65
3.2. Assessment of MDR reversal activity.....	67

Chapter 4

Jolkinol D derivatives as MDR reversers: SAR studies. Results and Discussion.....	69
4.1. Chemistry.....	72
4.2. Assessment of MDR reversal activity.....	76
4.2.1. Antiproliferative activity.....	76
4.2.2. Modulation of P-gp efflux.....	76
4.2.3. Structure-activity relationships (SAR) studies.....	81
4.2.4. Chemosensitization: reversion of drug-induced resistance.....	86
4.2.5. Effects on the ATPase activity of P-gp.....	87

Chapter 5

***Euphorbia welwitschii*: from structural elucidation to MDR reversal**

activity. Results and Discussion.....91

5.1. Structure elucidation of isolated compounds.....94

5.1.1. Diterpenes with jatrophane-type scaffold.....94

5.1.1.1. Welwitschine A - 3 β ,5 α ,11 β -triacetoxy-7 β ,8 α -diisobutyryloxy-9 α -nicotinoyloxy-12,15-epoxy-12,17-cyclojatroph-6 α -ol-14-one (**19**).....94

5.1.1.2. Welwitschine B - 3 β ,11 β -diacetoxy-7 β ,8 α -diisobutyryloxy-9 α -nicotinoyloxy-12,15-epoxy-12,17-cyclojatroph-5 α ,6 α -diol-14-one (**20**).....99

5.1.1.3. Epoxiwelwitschene - 3 β ,5 α ,-diacetoxy-7 β ,8 α -diisobutyryloxy-9 α -nicotinoyloxy-11,12-epoxy-jatroph-6(17)-en-15 β ol-14-one (**22**).....105

5.1.1.4. Esulatin M (**23**).....106

5.1.2. Biogenic interrelationships.....108

5.1.3. Structure elucidation of flavonoids.....109

5.1.3.1 Quercetin 3-O- α -L-3'',5''-diacetyl-arabinofuranoside (**24**).....109

5.1.3.2. Catechin (**25**).....111

5.2. Assessment of MDR reversal activity.....112

5.2.1. Modulation of P-gp efflux and ATPase activity.....112

5.2.1. Antiproliferative activity and chemosensitivity assays.....115

Chapter 6

Resensitizing MDR phenotypes: collateral sensitivity. Results and

Discussion.....117

6.1. Antiproliferative activity and collateral sensitivity.....119

6.2. Apoptosis assays.....127

Chapter 7

Conclusions.....129

7. Conclusions.....131

Chapter 8

Materials and Methods.....135

8.1. Chemistry.....137

8.1.1. General experimental procedures.....137

8.1.2. Phytochemical study of <i>Euphorbia piscatoria</i>	138
8.1.2.1. Plant Material.....	138
8.1.2.2. Extraction and Isolation.....	138
<i>Study of fraction G</i>	140
<i>Study of fraction I</i>	144
<i>Study of fraction J</i>	146
<i>Study of fraction K-N</i>	148
8.1.3. Phytochemical study of <i>Euphorbia welwitschii</i>	152
8.1.3.1. Plant Material.....	152
8.1.3.2. Extraction and Isolation.....	152
<i>Study of fraction G</i>	153
<i>Study of fraction I</i>	160
8.1.4. Preparation of a small library of macrocyclic lathyrane diterpenes.....	161
8.2. Biological Studies.....	188
8.2.1. Reversal of MDR mediated by P-glycoprotein.....	188
8.2.1.1. Cell lines and cultures.....	188
8.2.1.2. Antiproliferative assay.....	188
8.2.1.3. Assay for rhodamine 123 accumulation.....	189
8.2.1.4. Drug combination assay.....	189
8.2.1.5. ATPase Activity Assay.....	190
8.2.1.6. Curve fitting and data analysis.....	191
8.2.2. Collateral sensitivity assays.....	191
8.2.2.1. Cell lines, cell culture and cell proliferation assay.....	191
8.2.2.2. Apoptosis assay using Annexin V/PI staining.....	192
8.2.2.3. Statistical analysis.....	192
References.....	193

Tables Index

Table 1.1. Cellular and molecular resistance mechanisms to some chemotherapeutic agents.....	6
Table 1.2. Mechanisms of drug resistance presented by cancer stem cells.....	9
Table 3.1. ¹ H and ¹³ C NMR data (δ) for piscatolide (1), 400 and 101 MHz, respectively.....	47
Table 3.2. ¹ H and ¹³ C NMR data (δ) for compounds 2 and 7 (400 and 101 MHz, respectively).....	50
Table 3.3. ¹ H and ¹³ C NMR data (δ) for compounds 8 and 9 (400 and 101 MHz, respectively).....	54
Table 3.4. ¹ H and ¹³ C NMR data (δ) for piscatoriols A (3) and B (4) (400 and 101 MHz, respectively).....	56
Table 3.5. ¹ H and ¹³ C NMR data (δ) for compounds 5 and 6 (400 and 101 MHz, respectively).....	59
Table 3.6. ¹ H and ¹³ C NMR data (δ) for compound 10 (400 and 101 MHz, respectively).....	62
Table 3.7. ¹ H and ¹³ C NMR data (δ) for flavonoids 11-14 (400 and 101 MHz, respectively).....	64
Table 3.8. ¹ H and ¹³ C NMR data (δ) for compounds 15 and 16 (400 and 101 MHz, respectively).....	66
Table 3.9. ¹ H and ¹³ C NMR data (δ) for compounds 17 and 18 (400 and 101 MHz, respectively).....	66
Table 3.10. Evaluation of the interaction between compounds 3-5 and doxorubicin in human <i>MDR1</i> -gene transfected mouse lymphoma cells.....	67
Table 4.1. Antiproliferative activity of jolkinol D (6) and derivatives 6.1-6.27 in L5178Y mouse lymphoma cells (PAR cells) and in human <i>MDR1</i> -gene transfected mouse lymphoma cells (L5178Y-MDR cells).....	77
Table 4.2. Modulation of P-gp mediated rhodamine-123 efflux by jolkinol D (6) and derivatives (6.1-6.27).....	79
Table 4.3. Cluster analysis (K-means algorithm) of the compounds jolkinol D (6) and derivatives (6.1- 6.12 and 6.23). Grouping variables are physicochemical properties: molecular weight (MW), molecular volume (MV), octanol/water	82

partition coefficient ($\log P$), molar refractivity (MR), topological polar surface area (TPSA), accessible solvent area (ASA) and FAR values (at 2 μM).....	
Table 4.4. Effect of compounds 6 , 6.1-6.27 in combination with doxorubicin on L5178Y-MDR cells.....	88
Table 5.1. ^1H and ^{13}C NMR data (δ) for compounds 19 and 20 (400 and 101 MHz, respectively).....	95
Table 5.2. ^1H and ^{13}C NMR Data (δ) for compounds 21 (400 and 101 MHz) and 22 (300 and 101 MHz).....	104
Table 5.3. ^1H and ^{13}C NMR Data (δ) for compound 23 (400 and 101 MHz).....	107
Table 5.4. ^1H and ^{13}C NMR data (δ) for flavonoids 24 (400 and 101 MHz, respectively) and 25 (300 and 75 MHz, respectively).....	110
Table 5.5. Comparison of the proton coupling constants and ^{13}C shifts of compounds 25 , catechin and epicatechin, in different solvents.....	111
Table 5.6. Effect of compounds 21-24 on the P-gp mediated rhodamine-123 efflux, in <i>MDR1</i> -transfected L5178Y cells.....	112
Table 5.7. Antiproliferative activity of compounds 19-24 on L5178Y mouse lymphoma cells and in <i>MDR1</i> -transfected cells.....	115
Table 6.1. Characteristics of gastric, pancreatic and colon cancer cell lines and their drug selected sublines.....	120
Table 6.2. Antiproliferative activity of compounds 1-5 , 8 and 19-24 on pancreatic carcinoma cells: EPP85-181P (parental), EPP85-181RN (MDR phenotype) and EPP85-181RDB (MDR phenotype) and on gastric carcinoma cells: EPG85-257P (parental), EPG85-257RN (MDR phenotype) and EPG85-257RDB (MDR phenotype).....	123
Table 6.3. Antiproliferative activity of jolkinol D (6) and derivatives on gastric carcinoma cells: EPG85-257P (parental), EPG85-257RN (MDR phenotype) and EPG85-257RDB (MDR phenotype).....	124
Table 6.4. Antiproliferative activity of jolkinol D (6) and derivatives on pancreatic carcinoma cells: EPP85-181P (parental), EPP85-181RN (MDR phenotype) and EPP85-181RDB (MDR phenotype).....	125
Table 6.5. Antiproliferative activity of jolkinol D (6) and derivatives on colon carcinoma cells HT-29P (parental), HT-29RN (MDR phenotype) and HT-29RDB (MDR phenotype).....	126
Table 8.1. Crude fractions of the EtOAc soluble fraction of the methanol extract of <i>E. piscatoria</i>	139

Table 8.2. Crude fractions of the EtOAc soluble fraction of the methanol extract of <i>E. welwitschii</i>	152
--	-----

Schemes Index

Scheme 3.1. Piscatoric acid (2) as an intermediate on the biogenesis of <i>ent</i> -abietane α,β -unsaturated γ -lactones, such as helioscopinolide E (7).....	52
Scheme 3.2. Biogenetic interrelationships between lathyranes 3-6	61
Scheme 4.1. Jolkinoates A-G (6.1-6.7).....	72
Scheme 4.2. Jolkinoates I-J (6.8-6.12).....	73
Scheme 4.3. Jolkinoates J-T (6.13-6.19) and jolkinolates A-D (6.23-6.27). Reagents and conditions: 1 eq of jolkinol D (6); 1 eq of jolkinodiol (6.23); (a) Respective aroyl chlorides; TEA, CH ₂ Cl ₂ , DMAP (cat.), reflux 60 °C.....	74
Scheme 4.4. Jolkinoate U (6.20) and jolkinofornates A and B (6.21-6.22). Catalytic cycle for acylation of jolkinol D (6) using AgOTf.....	75
Scheme 5.1. Proposed biogenetic pathway for 12,17-cyclojatrophanes.....	108

Figures Index

Figure 1.1. Development of drug resistance. Treatment of a heterogeneous tumor population with a chemotherapeutic agent selects a drug resistant subpopulation. Adapted from Wilting and Dannenberg, 2012.....	3
Figure 1.2. Examples of cellular mechanism of drug resistance.....	5
Figure 1.3. Examples of anticancer drugs from different classes: anthracyclines (I.1), vinca alkaloids (I.2), epipodophyllotoxins (I.3), taxanes (I.4), anthracenediones (I.5), anti-metabolites (I.6 , I.11), platinum containing drugs (I.7), alkylating agents (I.8) and a tyrosine-kinase inhibitor (I.9).....	7
Figure 1.4. Tumor development from cancer stem cells or from cells with stem-cell-like properties.....	8
Figure 1.5. Overcoming MDR through nanotechnology-based drug delivery. Adapted from Conde <i>et al.</i> , 2013.....	10
Figure 1.6. Milestones of MDR-mediated by P-glycoprotein.....	12

Figure 1.7. Structure of P-glycoprotein. (A) P-gp is composed of one long chain that folds into two similar halves. The first half is colored green and the second half is colored blue. The flexible linker (magenta dotted line) is not seen in Aller's crystal structure (adapted from Goodsell, 2010). (B) Schematic structure showing the 12 transmembrane domains and the 2 ATP binding sites.....	13
Figure 1.8. Model of substrate transport by P-gp. (A) Substrate partitions into the bilayer from outside of the cell to the inner leaflet and enters the internal drug-binding pocket through an open portal. (B) ATP binds to the NBDs causing a large conformational change presenting the substrate to the outer leaflet/extracellular space. Adapted from Aller <i>et al.</i> , 2009.....	14
Figure 1.9. Example of compounds that have been tested in the clinical setting for MDR reversal.....	17
Figure 1.10. A 4-point pharmacophore. Specifications of the radius (A), distances (B), angles (C) and dihedral angle (D). Pharmacophoric points: Hyd (hydrophobic) and Acc (hydrogen bond acceptor) (Ferreira <i>et al.</i> , 2011).....	18
Figure 1.11. Collateral sensitivity phenomenon.....	20
Figure 1.12. Examples of collateral sensitivity.....	22
Figure 1.13. Collateral sensitivity mechanism of verapamil.....	23
Figure 1.14. Examples of natural products or its derivatives as anticancer drug.....	24
Figure 1.15. Ingenol 3-angelate.....	25
Figure 1.16. Types of diterpenic scaffolds synthesized by <i>Euphorbia</i> species.....	26
Figure 1.17. Terpenoid biosynthesis. Mevalonic acid (MVA) pathway and the 1-deoxy-D-xylulose 5-phosphate (DXP) pathway.....	28
Figure 1.18. Cyclization of GGPP yielding casbene. Biogenesis of casbene-derived diterpenes.....	29
Figure 1.19. Cyclization of GGPP leading to biosynthesis of polycyclic diterpenes.....	30
Figure 1.20. MDR reversal activity of jatrophanes isolated from <i>Euphorbia</i> species.....	32
Figure 1.21. MDR reversal activity of jatrophanes isolated from <i>Euphorbia</i> species.....	33
Figure 1.22. Structure–activity relationships of 5,17-epoxy lathyranes I.38-I.49 on P-gp modulation. FAR values presented at 2 and 20 μ M. Compounds I.38-I.42 were isolated from <i>E. boetica</i> . Epoxilathyrol (I.43) was obtained through hydrolysis of	34

I.38 and derivatives I.44-I.49 through acylation of I.43 (data from Vieira <i>et al.</i> , 2014).....	
Figure 1.23. The most active lathyrol derivative of Jiao <i>et al.</i> (2015) study.....	34
Figure 1.24. The most active P-gp modulator of Matos <i>et al.</i> (2015) study.....	35
Figure 1.25. Cytotoxic activity of jatrophanes isolated from <i>Euphorbia</i> species.....	36
Figure 1.26. Cytotoxic activity of <i>ent</i> -abietane lactones isolated from <i>Euphorbia</i> species...	36
Figure 1.27. Cytotoxic activity of lathyranes isolated from <i>Euphorbia</i> species.....	37
Figure 1.28. Anti-viral activity of jatrophanes and <i>ent</i> -abietane lactones isolated from <i>Euphorbia</i> species.....	38
Figure 3.1. Key COSY and HMBC correlations and NOESY interactions observed for piscatolide (1).....	48
Figure 3.2. Key COSY and HMBC correlations for piscatoric acid (2). Spin systems (A-B-C), their connection through the main heteronuclear $^2J_{C-H}$ and $^3J_{C-H}$ correlations...	51
Figure 3.3. 1H -spin systems (A-B), their connection through the main heteronuclear $^2J_{C-H}$ and $^3J_{C-H}$ correlations and key NOESY interactions of compound 3	57
Figure 4.1. Flow cytometry histograms showing reversal of the MDR phenotype: Jolkinoate G (A) and K (B) at 2 μ M and 20 μ M, in comparison with Jolkinol D (20 μ M). MDR: L5178Y-MDR chemo-resistant cells; PAR: parental chemo-sensitive cells.....	78
Figure 4.2. Relation between fluorescence activity ratio (FAR; lines) and percentage of MDR cells that reverted to a PAR phenotype (bars), for compounds 6.8-6.10 and 6.12 . This analysis clearly shows the dose-dependent inhibitory effect of P-gp efflux.....	80
Figure 4.3. Resume of structure–activity relationships of jolkinol D (6) and derivatives 6.1-6.12 and 6.23 . FAR values at 2 μ M.....	83
Figure 4.4. Cluster analysis of compounds 6.13-6.22 and 6.24-6.27 . Box and whiskers plot representing each grouping variable: FAR values (2 μ M), molecular weight (MW), molecular volume (MV), octanol/water partition coefficient (logP), molar refractivity (MR), topological polar surface area (TPSA), and accessible solvent area (ASA). Physicochemical properties were calculated using JME molecular editor, version July 2015, http://www.molinspiration.com/jme	84
Figure 4.5. Structure–activity relationships of jolkinol D derivatives: effects of electron withdrawing/donating groups and bulky substituents. FAR values at 2 μ M.....	85

Figure 4.6. (A) Effect of jolkinol D (6) and (B) jolkinoate P (6.15) on P-gp ATPase activity. Activation assay: to test the effect on the basal ATPase activity. Inhibition assay: to test the effect on drug-stimulated ATPase activity, measured in the presence of verapamil (40 μ M). Results are expressed as the mean \pm SD from experiments performed in duplicate. The effects of compounds were presented as the relative ATPase activity, in which, the verapamil-stimulated vanadate-sensitive ATPase activity is taken as 100% and the baseline vanadate-sensitive ATPase activity as 0%.....	90
Figure 5.1. Key COSY and HMBC correlations for welwitschine (19). The spin systems A and B and their connection through the main heteronuclear $^2J_{C-H}$ and $^3J_{C-H}$ correlations.....	97
Figure 5.2. Key NOESY correlations of welwitschine A (19).....	99
Figure 5.3. Crystallographic structure of 19 : (A) ORTEP diagram of welwitschine A (19); (B) Hydrogen bonds forming pairs of crystallographically independent molecules of 19 (hydrogen atoms were omitted for clarity).....	99
Figure 5.4 (A) Key NOESY correlations of welwitschine B. (B) ORTEP diagram of 20	101
Figure 5.5. Hydrogen bonds in compound 20 giving rise to zigzag chains in a view along the c axis. Hydrogen atoms (except the ones involved in the hydrogen bonds in the respective images) were omitted for clarity.....	101
Figure 5.6. Key COSY and HMBC correlations for welwitschene (21). Spin systems A, B and C and their connection through the main heteronuclear $^2J_{C-H}$ and $^3J_{C-H}$ correlations.....	103
Figure 5.7. (A) Main NOESY correlations of welwitschene (21); dot bold: α -protons correlation and dash: β -protons correlation. (B) NOE signals that suggest a preferential <i>endo</i> -type conformation for welwitschene (21).....	113
Figure 5.8. Effect of epoxiwelwitschene (22) on P-gp ATPase activity. Activation assay: to test the effect on the basal ATPase activity. Inhibition assay: to test the effect on drug-stimulated ATPase activity, measured in the presence of verapamil (40 μ M). Results are expressed as the mean \pm SD from experiments performed in duplicate. The effects of compounds were presented as the relative ATPase activity, in which, the verapamil-stimulated vanadate-sensitive ATPase activity is taken as 100% and the baseline vanadate-sensitive ATPase activity as 0%.....	114

Figure 5.9. Effect of compounds 19-23 in combination with doxorubicin in L5178Y-MDR cells. Combination index (CI) values are mean \pm standard deviation for an inhibitory concentration of 50 % (IC ₅₀). CI < 0.1: very strong synergism; 0.1 < CI < 0.3: strong synergism; 0.3 < CI < 0.7: synergism; 0.7 < CI < 0.9: moderate to slight synergism; 0.9 < CI < 1.1: nearly additive; 1.10 < CI < 1.45: moderate antagonism; 1.45 < CI < 3.30: antagonism (Chou, 2006, 2010).....	116
Figure 6.1. Induction of apoptosis on gastric (A) and pancreatic (B) cell lines. Total apoptosis (cells on the annexin V+/PI- quadrant, plus annexin V+/PI+ quadrant). Fold increase (treated sample/untreated sample).....	128
Figure 7.1. Summary of the main achievements obtained in this work.....	132
Figure 8.1. Study of <i>Euphorbia piscatoria</i> :: extraction, fractionation procedures, and compounds isolated from Fractions G, I, J and K-N.....	139
Figure 8.2. <i>Euphorbia. welwitschii</i> : study of fraction G and respective isolated compounds.....	153

Abbreviations

$[\alpha]_D^{26}$	Specific rotation
$[M]^+$	Molecular ion
$^2J_{C-H}$	C-H coupling through two bonds
$^3J_{C-H}$	C-H coupling through three bonds
ABC	ATP-binding cassette
ADME	Absorption, distribution, metabolism and elimination
AgOTf	Silver trifluoromethanesulfonate
ASA	Accessible solvent area
ATP	Adenosinetriphosphate
BCRP	Breast cancer resistance protein
bd	Broad doublet
bs	Broad singlet
<i>c</i>	Concentration
calcd.	Calculated
CDCl₃	Deuterated chloroform
CI	Combination index
COSY	Correlation spectrometry
CPP	Copalyl pyrophosphate
CSC	Cancer stem cells
d	Doublet
dd	Doublet of doublets
ddd	Doublet of doublet of doublets
DEPT	Distortionless Enhancement by Polarization
DMAP	4-dimethylaminopyridine
DMAPP	Dimethylallyl diphosphate
DMSO	Dimethyl sulphoxide
DNA	Deoxyribonucleic acid
dt	Doublet of triplets
DXP	1-deoxy-D-xylulose 5-phosphate
eq	Equivalent
ESIMS	Electrospray ionization mass spectrometry
ESI-TOF-HRMS	Electrospray ionization time-of-flight high resolution mass spectrometry
EtOAc	Ethyl acetate
FAR	Fluorescence activity ratio
FITC	Fluorescein isothiocyanate
FSC	Forward scatter
GGPP	Geranyl geranyl diphosphate
GPC3	Glypican 3
GSH	Glutathione
GST	Glutathione-S-transferase
HB	Hydrogen bond
HIV	Human immunodeficiency virus
HMBC	Heteronuclear multiple bond correlation
HMQC	Heteronuclear multiple quantum correlation
HPLC	High performance liquid chromatography
IC₅₀	Half maximal inhibitory concentration
IPP	Isopentenyl diphosphate
IR	Infrared
<i>J</i>	Coupling constant
KSP	Kinesin spindle protein

log <i>P</i>	Octanol/water partition coefficient
m	Multiplet
m.p.	Melting point
<i>m/z</i>	Ratio of mass to charge
MDR	Multidrug resistance
Me	Methyl
MeCN	Acetonitrile
MeOD	Deuterated methanol
MeOH	Methanol
MMR	Mismatch repair
MR	Molar refractivity
mRNA	Messenger Ribonucleic acid
MRP	Multidrug resistance associated protein
MS	Mass spectrometry
MTT	3-(4,5-dimethylthiazol-2-yl)-2,5-diphenyltetrazolium bromide
MV	Molecular volume
MVA	Mevalonic acid
MW	Molecular weight
MXR	Mitoxantrone-resistance protein
NBD	Nucleotide binding domain
NMR	Nuclear magnetic resonance
NOE	Nuclear overhauser effect
NOESY	Nuclear overhauser enhancement spectroscopy
PAR	Parental cells
PARP	Poly (ADP-ribose) polymerase
PBS	Phosphate buffer saline
P-gp	P-glycoprotein
PI	Propidium iodide
ppm	Parts per million
QSAR	Quantitative structure-activity relationships
Rel. int.	Relative intensity
ROS	Reactive oxygen species
RR	Relative resistance
RT	Room temperature
s	Singlet
SAR	Structure-activity relationships
SD	Standard deviation
siRNA	Small interfering Ribonucleic acid
SSC	Side scatter
t	Triplet
TAP	Transporter of antigenic peptides
td	Triplet of doublets
TEA	Triethylamine
TfOH	Trifluoromethanesulfonate alcohol
TLC	Thin layer chromatography
TMD	Transmembrane domain
Topo II	Topoisomerase II
TPSA	Topological polar surface area
UV	Ultraviolet
VEGF	Vascular endothelial growth factor
δ	Chemical shift
Δ	Unsaturated bond
δ_C	Carbon chemical shift
δ_H	Proton chemical shift
ν_{max}	Maximum wave number

Chapter 1

Introduction

1.1. Multidrug resistance in cancer

In 2012, cancer was the cause of death for 8.2 million people worldwide and in the next twenty years, with the occurrence of new cases, it is expected to extend by 70% (Ferlay *et al.*, 2015). In addition to this perspective, drug resistance accounts for 90% of treatment failure (Longley and Johnston, 2005). This affects patients with a variety of blood cancers and solid tumors, including breast, ovarian, lung, and lower gastrointestinal tract cancers. Resistance can be classified as intrinsic or acquired; tumors with intrinsic resistance fail to respond to the first chemotherapy given, since resistance-mediating factors are originally present in the tumor population. On the other hand, in acquired resistance, tumors innately respond to chemotherapy, but eventually relapse in spite of the following treatment (Gottesman *et al.*, 2002). The development/selection of various adaptive responses (Figure 1.1) is most probably attributed to the intratumor molecular heterogeneity found in tumor populations (Swanton, 2012). In fact, recent advances in this area revealed the co-existence of diverse clones within the same tumor that present distinct sensitivity upon treatment (Kreso *et al.*, 2013). Therefore, within the same tumor different clones can exhibit distinct mechanisms of resistance.

If resistance phenotype occurs to a broad spectrum of structurally and mechanistically diverse antitumor agents, it is designated as multidrug resistance (MDR). The phenomenon of MDR is considered to be the major hurdle for chemotherapy success since multiple drugs of different classes are used to treat most cancers (Lehnert, 1996; Gottesman *et al.*, 2002; Baird, 2003).

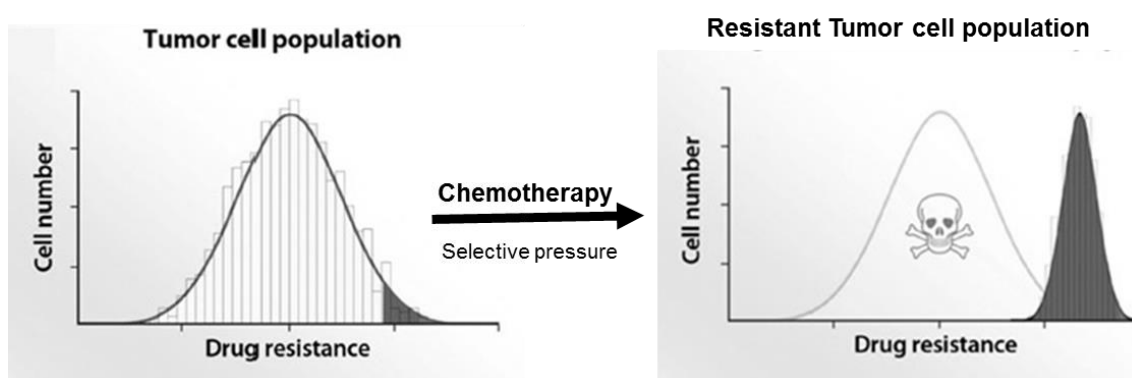


Figure 1.1. Development of drug resistance. Treatment of a heterogeneous tumor population with a chemotherapeutic agent selects a drug resistant subpopulation. Adapted from Wilting and Dannenberg, 2012.

1.1.1. Mechanisms of drug resistance

There are two main biological mechanisms that account for MDR, being classified as pharmacological and cellular mechanisms. The pharmacological mechanisms mainly affect the pharmacokinetics of drugs, namely ADME (absorption, distribution, metabolism and elimination) factors. For instance, the hypoxic niches found in tumor micro-environment lead to the production of lactic acid. This acidic environment affects the uptake of drugs that are pH-dependent, resulting in drug resistance. Other examples of drug resistance caused by non-efficient diffusion and availability of drugs can be attributed to the degree of vascularization of the tumor and to the binding of drugs with albumin and/or to other proteins (Lage, 2008; Baguley, 2010; Kartal-Yandim *et al.*, 2015).

The cellular mechanisms used or developed by cancer cells to evade chemotherapy have been recently reviewed (Holohan *et al.*, 2013; Housman *et al.*, 2014; Wu *et al.*, 2014; Kartal-Yandim *et al.*, 2015). The general consensus is that they are far from being completely understood and that are likely to occur simultaneously or in a cascade of events during the establishment of the MDR phenotype. In fact, MDR can be considered as multifactorial phenomenon with more than one mechanism being present (Larsen and Skladanowski, 1998). Some of the most common cellular mechanisms that have been implicated in MDR include (Figure 1.2): (i) alterations in the cell cycle checkpoints; (ii) failure of the apoptotic mechanisms; (iii) repair of damaged cellular targets; (iv) alterations in drug targets; (v) drug activation and inactivation; (vi) decreased drug uptake and (vii) reduced drug accumulation through drug efflux or vesicular sequestration by ATP binding cassette (ABC) transporters.

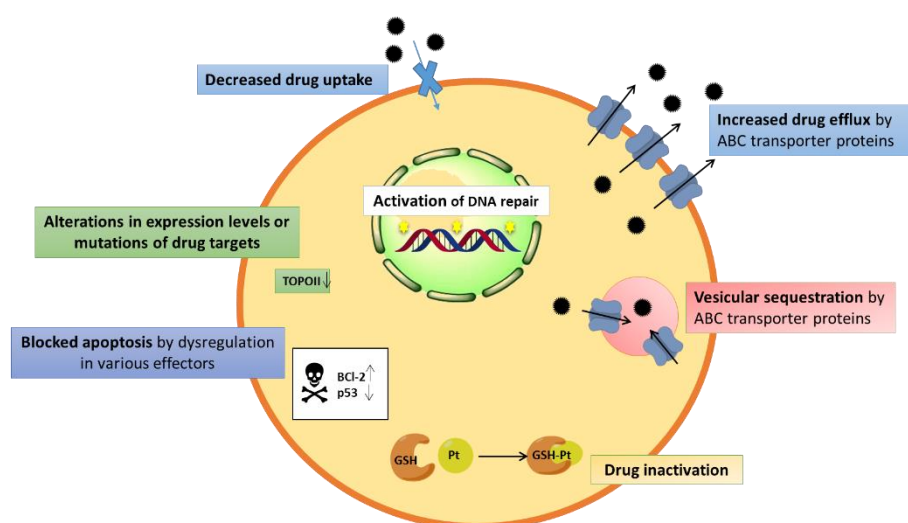


Figure 1.2. Examples of cellular mechanism of drug resistance.

These cellular mechanisms can be subdivided in “non-classical” MDR phenotypes and in “transport-based classical” MDR phenotypes. The last are strongly related with the overexpression of the ABC efflux pumps, which actively expel chemotherapeutic drugs from cells, allowing them to avoid the cytotoxic effects. The “non-classical” MDR comprises mechanisms not associated with a drug transport defect or overexpression of ABC transporters. A summary of the most relevant cellular and molecular resistance mechanisms, mostly observed in *in vitro* studies, is presented at Table 1.1 and examples of anticancer drugs involved in MDR are presented at Figure 1.3 (Longley and Johnston, 2005; Lage, 2008; Baguley, 2010; Holohan *et al.*, 2013; Kartal-Yandim *et al.*, 2015).

Table 1.1. Cellular and molecular resistance mechanisms to some chemotherapeutic agents.

Type	Mechanisms	Characteristics
Transport-based classical MDR		
P-gp-MDR	Overexpression of MDR1/P-gp/ABCB1	Resistance to a broad class of natural product-related anticancer drugs: anthracyclines (I.1), <i>Vinca</i> alkaloids (I.2), epipodophyllotoxins (I.3), or taxanes (I.4) Reduced drug accumulation due to enhanced drug efflux
MRP family-MDR	Expression of MRP1/ABCC1 (most commonly associated to clinical drug resistance) Other members of MRP family (MRP2/ABCC2, MRP3/ABCC3, MRP6/ABCC6, MRP7/ABCC10)	Resistance profile similar to P-gp-MDR Resistance to non-P-gp substrate methotrexate (I.6) Little resistance to taxanes (I.4) Exports drugs modified by glycosylation, sulfonation and glutathione
BCRP-MDR	Expression of BCRP/ABCG2	Cross-resistance to mitoxantrone (I.5) and anthracyclines (I.1) <i>Vinca</i> alkaloids (I.2), paclitaxel (I.4) are not transported by BCRP
Non-classical MDR		
Alteration in drug targets	Decreased topoisomerase II activity (by diminished levels of expression or mutations)	Resistance to Topo II drugs: epipodophyllotoxins (I.3), anthracyclines (I.1)
	Increased target expression (<i>e.g.</i> thymidylate synthase)	Resistance to antimetabolites: 5-fluorouracil (I.11) and methotrexate (I.6)
	Tubulin mutations	Resistance to paclitaxel (I.4) and <i>Vinca</i> alkaloids (I.2)
	Mutations of the target kinases	Resistance to the tyrosine-kinase inhibitor imatinib (I.9)
Drug inactivation	Increased content of thiol glutathione (GSH) and/or increased activity of GST	Resistance to cisplatin (I.7), melphalan (I.8)
	Gene encoding by thymidine phosphorylase inactivated by methylation	Resistance to capecitabine (I.10) (fluoropyrimidine prodrug converted to 5-fluorouracil by thymidine phosphorylase)
Decreased drug activation	Conversion enzymes absent (<i>e.g.</i> uridine phosphorylase)	Resistance to antimetabolites such as 5-fluorouracil (I.11) and methotrexate (I.6) by lack of conversion to the most active forms
Deregulation of apoptosis	Blocked apoptosis due to mutations of p53 Dysfunction of genes involved in apoptosis. Increased expression of anti-apoptotic proteins (<i>e.g.</i> BCL-2)	Resistance to most cytotoxic drugs
DNA damage repair	Several DNA repair pathways are changed to influence drug sensitivity (<i>e.g.</i> mismatch repair (MMR) system – hypermethylation of the MMR gene <i>MLH1</i>)	Resistance to platinum drugs (I.7), alkylating agents (I.8), anthracyclines (I.1) and epipodophyllotoxins (I.3)

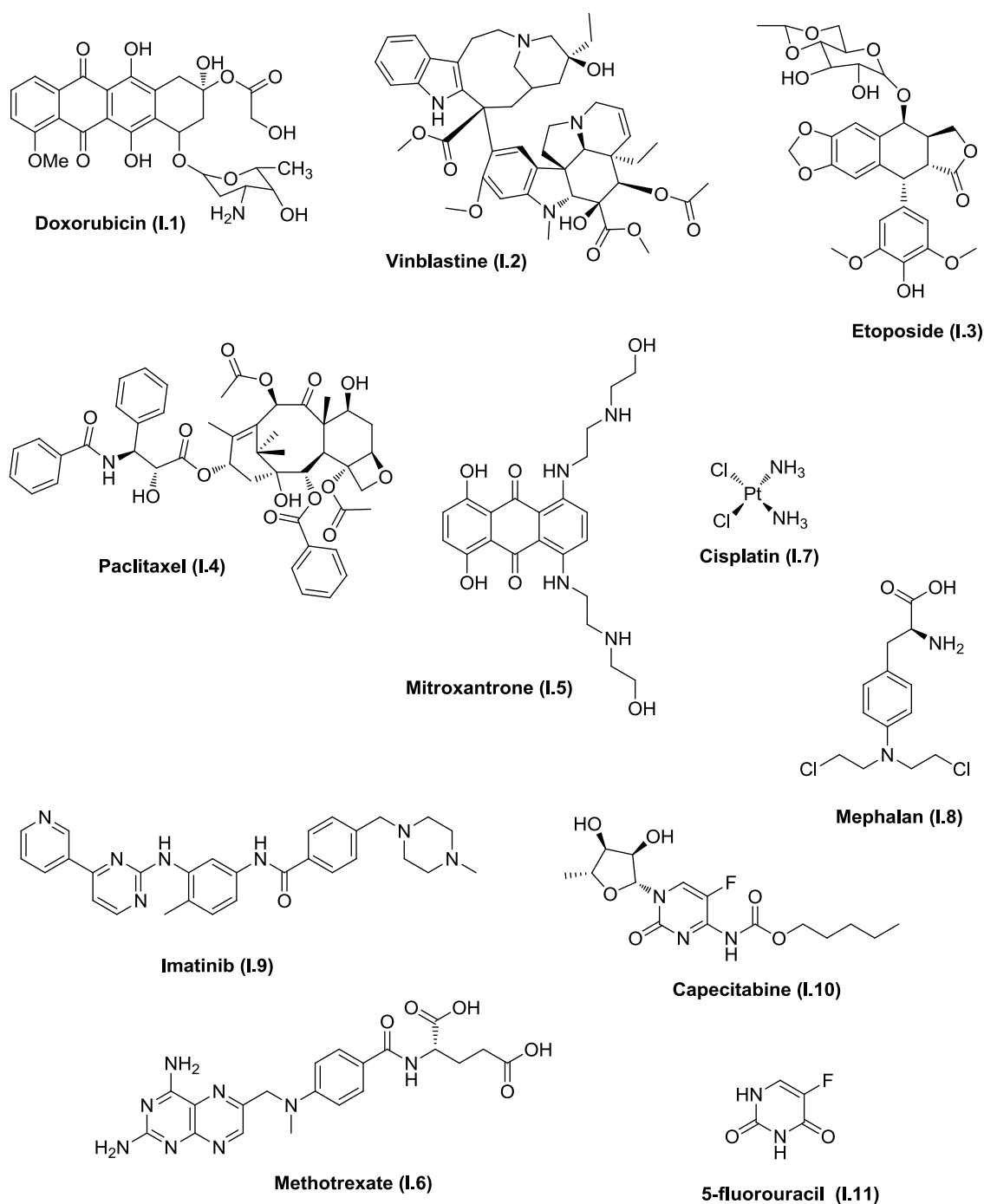


Figure 1.3. Examples of anticancer drugs from different classes: anthracyclines (**I.1**), vinca alkaloids (**I.2**), epipodophyllotoxins (**I.3**), taxanes (**I.4**), anthracenediones (**I.5**), anti-metabolites (**I.6**, **I.11**), platinum containing drugs (**I.7**), alkylating agents (**I.8**) and a tyrosine-kinase inhibitor (**I.9**).

More recently, another source of relapse and progression of cancer is being attributed to the presence of cancer stem cells (CSCs) that are intrinsically resistant to anticancer therapy (Baguley, 2010; Cojoc *et al.*, 2014). The CSC hypothesis for cancer development proposes that tumorigenic CSCs have the properties of self-renewal, clonal tumor initiation and clonal long-term repopulation potential (Figure 1.4). These CSCs have their origin in normal stem cells that escaped regulation. If a normal progenitor cell also escapes regulation may originate cancer cells with stem-cell-like properties (Holohan *et al.*, 2013; Plaks *et al.*, 2015).

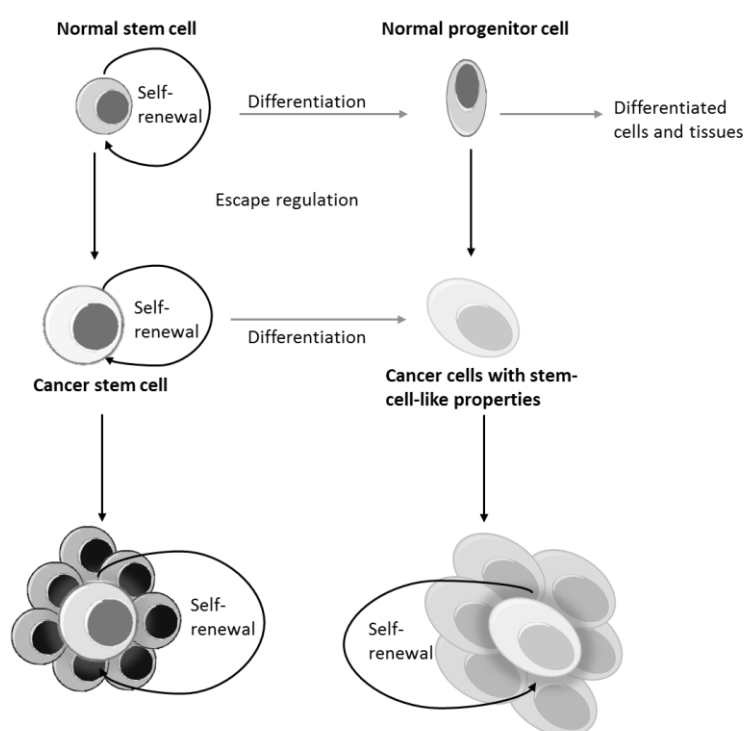


Figure 1.4. Tumor development from cancer stem cells or from cells with stem-cell-like properties.

CSCs or stem-cell-like cancer cells have been regarded as highly resistant to conventional chemotherapy. This resistance can be attributed to their quiescent or slow self-renewal state, since conventional chemotherapy is targeted to rapidly dividing cells. Moreover, other mechanisms of CSC resistance are summarized in Table 1.2 (Baguley, 2010; Holohan *et al.*, 2013; Cojoc *et al.*, 2014).

Table 1.2. Mechanisms of drug resistance presented by cancer stem cells.

Mechanism	Characteristics
High expression of drug efflux proteins	Mostly BCRP/ABCG2 P-gp/ABCB1 and MRP1/ABCC1
High aldehyde dehydrogenase activity	This enzyme contributes to the synthesis of retinoic acid and γ -amino butyric acid that contribute to the maintenance and differentiation of cells
Enhanced DNA damage response	Upregulation of DNA repair genes Protection from oxidative stress by efficient scavenging of reactive oxygen species
Activation of developmental pathways	Activation of signaling molecules of the Notch and Hedgehog pathways; these signaling pathways are involved in differentiation, development and proliferation of cells
CSC micro-environment	Hypoxic niches can protect cells by lack of oxygen. This promotes activation of hypoxia-inducible factors that will activate regulators of the Notch and Hedgehog pathways Tumor and stroma-derived growth factors and cytokines promote survival of CSCs

In conclusion, a better understanding of MDR nature and the comprehension of the underlying resistance mechanisms is essential for overcoming MDR in tumor cells and this is of the utmost importance for the success of future clinical treatments.

1.1.2. Strategies to overcome cancer MDR

To enhance the efficacy of chemotherapy several approaches have been developed to circumvent MDR. It is widely accepted that combination of two or more strategies will maximize the positive outcomes of treatment (Ozben, 2006; Pajeva and Wiese, 2009; Shukla *et al.*, 2011; Pluchino *et al.*, 2012; Saraswathy and Gong, 2013; Callaghan *et al.*, 2014; Szakács *et al.*, 2014).

These include:

- *New anticancer drugs that could evade efflux by ABC transporters (non-substrates): e.g. second- and third-generation taxanes and other microtubule and topoisomerase inhibitors (Nobili *et al.*, 2012);*
- *MDR modulators or chemosensitizers: as ABC efflux pump modulators;*
- *Drugs that specifically target MDR cells by exploiting the collateral sensitivity effect;*

- *Control the expression of MDR proteins* through antisense oligonucleotide approach and post transcriptional gene silencing using siRNA: *e.g.* ALN-VSP02 (Alnylam Pharmaceuticals), a therapeutic agent with two distinct siRNAs encapsulated within a lipid nanoparticle. This agent targets vascular endothelial growth factor (VEGF) and kinesin spindle protein (KSP). Being well tolerated in a phase I trial for liver cancer treatment (Xu and Wang, 2014);
- *Nanotechnology-based drug delivery* (Figure 1.5). Nanomaterials (liposomes, polymeric, magnetic, silica, and gold nanoparticles) can be used to circumvent essential MDR mechanisms through target delivery of MDR modulators, anticancer drugs, molecularly target agents and gene therapy agents;
- *Multimodal strategy*. Simultaneous cytotoxic activity towards CSCs and the corresponding differentiated tumor cells (Nobili *et al.*, 2015).

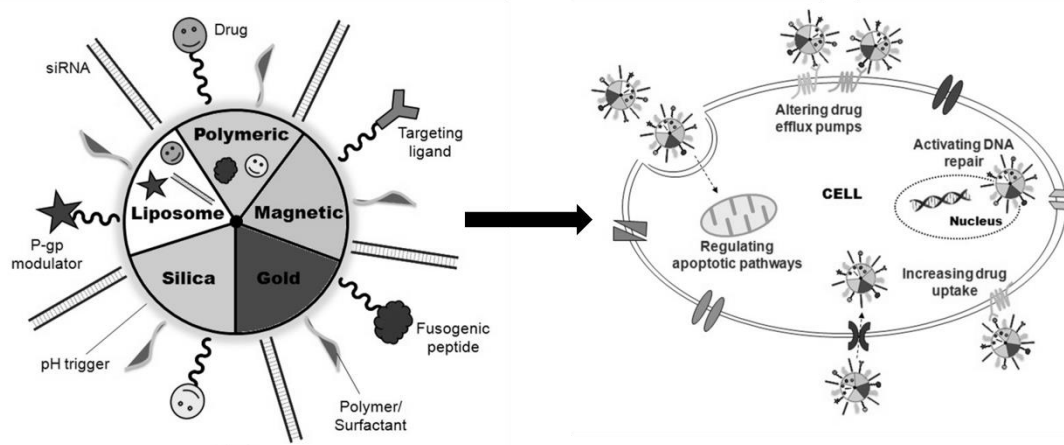


Figure 1.5. Overcoming MDR through nanotechnology-based drug delivery. Adapted from Conde *et al.*, 2013.

1.2. P-glycoprotein and multidrug resistance

Multidrug resistance transporters belong to the evolutionarily conserved family of the ATP binding cassette (ABC) proteins, which are present from prokaryotes to eukaryotes. In humans, the three major types of ABC proteins related to MDR include members of the subfamilies ABCB (ABCB1/MDR1/P-glycoprotein), the ABCC (ABCC1/MRP1, ABCC2/MRP2), and the ABCG (ABCG2/MXR/BCRP). In non-malignant cells, these efflux pumps constitute part of the complex cellular defense since they are able to recognize a number of structurally different and apparently unrelated molecules (xenobiotics) and extrude them into the extracellular space. Moreover, they are pharmacologically important proteins that participate in both distribution and elimination of drugs from the body (Gottesman *et al.*, 2002).

P-glycoprotein (ABCB1, P-gp) was the first human ABC transporter to be described, and consequently is one of the most known and studied efflux pumps associated with MDR (Figure 1.6) (McDevitt and Callaghan, 2007). The overexpression of P-gp in malignant cancer cells results in reduced intracellular concentration of anticancer drugs to levels that lead to treatment failure, causing cross-resistance to several cytotoxic drugs such as the *Vinca* alkaloids (*e.g.* vinblastine **I.2**, vincristine), podophyllotoxins (*e.g.* etoposide **I.3**, teniposide), anthracycline derivatives (*e.g.* doxorubicin **I.1**, daunorubicin), taxanes (*e.g.* paclitaxel **I.4**, docetaxel), and tyrosine kinase inhibitors (*e.g.* imatinib **I.9**, nilotinib) (Gottesman *et al.*, 2002; Sarkadi *et al.*, 2006; Szakács *et al.*, 2006; Kathawala *et al.*, 2015). Moreover, the *MDR1* promoter activity is up-regulated by various stimuli, such as anticancer drugs, DNA-damaging agents, heat shock, serum starvation and ultraviolet radiation. *MDR1* expression can also be up regulated as a consequence of tumor progression, such as mutation of the tumor suppressor gene *p53* and activation of *ras* oncogene (Tsuruo *et al.*, 2003).

Hence, research on selective and potent P-gp reversal agents that impair the efflux mechanism when co-administered with anticancer drugs represents a valuable approach to avoid the chemotherapy failure. However, a better understanding of the molecular basis of its function is essential to a rational drug design.

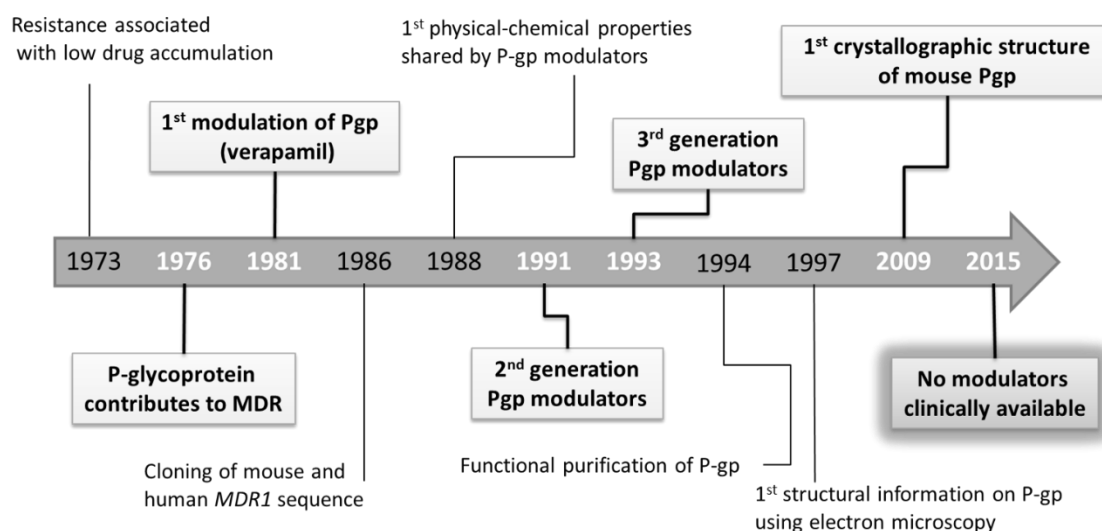


Figure 1.6. Milestones of MDR-mediated by P-glycoprotein.

1.2.1. Structure and function of P-glycoprotein

P-gp/ABCB1, the product of the human multidrug resistance (*MDR1*) gene, is a 170 kDa transmembrane protein. This transporter consists of 1280 amino acids organized in two tandem repeats of 610 amino acids joined by a linker region of 60 amino acids. This flexible linker connects the two halves of the protein ensuring proper interaction of two subunits (Figure 1.7A). P-gp is classified as a pseudosymmetrical heterodimer where each monomer consists of a transmembrane domain (TMD) as well as a nucleotide binding domain (NBD) (Figure 1.7A). Each TMD is composed of six membrane spanning segments (α -helices) separated by hydrophilic loops (Figure 1.7B). The intracellular loops comprise coupling helices, which account for the interaction between TMD and NBD. The TMDs mediate the recognition and transport of substrates and the NBDs are responsible for the ATP-binding, and hydrolysis and consequently for the generation of conformational changes on the protein (Ambudkar *et al.*, 2003; Sauna *et al.*, 2007; Aller *et al.*, 2009; Gutmann *et al.*, 2010). A large hydrophobic chamber of approximately 6.000 \AA^3 , constituted by the TMDs, was characterized on the X-ray structure of mouse P-gp. This presumptive drug binding pocket contains residues mostly of hydrophobic and aromatic nature in the upper half. While in the lower half more polar and charged residues are present (Aller *et al.*, 2009).

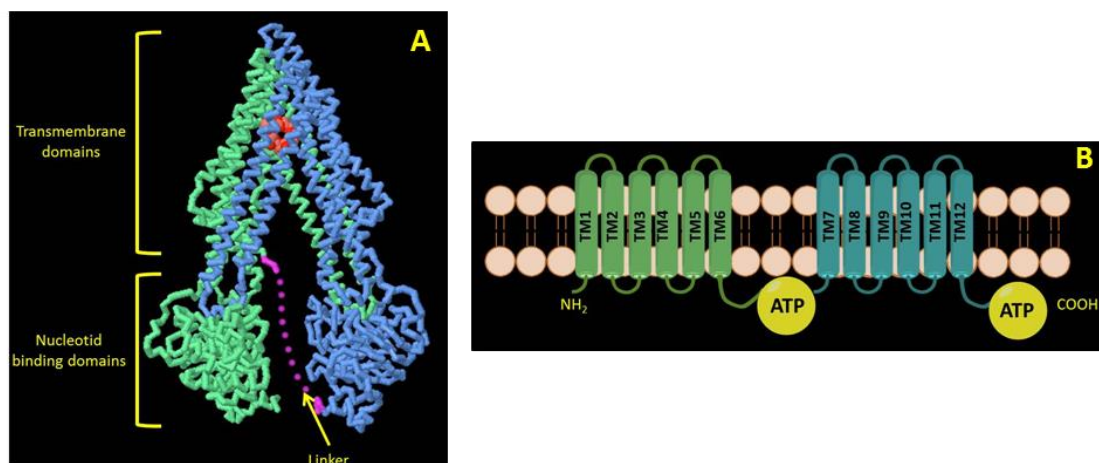


Figure 1.7. Structure of P-glycoprotein. (A) P-gp is composed of one long chain that folds into two similar halves. The first half is colored green and the second half is colored blue. The flexible linker (magenta dotted line) is not seen in Aller's crystal structure (adapted from Goodsell, 2010). (B) Schematic structure showing the 12 transmembrane domains and the 2 ATP binding sites.

The mechanism of P-gp efflux is not fully understood, therefore, some models have been proposed along the years. On the early years of study, Borst and Schinkel (1997) suggested the “membrane pore” model, in which the substrates are directly translocated from the cytoplasm to the extracellular location. More currently, there are two models that are most accepted. They are not mutually exclusive and are designated as the “flippase” and the “hydrophobic vacuum cleaner” models. In the “flippase” model, drugs partition into the inner membrane leaflet and interact with the P-gp substrate-binding pocket. Then are flipped to the outer membrane leaflet followed by rapid partitioning into the extracellular medium. In the “hydrophobic vacuum cleaner” model, drugs partition into the membrane and gain access to the P-gp substrate-binding pocket from within the bilayer interior. They are subsequently effluxed into the extracellular aqueous phase followed by rapid partitioning into the outer leaflet (Ferreira *et al.*, 2014b; Sharom, 2014)

Taking these models together and based on the information inferred from crystallographic and biochemical data, the catalytic cycle for substrate transport can be suggested as the following (Figure 1.8). Substrates partition into the bilayer, from outside of the cell to the inner membrane leaflet, entering the internal drug-binding pocket

through an open portal. This takes place when P-gp presents the inward facing conformation. It is assumed that substrates and membrane lipids remain together during initial entry into the internal cavity, since these lipids are a requirement for the promotion of the ATPase activity. Consequently, when ATP binds to the NBS, one molecule of ATP is hydrolyzed, causing a large conformational change that presents the substrate and drug-binding site(s) to the outer leaflet and/or extracellular space. The binding site is thought to reduce its affinity for the ligand by decreasing favorable intermolecular contacts. Thereafter, the second ATP is hydrolyzed and resets the system back to inward facing conformation, reinitiating the transport cycle (Sauna and Ambudkar, 2000; Loo and Clarke, 2005; Sauna *et al.*, 2007; Aller *et al.*, 2009).

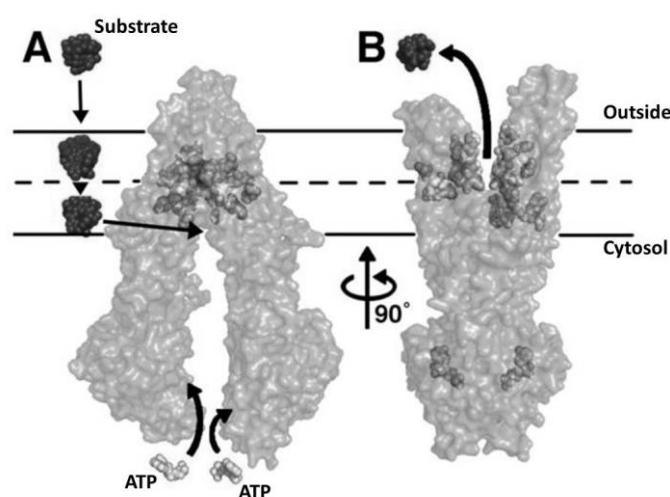


Figure 1.8. Model of substrate transport by P-gp. (A) Substrate partitions into the bilayer from outside of the cell to the inner leaflet and enters the internal drug-binding pocket through an open portal. (B) ATP binds to the NBDs causing a large conformational change presenting the substrate to the outer leaflet/extracellular space. Adapted from Aller *et al.*, 2009.

The substrate polyspecificity of P-gp is vast. Up to 300 molecules are known to interact with the transporter. These include not only the referred anticancer drugs (Figure 1.3), but also therapeutic agents such as, HIV-protease inhibitors (saquinavir; indinavir), antibiotics (actinomycin D), immunosuppressives (sirolimus), cardiac glycosides (digoxin), and endogenous neutral and cationic organic compounds (Ambudkar *et al.*, 1999; Chen *et al.*, 2012).

This polyspecificity is partly explained by the existence of several drug-binding sites. It is proposed that interaction between drug-binding sites enables allosteric regulation, as binding to one site may switch the other sites to a low affinity conformation (Aller *et al.*, 2009; Zinzi *et al.*, 2014).

1.2.2. Current status of P-glycoprotein modulators

P-gp modulators should be devoided of intrinsic toxicity, and when co-administered with an anticancer drug should be able to circumvent its efflux (Robert and Jarry, 2003; Ozben, 2006; Callaghan *et al.*, 2014). In addition, another possible mechanism for P-gp modulation can be through interaction with membrane phospholipids. Disturbance of the P-gp lipid environment would modify the physico-chemical properties of the membrane, triggering a loss of function by modifications on the secondary or tertiary structure of the protein (Maki *et al.*, 2003; Hennessy and Spiers, 2007; Murthy and Shah, 2007).

In this manner, in the past 30 years, a considerable number of natural and synthesized compounds have been described in the literature as P-gp reversal agents. Nevertheless, despite encouraging *in vitro* findings, up to date there are no reversal agents clinically available (O'Connor and Connor, 2009; Shukla *et al.*, 2011; Callaghan *et al.*, 2014; Cort and Ozben, 2015; Kathawala *et al.*, 2015). Figure 1.9 presents an example of compounds that have been tested in clinical setting, divided by the corresponding drug-generations: the first generation comprises drugs that are currently used in clinic for other applications; the second generation drugs are analogues of the first generation; and the third generation drugs were developed for the purpose of MDR reversal.

For instance, first-generation drugs, like verapamil (Tsuruo *et al.*, 1981) and cyclosporin A (Slater *et al.*, 1986), besides revealing low affinity for MDR transporters have other pharmacological actions. Therefore, the high serum concentrations required for P-gp inhibition resulted in cytotoxicity. To surpass this, analogs of these drugs were designed (second-generation modulators), but despite the absence of other pharmacological activity, dexverapamil demonstrated high toxicity (Warner *et al.*, 1998) and valsopodar demonstrated to affect pharmacokinetics of cytotoxic drugs (Boote *et al.*, 1996). The inhibition of hepatic and intestinal cytochrome P450 enzymes caused toxicity

due to decreased metabolism and clearance of the cytotoxic drugs. The lack of significant efficacy and safety in clinical trials did not allow further developments (Kathawala *et al.*, 2015). The third-generation of MDR modulators, like tariquidar (XR9576) (Mistry *et al.*, 2001) and zosuquidar (LY335979) (Dantzig *et al.*, 2001) inhibited P-gp at a nanomolar level. These compounds were less toxic, as well as, inhibitors of BCRP/ABCG2 and MRP1/ABCC1. Though regarded as potent and specific in pre-clinical models, in clinical trials showed lack of efficacy in combination with docetaxel, anthracycline or taxanes (Holohan *et al.*, 2013; Kartal-Yandim *et al.*, 2015).

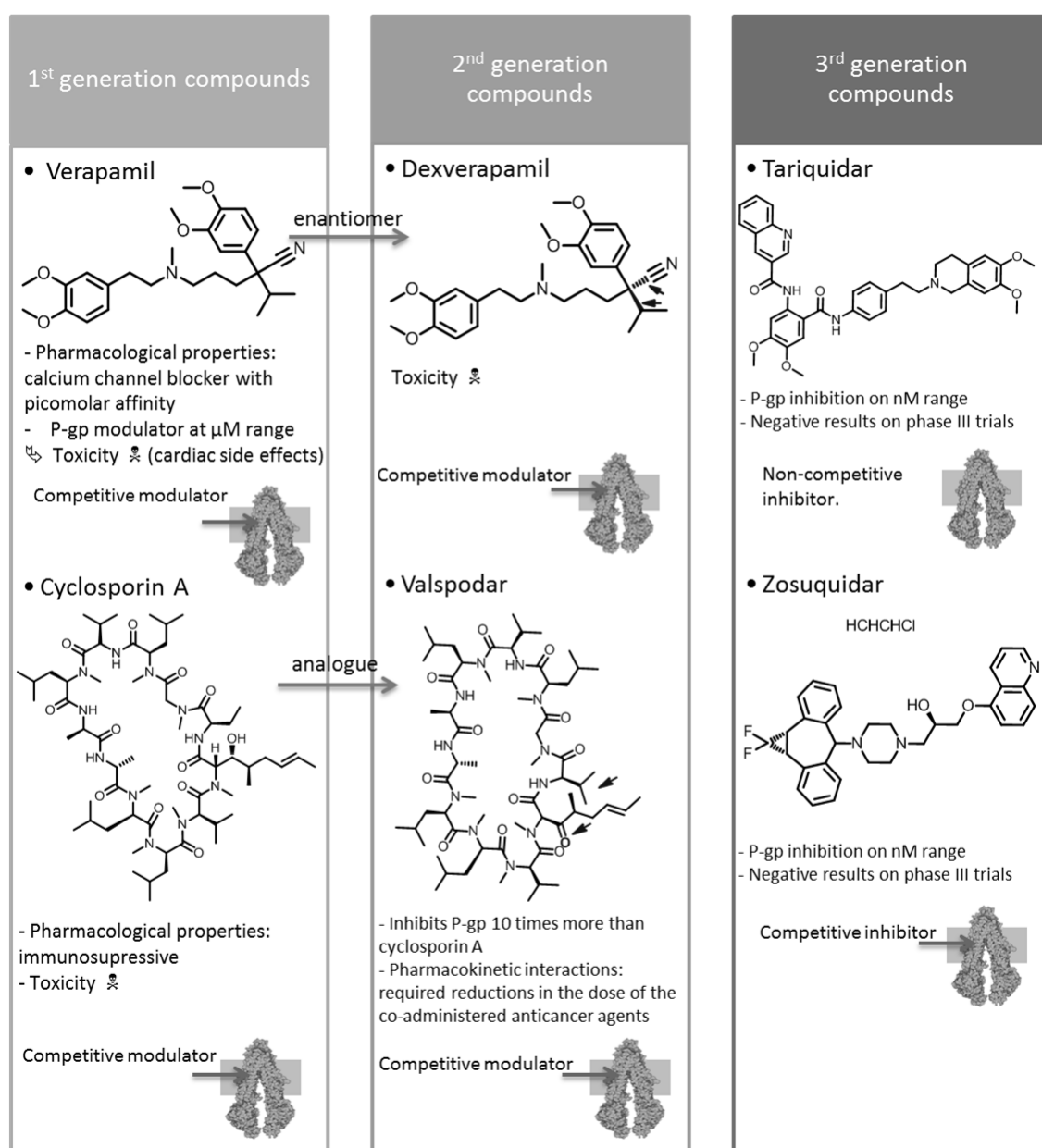


Figure 1.9. Example of compounds that have been tested in the clinical setting for MDR reversal.

Despite all the advances, no MDR modulator is currently in clinical usage. The bottleneck of these three generations can be greatly attributed to simultaneous inhibition of P-gp and the drug metabolizing cytochrome enzyme P450 (CYP3A4 isoform) as well as the inability of modulators/inhibitors to discriminate between “physiological” P-gp expressed in normal tissues and P-gp expressed in cancerous ones. Inhibition of these proteins can cause unwanted side effects on non-tumor sites of the body, modifying the pharmacokinetics of drugs (Callaghan *et al.*, 2014). Therefore, the search for a “fourth generation of modulators” is an ongoing field of research, covering compounds extracted from natural origins and their derivatives, surfactants and lipids, and peptidomimetics. Besides, this fourth generation has its focus on discovering/developing multifunctional drugs that have the ability to interact with multiple targets (Wu *et al.*, 2011; Palmeira *et al.*, 2012; Silva *et al.*, 2014).

1.2.3. Ligand-based and structure-based studies for P-gp modulators

Over the last few years, X-ray structures have been determined for bacterial ABC transporters *e.g.* *Escherichia coli* MsbA, *Staphylococcus aureus* Sav1866 (Dawson and Locher, 2007). Based on these structures, homology models were generated for investigating human P-gp-ligand interactions. However, these bacterial homologues only share 20% sequence identity with human P-gp in the transmembranar domains (Klepsch and Ecker, 2010). Alignments when there is less than 30% of sequence identity are in the so called “twilight-zone” for homology modeling (Martin *et al.*, 2000). For this reason, the design of modulators predominantly followed the classical ligand-based approach, through structure-activity relationships (SAR), Q(quantitative)SAR and pharmacophore modeling (Wiese and Pajeva, 2001; Stouch and Gudmundsson, 2002; Robert and Jarry, 2003; Raub, 2006). The structural diversity of molecules that interact with P-gp is wide, so it is difficult to identify the common structural elements they share. Nevertheless, some physicochemical features could be recognized: (i) lipophilicity - a general property the MDR related drugs; (ii) molecular weight - varies from about 250 to 2000, but remains a very unspecific steric requirement; (iii) hydrogen bond (HB) acceptors and donors – with the predominant role of HB acceptors over HB donor interactions; (iv) at least two

aromatic rings; and (v) a basic nitrogen (Wiese and Pajeva, 2001; Stouch and Gudmundsson, 2002; Robert and Jarry, 2003).

Pharmacophore modeling gives a more detailed understanding about the spatial arrangement of the molecule features relevant for P-gp modulation. Recently, our group proposed a 4-point pharmacophore for P-gp modulators, comprising three hydrophobic and one HB acceptor points (Figure 1.10). This pharmacophore was constructed based on data from previous studies and pharmacophores described in the literature, with the additional advantage of detecting the natural compounds jatrophone and lathyrane macrocyclic diterpenes, molecules capable of modulating P-gp (Ferreira *et al.*, 2011).

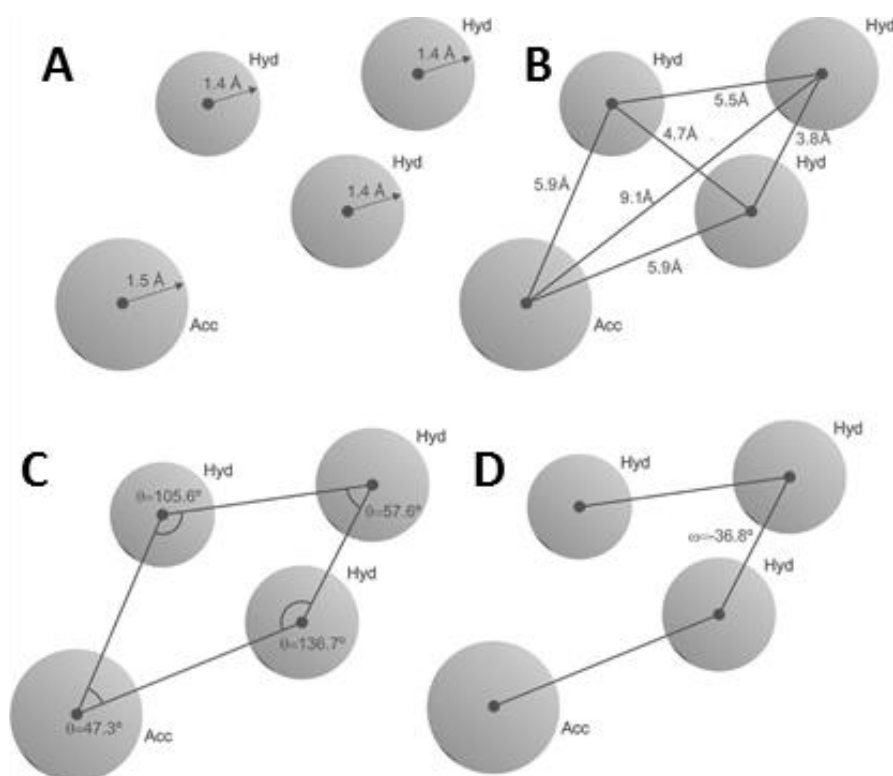


Figure 1.10. A 4-point pharmacophore. Specifications of the radius (A), distances (B), angles (C) and dihedral angle (D). Pharmacophoric points: Hyd (hydrophobic) and Acc (hydrogen bond acceptor) (Ferreira *et al.*, 2011).

Meanwhile, in 2009 the structure of the first murine ABC transporter was published (Aller *et al.*, 2009). This structure has 87% sequence identity to human P-gp, serving as a good template for homology modeling. This represented a great breakthrough for the development of structure-based drug design approaches, and several homology models have been produced.

The computational method of ligand docking is a good way to validate experimentally derived binding pockets or even to propose new areas of binding. In 2009, Pajeva *et al.* used the P-gp binding cavity, based on Aller *et al.* structure, to dock a series of quinazolinones, indolo- and pyrrolopyrimidines, molecules with P-gp modulatory effect. The docking results confirmed the P-gp pharmacophoric features, and identified the interactions between some functional groups and particular protein residues (Pajeva *et al.*, 2009). The clarification between substrates and modulators/inhibitors represented some challenges for docking studies. This was attributed to the polyspecific nature of the drug-binding site, because only one active binding pocket (with $\sim 6000 \text{ \AA}^3$) was being used in the same docking environment (Tarcsay and Keseru, 2011; Chen *et al.*, 2012). Dolgih and co-workers tested flexible docking versus rigid docking method to differentiate binders from nonbinders of P-gp. It was verified that treating P-gp binding cavity as flexible was critical for obtaining good results. This reflects the intrinsic flexibility of the binding site (Dolghih *et al.*, 2011).

Recently, Ferreira *et al.* proposed a classification scheme to discriminate non-substrates, substrates, non-transported substrates, and modulators, based on docking results using the whole drug-binding pocket as the docking-box. This study identified three putative drug binding sites that match other docking and experimental results (Ferreira *et al.*, 2013). In overall, the structure-based prediction models for P-gp are considered important for the analysis of transporter-ligand interactions (Ferreira *et al.*, 2014b).

1.3. Targeting MDR cancer cells by collateral sensitivity effect

In resistant cancer cells each genomic, proteomic or metabolomic alteration that conferred advantage during chemotherapeutic pressure, might at the same time, create vulnerabilities. Taking advantage of these vulnerabilities, by converting them into new therapeutic targets, is also a possible approach to overcome resistance. This concept was primarily observed in bacteria, in the early 1952. It was concluded that resistant *Escherichia coli* was hypersensitive to other unrelated drugs and termed this phenomenon as collateral sensitivity (Hall *et al.*, 2009a; Pluchino *et al.*, 2012). This concept was then applied to MDR cancer cells, in order to improve the efficacy of chemotherapy (Jensen *et al.*, 1997). Therefore, cancer cells that developed *in vitro* resistance to one agent, can be more sensitive to alternate agents than the original parental cell line (Figure 1.11) (Callaghan *et al.*, 2014; Szakács *et al.*, 2014). The mechanisms by which some compounds exert a selective activity against MDR cells are still under investigation. Some works associated this selectivity to ABC transporters expression, nevertheless, others found it to be independent.

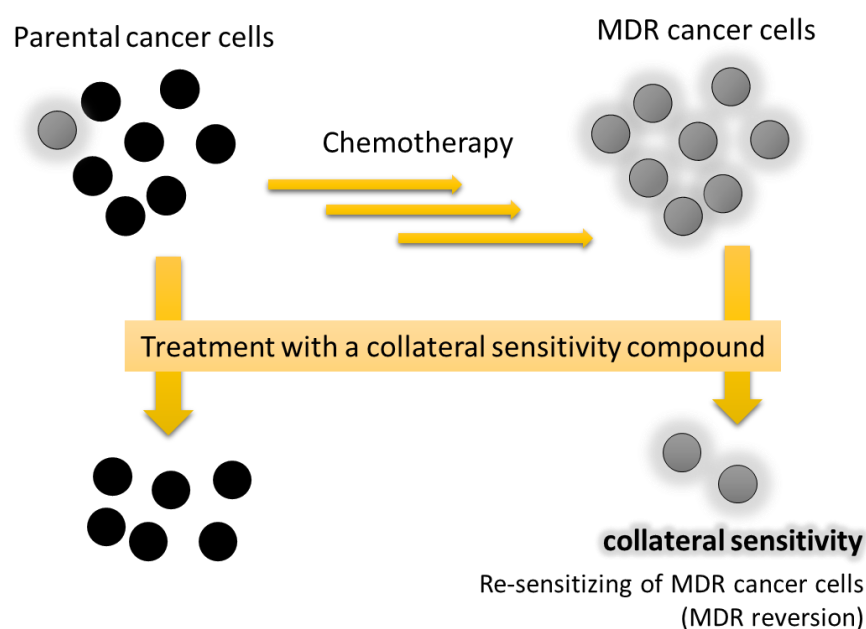
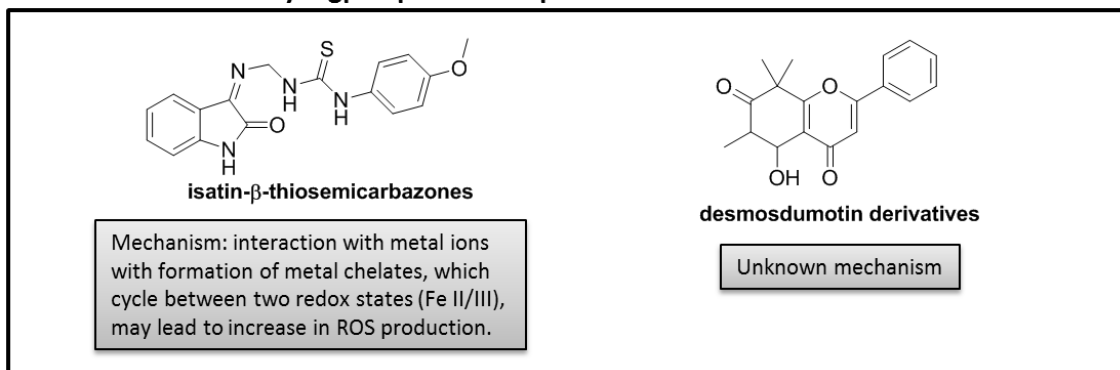


Figure 1.11. Collateral sensitivity phenomenon.

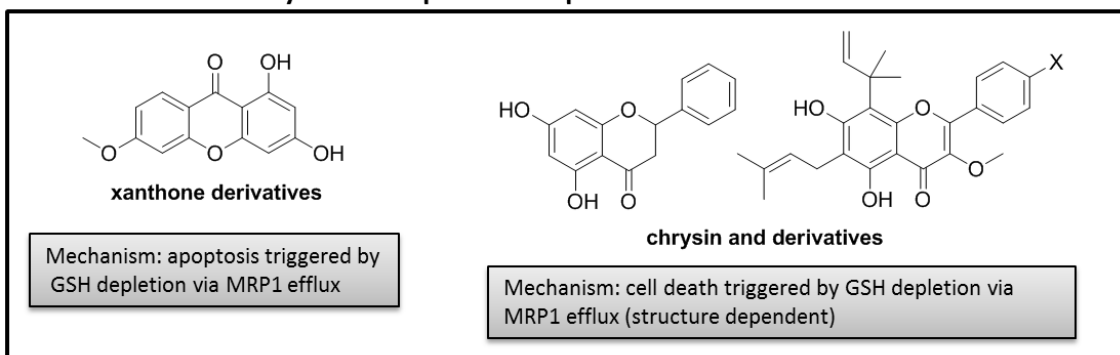
Selective cytotoxicity towards P-gp overexpressing cells, in comparison with normal or P-gp negative cells, was observed when drug-selected or transfected cells were treated with verapamil, non-ionic triton X detergents, steroid hormones and isatin- β -thiosemicarbazones (Figure 1.12) (Bech-Hansen *et al.*, 1976; Vvarr and Fergusson, 1988; Ludwig, 2006; Laberge *et al.*, 2009, 2014; Hall *et al.*, 2009b; 2011). Moreover, expression of ABCC1/MRP1 showed to elicit collateral sensitivity to verapamil, xanthone and flavone derivatives (Figure 1.12) (Laberge *et al.*, 2007; Genoux-Bastide *et al.*, 2011; Lorendeau *et al.*, 2014). Also, cases of collateral sensitivity dependent on ABCG2/BCRP expression were observed for the oxidants hydrogen peroxide, tert-butylperoxide, and 2,2-azobis(2-methylpropionamidine) dihydrochloride (Krzyżanowski *et al.*, 2014; Szakács *et al.*, 2014).

Interestingly, verapamil showed collateral sensitivity effect in P-gp and MRP1-expressing cells. In P-gp expressing cells, the collateral sensitivity mechanism is proposed to occur through production of reactive oxygen species (ROS), via futile hydrolysis of ATP (Figure 1.13). Verapamil is a P-gp substrate at low concentrations, but once inside the cells it is actively effluxed by P-gp with ATP consumption. The rapid cyclical efflux, re-entry and efflux leads to ATP depletion (ATP futile cycle). In turn, this will activate oxidative phosphorylation to increase the ATP levels, leading to higher ROS production, oxidative stress and cell death. Nevertheless, instead of oxidative phosphorylation, glycolysis is the process that has always been thought to support the energy of cancer. Therefore, this hypothesis has still limited evidence (Laberge *et al.*, 2009; Hall *et al.*, 2009a; Pluchino *et al.*, 2012). The mechanism of collateral sensitivity in MRP1-expressing cells is suggested to occur due to increase sensitivity to changes in energy levels and extrusion of an endogenous substrate, essential for cell survival (Figure 1.13). Therefore, in this cellular context, it is suggested that verapamil stimulates glutathione (GSH) efflux leading to oxidative stress and induction of apoptosis (Pluchino *et al.*, 2012).

① Collateral sensitivity P-gp-expression dependent



② Collateral sensitivity MRP1- expression dependent



③ Collateral sensitivity not related with ABC-transporters expression

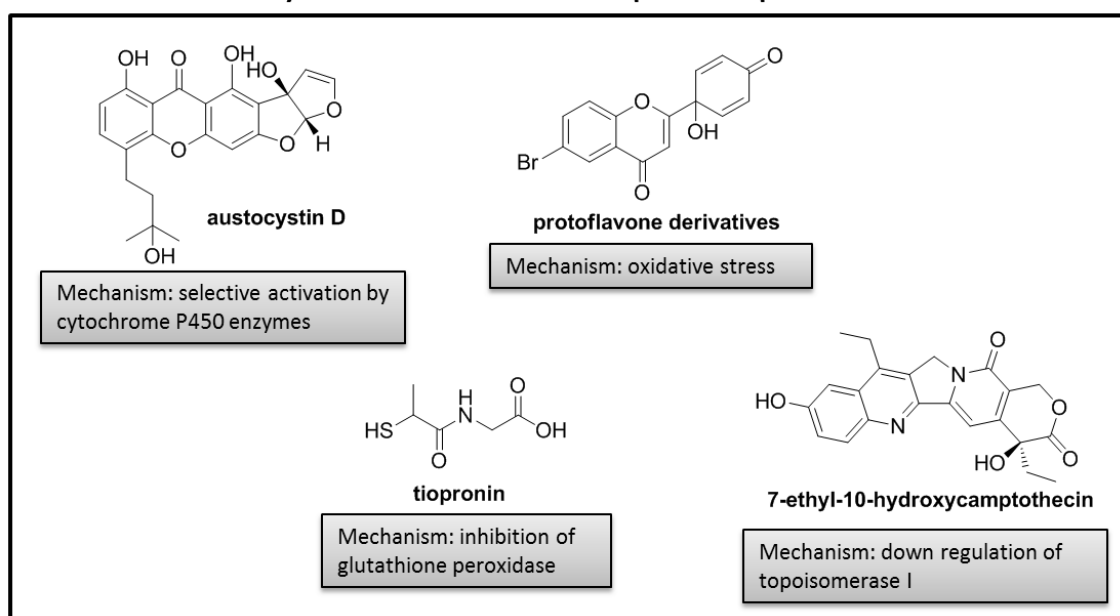


Figure 1.12. Examples of collateral sensitivity.

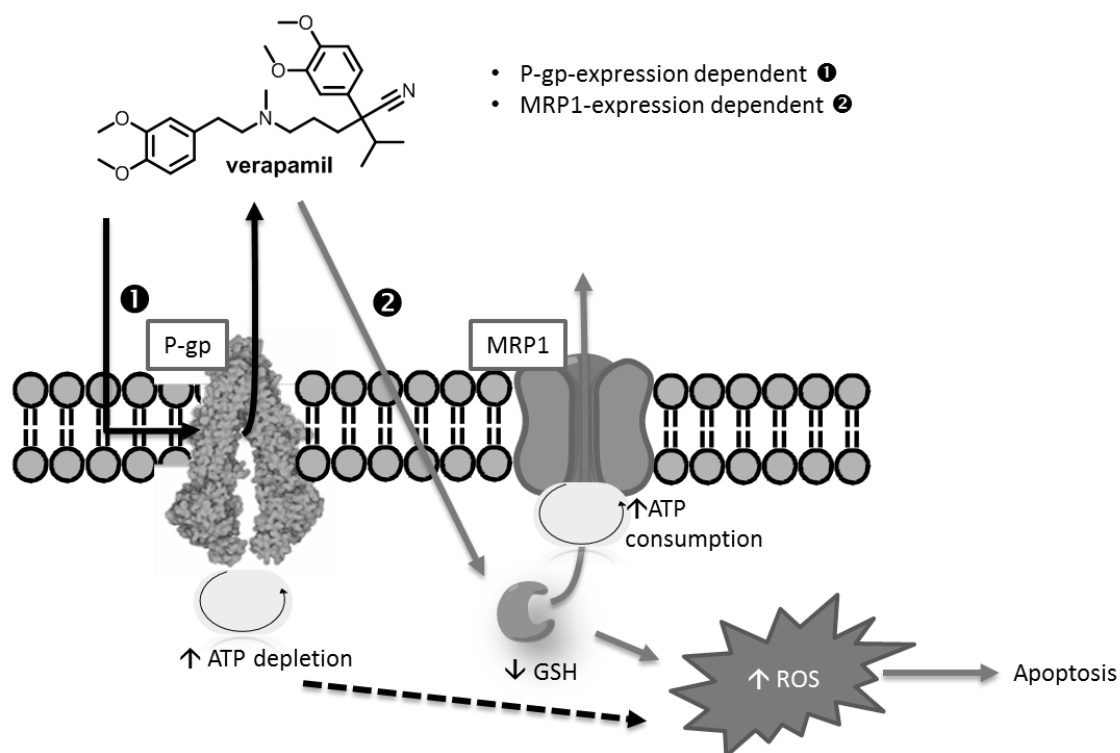


Figure 1.13. Collateral sensitivity mechanism of verapamil.

On the other hand, some compounds produce hypersensitivity in MDR cells independently from ABC transporters expression (Figure 1.12) (Wangpaichitr *et al.*, 2009; Hall *et al.*, 2014; Szakács *et al.*, 2014; Stanković *et al.*, 2015). For example, in cisplatin resistant cells, down regulation of topoisomerase I rendered sensitivity to 7-ethyl-10-hydroxycamptothecin (topoisomerase I inhibitor). Also, in human colon carcinoma cells, selective cytotoxic activity of austocystin D arose from its activation by cytochrome P450, enzymes upregulated in these cells (Szakács *et al.*, 2014).

In general terms, it appears that collateral sensitivity depends on each compound tested and MDR adaptive cell environment. In point of fact, it seems that there is no main mechanism, though, hypersensitivity to reactive oxygen species was transversal in the different studies.

1.4. Natural products as a source of bioactive molecules for cancer MDR reversion

Natural products scaffolds are strategic in drug discovery programs. Nature presents a vast chemical space that was selected through evolution to interact with a wide variety of proteins and other biological targets. Therefore, it is not surprising why natural products have become effective drugs in a wide variety of therapeutic indications. For instance, a total of 19 natural products based drugs were approved worldwide between 2005-2010 (Mishra and Tiwari, 2011). In the case of cancer therapy, 42% (34/81) of the approved anticancer drug candidates, between 1981-2006, comprised natural products and their synthetic derivatives (Newman and Cragg, 2007). The first natural product used as an anticancer drug was podophyllotoxin (Figure 1.14) isolated from *Podophyllum peltatum*. Also important as anticancer agents were its chemical derivatives etoposide (Figure 1.3) and teniposide (Figure 1.14); the vinca alkaloids vinblastine (Figure 1.3) and vincristine (Figure 1.14); and paclitaxel (Figure 1.3), obtained from *Taxus brevifolia* (Koehn and Carter, 2005; Mishra and Tiwari, 2011; Eid *et al.*, 2015).

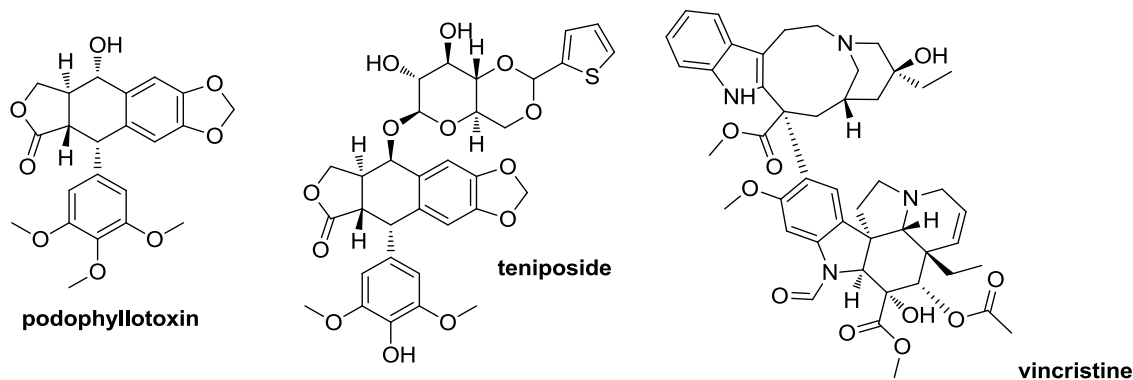


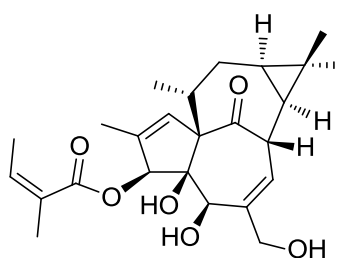
Figure 1.14. Examples of natural products or its derivatives as anticancer drug.

Concerning P-gp modulation, a large number of natural products has been discovered along the years. These include flavonoids, coumarins, cannabinoids, sesqui-, di- and tri-terpenes, alkaloids, lignans and others (Wu *et al.*, 2011; Palmeira *et al.*, 2012; Eid *et al.*, 2015). The aim of this thesis laid on the discovery of new diterpenes with macrocyclic and *ent*-abietane skeletons with MDR reversion potential. Therefore, this topic will have its main focus on the following sections.

1.4.1. Diterpenoids from *Euphorbia* species

Plants from the genus *Euphorbia* (Euphorbiaceae) have a widespread habitat range. These species are distributed from tropical to temperate regions, presenting diverse morphologies, such as annual or perennial herbs, shrubs, trees, succulents and cactus-like (Mwine and Van Damme, 2011). This remarkable biodiversity is also reflected in a wide variety of unique secondary metabolites. In traditional medicine, *Euphorbia* species are commonly named as spurge, due to the use of the plant latex as purgative. However, the fresh latex can also be used to treat cancer, tumors and warts. In addition, they can also have ethnobotanical uses such as fish poisons and arrow poisons (Rivera, 1995; Graham *et al.*, 2000; Mwine and Van Damme, 2011).

Beyond the traditional uses, some species of this genus are considered potent medicinal plants and their extracts have been patented (US patents) as modern anticancer drugs (*e.g.* extract of *E. antiquorum* - US 2003/0165579A1; extracts of *E. peplus*, *E. hirta*, *E. drummondii* - US 6432452) (Mwine and Van Damme, 2011). Another interesting example is ingenol 3-angelate (Figure 1.15), obtained from *E. peplus* that was recently launched for the treatment of actinic keratosis (ingenol mebutate, PEP005, Picato®, LEO Pharma). This compound is an activator of protein kinase C (Vasas *et al.*, 2012).



ingenol 3-angelate

Figure 1.15. Ingenol 3-angelate.

In fact, over 650 diterpenoids, including more than 20 skeletons were isolated from *Euphorbia* species. The result of almost 40 years of research until 2012 are compiled in two review articles (Shi *et al.*, 2008; Vasas and Hohmann, 2014). The most commonly found diterpenes present skeletons of the following types: casbane, daphnane, tigliane, ingenane, jatrophone, lathyrane, paraliene, pepluane, myrsinane, premyrsinane and cyclomyrsinane (Figure 1.16). These scaffolds have been found only in plants of the Euphorbiaceae and Thymelaeaceae families. Additionally, polycyclic diterpenes with rosane, *ent*-abietane, atisane and *ent*-kaurane scaffolds have also been reported (Figure 1.16) (Shi *et al.*, 2008; Vasas and Hohmann, 2014).

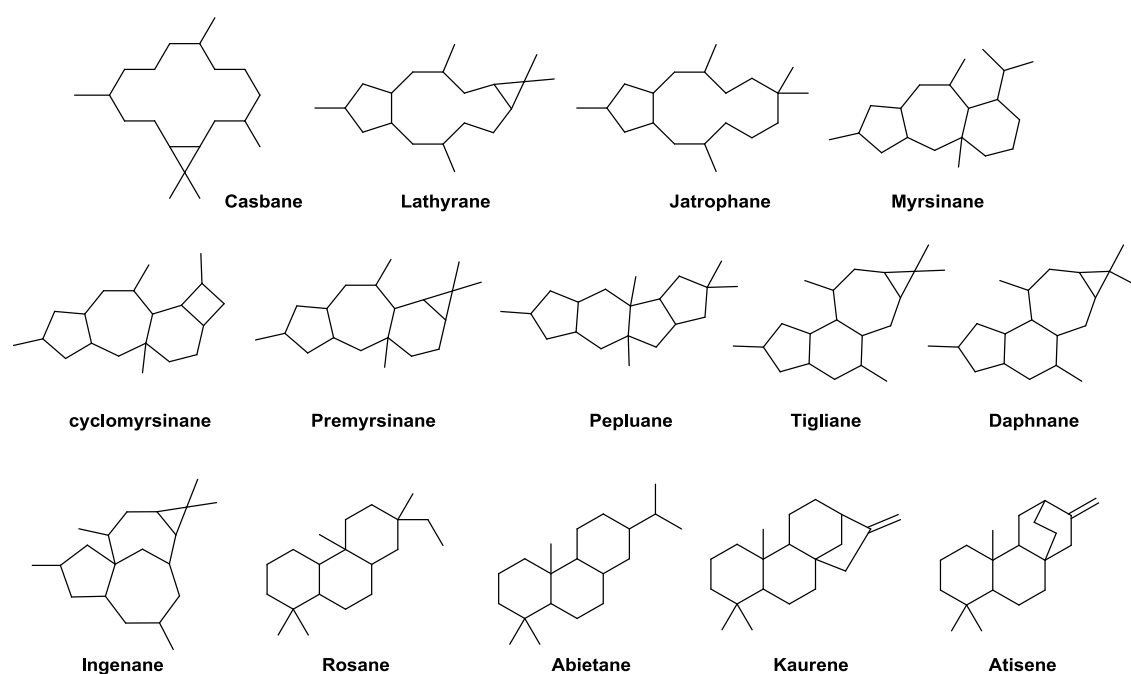


Figure 1.16. Types of diterpenic scaffolds synthesized by *Euphorbia* species.

1.4.1.1. Biosynthesis of diterpenes

Terpenoids constitute a large and diverse group of secondary metabolites derived from C₅ isoprene units. These are arranged mostly in a head-to-tail fashion originating monoterpenes (C₁₀), sesquiterpenes (C₁₅), diterpenes (C₂₀), sesterterpenes (C₂₅), triterpenes (C₃₀) and tetraterpenes (C₄₀). The isoprenoid units - dimethylallyl diphosphate (DMAPP) and isopentenyl diphosphate (IPP) - may be originated from two metabolic pathways: the mevalonic acid (MVA) pathway or the 1-deoxy-D-xylulose 5-phosphate (DXP) pathway (Figure 1.17). In plants, both pathways are present and compartmentalized with MVA being prevalent in the cytosol and DXP in the plastids. Consequently, monoterpenes, diterpenes and tetraterpenes arise via DXP in the plastids and sesquiterpenes and triterpenes via MVA in the cytosol (McGarvey and Croteau, 1995; MacMillan and Beale, 1999; Dewick, 2009a). This section will focus only on the general biosynthetic pathway of diterpenes.

Thus, IPP is isomerized by IPP isomerase to DMAPP, which is sequentially elongated by prenyltransferases, in a head-to-tail fashion, to yield geranylgeranyl diphosphate (GGPP) (Figure 1.17). In turn, diterpenes cyclases catalyze the cyclization of GGPP via electrophilic reactions. Accordingly, these are mediated by carbocation formation, which can be initiated by ionization of the diphosphate ester or by internal deprotonation or protonation. These cyclization reactions together with subsequent Wagner–Meerwein rearrangements are the main source of structural diversity of diterpenes. Rearrangements of this type include migration of carbons or hydride, in order to achieve a stable tertiary carbocation (McGarvey and Croteau, 1995; MacMillan and Beale, 1999; Dewick, 2009a).

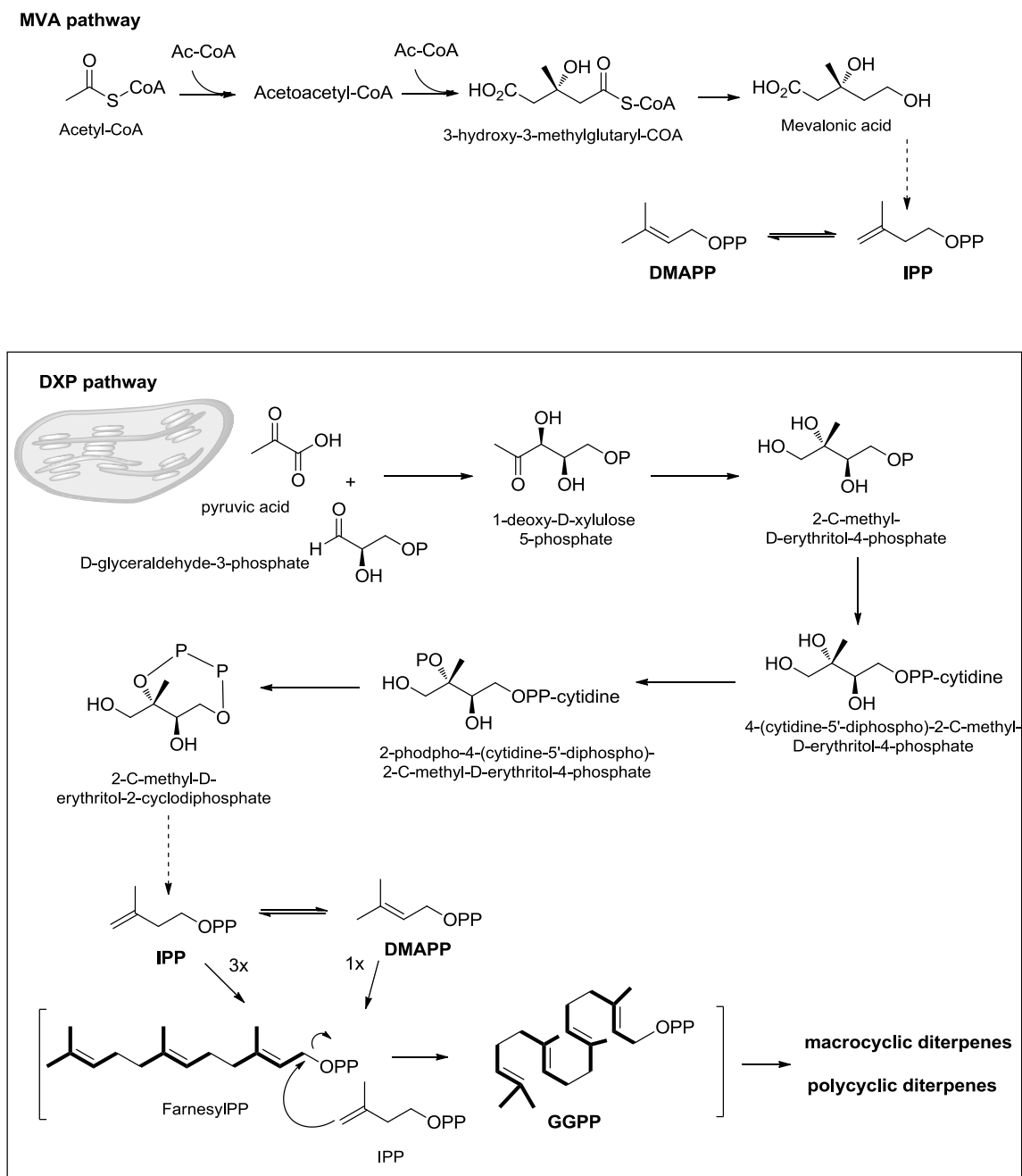


Figure 1.17. Terpenoid biosynthesis. Mevalonic acid (MVA) pathway and the 1-deoxy-D-xylulose 5-phosphate (DXP) pathway.

Diterpenes like jatrophanes, lathyranes, tiglianes, daphnanes and ingenanes are derived from casbene (Figure 1.18). The ionization of GGPP diphosphate and its subsequent cyclization generates the cembrene cation (14-membered ring system). Through the loss of a proton and cyclopropane ring formation casbene is yielded. The further steps for the biosynthesis of casbene-derived diterpenoids have not been identified so far (King *et al.*, 2014; Rinner, 2015). The succeeding reactions include a series of oxidations, ring closures and addition of acyl groups. In plants, cytochrome P450s are responsible for the majority of oxidation reactions that occur in secondary metabolism. It is also possible that these enzymes are involved in the origin of the intramolecular carbon-carbon bonds, characteristic of the macrocyclic diterpenes and re-arranged derivatives (Mizutani, 2012; King *et al.*, 2014). Concerning the ester biosynthesis the BAHD¹ acyltransferases are thought to be involved in this process (D'Auria, 2006; King *et al.*, 2014).

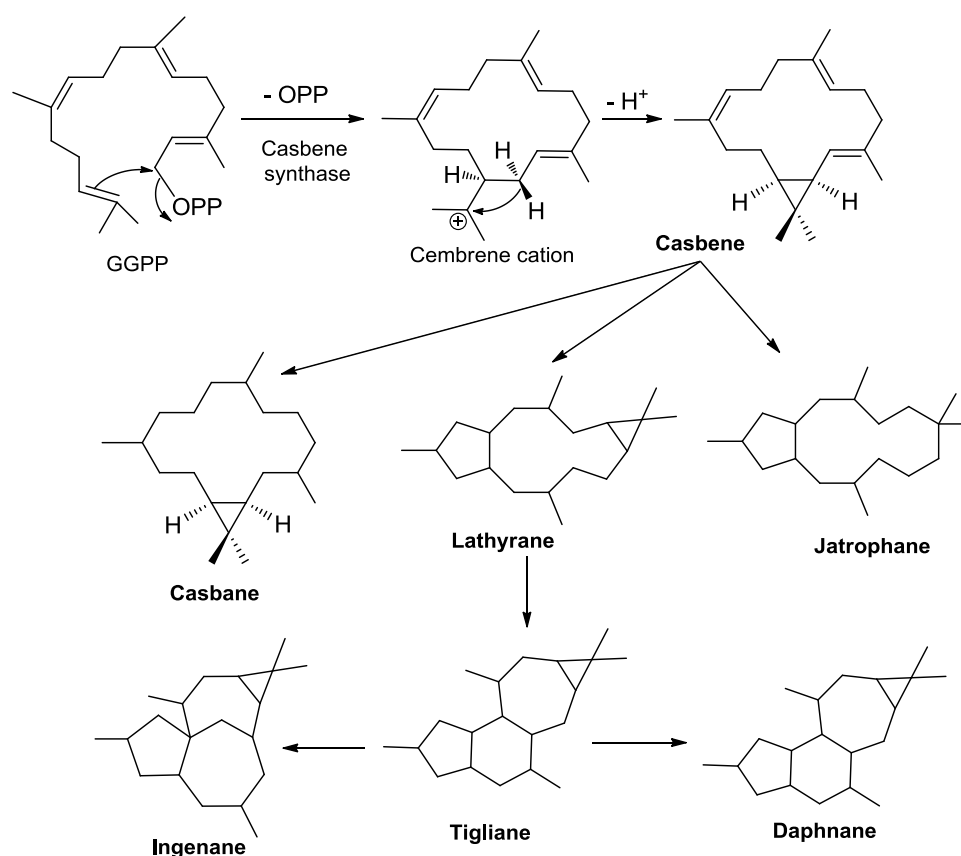


Figure 1.18. Cyclization of GGPP yielding casbene. Biogenesis of casbene-derived diterpenes.

¹ The BAHD acyltransferase is named according to the first letter of each of the first four biochemically characterized enzymes of this family (BEAT, AHCT, HCBT, and DAT). Benzylalcohol *O*-acetyltransferase (BEAT), *O*-hydroxycinnamoyltransferase (AHCT), *N*-hydroxycinnamoyl/benzoyltransferase (HCBT) and deacetylvindoline 4-*O*-acetyltransferase (DAT).

Polycyclic diterpenoids like *ent*-abietanes, *ent*-atisanes, *ent*-kauranes, *ent*-isopimaranes, and *ent*-pimaranes are formed through protonation of GGPP (Figure 1.19). This initiates a concerted cyclization sequence, terminated by loss of a proton from a methyl, yielding copalyl pyrophosphate (CPP). From CPP, a sequence of cyclizations and rearrangements lead to the different classes of polycyclic diterpenes (Figure 1.19).

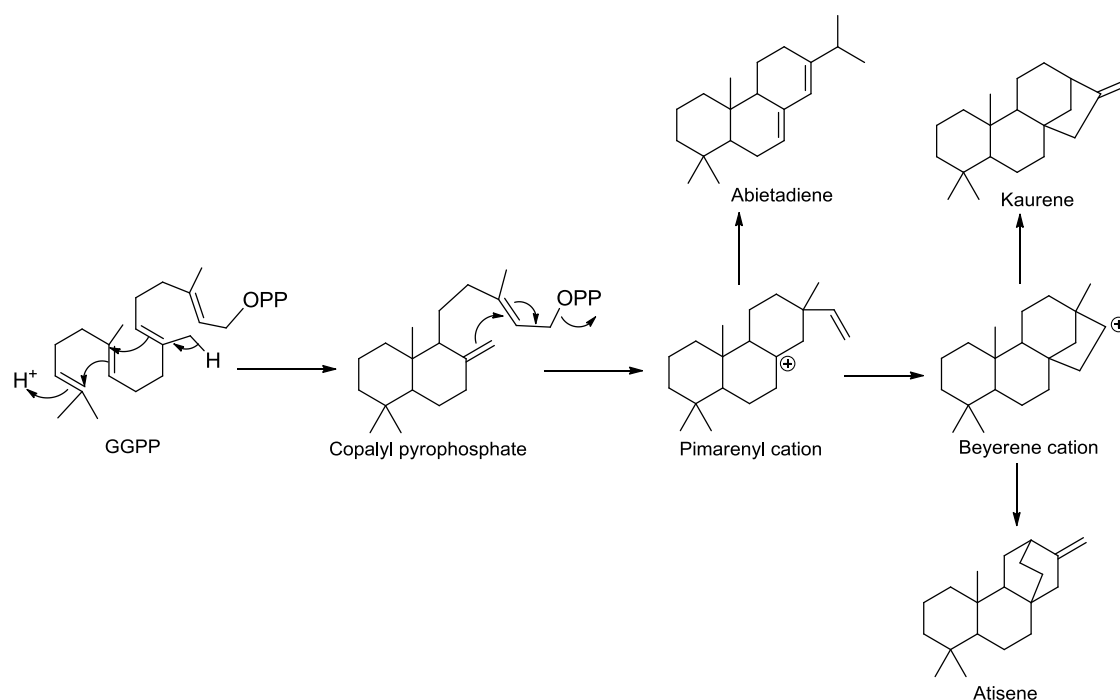


Figure 1.19. Cyclization of GGPP leading to biosynthesis of polycyclic diterpenes.

1.4.2. Bioactive diterpenes from *Euphorbia* species

In general terms, compounds presenting the daphnane, tiglane, and ingenane scaffolds have been associated with toxicity, skin-tumor promotion and pro-inflammatory activity (Jassbi, 2006; Shi *et al.*, 2008; Vasas *et al.*, 2012). While the polyoxygenated jatropane and lathyrane-type macrocyclic diterpenes are promising MDR reversers in cancer, mainly through P-gp modulation (Hohmann *et al.*, 2002; Valente *et al.*, 2004; Duarte *et al.*, 2007; Corea *et al.*, 2009; Reis *et al.*, 2012; Ferreira *et al.*, 2014a). Diterpenes of the *ent*-abietane-type, usually found in *Euphorbia* species as α,β -unsaturated lactones, were identified as having cytotoxicity against various types of tumor cells (Shi *et al.*, 2008; Wu *et al.*, 2009) and selective antiproliferative activity towards cancer cells with MDR phenotype (Lage *et al.*, 2010).

Examples of these biological activities will be given in the following sections, covering works published between 2013 and 2015.

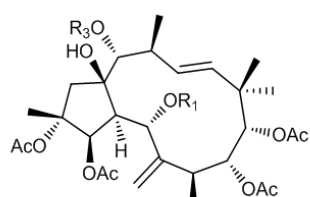
1.4.2.1. MDR reversal activity

Jatrophanes have a flexible twenty carbon skeleton, with a 5:12 fused ring system, which is generally polyacylated. This class of compounds is also characterized by a great structural variability in terms of the number and positions of double bonds (endocyclic or exocyclic), oxygen functions (ketone, epoxy, hydroxy, ether and ester) and configuration of the diterpenic core. There are few MDR structure-activity relationship studies for jatrophanes, possible due to the high structural variability found (Corea *et al.*, 2009; Ferreira *et al.*, 2014a). However, the factors contributing to MDR modulation were accounted for the combination between:

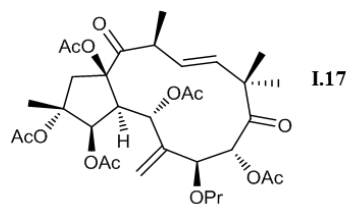
- i. acylation pattern and other chemical functions (ketone, epoxy, hydroxy, ether, double bonds);
- ii. stereochemistry and;
- iii. different conformations (*endo*- and *exo*-type).

In fact, conformational flexibility seems to be important for P-gp modulation, since molecules with the jatrophane skeleton were generally found to be more active than the rearranged polycyclic derivatives (Reis *et al.*, 2012; Ferreira *et al.*, 2014a).

The most recent studies on jatrophanes with MDR activity are summarized in Figures 1.20 and 1.21. Compounds **I.13**, **I.22**, **I.25** and **I.37** showed modulation of human P-gp, while compounds **I.33** and **I.35** modulated *Candida albicans* MDR transporters.

E. sororia (acetone extract of fruits)

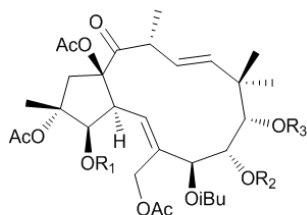
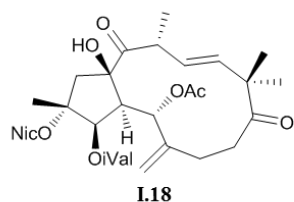
	R ₁	R ₂	R ₃
I.12	Bz	iBu	Ac
I.13	Bz	iBu	Bz
I.14	iBu	iBu	Bz
I.15	iBu	Pr	Bz
I.16	Pr	iBu	Bz



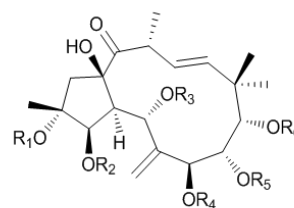
MDR-reversal activity:

- Compound **I.13** showed a **potent inhibition** of P-gp efflux activity at 10 μM, on KBv200 cells

No antiproliferative activity on human mammary adenocarcinoma (MCF-7) and human lung adenocarcinoma (A549) cells (Lu *et al.*, 2014)

E. dendroides (latex)

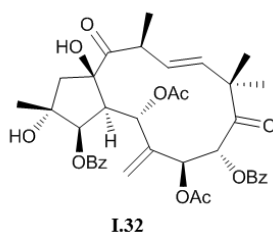
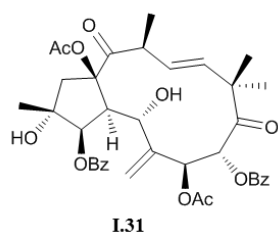
	R ₁	R ₂	R ₃
I.19	Pr	Ac	Nic
I.20	Ac	Nic	Nic
I.21	Ac	Ac	Bz



	R ₁	R ₂	R ₃	R ₄	R ₅	R ₆
I.22	H	Pr	Ac	iBu	Bz	Nic
I.23	H	Pr	Ac	iBu	Nic	Nic
I.24	H	Pr	Ac	iBu	iBu	Nic
I.25	H	iBu	Ac	iBu	Bz	Nic
I.26	H	iBu	Ac	iBu	Nic	Nic
I.27	H	iBu	Ac	Ac	Nic	Ac
I.28	H	Ac	Ac	iBu	Ac	Nic
I.29	OAc	iBu	Ac	iBu	Ac	Nic
I.30	OAc	iBu	Nic	iBu	Ac	Nic

MDR-reversal activity:

- **I.22** and **I.25** demonstrated a **powerful inhibition** of P-gp at 10 μM, on DLD1-TxR colorectal MDR cells and on NCI-H460/R cell lung carcinoma (Jadranin *et al.*, 2013).

E. cyparissias (EtOAc extract of the whole plant)

MDR-reversal activity:

- **weak P-gp inhibition** on MCF-7 ADR cells (Lanzotti *et al.*, 2015)

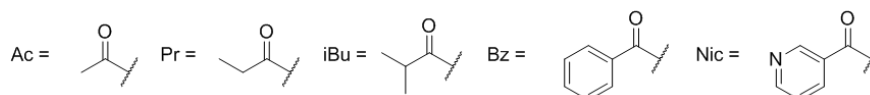
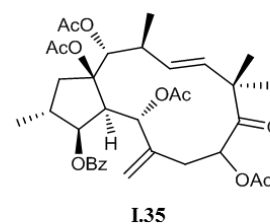
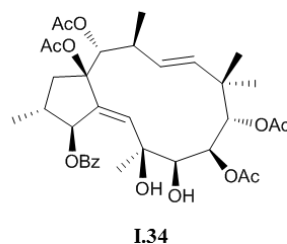
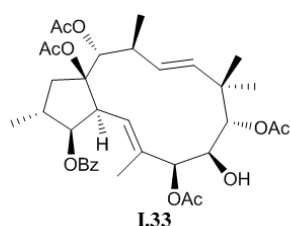


Figure 1.20. MDR reversal activity of jatrophanes isolated from *Euphorbia* species.

E. squamosa (acetone extract of the aerial parts)



MDR reversal activity:

- Inhibition of *Candida albicans* MDR transporters (*CaCdr1p* and *CaMdr1p*).

I.33 and **I.35** inhibited 40-60% the *CaCdr1p* efflux

I.35 inhibited 40% the *CaMdr1p* efflux – **dual inhibitor**

- Cytotoxicity against yeast strains

AD1-8u^r (control), AD-CDR1 (*CaCdr1p*), AD-MDR1 (*CaMdr1p*)

I.33 low IC₅₀ (2.3-3.7 μM) to all yeast strains

I.35 low IC₅₀ (2.3 μM) only on the control strain

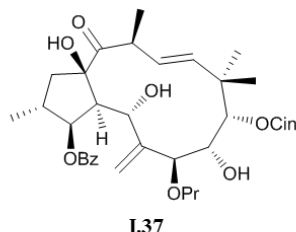
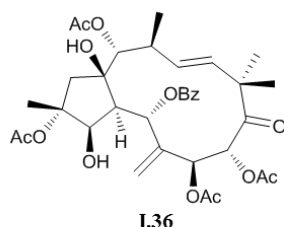
-Combination assay

I.33 and **I.35** showed **synergistic interaction**

with fluconazole on AD-CDR1 (*CaCdr1p*) strain

(Rawal *et al.*, 2014)

E. exigua (MeOH extract of the whole plant)



MDR reversal activity:

- **I.37** showed a **strong inhibition** of P-gp at 8 μg/ml (Rédei *et al.*, 2015)

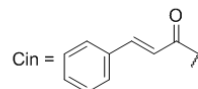


Figure 1.21. MDR reversal activity of jatrophanes isolated from *Euphorbia* species.

Lathyranes bear a 5:11:3-membered ring system presenting similar structural variability as the jatrophanes. But contrary to these, lathyranes present recent structure-activity studies related with P-gp modulation (Vieira *et al.*, 2014; Jiao *et al.*, 2015; Matos *et al.*, 2015).

For instance, the SAR study of 6,17-epoxylathyrane diterpenes **I.38-I.49** (Figure 1.22) showed that P-gp modulation was not associated with the number of aromatic rings, since molecules with two or three aromatic rings (**I.44-I.49**) were not the most active. The optimal combination for P-gp modulation was obtained for compound **I.42**, with an aryl substituent at C-3 and two acetates at C-5 and C-15.

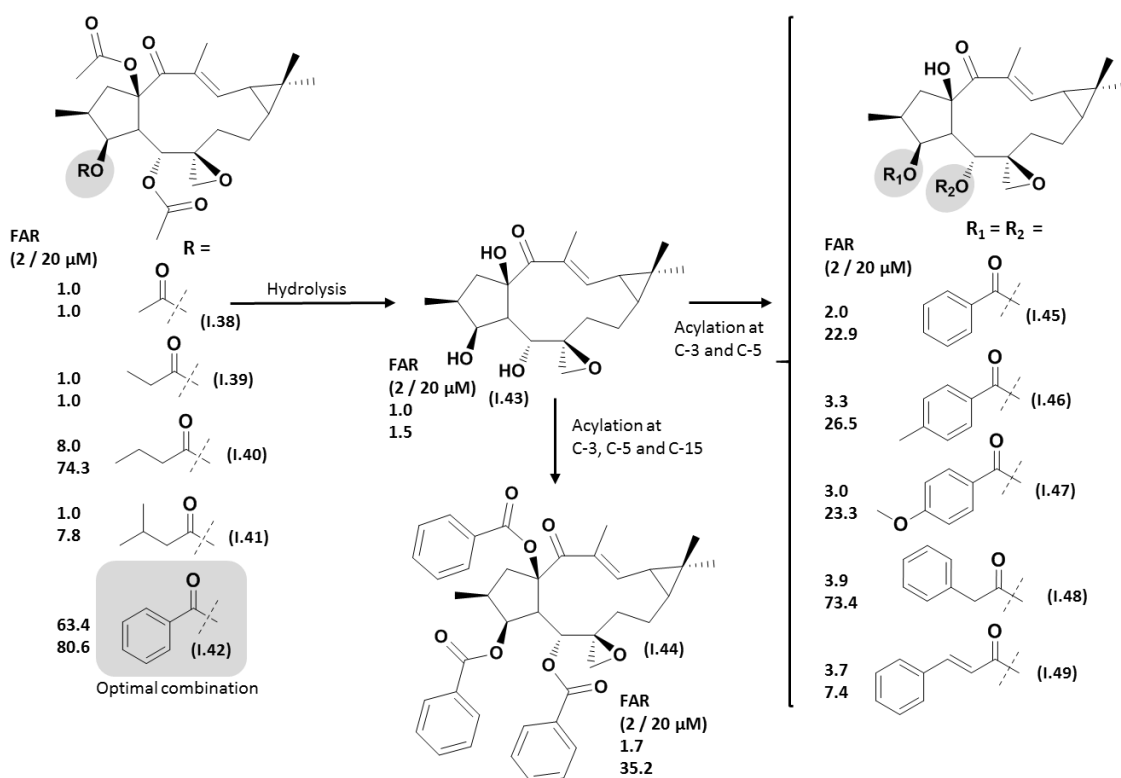


Figure 1.22. Structure–activity relationships of 5,17-epoxy lathyranes **I.38-I.49** on P-gp modulation. FAR values presented at 2 and 20 μM . Compounds **I.38-I.42** were isolated from *E. boetica*. Epoxilathyrol (**I.43**) was obtained through hydrolysis of **I.38** and derivatives **I.44-I.49** through acylation of **I.43** (data from Vieira *et al.*, 2014).

Studies on lathyrol (**I.50**) derivatives, which were obtained by modifying the hydroxyl moiety of C-3 and C-5, showed that the presence of benzoyl groups at these positions produced the most active modulator of the study (**I.51**, Figure 1.23) (Jiao *et al.*, 2015).

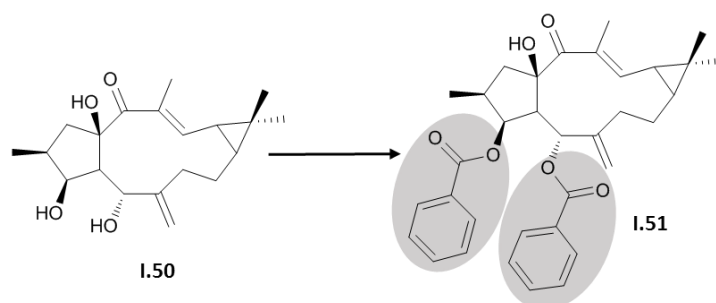


Figure 1.23. The most active lathyrol derivative of Jiao *et al.* (2015) study.

Using epoxyboetirane A (**I.52**, Figure 1.24) as starting material, several derivatives were obtained. The SAR study showed the 3,17-disubstituted aromatic ester (**I.53**), derived from a Payne-rearranged Michael adduct, considerable modulated P-gp efflux at 200 nM (Matos *et al.*, 2015).

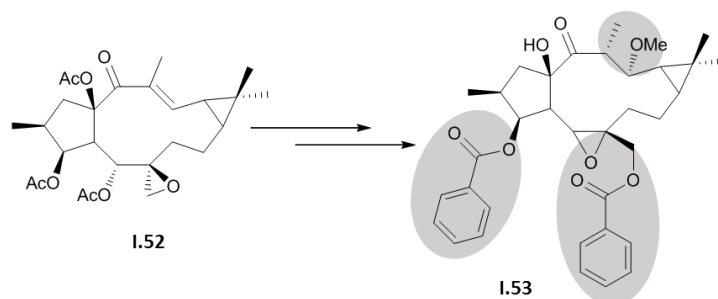


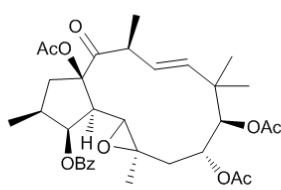
Figure 1.24. The most active P-gp modulator of Matos *et al.* (2015) study.

1.4.2.2. Cytotoxic and anti-viral activity

Compounds with the jatropane and lathyrene skeletons are usually considered to lack cytotoxic activity, however some exceptions have been found (Vasas and Hohmann, 2014). Accordingly, the jatrophanes **I.54-I.58**, reported between 2013 and 2015, were tested for their potential cytotoxicity. None of the compounds showed activity against the tested cancer cells (Figure 1.25). From the reported *ent*-abietane lactones and lathyrenes, only compounds **I.77** (Figure 1.26), **I.59**, **I.64**, **I.70** and **I.71** (Figure 1.27) showed significant cytotoxic activities against cancer cell lines.

In regard to the anti-viral activity, the phytochemical studies on *E. amygdaloides* spp. *semiperfoliata* and on *E. nerifolia* afforded the isolation of promising compounds (Figure 1.28). Compounds **I.81**, **I.88** and **I.89** exhibited a strong and selective anti-HIV activity. Additionally, jatrophanes **I.81** and **I.83** also showed strong activities against the Chikungunya virus. This is an emerging arthropod-borne virus, associated with severe morbidity in tropical areas.

E. connate (CH₂Cl₂:acetone extract of the aerial parts)

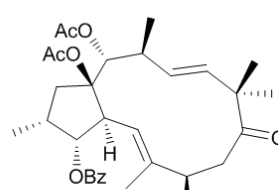


I.54

Breast cancer cells:

- **weak cytotoxicity** against MDA-MB (IC₅₀ > 30 μM)
- **moderate cytotoxicity** against MCF-7 cell line (IC₅₀ = 24.33 ± 3.21 μM) (Shadi *et al.*, 2015).

E. lunulata (EtOH extract of the aerial parts)

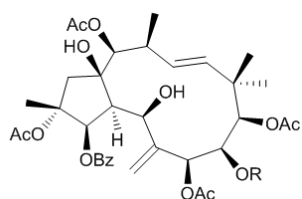


I.55

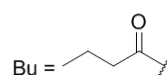
Human NCI-H460 and MCF-7 HeLa cancer cells:

- **weak cytotoxicity** against the two cell lines (IC₅₀ > 30 μM) (Liu *et al.*, 2014).

E. osyridea (CH₂Cl₂:acetone extract of the aerial flowering parts)



R
I.56 Bu
I.57 Pr
I.58 Ac

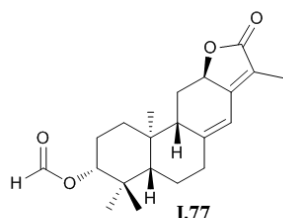


Human ovarian cancer cells (OVCAR-3 and Caov-4):

- **weak –none** cytotoxic activity cells. IC₅₀ ranging from 40 to 86 μM (Ghanadian *et al.*, 2015).

Figure 1.25. Cytotoxic activity of jatrophanes isolated from *Euphorbia* species.

E. lunulata (EtOH extract of the aerial parts)

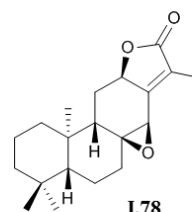


I.77

Human NCI-H460 and MCF-7 HeLa cancer cells:

- **marked activity** against the two cell lines with the IC₅₀ values 19.5 μM (NCI-H460) and 18.6 μM (MCF-7).
- Cis-platinum (positive control) 29.7 μM (NCI-H460) and 27.7 μM (MCF-7) (Liu *et al.*, 2014)

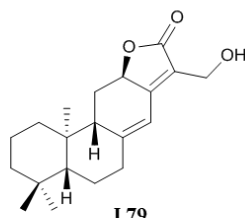
E. pilosa (EtOH extract of the whole plant)



I.78

- **no activity** against five human cancer cell lines (HL-60, SMMC-7721, A-549, MCF-7 and SW-480) (Zhang *et al.*, 2014)

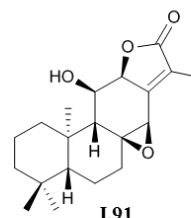
E. stracheyi (EtOH extract of the whole plant)



I.79

- **weak** cytotoxicity activity of A549 cell line (IC₅₀ = 29.44 μM) (Yang *et al.*, 2014).

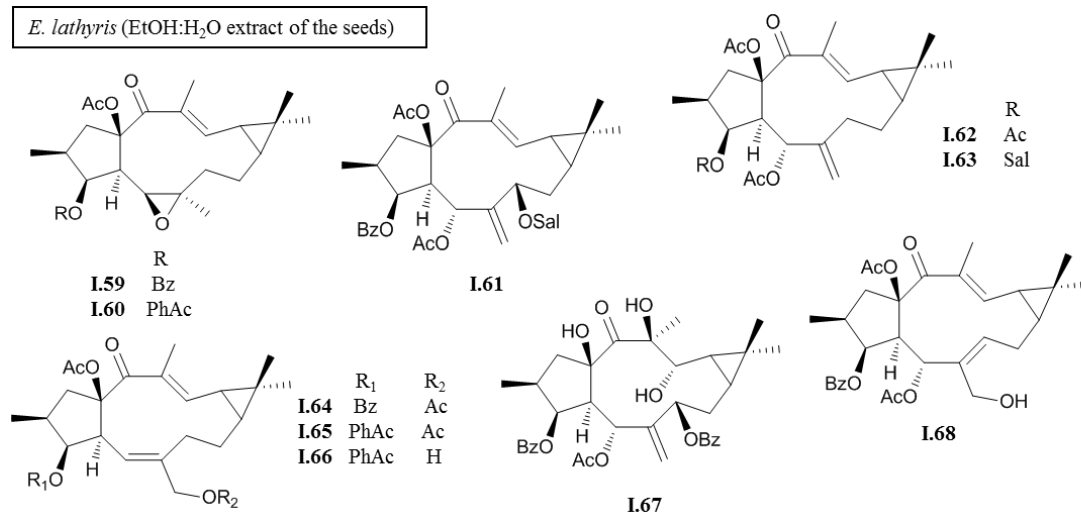
E. fischeriana (EtOH extract of the roots)



I.91

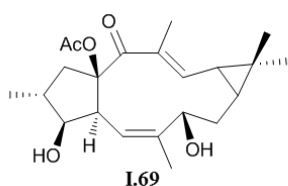
- **no activity** against four human cancer cell lines (A549, BEL7402, HTC116 and MDA-MB-231, IC₅₀ > 50 μM) (Wang *et al.*, 2013).

Figure 1.26. Cytotoxic activity of *ent*-abietane lactones isolated from *Euphorbia* species.

E. lathyris (EtOH:H₂O extract of the seeds)

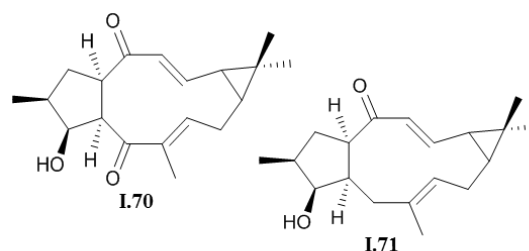
- compounds **I.59** and **I.65** showed **cytotoxicity** against MCF-7 (IC₅₀ = 12.4–13.1 μM) and compound **I.63** against the C6 cell line (IC₅₀ = 15.3 μM)

- **all inactive** against the HeLa and HepG2 cell lines (IC₅₀ > 50 μM) (Lu *et al.*, 2014).

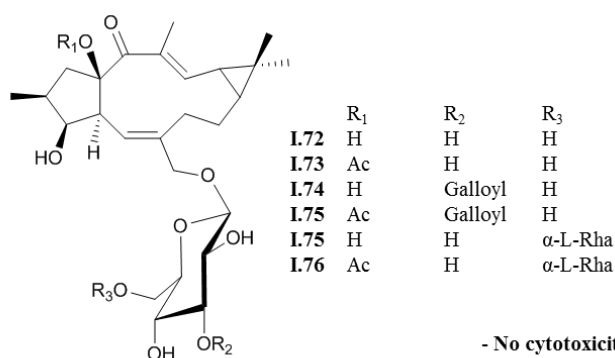
E. altotibetica (EtOH:H₂O extract of the whole plant)

- **inactive** against gastric SGC-7901 and hepatocarcinoma SMCC-7721 cell lines

- **weak activity** against K562 cells (IC₅₀ = 34.32 μg/mL) (Zhang *et al.*, 2014)

E. kansuensis (EtOH:H₂O extract of the roots)

- **cytotoxic activity** against HeLa and Hep-G2 cells (IC₅₀ values in the range of 3.6–9.7 μg/ml) (Zhang *et al.*, 2013)

E. dracunculoides (acetone:H₂O extract of the aerial parts)

- **No cytotoxicity** against HL-60, SMMC-7721, A-549, MCF-7, and SW480 human cancer cell lines (Wang *et al.*, 2015)

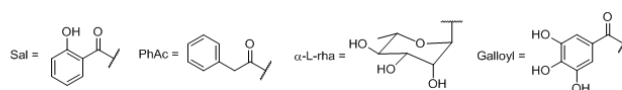
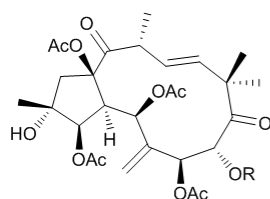
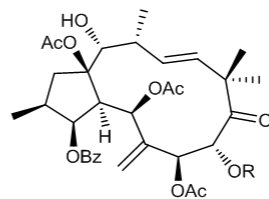


Figure 1.27. Cytotoxic activity of lathyranes isolated from *Euphorbia* species.

E. amygdaloides ssp. *semiperfoliata* (EtOAc extract of the whole plant)



R
I.80 Ac
I.81 Tig
I.82 iBu
I.83 Bz

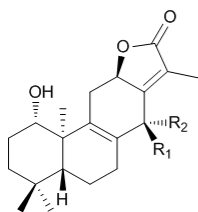


R
I.84 iBu
I.85 MeBu

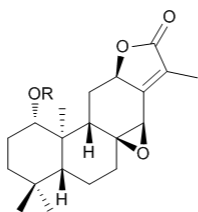
- compound **I.81** and **I.83** were the most **potent and selective inhibitors** of Chikungunya virus (CHIKV) replication ($EC_{50} = 0.76 \pm 0.14 \mu\text{M}$, $SI = 208$, and $EC_{50} = 4.3 \pm 0.2 \mu\text{M}$, $SI = 29$, respectively)

- compound **I.81** showed a **strong and selective** antiviral effect on HIV-1 and HIV-2 virus replication ($IC_{50} = 0.34 \pm 0.05 \mu\text{M}$, $SI > 96$ and $IC_{50} = 0.043 \pm 0.005 \mu\text{M}$, $SI > 751$, respectively) (Nothias-Scaglia *et al.*, 2014).

E. nerifolia (EtOH extract of the twigs and leaves)



R₁ R₂
I.86 H OH
I.87 OH H
I.88 OAc H



R
I.89 H
I.90 Ac

- eurifoloids E (**I.88**) and F (**I.89**) exhibited **significant anti-HIV activities**, with $EC_{50} = 3.58 \pm 0.31 \mu\text{M}$ ($SI = 8.6$) and $EC_{50} = 7.40 \pm 0.94 \mu\text{M}$ ($SI = 10.3$), respectively (Zhao *et al.*, 2014).

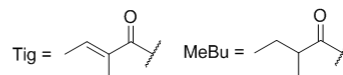


Figure 1.28. Anti-viral activity of jatrophanes and *ent*-abietane lactones isolated from *Euphorbia* species.

Chapter 2

Objectives

2.1 Objectives

Circumventing MDR in cancer is a cornerstone to chemotherapy success. Among several approaches proposed, modulation of P-glycoprotein is the most highlighted to overcome MDR. Another valuable approach is the collateral sensitivity effect, where some compounds may selectively exert a more pronounced cytotoxicity on cells with MDR phenotype than on the parental ones.

Euphorbia diterpenes have been recognized of substantial importance in natural products drug discovery programs, due to conjugation of potential biological activities with chemical structural diversity. Our group, has been conducting research in *Euphorbia* spp. from the Portuguese flora with the purpose of finding new anticancer agents (Ferreira *et al.*, 2014a).

Therefore, the main goal of this work was to find out effective MDR reversal compounds, as P-gp modulators and/or collateral sensitivity agents, from *Euphorbia* species.

The main goal was accomplished with:

- (i) **Phytochemical studies**; directed for isolation of macrocyclic lathyrane and jatrophane diterpenes and *ent*-abietane diterpenic lactones, from *Euphorbia piscatoria* and *E. welwitschii*.
- (ii) **Molecular derivatization of isolated compounds**; optimization of macrocyclic diterpenes, as lead compounds for the development of selective P-gp modulators.
- (iii) **Selective targeting of MDR cancer cells**; search for diterpenes with selective antiproliferative activity, targeting MDR in human cancer cells, followed by investigation of the mechanism of action, for the most active compounds.

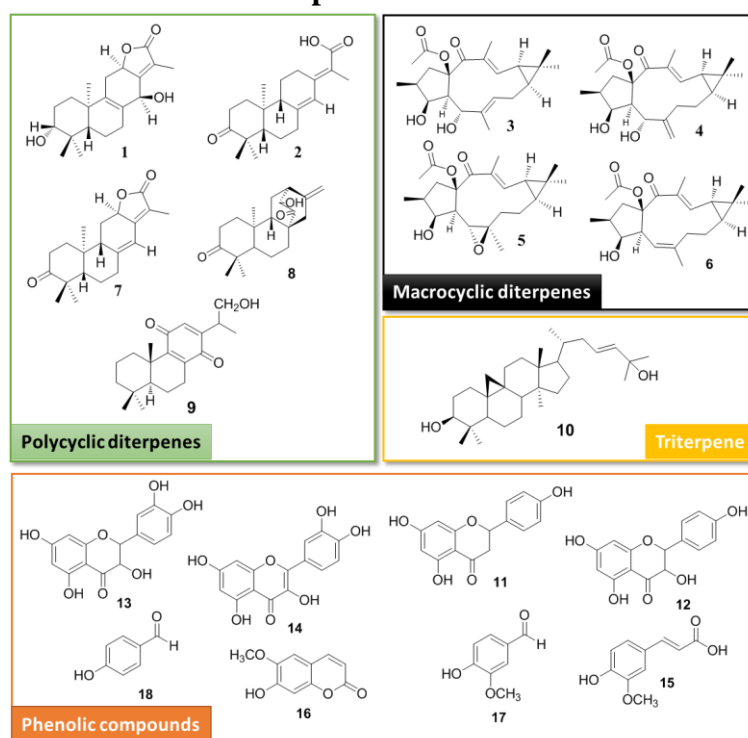
Chapter 3

Phytochemical investigations of *Euphorbia piscatoria* Results and Discussion

Four new diterpenes were isolated from the methanolic extract of *Euphorbia piscatoria*, two *ent*-abietanes (**1**, **2**) and two lathyrane-type macrocyclic diterpenes (**3**, **4**). Compound **2**, with an unusual structure, might be considered intermediate in the biogenesis of *ent*-abietane α,β -unsaturated lactones, commonly found in *Euphorbia* species. Therefore, a possible biogenetic pathway is proposed. Other known macrocyclic and polycyclic diterpenes were also isolated: 15-acetoxy-5,6-epoxylathyr-12-en-3-ol-14-one (**5**), jolkinol D (**6**), helioscopinolide E (**7**), *ent*-13[*R*]-hydroxy-3,14-dioxo-16-atisene (**8**) and portlanquinol (**9**). In addition, cycloart-23-ene-3 β ,25-diol (**10**) and several phenolic compounds, such as, naringenin (**11**), aromadendrin (**12**), taxifolin (**13**), quercetin (**14**), ferulic acid (**15**), scopoletin (**16**), vanillin (**17**) and *p*-hydroxybenzaldehyde (**18**) were also obtained from this plant. Their structures were characterized by spectroscopic methods mainly 1D and 2D NMR (^1H , ^{13}C , DEPT, COSY, HMBC, HMQC, and NOESY) experiments and comparison with literature data.

The MDR reversal potential of macrocyclic diterpenes **3-5** was evaluated through a drug combination assay, using the L5178Y mouse T lymphoma cell line transfected with the human *MDR1* gene. Compounds **3-5** were able to enhance, synergistically, the antiproliferative activity of doxorubicin (combination indexes < 0.5).

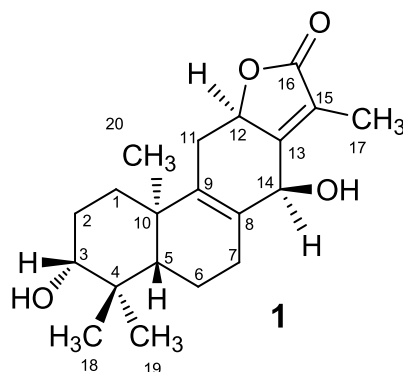
Graphical abstract



3.1. Structure elucidation of isolated compounds

3.1.1. Diterpenes with polycyclic scaffold

3.1.1.1. Piscatolide - 3 α ,14 β -dihydroxy-ent-abieta-8,13(15)-dien-16,12-olide (**1**)



Compound **1**, named piscatolide, was isolated as a white powder. The IR absorptions at 1734 and 3385 cm^{-1} suggested the presence of an α,β -unsaturated γ -lactone and a hydroxyl group (Borghi *et al.*, 1991; Che *et al.*, 1999; Yuan *et al.*, 2004). The molecular formula was deduced as $\text{C}_{20}\text{H}_{28}\text{O}_4$, from its ESI-TOF-HRMS spectrum, indicating the presence of seven degrees of unsaturation. The ^1H NMR spectrum of compound **1** displayed three singlets corresponding to tertiary methyls (δ_{H} 1.00, 1.19, 1.22), one vinylic methyl group at δ_{H} 2.19 and three signals of protons at carbons bearing oxygen atoms (δ_{H} 5.15, 4.92 and 3.34). The ^{13}C NMR and DEPT spectra of piscatolide (**1**) were consistent with an abietane skeleton (Uemura *et al.*, 1976; Ohba *et al.*, 1983; Borghi *et al.*, 1991; Che *et al.*, 1999; Yuan *et al.*, 2004), showing twenty carbon resonances corresponding to four methyls, five methylenes, four methines (three corresponding to oxymethines at δ_{C} 70.1, 78.7 and 79.1) and seven quaternary carbons (four olefinic at δ_{C} 121.6, 130.4, 137.8, 162.7 and a carbonyl at δ_{C} 176.9). Detailed structure information was obtained from two-dimensional NMR data (^1H - ^1H COSY, HMQC and HMBC), which allowed the clear assignment of all the carbons (Table 3.1) and the location of the functional groups.

The ^1H - ^1H COSY experiments revealed three key fragments (Figure 3.1), which were connected by heteronuclear $^2J_{\text{C-H}}$ and $^3J_{\text{C-H}}$ HMBC correlations. The HMBC correlations between the vinylic methyl (C-17) and the carbonyl signal at δ_{C} 175.2 (C-16) and the quaternary olefinic carbons at δ_{C} 121.6 (C-15) and 162.7 (C-13) corroborated the presence of the α,β -unsaturated γ -lactone moiety. The location of the hydroxyl group at C-14 (δ_{C} 70.1; δ_{H} 5.15 s) was assigned by comparison of the NMR data of **1** with those reported for phlogacantholide B (δ_{C} 69.9, C-14; δ_{H} 5.16 s, H-14) (Yuan *et al.*, 2004) that differs from piscatolide (**1**) at ring A, having a primary hydroxyl group at C-19, whereas compound **1** is oxidized at C-3.

Table 3.1. ^1H and ^{13}C NMR data (δ) for piscatolide (**1**), 400 and 101 MHz, respectively.

position		Piscatolide (1) ^a	
		δ_{H} (J in Hz)	δ_{C}
1	a	1.92 dt (12.6, 2.9)	34.6
	b	1.38 m	
2	a	1.85 m ^b	27.4
	b	1.85 m ^b	
3		3.34 m	78.7
4		-	38.6
5		1.34 m	51.4
6	a	2.00 m	18.6
	b	1.71 m	
7	a	2.65 m	29.2
	b	2.25 m	
8		-	130.4
9		-	137.8
10		-	39.2
11	a	3.05 dd (15.3, 6.6)	32.9
	b	2.07 m	
12		4.92 t (8.2)	79.1
13		-	162.7
14		5.15 s	70.1
15		-	121.6
16		-	176.9
17		2.19 s	9.0
18		1.00 s	16.0
19		1.19 s	28.3
20		1.22 s	19.1

^aspectra recorded in a mixture $\text{CDCl}_3/\text{CD}_3\text{OD}$ (1:1); ^bsignal partially overlapped

The relative stereochemistry of compound **1** was determined by a NOESY experiment (Figure 3.1) taking into account the coupling constant values that were compared to those reported in the literature for similar compounds (Yuan *et al.*, 2004). The *trans* ring junction between rings A and B in **1** was based on biogenic considerations (Dewick, 2009a). In the NOESY experiment, the cross peaks observed between H-3/H-18 and H-3/H-5 indicated that these protons lie on the same side of the molecule. The NOE interactions H-20/H-11a, H-11a/H-14, H-11a/H-7a and H-7a/H-14 were also observed, indicating the same orientation for these protons. The configuration at C-12 was assigned based on the coupling constant value of H-12 (δ_{H} 4.92 t; $J = 8.2$ Hz) that was similar to that described for phlogacantholide B (δ_{H} 4.86 t, $J = 8.4$ Hz), whose stereochemistry was confirmed by X-ray crystallography (Yuan *et al.*, 2004). In the same way, the relative configuration at C-14 (β -OH; δ_{C} 70.1; δ_{H} 5.15 s) was further confirmed by comparison of C-14 and H-14 chemical shifts with those reported for phlogacantholide B (β -OH at C-14; δ_{C} 69.9; δ_{H} 5.16 s) and with its epimer phlogacantholide C (α -OH at C-14; δ_{C} 64.9; δ_{H} 4.98 s) (Yuan *et al.*, 2004).

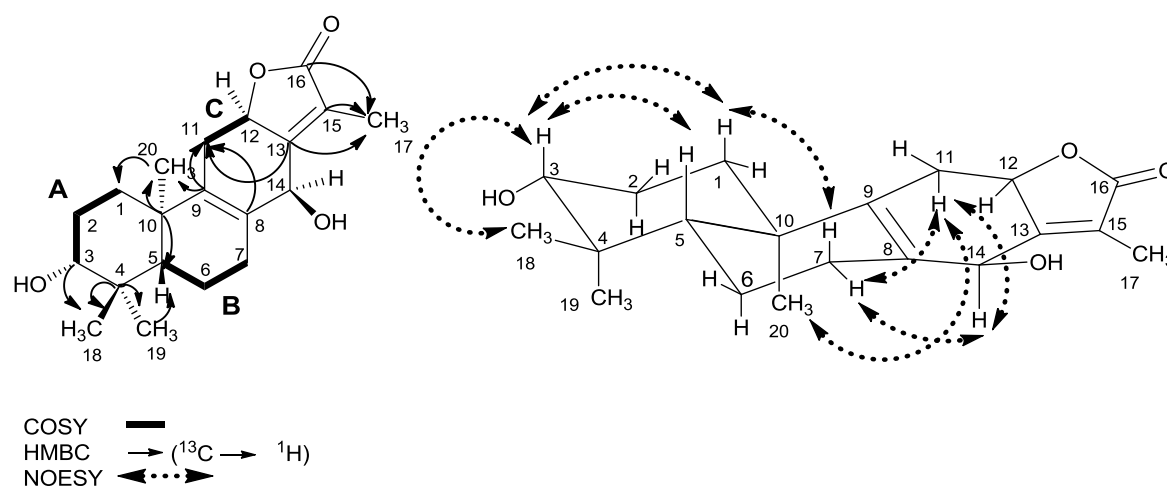
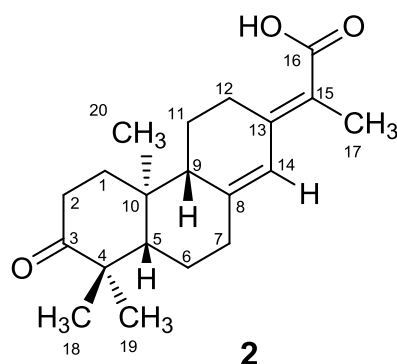


Figure 3.1. Key COSY and HMBC correlations and NOESY interactions observed for piscatolide (**1**).

3.1.1.2. Piscatoric acid - 3-oxo-ent-abieta-8(14),13(15)-dien-16-oic acid (2)

Compound **2**, named piscatoric acid, was obtained as a white powder. The molecular formula was deduced as $C_{20}H_{28}O_3$, from its ESI-TOF-HRMS spectrum, indicating the presence of seven degrees of unsaturation. The IR spectrum suggested the presence of a α,β -unsaturated carboxyl group ($3288\text{--}2500\text{ cm}^{-1}$, OH; 1665 cm^{-1} , C=O) and a ketone function (1705 cm^{-1}). These findings were corroborated by the ^{13}C NMR signals at δ_{C} 175.0 (α,β -unsaturated carboxylic acid) and δ_{C} 216.6 (ketone). The ^{13}C NMR and DEPT spectra showed twenty carbon resonances corresponding to four methyl groups, six methylenes, three methines (one vinylic carbon δ_{C} 123.4) and seven quaternary carbons (three vinylic carbons at δ_{C} 118.4, 147.4 148.6, and two carbonyls at δ_{C} 175.0 and 216.6). Moreover, the ^1H NMR spectrum of **2** displayed signals for four methyls: three singlets corresponding to tertiary methyls (δ_{H} 0.96, 1.08, 1.11) and one vinylic methyl group at δ_{H} 1.97. A broad singlet at δ_{H} 6.31, corresponding to an olefinic proton, was also recorded. Further structural details were obtained by two-dimensional NMR experiments (COSY, HMQC and HMBC), allowing unambiguous assignment of all carbon signals (Table 3.2).

As shown in Figure 3.2, the ^1H - ^1H COSY experiments allowed the establishment of three spin systems, which were linked together through $^2J_{\text{C-H}}$ and $^3J_{\text{C-H}}$ HMBC correlations. The HMBC correlation between the vinylic methyl group (H-17) and the carbonyl signal at δ_{C} 175.0 confirmed the unusual α,β -unsaturated carboxylic function at C-16. Comparing the ^1H and ^{13}C NMR data of **2** with those of compound **1** and helioscopinolide E (**7**) (Borghi *et al.*, 1991), shows that these compounds have the same general structure concerning rings A-C.

However, the α,β -unsaturated γ -lactone ring of **1** and **7** is absent in compound **2**. In fact, in both piscatolide (**1**) and in helioscopinolide E (**7**), C-12 corresponds to an

oxymethine (δ_C 79.1, δ_H 4.92 and δ_C 75.6 and δ_H 4.89, respectively), whereas in compound **2** corresponds to a methylene group [δ_C 27.5; δ_H 3.39 (dt, $J = 15.3, 4.0$ Hz, H-12a); δ_H 2.13, m, H-12b]. The relative stereochemistry of compound **2** was deduced from the analysis of NOE correlations and was found to be the same as helioscopinolide E (Borghi *et al.*, 1991). NOE correlations between H-20 and H-1a, H-2a, H-6a and H-11b, and between H-2a/H-6a, H-2a/H-19 indicated that H-20 and H-19 lie on the same side of the molecule. Nuclear Overhauser cross peaks were also observed between H-2b and H-5, H-9 and H-18 corroborating the assigned relative stereochemistry (Ohba *et al.*, 1983; Borghi *et al.*, 1991).

Table 3.2. ^1H and ^{13}C NMR data (δ) for compounds **2** and **7** (400 and 101 MHz, respectively).

position	Piscatoric acid (2) ^a		Helioscopinolide E (7) ^a	
	δ_H (J in Hz)	δ_C	δ_H (J in Hz)	δ_C
1	a	2.00 m ^b	2.19 m ^b	37.7
	b	1.52 m	1.57m ^b	
2	a	2.66 td (15.0, 5.7)	2.64 m	34.4
	b	2.31 m	2.46 ddd (15.7, 5.7, 3.6)	
3	-	216.6	-	215.5
4	-	48.0	-	47.5
5	-	55.0	1.64 m ^b	54.8
6	a	1.64 m	1.80 m	24.6
	b	1.55 m ^b	1.57 m ^b	
7	a	2.53 m	2.55m ^b	36.6
	b	2.26 m	2.19 m ^b	
8	-	148.6	-	150.2
9	-	50.8	2.26 d (8.6)	50.7
10	-	38.3	-	40.9
11	a	1.81 m	2.55 m ^b	27.8
	b	1.42 m	1.57 m ^b	
12	a	3.39 dt (15.3, 4.0)	4.88 dd (13.2, 5.5)	75.6
	b	2.13 m		
13	-	147.4	-	155.6
14	-	123.4	6.33 bs	114.7
15	-	118.4	-	117.1
16	-	175.0	-	175.0
17	-	14.8	1.84 d (1.3)	8.3
18	-	25.8	1.13 s	26.5
19	-	22.5	1.06 s	21.8
20	-	14.9	1.10 s	16.2

^aspectra recorded in CDCl_3 ; ^bsignal partially overlapped

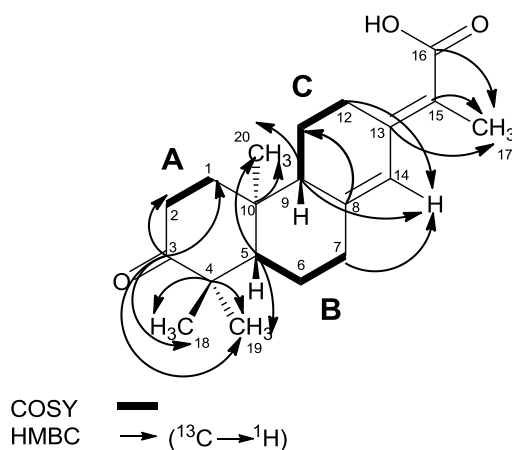
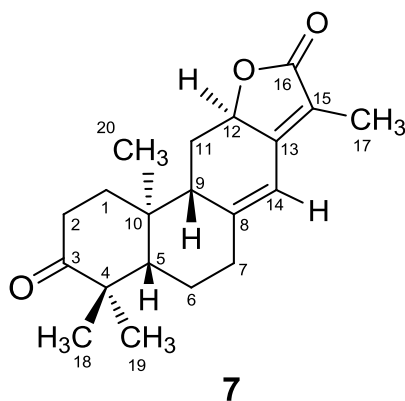


Figure 3.2. Key COSY and HMBC correlations for piscatoric acid (**2**). Spin systems (A-B-C), their connection through the main heteronuclear $^2J_{\text{C-H}}$ and $^3J_{\text{C-H}}$ correlations.

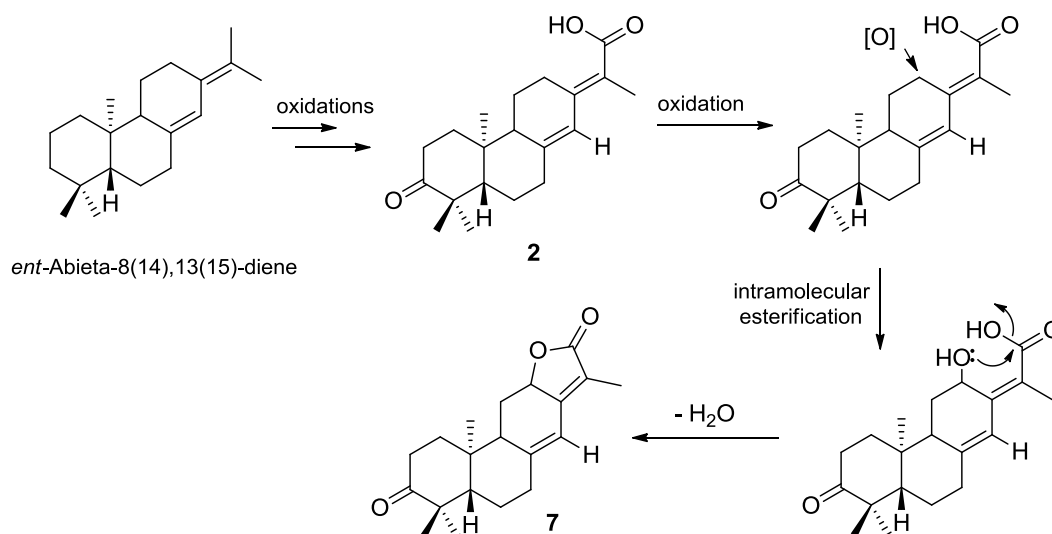
3.1.1.3. Helioscopinolide E (**7**)



Compound **7** was obtained as white crystals of m.p. 180 – 183 °C and $[\alpha]_D^{25} + 283.2$. The IR spectrum suggested the presence of an α,β -unsaturated γ -lactone and a ketone carbonyl group (bands at 1745 and 1699 cm^{-1} , respectively). The ESIMS spectrum presented a pseudomolecular ion at m/z 337 $[\text{M} + \text{Na}]^+$, corresponding to the molecular formula $\text{C}_{20}\text{H}_{26}\text{O}_3$, from which eight degrees of unsaturation were deduced. These findings were corroborated by the ^1H and ^{13}C NMR data (Table 3.2), which led to the identification of compound **7** as the *ent*-abietane lactone helioscopinolide E (Borghi *et al.*, 1991).

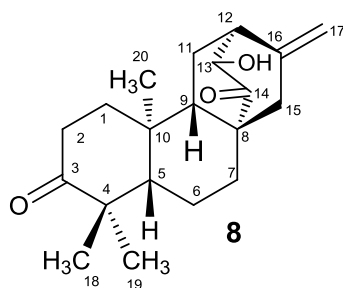
3.1.1.4. Proposed biogenetic pathway for *ent*-abietane α,β -unsaturated γ -lactones

Piscatoric acid (**2**), with an unprecedented structure, might be an intermediate on the biogenesis of *ent*-abietane α,β -unsaturated γ -lactones, such as helioscopinolide E (**7**), found in *Euphorbia* species, and therefore a possible biogenetic pathway is proposed (Scheme 3.1). In this way, the precursor *ent*-abieta-8(14),13(15)-diene could be sequentially oxidized giving piscatoric acid (**2**), which would be further oxidized at C-12. Nucleophilic attack of the OH-12 on the carbonyl group of the carboxylic acid would lead to intramolecular esterification, forming the favorable five-membered lactone ring.



Scheme 3.1. Piscatoric acid (**2**) as an intermediate on the biogenesis of *ent*-abietane α,β -unsaturated γ -lactones, such as helioscopinolide E (**7**).

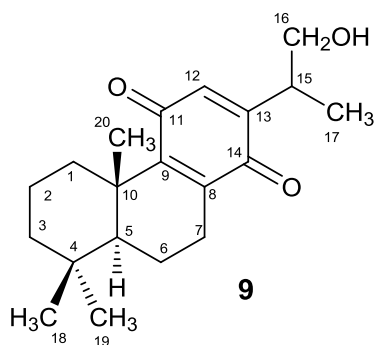
3.1.1.5. *ent*-13[*R*]-hydroxy-3,14-dioxo-16-atisene (**8**)



Compound **8**, with m.p. 174-177 °C and $[\alpha]_D^{26} + 38$, was identified as *ent*-13[*R*]-hydroxy-3,14-dioxo-16-atisene, through the comparison of the obtained physical and spectroscopic data with those reported on the literature for this compound (Lal *et al.*,

1989, 1990). This compound was first isolated from the ether extract of *Euphorbia fidjiana*. The IR spectrum showed the presence of a hydroxyl (3460 cm^{-1}) and two carbonyl groups (1720 and 1690 cm^{-1}). The molecular ion at m/z 317 $[M + H]^+$, recorded on ESIMS, was consistent with the molecular formula $C_{20}H_{28}O_3$. These features were corroborated by the 1H and ^{13}C NMR spectra (Table 3.3), where an oxymethine group (δ_C 75.3, δ_H 3.88) and two high-field carbonyl signals at δ 218.1 and 216.2 were recorded. Moreover, the 1H NMR spectrum displayed two olefinic protons as broad singlets at δ 5.02 and 4.86, indicating the presence of an exocyclic terminal double bond and three tertiary methyl groups (singlets at δ 1.08, 1.00 and 0.84).

3.1.1.6. Portlanquinol - 16-hydroxy-abieta-8,12-diene-11,14-dione (9)



Compound **9**, $[\alpha]_D^{26} + 30$, was isolated as a yellow oil. Analysis of its spectroscopic data indicated that compound **9** was a known quinoid-type abietane diterpene, named portlanquinol, which was isolated for the first time from the acetone extract of *Euphorbia portlandica* (Madureira *et al.*, 2004). The 1H and ^{13}C NMR data (Table 3.3) clearly indicated the presence of the diagnostic signals: the 2-hydroxyisopropyl group (oxymethylene at δ_C 66.8, δ_H 3.63 d; secondary methyl at δ_C 15.5, δ_H 1.12 d and a methine group at δ_C 34.6, δ_H 3.08 m); the three tertiary methyl groups (δ_H 1.27 s, 0.92 s and 0.89 s) and the benzoquinone ring. The latter was evidenced by the downfield signals of the conjugated carbonyls at δ_C 188.7 and 187.8, the olefinic carbons at δ_C 151.4, 148.7, 142.9 and 134.2 and the singlet at δ_H 6.39 assigned to the olefinic proton. The ESIMS corroborated the attribution of this structure, showing a molecular ion at m/z 338 $[M + Na]^+$ consistent with the molecular formula $C_{20}H_{28}O_3$ (seven degrees of unsaturation).

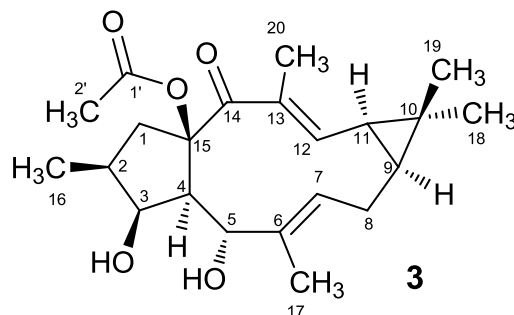
Table 3.3. ¹H and ¹³C NMR data (δ) for compounds **8** and **9** (400 and 101 MHz, respectively).

Position	<i>ent</i> -13[<i>R</i>]-hydroxy-3,14-dioxo-16-atisene (8) ^a		Portlanquinol (9) ^a		
		δ_{H} (J in Hz)	δ_{C}	δ_{H} (J in Hz)	δ_{C}
1	a	1.86 ddd (13.3, 6.4, 3.2)	36.8	1.12 m*	36.5
	b	1.39 td (13.3, 5.6)		2.71 m	
2	a	2.55 ddd (15.8, 13.2, 6.4)	34.2	1.52 m	19.1
	b			2.36 m	
3	a	-	216.2	1.19 m	41.5
	b			-	
4		-	47.6	-	33.7
5		1.31 m	55.3	1.10 m*	51.7
6	a	1.51 m	20.1	1.86 m	17.5
	b	1.50 m		1.42 m	
7	a	2.41 dt (13.5, 3.2)	30.5	2.29 m	26.2
	b	0.94 m		2.65 d (5.5)	
8		-	47.4	-	142.9
9		1.65 dd (11.5, 6.1)	51.2	-	151.4
10		-	37.7	-	38.7
11	a	1.75 ddd (14.0, 6.1, 2.7)	25.5	-	188.7
	b			2.00 m	
12		2.81 dd (5.9, 2.7)	44.9	6.39 s	134.2
13		3.88 d (2.7)	75.3	-	148.7
14			218.1	-	187.8
15		2.32 bs	43.9	3.08 sext (6.4)	34.6
16			142.3	3.63 d (5.7)	66.8
17	a	5.02 s	111.3	1.12 d (6.9)*	15.5
	b	4.86 s			
18		1.08 s	26.3	0.92 s	33.6
19		1.00 s	22.0	0.89 s	21.9
20		0.84 s	13.8	1.27 s	20.3

^aspectra recorded in CDCl₃; *signal partially overlapped

3.1.2. Diterpenes with lathyrane-type scaffold

3.1.2.1. Piscatoriol A - 15 β -acetoxy-lathyra-6,12-diene-3 β ,5 α -diol-14-one (**3**)



Compound **3**, named piscatoriol A, was obtained as a white powder. The molecular formula was deduced as $C_{22}H_{32}O_5$, from its ESI-TOF-HRMS spectrum, indicating seven degrees of unsaturation. IR absorption bands at 3311, 1747 and 1625 cm^{-1} suggested the presence of hydroxyl, ester carbonyl and an enone system. These structural features were corroborated by the NMR data of compound **3** (Table 3.4), which revealed the presence of two oxymethines (δ_C 79.8, δ_H 4.34 t; δ_C 65.8, δ_H 5.37 d) and one acetyl group (δ_C 170.1; δ_C 22.2; δ_H 2.09 s). Moreover, the presence of an α,β -unsaturated ketone was indicated by the relatively high-field carbonyl signal at δ_C 197.9 and a downfield vinylic proton resonance at δ 6.44 (H-12, dd, $J = 11.4, 1.0$ Hz), providing evidence of mesomeric effects. Besides these signals, the remaining ^{13}C NMR and DEPT data showed another seventeen resonances corresponding to five methyls, two methylenes, six methines (two vinylic at δ_C 142.7 and 126.8) and four quaternary carbons (two olefinic carbons at δ_C 135.5 and 133.5 and one oxygenated carbon at 92.7). Further structural details were obtained by 2D NMR measurements (COSY, HMQC and HMBC), which allowed the assignment of the remaining NMR resonances (Table 3.4; Figure. 3.3). The absence of HMBC correlations between oxymethine protons H-3 and H-5 with the ester carbonyl carbon located the acetyl ester was placed at C-15.

The relative stereochemistry of piscatoriol A (**3**) was deduced from the NOESY spectrum (Figure 3.3). The α -oriented H-4 was taken as a reference point (Liu and Tan, 2001; Tian *et al.*, 2011). Strong NOE interactions between H-4 and H-3, H-2 and H-1a indicated α -orientation for these three protons. The stereochemistry at C-2 was further confirmed by comparing the coupling constant values $J_{2,3}$ and $J_{3,4}$ ($J_{2,3} = J_{3,4} = 3.6$ Hz)

with literature data, which are in agreement with a β configuration for H-16 (Tian *et al.*, 2011) (H-16 α , $J_{2,3} \approx 2.0 - 3.5$ Hz and $J_{3,4} \approx 7.5$ Hz) (Valente *et al.*, 2012). The C6-C7 double bond of piscatoriol A is an uncommon feature in this type of compounds (Shi *et al.*, 2008).

Table 3.4. ^1H and ^{13}C NMR data (δ) for piscatoriols A (**3**) and B (**4**) (400 and 101 MHz, respectively).

position	Piscatoriol A (3) ^a		Piscatoriol B (4) ^a	
	δ_{H} (J in Hz)	δ_{C}	δ_{H} (J in Hz)	δ_{C}
1	a	3.33 dd (13.5, 7.6)	3.40 dd (13.7, 7.9)	47.3
	b	1.69 m	1.90 m	
2		2.06 m ^b	2.09 m	37.5
3		4.34 t (3.6)	4.32 bs	79.6
4		2.11 dd (6.3, 3.6) ^b	2.43 dd (8.6, 3.4)	54.2
5		5.37 d (6.3)	4.81 bs	66.8
6		-	-	148.2
7	a	5.25 dd (11.2, 4.9)	2.72 dd (13.6, 5.5)	35.4
	b		2.15 m ^b	
8	a	2.35 m	2.01 m ^b	22.0
	b	2.39 m	1.57 m	
9		1.26 m ^b	1.12 m ^b	34.6
10				24.8
11		1.42 dd (11.4, 8.5)	1.37 dd (11.2, 8.4)	28.4
12		6.44 dd (11.4, 1.0)	6.33 bd (11.2)	145.5
13		-	-	133.7
14		-	-	197.2
15		-	-	92.8
16		1.07 d (6.8)	1.09 d (7.3)	13.5
17		1.65 s	4.95 bs; 4.75 bs	113.6
18		1.23 s	1.08 s	16.7
19		1.16 s	1.15 s	29.1
20		1.75 d (1.0)	1.70 s	12.6
1'		-	-	169.9
2'		2.09 s	2.06 s	22.1

^aspectra recorded in CDCl_3 ^bsignal partially overlapped

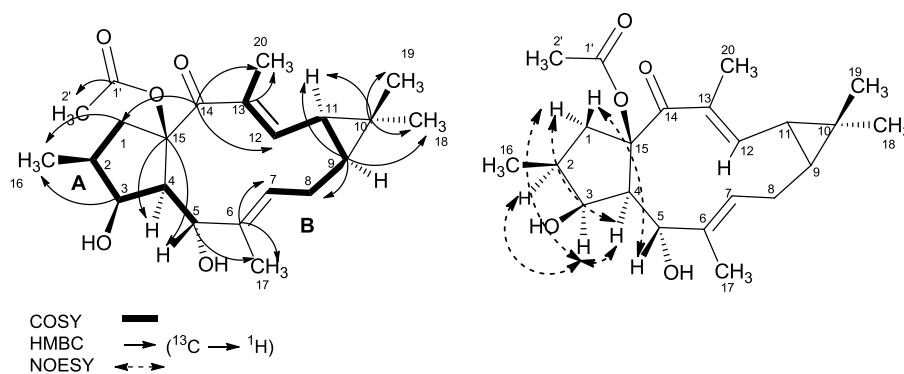
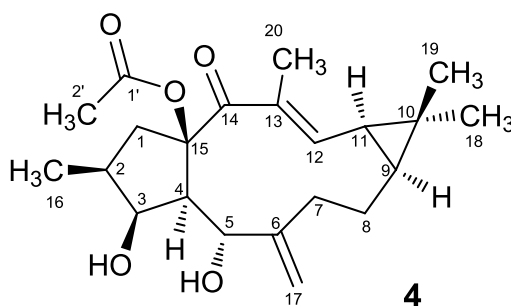


Figure 3.3. ¹H-spin systems (A-B), their connection through the main heteronuclear ²J_{C-H} and ³J_{C-H} correlations and key NOESY interactions of compound **3**.

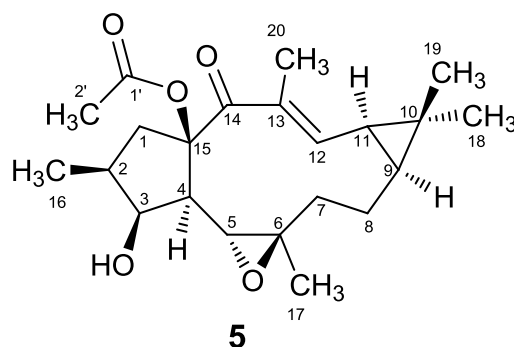
3.1.2.2. Piscatoriol B - 15β-acetoxy-lathyra-6(17),12-diene-3β,5α-diol-14-one (**4**)



Compound **4**, named piscatoriol B, was obtained as a white powder. The low resolution positive ESIMS of compound **4** exhibited a pseudomolecular ion at m/z 399 $[M + Na]^+$. The molecular formula was deduced as $C_{22}H_{32}O_5$, from its ESI-TOF-HRMS spectrum, indicating the presence of seven degrees of unsaturation. The spectroscopic data of piscatoriol B (**4**) revealed the same functional groups (alcohol, ester and α,β -unsaturated ketone) of piscatoriol A (**3**). The comparison of ¹³C and ¹H NMR data of compounds **4** and **3** (Table 3.4) pointed piscatoriol B as a lathyrane macrocycle diterpene, bearing an acetyl group at C-15 (δ_C 169.9; δ_C 22.1; δ_H 2.06 s), an enone system (δ_{C14} 197.2; δ_{C13} 133.7; δ_{C12} 145.5; δ_{H12} 6.33 bd) and two hydroxyl groups at C-3 (δ_C 79.6; δ_H 4.32 bs) and C-5 (δ_C 66.8; δ_H 4.81 bs). Nevertheless, the ¹H NMR data of piscatoriol B (**4**) revealed an exocyclic terminal double bond between C-6 and C-17, displayed as two broad singlets at δ_H 4.95 and 4.75, instead of the double bond between C-6 and C-7 found in **3**. The relative stereochemistry of piscatoriol B (**4**) was deduced from the NOESY spectrum through the same approach as used for compound **3**. The free hydroxyls at C-3

and C-5, present on both piscatoriols A (**3**) and B (**4**), are not common in lathyrane diterpenoids as these compounds are usually found as polyesters (Shi *et al.*, 2008; Tian *et al.*, 2011).

3.1.2.3. 15-acetoxy-5,6-epoxylathyr-12-en-3-ol-14-one (**5**)



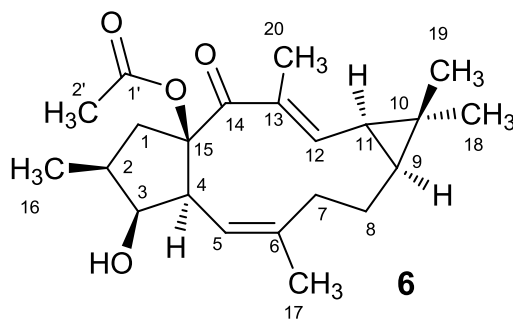
Compound **5**, $[\alpha]_D^{26} - 8.7$, was isolated as a white powder. Its spectroscopic data provided evidence for a lathyrane-type diterpene with the same functional groups (alcohol, ester and α,β -unsaturated ketone) found in piscatoriols A (**3**) and B (**4**). The low resolution ESIMS of **5** exhibited a pseudomolecular ion at m/z 399 $[M + Na]^+$, consistent with the molecular formula $C_{22}H_{32}O_5$. The ^{13}C and 1H NMR spectra (Table 3.5) presented signals for an acetyl group at C-15 (δ_C 169.7; δ_C 21.6; δ_H 2.07 s), an enone system (δ_C 195.3; 134.5; 143.9; δ_H 6.92 dd), one hydroxyl group at C-3 (δ_C 78.7; δ_H 4.07 bs) and an 5,6-epoxy ring (δ_C 58.1; δ_H 3.51 d; δ_C 63.9). Therefore, combining its physical and spectroscopic data it was concluded that compound **5** was 15-acetoxy-5,6-epoxylathyr-12-en-3-ol-14-one, isolated for the first time from the ethanol extract of *Euphorbia micractina* roots (Tian *et al.*, 2011).

Table 3.5. ¹H and ¹³C NMR data (δ) for compounds **5** and **6** (400 and 101 MHz, respectively).

position	15-acetoxy-5,6-epoxylathyr-12-en-3-ol-14-one (5) ^a		Jolkinol D (6) ^a		
	δ_{H} (J in Hz)	δ_{C}	δ_{H} (J in Hz)	δ_{C}	
1	a	3.45 dd (13.5, 7.4)	45.0	3.49 dd (14.0, 8.1)	44.1
	b	1.61 m		1.53 m ^b	
2		1.94 m	38.4	2.04 m	39.4
3		4.07 bs	78.7	3.91 dd (8.2, 3.6)	80.1
4		1.49 dd (9.4, 3.6)	53.6	2.38 dd (10.9, 3.6)	52.8
5		3.51 d (9.4)	58.1	5.67 d (10.9)	119.6
6		-	63.9	-	143.2
7	a	2.03 m	38.8	2.57 d (13.3)	36.9
	b	1.54 m		1.77 td (13.1, 6.5)	
8	a	2.09 m	23.3	2.21 ddd (14.5, 6.8, 3.3)	28.5
	b	1.51 m ^b		1.53 m ^b	
9		1.14 dd (8.0, 5.0)	33.8	1.06 m	34.4
10		-	26.3	-	24.6
11		1.51 m ^b	29.9	1.40 dd (11.4, 8.2)	29.8
12		6.92 dd (10.9, 1.0)	143.9	6.65 d (11.4)	146.7
13		-	134.5	-	132.3
14		-	195.3	-	195.5
15		-	92.0	-	95.4
16		1.07 m ^b	13.3	1.08 d (6.7)	13.9
17		1.17 s	20.1	1.46 s	21.1
18		1.20 s	29.2	1.17 s	29.4
19		1.07 m ^b	16.5	1.04 s	16.6
20		1.86 d (1.0)	12.6	1.83 s	12.5
1'		-	169.7	-	170.0
2'		2.07 s	21.6	2.01 s	21.8

^aspectra recorded in CDCl₃ ^bsignal partially overlapped

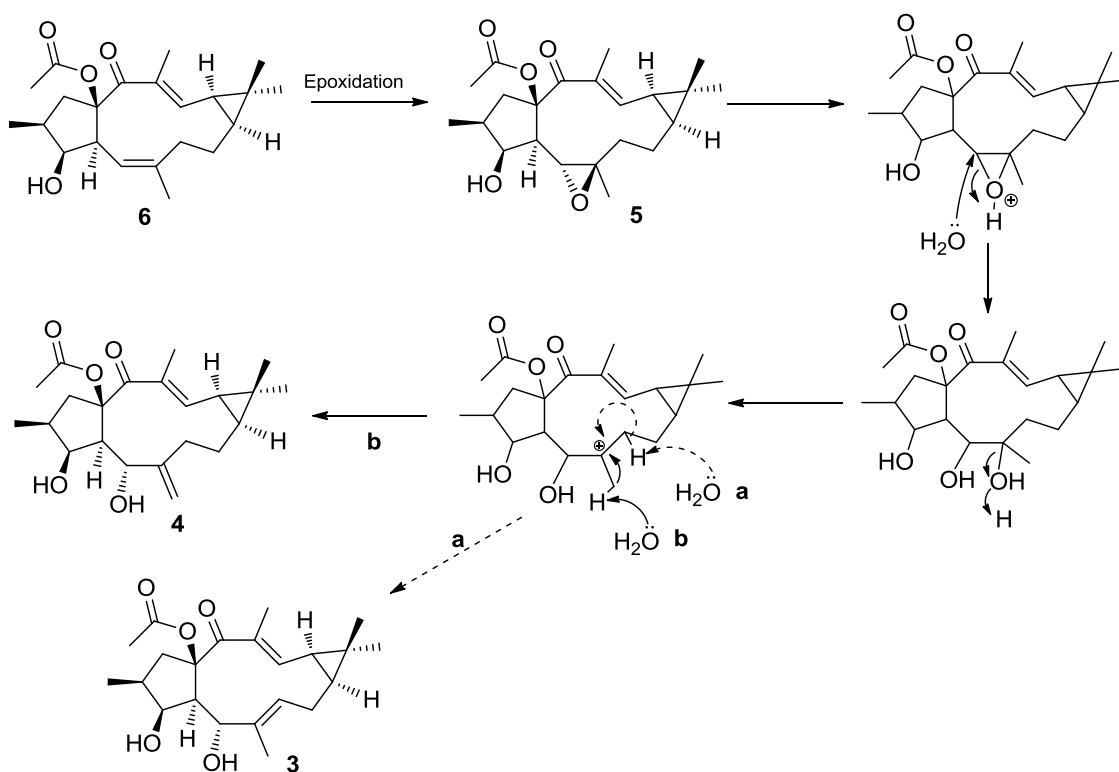
3.1.2.4. Jolkinol D (6)



Compound **6**, $[\alpha]_D^{25} + 27.9$, was isolated in large amount (2.1 g) as white crystals of m.p. 186- 188 °C. Its spectroscopic data resemble those of the other lathyranes described so far (**3-5**). Using the same approach as described before, compound **6** was identified as jolkinol D, first isolated from *Euphorbia jolkinii* (Uemura *et al.*, 1976). In this way, the ESIMS exhibited a pseudomolecular ion at m/z 383 $[M + Na]^+$, according to the molecular formula $C_{22}H_{32}O_4$. From the 1H and ^{13}C NMR spectra (Table 3.5) the characteristic acetyl group at C-15 (δ_C 170.0; δ_C 21.8; δ_H 2.01 s), a conjugated ketone (δ_{C14} 195.5; δ_{C13} 132.3; δ_{C12} 146.7; δ_{H12} 6.65 d), one hydroxyl group at C-3 (δ_C 80.1; δ_H 3.91 dd) and a 5,6-double bond (δ_{C5} 119.6; δ_{H5} 5.67 d; δ_{C6} 143.2) could be depicted.

3.1.2.5. Biogenic relationships of lathyranes 3-6

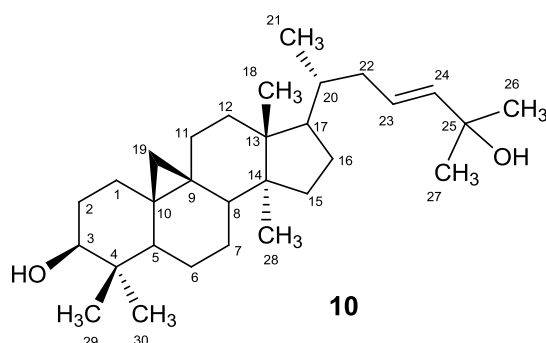
The lathyrane diterpenes **3-6** seem to be derivatives of each other, conserving the same functional groups at C-15, C-14, C-13, C-12 and C-3, but differing from their substituents between C-5 and C-7. In this way, a biogenetic relationship between these lathyranes is proposed (Scheme 3.2). The 5,6-epoxidation of jolkinol D (**6**) yields compound **5** (Uemura *et al.*, 1976; Tian *et al.*, 2011). Hydrolysis of **5** leads to epoxide opening to the corresponding vicinal diol. Subsequent dehydration at C-6, followed by deprotonation, yields compounds **3** (Scheme 3.2 **a**) and **4** (Scheme 3.2 **b**).



Scheme 3.2. Biogenetic interrelationships between lathyranes 3-6.

3.1.3. Cycloartane-type triterpene

3.1.3.1. Cycloart-23-ene-3 β ,25-diol (10)



Compound **10**, $[\alpha]_D^{18} + 42.8$, was obtained as white crystals of m.p. 212 – 215 °C, being identified as cycloart-23-ene-3 β ,25-diol on the basis of its physical and spectroscopic data (De Pascual *et al.*, 1987). The presence of the hydroxyl groups was suggested by the IR absorption band at 3352 cm⁻¹. The secondary hydroxyl at C-3 was

corroborated by the oxymethine signal at δ_C 79.0 and δ_H 3.28 dd ($J = 10.9, 4.3$ Hz) and the hydroxyl at C-25 by the oxygenated quaternary carbon at δ_C 70.9 (Table 3.6). The characteristic 1H signals of cyclopropane ring were observed in the spectrum as two shielded doublets at δ 0.55 and 0.33 ($J = 4.0$ Hz). Moreover, two olefinic protons were displayed as an overlapped signal at δ 5.59 (bs). Seven methyl groups were recorded; the secondary methyl H-21 was displayed as a doublet (δ 0.85, $J = 6.4$ Hz) and the geminal tertiary methyls H-26 and H-27 as an overlapped deshielded signal at δ 1.31 bs.

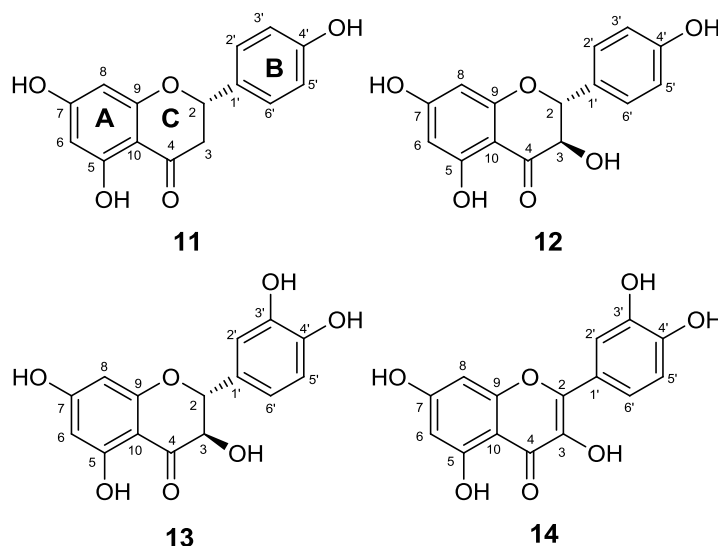
Table 3.6. 1H and ^{13}C NMR data (δ) for compound **10** (400 and 101 MHz, respectively).

			Cycloart-23-eno-3β,25-diol (10)^a	
position			δ_H (J in Hz)	δ_C
3			3.28 dd (10.9, 4.3)	79.0
18			0.96 s ^b	18.2
19	a		0.55 d (4.0)	30.5
	b		0.33 d (4.0)	
21			0.85 d (6.4)	18.4
23			5.59 bs ^b	125.8
25			-	70.9
24			5.59 bs ^b	139.5
26			1.31 bs ^b	30.0
27			1.31 bs ^b	30.1
28			0.88 s	19.4
29			0.96 s ^b	14.2
30			0.80 s	25.6

^aspectra recorded in $CDCl_3$; ^bsignal partially overlapped

3.1.4. Phenolic compounds

3.1.4.1. Naringenin (11), aromadendrin (12), taxifolin (13) and quercetin (14)



The well-known flavonoids **11-14** were also isolated from the aerial parts of *E. piscatoria*. Their identification was performed mainly by ^1H and ^{13}C NMR experiments (Table 3.7).

In regard to the flavonoid classification, naringenin (**11**) is a flavanone whereas aromadendrin (**12**) and taxifolin (**13**) belong to the flavanonols subclass. The last differ from flavanones due to the oxidation at C-3 (Dewick, 2009b). Therefore, compound **11** bears a methylene group at C-3 (δ_{C} 44.0, δ_{H} 3.07 dd and 2.65 dd) while compounds **12** and **13** present an oxymethine group (δ_{C} 73.6, δ_{H} 4.51 d; δ_{C} 73.1, δ_{H} 4.61 d, respectively). Quercetin (**14**) belongs to the flavonols subclass characterized by having a 2,3-double bond oxidized at C-3 (δ_{C} 147.9 and 137.2, C-2 and C-3 respectively).

The ring A 5,7-substitution pattern was assumed from the observation of aromatic signals at δ_{C} 5.84 – 6.39, with *meta* coupling constant ($J \sim 2$ Hz). Regarding the oxygenation pattern of ring B, it was reflected on the proton splitting pattern and coupling constants as well as on the carbon chemical shifts. In the spectra of the monohydroxylated flavonoids **11** and **12** the ring B protons H-2'/H6' and H-3'/H-5' were present as doublets (δ_{H} 7.22; 7.32 and 6.78; 6.80, respectively), with *ortho* coupling constants ($J \sim 8.5$ Hz), characteristic of *para*-substituted aromatic rings. While in the spectra of the

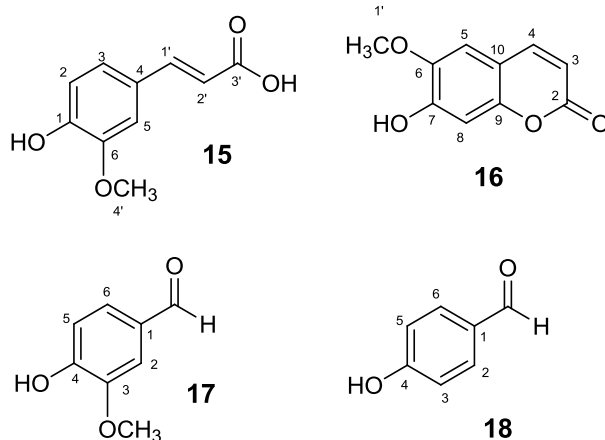
dihydroxylated compounds **13** and **14**, H-2' is presented as a doublet (δ_{H} 7.04; 7.74, respectively) with a *meta* coupling constant ($J \sim 2$ Hz), H-5' as a doublet (δ_{H} 6.86; 6.85, respectively) with $J \sim 8$ Hz (*ortho* coupling) and H-6' as a doublet of doublets (δ_{H} 6.92; 7.64, respectively) with the corresponding *ortho* and *meta* coupling constants. The oxygenated aromatic carbons of these flavonoids resonated at the characteristic δ_{C} 144.6-159.2.

Table 3.7. ^1H and ^{13}C NMR data (δ) for flavonoids **11-14** (400 and 101 MHz, respectively).

position	Naringenin (11) ^a		Aromadendrin (12) ^a		Taxifolin (13) ^b		Quercetin (14) ^a	
	δ_{H} (J in Hz)	δ_{C}	δ_{H} (J in Hz)	δ_{C}	δ_{H} (J in Hz)	δ_{C}	δ_{H} (J in Hz)	δ_{C}
2	5.29 dd (13.0, 2.9)	80.4	4.94 d (11.6)	84.9	5.03 d (11.4)	84.4	-	147.9
3a	3.07 dd (17.1; 13.0)	44.0	4.51 d (11.6)	73.6	4.61 d (11.4)	73.1	-	137.2
3b	2.65 dd (17.1; 2.9)							
4	-	197.7	-	198.4	-	198.1	-	177.2
5	-	163.7	-	165.2	-	164.1	-	162.4
6	5.85 d (2.2)	97.0	5.89 d (2.1)	97.3	5.99 d (2.1)	96.9	6.19 d (2.0)	99.1
7	-	168.3	-	168.7	-	167.6	-	165.5
8	5.84 d (2.2)	96.1	5.84 d (2.1)	96.3	5.95 d (2.1)	96.9	6.39 d (2.0)	94.3
9	-	164.8	-	164.5	-	164.9	-	158.1
10	-	103.3	-	101.8	-	101.5	-	104.4
1'	-	131.1	-	129.3	-	129.7	-	124.1
2'	7.27 d (8.5)	129.0	7.32 d (8.6)	130.3	7.07 d (1.8)	115.8	7.74 d (2.0)	115.9
3'	6.78 d (8.5)	116.3	6.80 d (8.6)	116.1	-	145.4	-	146.1
4'	-	159.0	-	159.2	-	144.6	-	148.6
5'	6.78 d (8.5)	116.3	6.80 d (8.6)	116.1	6.86 d (8.1)	115.6	6.85 d (8.4)	116.1
6'	7.27 d (8.5)	129.0	7.32 d (8.6)	130.3	6.92 dd (8.1; 1.8)	120.8	7.64 dd (8.4, 2.0)	121.6

^aspectra recorded in MeOD; ^bspectra recorded in Acetone-d₆

3.1.4.2. Ferulic acid (**15**), scopoletin (**16**), vanillin (**17**) and *p*-hydroxybenzaldehyde (**18**)



Ferulic acid (**15**) is a hydroxycinnamic acid (C_6C_3 scaffold). The hydroxylation of hydroxycinnamic acids, *ortho* to the side chain and subsequent lactonization originates the coumarins of which scopoletin (**16**) is a representative (Dewick, 2009b).

In the 1H NMR spectra (Table 3.8), the characteristic H-3 and H-4 *cis* olefinic protons of compound **16** were observed as doublets at δ 7.60 ($J = 9.5$ Hz) and 6.27 ($J = 9.5$ Hz), respectively, while the corresponding H-2' and H-1' *trans* olefinic protons of ferulic acid (**15**) resonated at δ 7.55 (d, $J = 15.9$ Hz) and 6.28 (d, $J = 15.9$ Hz). The relatively low field resonance of H-4 (**16**) and H-1' (**15**) can be attributed to mesomeric effects, due to their beta position in relation to the carbonyl group. Regarding the substitution pattern of the aromatic moiety, ferulic acid (**15**) presents a trisubstituted pattern, displaying in the 1H NMR spectrum a broad singlet at δ 7.14 (H-5) and two doublets at δ 7.02 ($J = 8.2$ Hz, H-3) and 6.77 ($J = 8.2$ Hz, H-2). In contrast, as expected, scopoletin (**16**) displayed two proton singlets (δ_H 6.92 and 6.84, H5 and H8 respectively). In addition, the 1H NMR spectra of compounds **15** and **16** displayed signals assignable to the methoxyl group at δ_H 3.85 and 3.95, respectively. The ^{13}C spectra of both compounds displayed ten resonances, the typical aromatic and olefinic carbons were recorded at δ_C 107.6 – 150.4 (Table 3.8). The corresponding methoxyl groups were assigned at δ_C 56.4 and 56.6 (**15** and **16**, respectively). For compound **15**, the low field resonance at δ_C 171.0 was assigned to the carboxylic acid ketone. In the same way, for compound **16**, the carbonyl of the lactone function was recorded at δ_C 161.6.

Vanillin (**17**) and *p*-hydroxybenzaldehyde (**18**) are simple C₆C₁ phenols that differ at C-5, as vanillin has a methoxyl substituent (δ_{H} 3.96; δ_{C} 56.1). Their ¹H and ¹³C NMR spectra (Table 3.9) allowed the unambiguous assignment of their structures, confirming their aromatic structure (δ_{H} 6.96 - 7.81 and δ_{C} 109.3 – 147.5) and the aldehyde function (δ_{H} 9.82 and 9.87; δ_{C} 191.2 and 191.2, **17** and **18** respectively).

Table 3.8. ¹H and ¹³C NMR data (δ) for compounds **15** and **16** (400 and 101 MHz, respectively).

Ferulic acid (15) ^a			Scopoletin (16) ^b		
position	δ_{H} (J in Hz)	δ_{C}	position	δ_{H} (J in Hz)	δ_{C}
1	-	150.4	2	-	161.6
2	6.77 d (8.2)	116.2	3	6.27 d (9.5)	113.5
3	7.02 d (8.2)	123.9	4	7.60 d (9.5)	143.5
4	-	127.8	5	6.92 s	103.3
5	7.14 s	111.6	6	-	144.1
6	-	149.3	7	-	150.2
1'	7.55 d (15.9)	146.7	8	6.84 s	107.6
2'	6.28 d (15.9)	116.4	9	-	149.3
3'	-	171.0	10	-	111.6
4'	3.85 s	56.4	1'	3.95	56.6

^aspectra recorded in MeOD; ^bspectra recorded in CDCl₃

Table 3.9. ¹H and ¹³C NMR data (δ) for compounds **17** and **18** (400 and 101 MHz, respectively).

Vanillin (17) ^a			<i>p</i> -hydroxybenzaldehyde (18) ^a		
position	δ_{H} (J in Hz)	δ_{C}	δ_{H} (J in Hz)	δ_{C}	
1	-	129.8	-	129.9	
2	7.43 m*	109.3	7.81 d (8.4)	132.6	
3	-	147.5	6.96 m*	116.1	
4	-	152.2	-	161.7	
5	7.05 d (8.1)	114.8	6.96 m*	116.1	
6	7.43 m*	127.5	7.81 d (8.4)	132.6	
COH	9.82 s	191.2	9.87 s	191.3	
OCH ₃	3.96 s	56.1	-	-	

^aspectra recorded in CDCl₃,* signal partially overlapped

3.2. Assessment of MDR reversal activity

Macrocyclic diterpenes **3-5** were evaluated for their drug-interaction effect and as P-gp efflux modulators on *MDR1*-transfected L5178Y mouse T lymphoma cell model. The results of the chemosensitivity assay are presented in Table 3.10. As it can be observed, when tested alone, lathyranes **3-5** presented a weak antiproliferative effect. However, their combination with doxorubicin resulted in a synergistic enhancement of the antiproliferative activity of this anticancer drug. This was observed throughout the inhibitory concentration range (Table 3.10). Since this cell model overexpresses P-gp, we further investigated if this synergistic effect could be related with inhibition of P-gp efflux, by using the rhodamine-123 efflux assay. However, diterpenes **3-5** did not show modulatory activity (data not shown).

These results might suggest the possible mechanisms of action. Either the lathyranes **3-5** act as P-gp substrates, competing with doxorubicin for the efflux. Hence, reduction of its efflux rate caused a higher cytotoxic effect. Or these macrocycle lathyranes had MDR reversal effect independent from P-gp, by targeting other cellular pathways. This multifactorial character of MDR is well described (Longley and Johnston, 2005; Lage, 2008; Baguley, 2010).

Table 3.10. Evaluation of the interaction between compounds **3-5** and doxorubicin in human *MDR1*-gene transfected mouse lymphoma cells.

Compound	Single drug	Drug combination		
	IC ₅₀ ± SD (µM)	CI ± SD ^a for IC ₅₀ (interaction)	CI ± SD ^a for IC ₇₅ (interaction)	CI ± SD ^a for IC ₉₀ (interaction)
3	69.80 ± 0.12	0.25 ± 0.03 (strong synergy)	0.23 ± 0.03 (strong synergy)	0.25 ± 0.05 (strong synergy)
4	81.50 ± 0.06	0.39 ± 0.05 (synergy)	0.33 ± 0.04 (synergy)	0.27 ± 0.04 (strong synergy)
5	59.80 ± 0.06	0.23 ± 0.04 (strong synergy)	0.09 ± 0.02 (very strong synergy)	0.04 ± 0.01 (very strong synergy)
Doxorubicin	1.82 ± 0.49			

^a Combination index (CI) values are the mean ± standard deviation (SD) for an given inhibitory concentration. CI < 0.1: very strong synergism; 0.1 < CI < 0.3: strong synergism; 0.3 < CI < 0.7: synergism; 0.7 < CI < 0.9: moderate to slight synergism; 0.9 < CI < 1.1: nearly additive; 1.10 < CI < 1.45: moderate antagonism; 1.45 < CI < 3.30: antagonism (Chou, 2006, 2010).

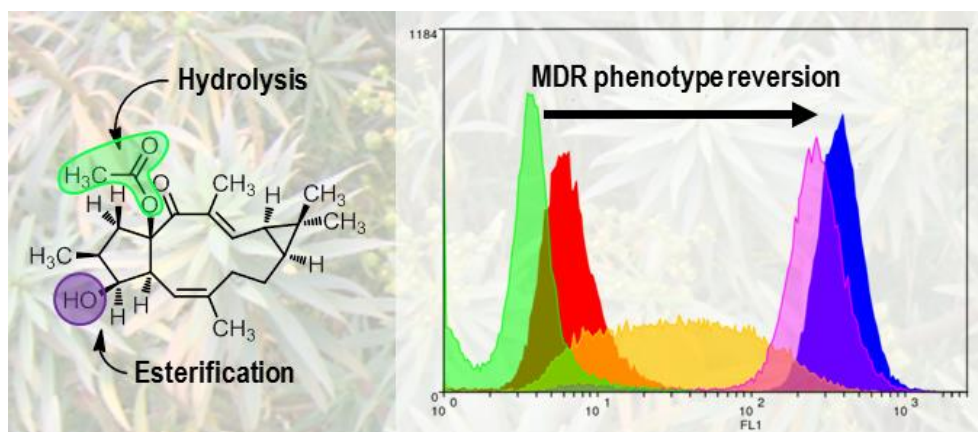
Chapter 4

**Jolkinol D derivatives as MDR reversers: SAR studies
Results and Discussion**

The phytochemical study of *Euphorbia piscatoria* afforded the isolation of jolkinol D (**6**) in large amount. As a result, a small library of 27 derivatives was designed to establish structure-activity relationships. The P-gp efflux activity was assessed through a rhodamine-123 transport assay, on a *MDR1*-transfected cell model. The derivatives showed to be able to revert the P-gp-mediated MDR phenotype and the most relevant SAR results pointed towards the importance of the aroyl moiety and its pattern of substitution for the efficacy of efflux modulation. When these bioactive diterpenes were tested in a chemosensitivity assay, the majority was able to synergistically enhance the antiproliferative effect of an anticancer agent (doxorubicin).

In conclusion, the optimization of the lathyrane macrocyclic scaffold, provided a valuable approach to understand the mechanism of P-gp modulation and for the selection of promising lead compounds for cancer MDR reversal.

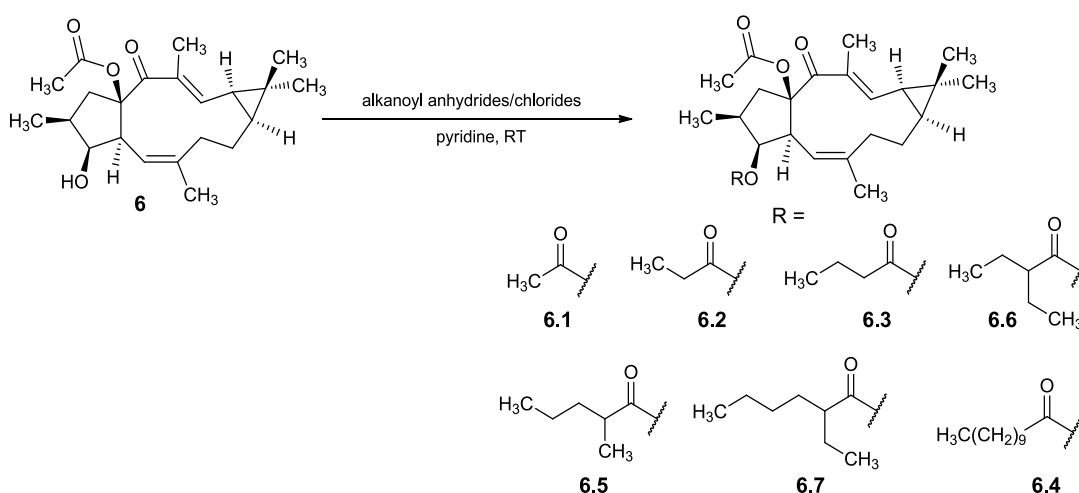
Graphical abstract



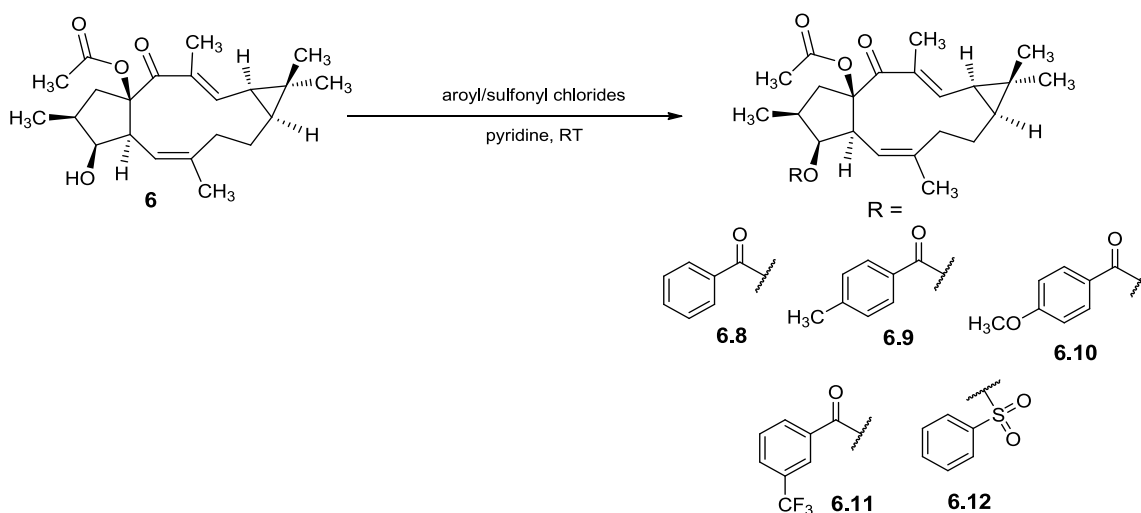
4.1. Chemistry

A small library of 27 macrocyclic lathyrane diterpenes targeted for P-gp efflux modulation was achieved by molecular derivatization of jolkinol D (**6**), mainly through acylation reactions. Compound **6** constitutes a good prototype for SAR since it only possesses one acylation point at C-3, and thus, the impact of structural modifications will be clearly assigned to modulation of P-gp efflux. The derivatization was guided through SAR studies. The rationale behind the design, predominantly followed the general physicochemical features of compounds recognized by P-gp, as well as, the indications given by previous pharmacophore modeling and QSAR studies, performed with macrocyclic diterpenes (Pajeva and Wiese, 2009; Ferreira *et al.*, 2011; Sousa *et al.*, 2012).

The first set of monoacylated derivatives at C-3 (**6.1-6.12**) was projected to clarify the potential activity of alkanoyl derivatives versus aryl and relate their physicochemical properties. Therefore, alkanoyl/aroyl/sulfonyl substituents were introduced into compound **6** scaffold. Alkanoyl derivatives **6.1-6.7** varied on the size of the side chain (from acetyl to lauroyl) as well as ramification pattern (Scheme 4.1). While, aromatic derivatives **6.8-6.12** differed mainly on the presence or absence of electron donor or acceptor groups (Scheme 4.2).



Scheme 4.1. Jolkinolates A-G (**6.1-6.7**).

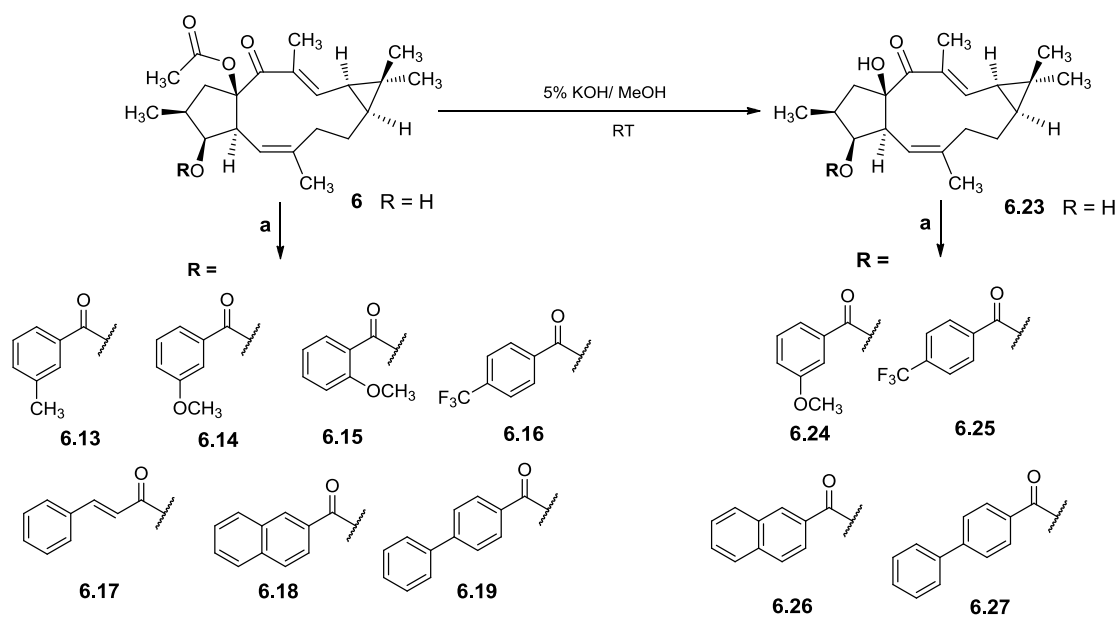


Scheme 4.2. Jolkinolates I-J (**6.8-6.12**).

Hence, chemical derivatization of the free hydroxyl group at C-3, with alkanoyl anhydrides and alkanoyl/aroyl/sulfonyl chlorides in pyridine, yielded twelve derivatives in 55–97% yields (Scheme 4.1 and 4.2). Moreover, hydrolysis of the ester function at C-15, produced compound **6.23** in 81% yield (Scheme 4.3). The derivatives were characterized by comparison of their spectroscopic data with those of jolkinol D (**6**). The main differences between the NMR data of compound **6** and the data of the acylated derivatives (**6.1-6.12**) were observed for the carbon and proton chemical shifts of the pentacyclic ring. The ^1H NMR data of compounds **6.1-6.12** showed significant paramagnetic effects at H-3, whose signal appeared approximately 1.0–1.6 ppm downfield. As expected, in the ^{13}C NMR spectra, similar paramagnetic effects at the α -carbons were also observed; C-3 of compounds **6.11** and **6.12** ($\Delta\delta_{\text{C}} = +2.9$ and $+11.3$ ppm, respectively) displayed the highest chemical shifts. The β -carbons C-2 and C-4 also showed predictable diamagnetic effects ($\Delta\delta_{\text{C}} \cong 0.9$ – 1.3 and 1.1 – 1.9 ppm, respectively). For the hydrolyzed derivative jolkinodiol (**6.23**), the α -carbon C-15 appeared upfield by 2.7 from its position in compound **6** and C-1, C-4, and C-14 (β -carbons) were shifted downfield ($\Delta\delta_{\text{C}} = +2.0$, $+0.5$, $+2.6$ ppm, respectively). The marked effect at C-14 (β -carbon) could also be explained by an intramolecular hydrogen bond between the corresponding ketone function and the free hydroxyl group at C-15. This effect was also observed at both H-12 and C-12 of the enone system due to mesomeric effect ($\Delta\delta_{\text{H}} = +0.8$ ppm and $\Delta\delta_{\text{C}} = +5.1$ ppm, respectively).

The SAR analysis of compounds **6.1-6.12** and **6.23** (section 4.2.3 of this chapter), established the best physicochemical properties for P-gp modulation and pointed the importance of the aromatic moiety. As a result, a new set of derivatives **6.13-6.22** and **6.24-6.28** was produced to investigate the role of aromatic electronic effects and hindrance effects on the activity of this efflux pump.

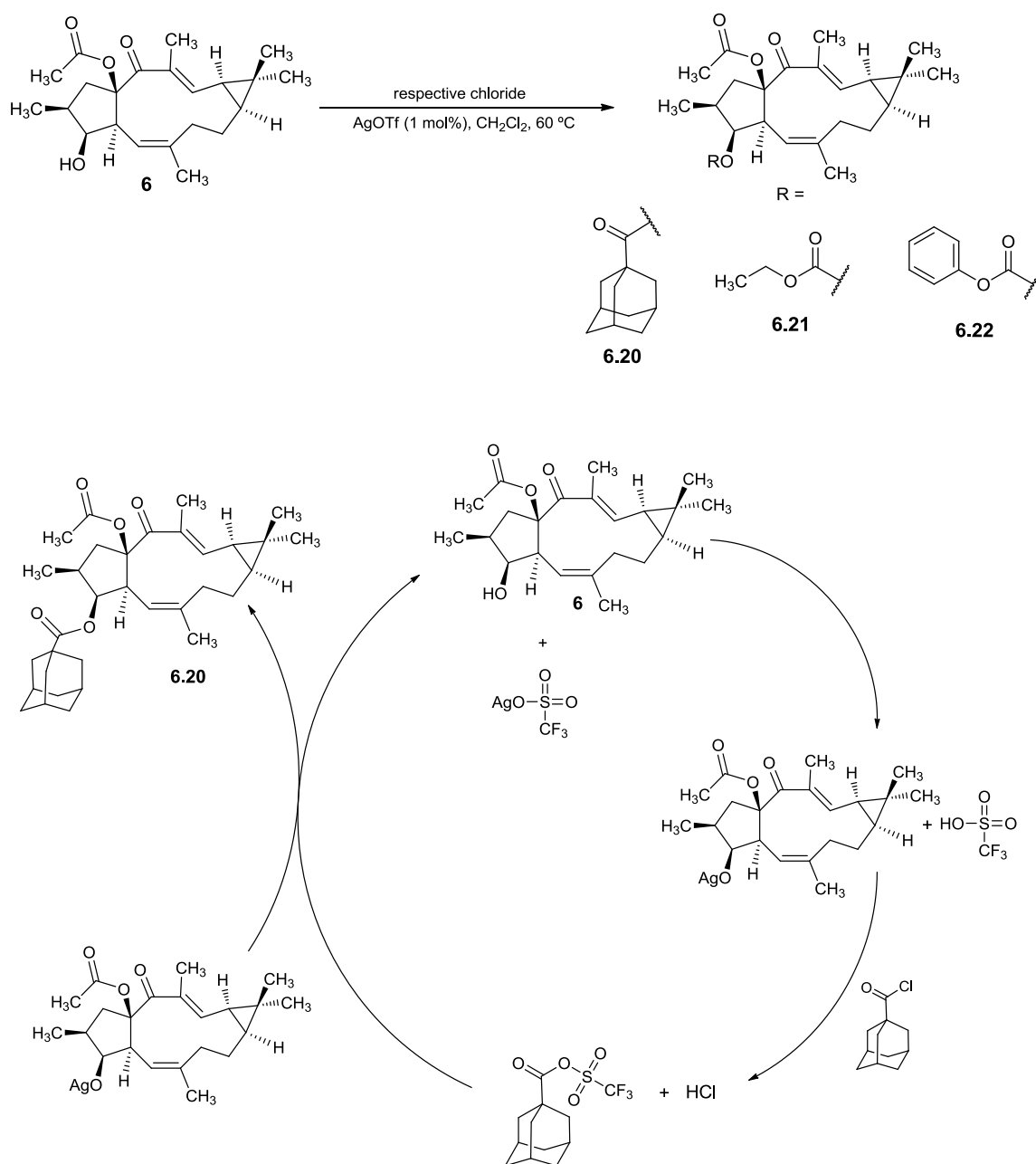
Derivatives **6.13-6.19** were synthesized by reaction of jolkinol D (**6**) with the respective aroyl chlorides in the presence of CH₂Cl₂, TEA and DMAP, in 28-96% yield (Scheme 4.3). No product was obtained when these reactions were attempted in pyridine. In parallel, to study the role of the substituent at C-15, derivatives **6.24-6.27** were synthesized, in 20-81% yield, using jolkinodiol (**6.23**) as parent molecule (Scheme 4.3). Concomitant acylation of compound **6.23** at C-15 and C-3 was not successful, even when strong reactional conditions were applied, such as using sodium hydride as base. The hydroxyl at C-15 tends to be less reactive, given its tertiary nature.



Scheme 4.3. Jolkinolates J-T (**6.13-6.19**) and jolkinolates A-D (**6.23-6.27**). Reagents and conditions: 1 eq of jolkinol D (**6**); 1 eq of jolkinodiol (**6.23**); (a) Respective aroyl chlorides; TEA, CH₂Cl₂, DMAP (cat.), reflux 60 °C.

Moreover, an adamantane derivative (**6.20**) and two formats, one aliphatic (**6.22**) and one aromatic (**6.21**), were prepared using silver triflate as catalyst, in 21-81% yield. The catalytic cycle for the acylation of jolkinol D (**6**) is shown in Scheme 4.4, as proposed by Das and Chakraborty (Das and Chakraborty, 2011). The TfOH is generated from the

reaction between AgOTf and jolkinol D (**6**) and is responsible for the further propagation of the reaction. Ag(I) plays a key role in substrate activation.



Scheme 4.4. Jolkinoinate U (**6.20**) and jolkinoinates A and B (**6.21-6.22**). Catalytic cycle for acylation of jolkinol D (**6**) using AgOTf.

4.2. Assessment of MDR reversal activity

Aiming to evaluate the MDR reversal potential of compounds **6** and **6.1-6.27** a P-gp overexpressing cell model (L5178Y mouse T lymphoma cell line transfected with *MDR1*) and its parental counterpart were used. This L5178Y-MDR cell line exclusively expresses P-gp/ABCB1, and thus constitutes a good model for the design and evaluation of MDR reversal experiments.

4.2.1. Antiproliferative activity

Antiproliferative assays were implemented so as to select nontoxic and low concentrations to use in the efflux and SAR studies. These tests were performed on parental (PAR) and P-gp-overexpressing (L5178Y-MDR) cell lines, using the MTT assay. In general, the derivatives **6.1-6.27** were more active than the parental compound jolkinol D (**6**), although none presented an IC₅₀ lower than 10 μM (Table 4.1). The determination of the selectivity index (Table 4.1) showed a general trend of a higher antiproliferative activity towards the parental cell line (chemo-sensitive). This effect was expectable, since it lacks the mechanisms of resistance present in L5178Y-MDR cells. On the basis of these results, 2 and 20 μM were chosen to use in the rhodamine-123 transport assay.

4.2.2. Modulation of P-gp efflux

In order to investigate compounds **6**, **6.1-6.27** as potential P-gp modulators, the rhodamine-123 transport assay was employed. This assay gives a direct quantitative assessment whether a compound inhibits/modulates the efflux. Rhodamine-123 is a fluorescent substrate of P-gp, therefore, its cytoplasmic accumulation can be quantified by flow cytometry through the Fluorescence Activity Ratio ($\text{FAR} = (\text{L5178Y-MDR}_{\text{FL-1treated}} / \text{L5178Y-MDR}_{\text{FL-1control}}) / (\text{PAR}_{\text{FL-1treated}} / \text{PAR}_{\text{FL-1control}})$; Figure 4.1). P-gp modulation takes place when FAR value is higher than 1, hence, when this ratio is higher than 10, compounds can be classified as strong modulators. Verapamil, a well-known modulator, was used as positive control in this assay.

Table 4.1. Antiproliferative activity of jolkinol D (**6**) and derivatives **6.1-6.27** in L5178Y mouse T lymphoma cells (PAR cells) and in human *MDR1*-gene transfected mouse T lymphoma cells (L5178Y-MDR cells).

Compounds	IC ₅₀ ^a (μM)		Selectivity index ^b
	PAR	L5178Y-MDR	
Jolkinol D (6)	89.87 ± 0.80	99.67 ± 4.53	1.1
Jolkinoate A (6.1)	38.21 ± 5.52	60.35 ± 1.25	1.6
Jolkinoate B (6.2)	18.33 ± 4.00	22.16 ± 3.94	1.2
Jolkinoate C (6.3)	23.99 ± 0.45	26.84 ± 5.32	1.1
Jolkinoate D (6.4)	38.66 ± 6.30	60.27 ± 6.43	1.6
Jolkinoate E (6.5)	17.20 ± 2.55	18.76 ± 3.11	1.1
Jolkinoate F (6.6)	14.34 ± 2.64	14.74 ± 0.73	1.0
Jolkinoate G (6.7)	20.58 ± 7.11	48.92 ± 4.16	2.4
Jolkinoate I (6.8)	34.70 ± 6.93	33.08 ± 5.44	1.0
Jolkinoate J (6.9)	41.16 ± 3.03	45.07 ± 3.33	1.1
Jolkinoate K (6.10)	21.67 ± 6.60	32.71 ± 5.17	1.5
Jolkinoate L (6.11)	43.99 ± 3.67	52.60 ± 3.84	1.2
Jolkinoate M (6.12)	12.13 ± 0.46	14.95 ± 4.33	1.2
Jolkinoate N (6.13)	67.71 ± 8.99	> 100	1.5
Jolkinoate O (6.14)	24.87 ± 1.22	36.35 ± 6.01	1.5
Jolkinoate P (6.15)	19.73 ± 1.34	24.17 ± 3.40	1.2
Jolkinoate Q (6.16)	47.50 ± 2.80	91.64 ± 7.95	1.9
Jolkinoate R (6.17)	20.94 ± 0.53	26.50 ± 0.69	1.3
Jolkinoate S (6.18)	27.06 ± 2.74	55.88 ± 0.45	2.1
Jolkinoate T (6.19)	33.05 ± 2.40	58.86 ± 7.84	1.8
Jolkinoate U (6.20)	24.71 ± 5.52	30.87 ± 3.68	1.2
Jolkinofornate A (6.21)	30.09 ± 5.50	40.15 ± 0.25	1.3
Jolkinofornate B (6.22)	49.51 ± 6.03	54.09 ± 2.68	1.1
Jolkinodiol (6.23)	36.42 ± 5.77	48.92 ± 4.16	1.3
Jolkinolate A (6.24)	47.12 ± 6.97	48.85 ± 5.65	1.0
Jolkinolate B (6.25)	62.42 ± 5.36	90.27 ± 6.70	1.4
Jolkinolate C (6.26)	53.91 ± 0.23	67.07 ± 0.48	1.2
Jolkinolate D (6.27)	70.20 ± 4.14	84.62 ± 2.43	1.2
DMSO (2%)	1.21 ± 0.51	1.46 ± 0.11	-

^a Values of IC₅₀ are means ± standard error of the mean of three independent experiments; ^b Selectivity index = IC₅₀ MDR cells / IC₅₀ PAR cells

Modulation of the P-gp mediated rhodamine-123 efflux is summarized in Table 4.2. When tested at 20 μM , the acylated derivatives **6.1-6.22**, **6.24**, **6.26** and **6.24** caused a strong impairment of P-gp transport activity, with FAR values ranging from 12.1 to 109.2. Moreover, jolkinodiol (**6.23**) and jolkinolate B (**6.25**) were the ones exhibiting the lowest activity (FAR = 3.2 and 9.9, respectively), along with the parent compound **6** that did not show ability as modulator. This suggests the structural modifications at C-3 and C-15 contributed to increase P-gp inhibitory activity. The strong modulators of this library were selected from the 2 μM data: two alkanoyl derivatives **6.7** (Figure 4.1 A) and **6.20**; plus eleven aryl derivatives **6.8**, **6.9**, **6.10** (Figure 4.1 B), **6.12**, **6.14**, **6.15**, **6.17-6.19**, **6.22** and **6.24**. These compounds showed FAR values from 10.6 – 33.3. These results are of particular interest since the MDR reversal activity of verapamil at 20 μM is approximately 12.5.

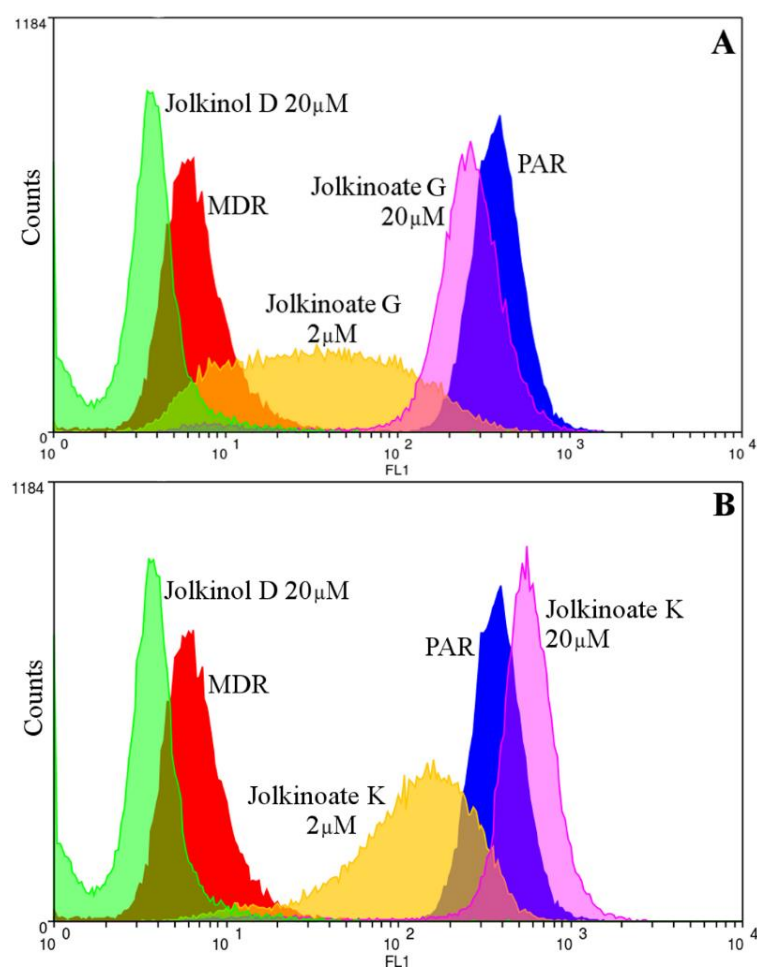


Figure 4.1. Flow cytometry histograms showing reversal of the MDR phenotype: Jolkinolate G (A) and K (B) at 2 μM and 20 μM , in comparison with Jolkinol D (20 μM). MDR: L5178Y-MDR chemo-resistant cells; PAR: parental chemo-sensitive cells.

Table 4.2. Modulation of P-gp mediated rhodamine-123 efflux by jolkinol D (**6**) and derivatives (**6.1-6.27**).

Compounds	Fluorescence activity ratio (FAR) ^a	
	2 μ M	20 μ M
Jolkinol D (6)	0.8	0.9
Jolkinoate A (6.1)	1.2	33.8
Jolkinoate B (6.2)	3.0	30.6
Jolkinoate C (6.3)	5.2	107.9
Jolkinoate D (6.4)	1.7	25.7
Jolkinoate E (6.5)	7.1	12.1
Jolkinoate F (6.6)	5.0	77.3
Jolkinoate G (6.7)	10.6	52.7
Jolkinoate I (6.8)	24.2	84.2
Jolkinoate J (6.9)	21.1	56.9
Jolkinoate K (6.10)	28.1	109.2
Jolkinoate L (6.11)	9.3	28.7
Jolkinoate M (6.12)	16.1	52.8
Jolkinoate N (6.13)	2.2	18.0
Jolkinoate O (6.14)	26.1	36.4
Jolkinoate P (6.15)	33.3	39.6
Jolkinoate Q (6.16)	9.4	25.4
Jolkinoate R (6.17)	28.6	41.5
Jolkinoate S (6.18)	11.9	31.9
Jolkinoate T (6.19)	11.6	37.2
Jolkinoate U (6.20)	12.6	29.0
Jolkinofornate A (6.21)	3.1	18.7
Jolkinofornate B (6.22)	10.8	19.5
Jolkinodiol (6.23)	0.84	3.38
Jolkinolate A (6.24)	12.0	32.8
Jolkinolate B (6.25)	3.0	9.9
Jolkinolate C (6.26)	8.3	16.7
Jolkinolate D (6.27)	4.8	19.0
Verapamil	-	12.5

^aFAR = (L5178Y-MDR_{FL-1treated} / L5178Y-MDR_{FL-1control}) / (PAR_{FL-1treated} / PAR_{FL-1control}). FL-1: mean fluorescence intensity of the cells. DMSO (2%) FAR = 0.87

To study whether P-gp efflux modulation had dose-effect dependence, some derivatives were tested at different concentrations (2, 20, 40/80 μM). The Overton cumulative histogram subtraction algorithm was calculated for compounds **6.8**, **6.9**, **6.10** and **6.12**. This algorithm subtracts histograms on a channel-by-channel basis to provide a percentage of positive cells (Overton, 1988), allowing to calculate the percentage of the population that reverted to a chemosensitive phenotype. The direct correlation between the increase of concentration and number of cells with a chemosensitive phenotype is an indicator of a dose-dependent inhibitory effect on the MDR reversal activity. For instance, jolkinolate K (**6.10**) and jolkinolate I (**6.8**) reverted 95% and 70.2% of the population of MDR cells to a chemosensitive phenotype at 20 μM (Figure 4.2).

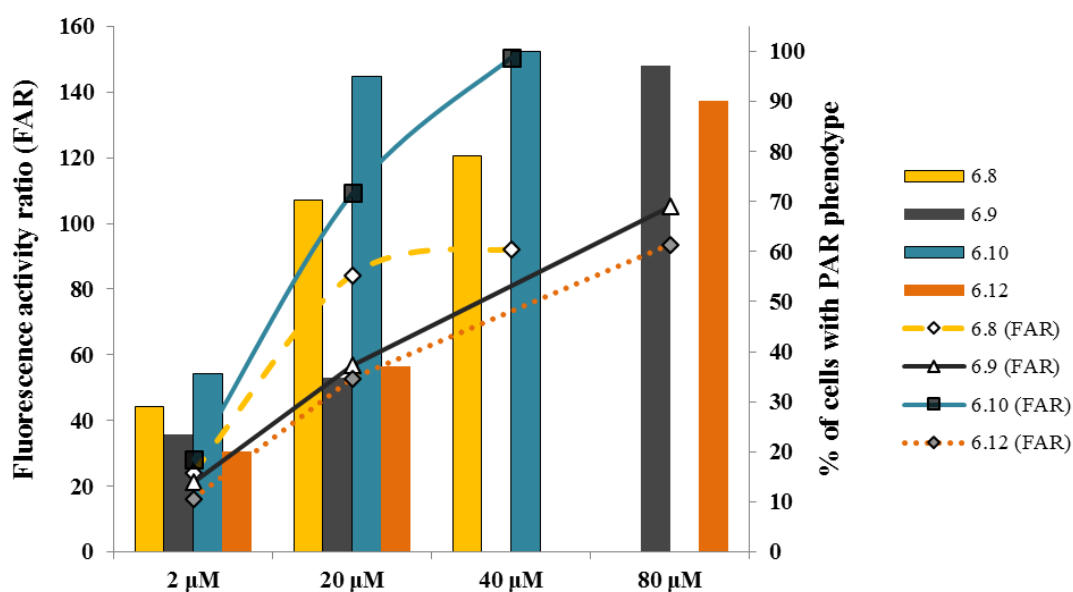


Figure 4.2. Relation between fluorescence activity ratio (FAR; lines) and percentage of MDR cells that reverted to a PAR phenotype (bars), for compounds **6.8-6.10** and **6.12**. This analysis clearly shows the dose-dependent inhibitory effect of P-gp efflux.

4.2.3. Structure-activity relationships (SAR) studies

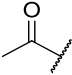
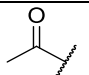
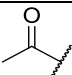
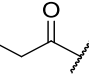
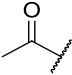
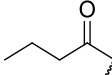
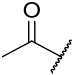
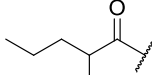
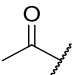
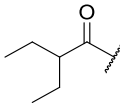
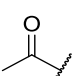
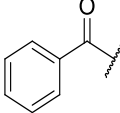
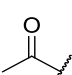
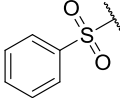
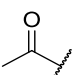
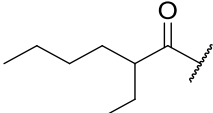
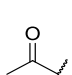
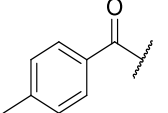
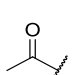
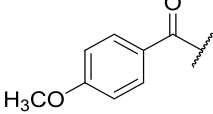
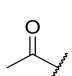
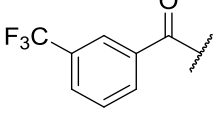
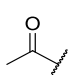
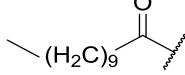
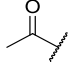
First set 6.1-6.12 and 6.23: K-means clustering and linear regression analysis.

The acylated derivatives at C-3 of jolkinol D constitute a good set of homologous compounds to determine structure-activity relationships. Therefore, some physicochemical properties of compounds **6**, **6.1-6.12** and **6.23** were determined and subdivided by the K-means cluster analysis into five main clusters, in which a high degree of similarity was found (Table 4.3).

Cluster **I** comprises compounds **6** and **6.23**, molecules that have a molecular weight below 400 g.mol⁻¹ and log*P* lower than 4.0, which are often considered poor P-gp substrates (Didziapetris *et al.*, 2003). Cluster **II** includes compounds **6.1**, **6.2** and **6.3** (Table 4.3), differing in the size of the ester side chain (one or two methylene units). In this group, and despite the low number of molecules, it was possible to correlate the increase in P-gp inhibitory activity with the increase of the molecular weight (MW, $r^2 = 0.96$) and solvent accessible area (ASA, $r^2 = 0.94$ at 2 μM , and at 20 μM , with ASA, $r^2 = 0.77$).

Cluster **III** comprises compounds **6.5**, **6.6**, **6.8** and **6.12** (Table 4.3). Within this group, a single correlation could be determined with ASA ($r^2 = 0.84$, 20 μM). However, compounds bearing an aromatic moiety (**6.8** and **6.12**) displayed higher MDR reversal activity at 2 μM when compared with all the alkanoyl derivatives. This observation is in agreement with previous studies by our group that identified aromatic moieties to be important for the establishment of additional hydrophobic interactions within the drug-binding pocket (Ferreira *et al.*, 2011; Ferreira *et al.*, 2014b). Cluster **IV** includes the most active molecules identified in this particular study, namely compounds **6.7** and **6.9-6.11** (Table 4.3). A strong correlation was found within this group between octanol/water partition coefficient and FAR (log*P*, $r^2 = 0.96$ and $r^2 = 0.86$ at 2 μM and 20 μM , respectively; these two properties are inversely proportional). Jolkinoate D (**6.4**) remained alone in Cluster **V**, because its physicochemical features are very dissimilar from the remaining compounds (Table 4.3).

Table 4.3. Cluster analysis (K-means algorithm) of the compounds jolkinol D (**6**) and derivatives (**6.1- 6.12** and **6.23**). Grouping variables are physicochemical properties: molecular weight (MW), molecular volume (MV), octanol/water partition coefficient ($\log P$), molar refractivity (MR), topological polar surface area (TPSA), accessible solvent area (ASA) and FAR values (at 2 μM).

Compound	Substituent		FAR (2 μM)	Physico-chemical properties ^a					
	C-3	C-15		MW	MV	$\log P$	MR	TPSA	ASA
Cluster I									
Jolkinol D (6)	H		0.79	360	377.4	3.8	10.1	63.6	587.01
Jolkinodiol (6.23)	H	H	0.84	318	339.0	3.3	9.0	57.5	540.04
Cluster II									
Jolkinolate A (6.1)			1.16	402	414.5	4.4	11.1	69.7	629.51
Jolkinolate B (6.2)			2.95	430	433.3	4.8	11.6	69.7	661.45
Jolkinolate C (6.3)			5.15	416	449.6	5.2	12.1	69.7	642.79
Cluster III									
Jolkinolate E (6.5)			7.14	459	486.0	5.8	13.0	69.7	695.65
Jolkinolate F (6.6)			4.99	458	486.9	5.8	13.0	69.7	686.88
Jolkinolate I (6.8)			24.15	465	477.6	5.7	13.2	69.7	698.05
Jolkinolate M (6.12)			16.06	501	488.6	5.2	13.6	86.7	699.81
Cluster IV									
Jolkinolate G (6.7)			10.55	486	520.9	6.6	13.9	69.7	734.80
Jolkinolate J (6.9)			21.11	476	492.9	6.0	13.6	69.7	732.92
Jolkinolate K (6.10)			28.09	492	503.4	5.7	13.8	78.9	746.18
Jolkinolate L (6.11)			9.32	533	503.4	7.0	13.8	69.7	736.54
Cluster V									
Jolkinolate D (6.4)			1.74	543	592.4	8.3	15.8	69.7	916.70

^a Physico-chemical properties were calculated in MOE v2010.10³⁴

The main conclusions of this first SAR analysis highlighted the importance of the lipophilicity and aromaticity for modulation ability of P-gp efflux (Figure 4.3). The aromatic residues of compounds that interact with P-gp are assumed to establish π - π interactions with phenylalanine or tyrosine residues within the drug-binding pocket (Baird, 2003). To further investigate this assumption, the subsequent derivatives were substituted with electron withdrawing/donating groups at different orientations, so as to relate the strength of the aromatic interactions with P-gp efflux modulation.

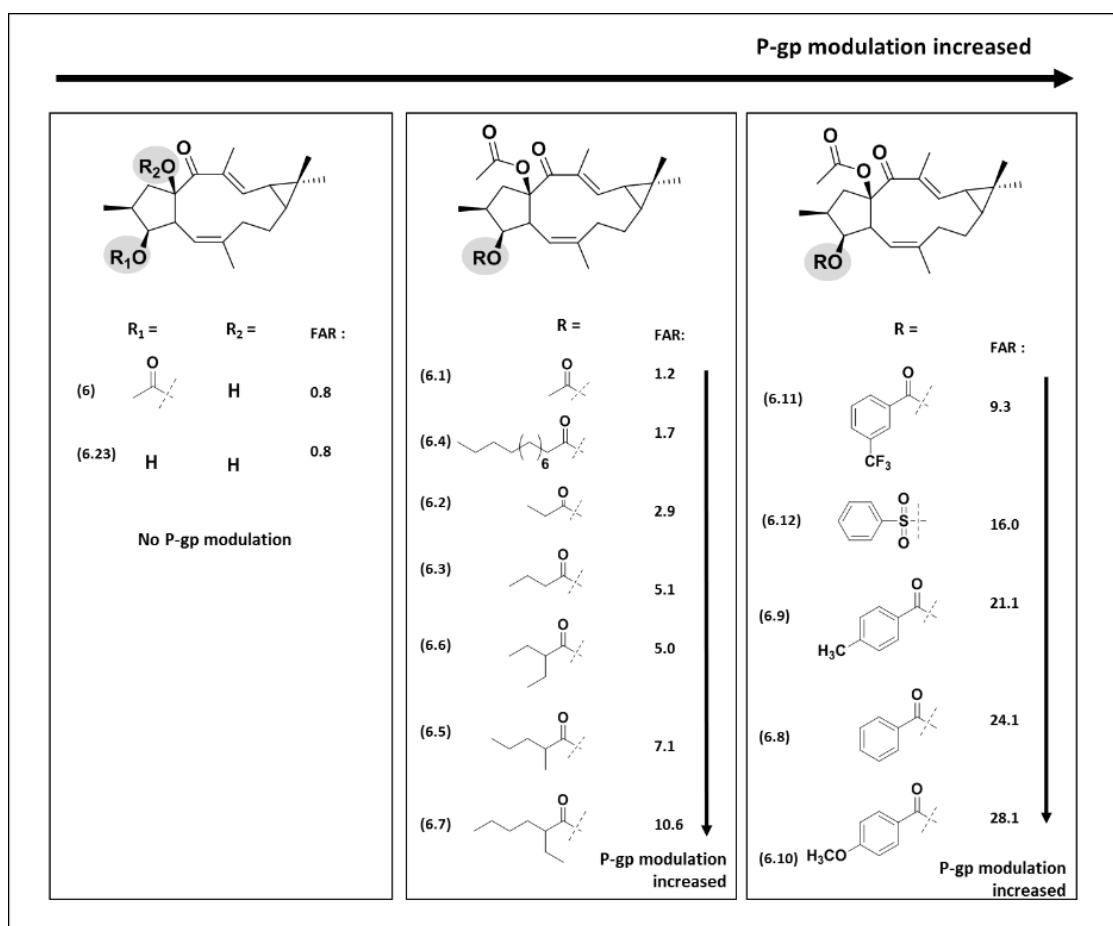


Figure 4.3. Resume of structure–activity relationships of jolkinol D (6) and derivatives 6.1–6.12 and 6.23. FAR values at 2 μ M.

Second set 6.13–6.22 and 6.24–6.27: K-means clustering and aromatic interactions

Compounds 6.13–6.22 and 6.24–6.27 were submitted to K-means clustering. Four groups that share a high degree of similarity, in terms of physicochemical properties and activity at 2 μ M, were created (Figure 4.4). The first cluster gathers compounds with the bulkier substituents (6.16, 6.18, 6.19, 6.20 and 6.27), therefore presented the higher MW,

MV, $\log P$, MR and ASA (Figure 4.4). The most active compounds **6.14**, **6.15** and **6.17** share physicochemical properties of compounds in clusters I and III, thus were grouped mainly due to the FAR values (Figure 4.4). Cluster III comprises the jolkinodiol derivatives **6.24-6.26** plus compounds **6.13** and **6.22**. Jolkinofornate A (**6.21**) is single at cluster IV.

Contrary to what was described for the first set of compounds, no significant correlations were found between the computed physicochemical properties and P-gp modulatory activity. This is suggestive of a stronger role of particular structural aspects, than the contribution of general physicochemical properties.

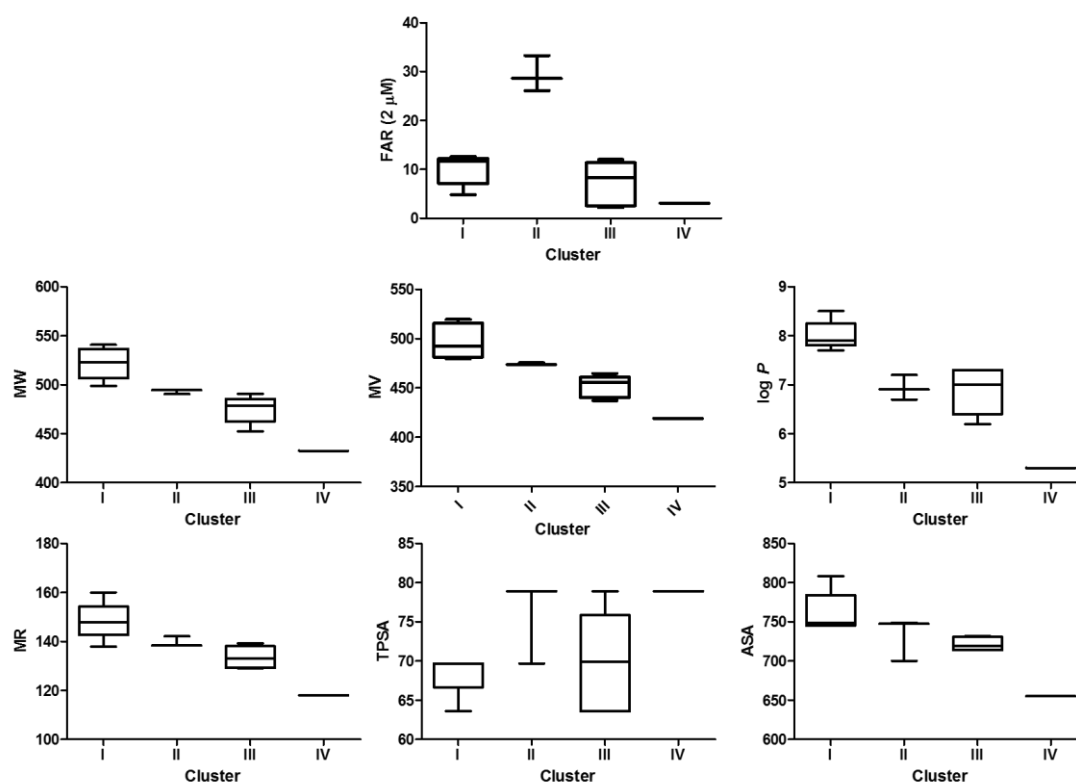


Figure 4.4. Cluster analysis of compounds **6.13-6.22** and **6.24-6.27**. Box and whiskers plot representing each grouping variable: FAR values ($2 \mu\text{M}$), molecular weight (MW), molecular volume (MV), octanol/water partition coefficient ($\log P$), molar refractivity (MR), topological polar surface area (TPSA), and accessible solvent area (ASA). Physicochemical properties were calculated using JME molecular editor, version July 2015, <http://www.molinspiration.com/jme>.

To investigate the relation between the aromatic electronic density and P-gp efflux modulation, electron withdrawing/donating groups at different orientations were tested (Figure 4.5). In this way, the introduction of trifluoromethyl, an electron-withdrawing group, at *meta* or *para* positions was verified to decreased the efflux modulatory efficiency in 2.5-fold (FAR = 9.3 and 9.4, respectively to **6.11** and **6.16**), in respect to jolkinolate I (**6.8**; FAR = 24.2). Likewise, jolkinofornate B (**6.22**; FAR = 10.8) with a phenyl formate substituent loss modulatory ability in comparison to **6.8**.

On the other hand, jolkinolate J (**6.9**) with a moderate electron-donating methyl group at *para* position, retained the strong modulatory character (FAR = 21.1). However, jolkinolate N (**6.13**; FAR = 2.2), displaying this group at *meta* position, showed to be almost inactive. The effects of a strong electron-donating group were investigated by using the methoxy group. Incorporation of this group at the *ortho* (**6.15**; FAR = 33.3) and *para* (**6.10**; FAR = 28.1) positions seemed to have a slightly higher electronic influence, due to the resonance effects, than its displacement at *meta* (**6.14**; FAR = 26.1). Nevertheless, differences in activity were not significant. Similarly, jolkinolate R (**6.17**; FAR = 28.6), bearing a cinnamoyl moiety, was also among the strongest modulators of the study, suggesting the aromatic conjugated system as a strong contributor for P-gp modulation.

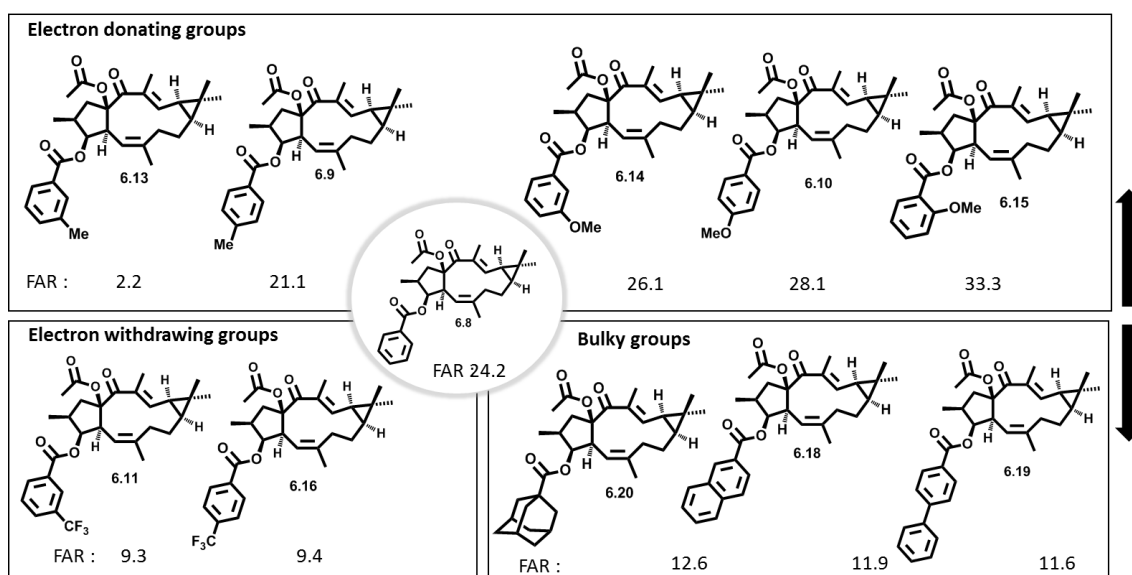


Figure 4.5. Structure–activity relationships of jolkinol D derivatives: effects of electron withdrawing/donating groups and bulky substituents. FAR values at 2 μ M.

The potential steric hindrance on P-gp efflux modulation was studied by inclusion of bulky groups like naphthoyl (**6.18**; FAR = 11.9), biphenyl (**6.19**; FAR = 11.6) and adamantly (**6.20**; FAR = 12.6). A reduction of about 2-fold of modulatory efficiency, when compared to **6.8**, may suggest the introduction of a bicyclic ring structure potentiates steric clashes within the drug-binding pocket of P-gp, independently from its aromatic nature. Similar observations were found by Jiao *et al.* These author verified that lathyrol derivatives with 1-naphthylacetyl or phenylacetyl substituents lost P-gp modulatory ability (Jiao *et al.*, 2015).

Moreover, derivatives of jolkinodiol (**6.23**) were included to test the role of the acetyl group at C-15. Jolkinolate A (**6.24**) with a methoxy group at *meta* position presented a 2-fold loss in efficacy in comparison to **6.14**. The same tendency was verified for compounds **6.25** and **6.27** in comparison to their respective counterparts (**6.18** and **6.19**). Therefore, the presence of the acetyl group at C-15 as a hydrophobic point or electron acceptor moiety might be more important for recognition/interaction with P-gp than a presence of a hydrogen bond donor. These findings are in accordance to the *in-house* pharmacophore model, based on macrocyclic diterpenes and other P-gp inhibitors, in which the recognition pattern contains three hydrophobic moieties and one hydrogen-bond acceptor group (Ferreira *et al.*, 2011).

The main conclusions of this second SAR emphasize the inclusion of electron donating groups, to the benzyl moiety, as favorable for the modulatory activity of jolkinolates, by increasing the electrostatic interactions and π -stacking at the drug binding pocket of P-gp.

4.2.4. Chemosensitization: reversion of drug-induced resistance

Since the studied compounds **6**, **6.1-6.27** showed activity as P-gp efflux modulators, the following step was to address what would be the outcomes of a combination with an antineoplastic drug, such as doxorubicin. This chemotherapeutic agent is not only transported by P-gp, but also induces its expression in cancer cells and, therefore, its cytostatic efficacy is limited by P-gp activity (Szakács *et al.*, 2006). The effect of drug interactions on L5178Y-MDR cells was assessed by the combination index (CI) as synergistic, additive or antagonistic (Chou, 2010). As can be observed in Table

4.4, most of the compounds synergistically enhanced cytotoxicity of doxorubicin (CI = 0.06 – 0.84). These resistance modulators were able to restore sensitivity to doxorubicin, which is in accordance with the assumption that a promising P-gp inhibitor would consequently be able to increase the action of a cytotoxic drug, due to greater efflux impairment. However, compounds **6.4**, **6.17**, **6.20** and **6.21**, strong P-gp inhibitors at 20 μ M, presented an antagonistic effect on the combination assay (CI = 1.11-2.02). Beyond the modulatory efflux activity, these derivatives might affect other cellular pathways, thus, may antagonize doxorubicin effect by competing or inhibiting its targets, independently from interaction with P-gp. On the other hand, jolkinol D (**6**) a non P-gp modulator, showed a synergistic effect with doxorubicin. This may suggest that other distinct mechanisms, besides the direct P-gp modulation, could be involved in MDR reversal.

4.2.5. Effects on the ATPase activity of P-gp

The P-gp mediated efflux is coupled to ATP hydrolysis, being often stimulated by the transported substrates (Ambudkar *et al.*, 1999; Chufan *et al.*, 2015). Measurement of this catalytic activity is an approach to investigate, whether, a candidate modulator acts as substrate or inhibitor. Assessment of ATPase activity can be carried out using isolated membrane vesicles from cells expressing high concentrations of P-gp (Özvegy *et al.*, 2001; Chang *et al.*, 2006). For instance, compounds like ketoconazole, paclitaxel, vinblastine and cyclosporine A present a dose dependent activation of ATPase activity at low concentrations, while at higher doses inhibition is found. Whereas, other substrates as erythromycin, nifedipine, quinidine, dexamethasone and verapamil, produce a saturable dose dependent activation of ATPase activity. Cyclosporin A, a known P-gp inhibitor, is able to abrogate the verapamil-stimulated ATPase activity of P-gp (Ambudkar *et al.*, 1999; Dongping, 2007).

Therefore, the parent compound jolkinol D (**6**) and the most active modulator of this set of lathyranes, jolkinoate P (**6.15**), were examined for their effect on the ATPase activity of P-gp. This activity was measured using SB-MDR1 PREADEASY™ ATPase kit, which uses purified insect membrane vesicles (Sf9) expressing high levels of human P-gp. The inorganic phosphate, resultant from ATP hydrolysis, can be detected by a simple colorimetric reaction.

Table 4.4. Effect of compounds **6**, **6.1-6.27** in combination with doxorubicin on L5178Y-MDR cells.

Combination Index (CI)			
Drug combination with	IC ₅₀		
Doxorubicin	Ratio ^a	CI ± SD ^b	Interaction
Jolkinol D (6)	40:1	0.26 ± 0.05	synergy
Jolkinoate A (6.1)	38:1	0.18 ± 0.03	strong synergism
Jolkinoate B (6.2)	8:1	0.34 ± 0.04	synergism
Jolkinoate C (6.3)	20:1	0.39 ± 0.04	synergism
Jolkinoate D (6.4)	5:1	2.02 ± 0.26	antagonism
Jolkinoate E (6.5)	4:1	0.23 ± 0.07	strong synergism
Jolkinoate F (6.6)	30:1	0.25 ± 0.04	strong synergism
Jolkinoate G (6.7)	65:1	0.31 ± 0.05	synergism
Jolkinoate I (6.8)	40:1	0.35 ± 0.06	synergism
Jolkinoate J (6.9)	33:1	0.26 ± 0.03	strong synergism
Jolkinoate K (6.10)	10:1	0.30 ± 0.04	synergism
Jolkinoate L (6.11)	18:1	0.27 ± 0.04	strong synergism
Jolkinoate M (6.12)	10:1	0.21 ± 0.05	strong synergism
Jolkinoate N (6.13)	-	-	-
Jolkinoate O (6.14)	25:1	0.84 ± 0.14	moderate synergism
Jolkinoate P (6.15)	10:1	0.09 ± 0.03	very strong synergism
Jolkinoate Q (6.16)	-	-	-
Jolkinoate R (6.17)	50:1	1.13 ± 0.37	slight antagonism
Jolkinoate S (6.18)	400:1	0.06 ± 0.02	very strong synergism
Jolkinoate T (6.19)	100:1	0.32 ± 0.08	synergism
Jolkinoate U (6.20)	15:1	1.11 ± 0.37	slight antagonism
Jolkinofornate A (6.21)	5:1	1.22 ± 0.28	moderate antagonism
Jolkinofornate B (6.22)	18:1	0.50 ± 0.07	synergism
Jolkinodiol (6.23)	23:1	0.65 ± 0.11	synergism
Jolkinolate A (6.24)	50:1	0.38 ± 0.16	synergism
Jolkinolate B (6.25)	-	-	-
Jolkinolate C (6.26)	200:1	0.20 ± 0.05	strong synergism
Jolkinolate D (6.27)	-	-	-

^aData is shown as the best combination ratio of the tested compounds and doxorubicin; ^bCombination index (CI) values are mean ± standard deviation (SD) for an inhibitory concentration of 50 % (IC₅₀). CI < 0.1: very strong synergism; 0.1 < CI < 0.3: strong synergism; 0.3 < CI < 0.7: synergism; 0.7 < CI < 0.9: moderate to slight synergism; 0.9 < CI < 1.1: nearly additive; 1.10 < CI < 1.45: moderate antagonism; 1.45 < CI < 3.30: antagonism (Chou, 2006, 2010).

Two complementary assays compose the ATPase kit: an activation and an inhibition assay. In the activation assay, compounds can be ranked as stimulating or inhibiting the baseline vanadate sensitive ATPase activity. The inhibition assay, which is performed in the presence of a known P-gp activator, is primarily used to characterize efflux inhibitors (or slowly transported substrates) through the reduction of verapamil-stimulated vanadate-sensitive ATPase activity by the tested compound. Verapamil (40 μM) and cyclosporin A (40 μM) were used as positive controls in the activation and inhibition assays, respectively.

Hence, compounds **6** and **6.15** were tested in a dose dependent manner. The ATPase activity is presented as relative, in which, the stimulated vanadate-sensitive ATPase activity is taken as 100% and the base line vanadate-sensitive ATPase activity as 0%.

Results from the ATPase assay indicate that jolkinol D (**6**) interacts with P-gp, enhancing 66-87% of the basal ATPase activity (Figure 4.6A, activation assay). However, this stimulation is not dose dependent. Also, this compound did not show any effect (stimulatory or inhibitory) in the verapamil-stimulated ATPase activity (Figure 4.6A, inhibition assay). As concluded in the rhodamine-123 assay, jolkinol D (**6**) had no modulatory effect on P-gp mediated efflux. Relating these observations, it might be concluded that jolkinol D (**6**) is a transported substrate, which does not compete with verapamil for the same binding sites. Moreover, this compound might have more affinity or compete with doxorubicin for efflux. The combination between this non modulator and the cytotoxic drug, presented a synergistic nature, which may suggest accumulation of doxorubicin in the detriment of jolkinol D efflux.

Interesting results were also obtained with the strong modulator jolkinoate P (**6.15**). This compound stimulated the basal ATPase activity of P-gp (Figure 4.6B, activation assay), but in a lower extent in comparison to verapamil (100%) or jolkinol D (**6**). Compound **6.15** was able to abrogate this basal activity for concentrations higher than 50 μM . When tested in the presence of second substrate, jolkinoate P (**6.15**) was able to reduce the verapamil-stimulated ATPase activity, and at 1.56 and 25 μM was able to completely inhibit this activity (Figure 4.6B, inhibition assay). A biphasic dose-response relationship is suggested by these results. The biphasic nature of P-gp ATPase dose-response was observed for numerous compounds (Calabrese, 2008) and may be due to

the polyspecificity of the drug binding sites. Therefore, jolkinolate P (**6.15**), in some extent, seems to have a different modulatory profile from verapamil, showing a lower stimulatory effect of the basal ATPase.

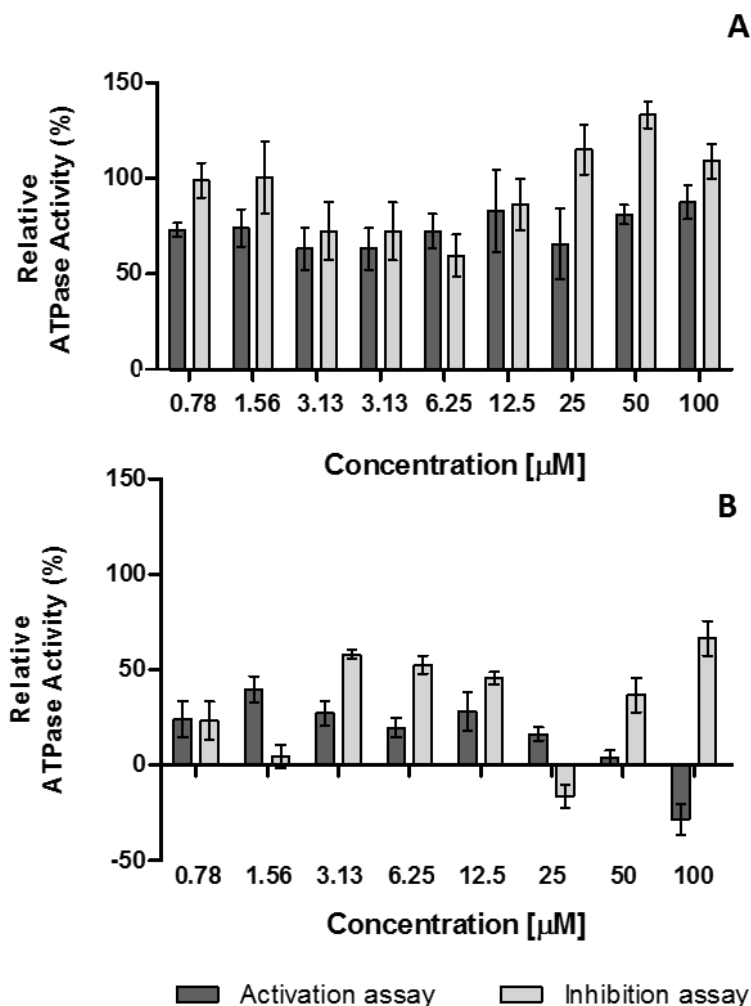


Figure 4.6. (A) Effect of jolkinol D (**6**) and (B) jolkinolate P (**6.15**) on P-gp ATPase activity. Activation assay: to test the effect on the basal ATPase activity. Inhibition assay: to test the effect on drug-stimulated ATPase activity, measured in the presence of verapamil (40 µM). Results are expressed as the mean ± SD from experiments performed in duplicate. The effects of compounds were presented as the relative ATPase activity, in which, the verapamil-stimulated vanadate-sensitive ATPase activity is taken as 100% and the baseline vanadate-sensitive ATPase activity as 0%.

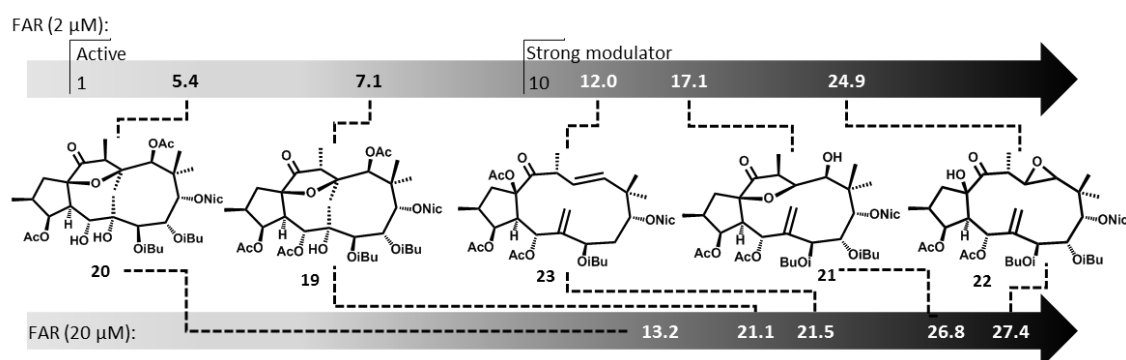
Chapter 5

***Euphorbia welwitschii*: from structural elucidation to
MDR reversal activity. Results and Discussion**

The phytochemical study of *Euphorbia welwitschii* afforded four new jatrophanes (**19-22**), together with the isolation of esulatin M (**23**), a known $\Delta^6(17),\Delta^{11}$ -jatropane, and two known flavonoids, quercetin 3-*O*- α -L-3'',5''-diacetyl-arabinofuranoside (**24**) and catechin (**25**). Welwitschines A (**19**) and B (**20**) present a unique combination of structural features: a 5/8/8 fused-ring system and an 12,15-ether bridge. Insights into the biogenetic pathway of 12,17-cyclojatrophanes were proposed using welwitschene (**21**) and epoxywelwitschene (**22**) as precursors of welwitschines A and B. Structures of compounds **19-25** were determined by spectroscopic methods, mainly by 1D and 2D NMR experiments, and X-ray crystallography for the 12,17-cyclojatrophanes **19** and **20**.

Compounds **19-24** were assessed for their potential MDR reversal activity. The results indicated the jatrophanes **19-23** as strong P-gp modulators. However, the conformational flexibility of the twelve-membered ring of jatrophanes **21-23**, seems to favor P-gp modulation, in contrast to the more rigid tetracyclic scaffold of diterpenes **19** and **20**. Epoxiwelwitschene (**22**), the strongest modulator of this group, may impair P-gp efflux through a competitive modulation mechanism, as concluded in the ATPase activity assay. Drug combination experiments also corroborated the anti-MDR potential of these diterpenes due to their synergistic interaction with doxorubicin.

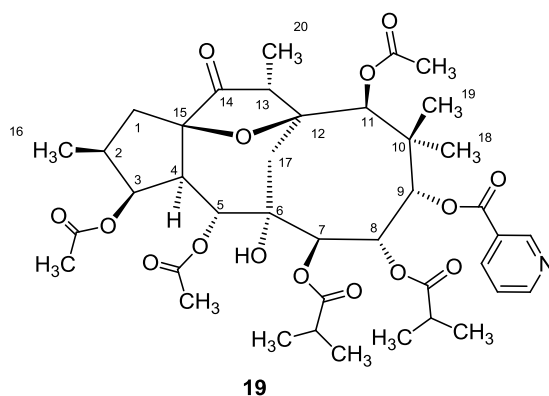
Graphical abstract



5.1. Structure elucidation of isolated compounds

5.1.1. Diterpenes with jatrophone-type scaffold

5.1.1.1. Welwitschine A - 3 β ,5 α ,11 β -triacetoxy-7 β ,8 α -diisobutyryloxy-9 α -nicotinoyloxy-12,15-epoxy-12,17-cyclojatrophone-6 α -ol-14-one (**19**)



Compound **19**, named welwitschine A, was obtained as white crystals (m.p. 225–228 °C; $[\alpha]_D^{24} + 2.9$). The IR absorptions at 3447 and 1738 and 1641 cm^{-1} suggested the presence of hydroxyl and carbonyl functions. The molecular formula $\text{C}_{40}\text{H}_{53}\text{NO}_{15}$, consistent with 15 degrees of unsaturation, was deduced from HRMS-ESI-TOF at m/z 788.3499 $[\text{M} + \text{H}]^+$ (calcd for $\text{C}_{40}\text{H}_{54}\text{NO}_{15}$ 788.3488).

The ^1H NMR spectrum of welwitschine A (**19**), when recorded in CDCl_3 , presented several broad and overlapped signals. Therefore the solvent was changed to C_6D_6 and better separated NMR resonances were obtained allowing the unambiguous assignments of all ^1H and ^{13}C signals. The ^1H and ^{13}C NMR data (Table 5.1) suggested compound **19** to be a polyester rearranged jatrophone-type diterpene. From the NMR spectra six ester residues could be identified as: three acetoxy, two isobutyryloxy groups and one nicotinoyloxy moiety. Moreover, the remaining signals corresponded to a C_{20} diterpenic scaffold (Table 5.1), constituted of five quaternary carbons (one carbonyl at δ_{C} 218.7), nine methines (six bearing oxygen), two methylenes and four methyl groups. The aforementioned data accounted, so far, for 11 degrees of unsaturation, which suggested the skeleton of welwitschine A (**19**) should be tetracyclic.

Table 5.1. ¹H and ¹³C NMR data (δ) for compounds **19** and **20** (400 and 101 MHz, respectively).

position	Welwitschine A (19)				Welwitschine B (20) ^b	
	δH (J in Hz) ^a	δC ^a	δH (J in Hz) ^b	δC ^b	δH (J in Hz)	δC
1a	1.68 dd (13.2, 6.5)		1.86 m		1.87 m*	
1b	1.93 m*	42.9	2.01 m*	43.1	2.07 m	43.0
2	2.19 m	37.5	2.26 m*	37.3	2.26 m	37.1
3	5.45 bs	77.5	5.36 t (3.8)	77.5	5.42 bs	77.9
4	3.04 dd (11.0, 4.7)	50.8	2.87 dd (11.1, 4.9)	50.2	2.60 dd (10.5, 4.9)	54.0
5	6.27 d (11.0)	69.0	5.96 d (11.1)	68.7 [†]	4.69 dd (10.5, 4.6)	68.2
6	-	74.0	-	73.7	-	72.7
7	5.91 d (10.0)	75.9	5.41 d (10.1)	75.5	5.51 d (8.0)	80.8
8	6.41 d (10.0)	69.2	6.00 d (10.1)	68.6 [†]	5.83 dd (8.0, 3.3)	74.6
9	6.01 s	82.7	5.53 bs	82.5	6.77 d (3.3)	74.2
10	-	44.4	-	43.9	-	43.0
11	5.40 s	75.0	5.07 s	74.8	5.27 s	81.3
12	-	84.9	-	84.8	-	84.9
13	2.68 m*	54.0	2.64 q (6.6)	53.8	2.36 m	54.7
14	-	218.1	-	218.7	-	220.2
15	-	86.1	-	85.5	-	85.6
16	0.73 d (6.4)	13.0	0.90 d (6.6)	13.1	0.98 d (6.6)	13.0*
17a	2.64 d (17.1)*		2.01 m*		2.84 d (16.3)	
17b	2.34 d (17.1)	42.4	2.30 m*	42.0	1.87 m*	53.8
18	1.06 s	31.2	1.00 s	31.1	1.30 s	23.6
19	1.96 s*	20.0	1.63 s	20.7	1.26 s	20.7
20	1.04 d (6.7)	7.6	1.02 d (6.6)	7.7	1.23 d (7.1)	13.0*
5-OH	-	-	-	-	3.62 d (4.6)	-
6-OH	3.13 s	-	2.96 s	-	4.09 s	-
3-OAc	-	170.1	-	171.3	-	172.7
	1.90 s	20.4	2.09 s	21.4	2.42 s	20.8 [†]
5-OAc	-	169.4	-	168.7	-	-
	1.75 s	20.6	1.98 s	21.4	-	-
11-OAc	-	168.8	-	170.1	-	170.1
	1.49 s	19.4	2.15 s	21.0	2.18 s	20.8 [†]
7-OiBu	-	175.2 [†]	-	175.3 [†]	-	175.5
2'	2.08 m	34.4 [†]	2.29 m*	34.0 [†]	2.44 m*	34.1* [†]
3'	0.83 d (6.9)	18.9 [†]	1.03 d (7.0)* [†]	18.5 [†]	1.02 d (7.0)* [†]	18.8* [†]
4'	0.93 d (6.9)	18.1 [†]	1.07 d (7.0)* [†]	18.8 [†]	1.04 d (7.0)* [†]	18.9* [†]
8- OiBu	-	175.0 [†]	-	175.4 [†]	-	176.4
2'	2.45 m	33.9 [†]	2.42 m	33.9 [†]	2.44 m*	34.2* [†]
3'	1.16 d (6.9)	18.0 [†]	1.13 d (7.0)* [†]	19.0 [†]	1.05 d (7.0)* [†]	19.0* [†]
4'	1.26 d (6.9)	18.5 [†]	1.15 d (7.0)* [†]	19.5 [†]	1.08 d (7.0)* [†]	19.2* [†]
9-ONic	-	164.9	-	164.2	-	164.6
2'	9.69 s	151.1	9.27 s	150.9	9.13 s	150.8
3'	-	125.7	-	125.6	-	125.9
4'	8.19 d (7.5)	136.6	8.30 d (7.9)	137.3	8.21 d (7.9)	137.2
5'	6.48 dd (7.5, 4.9)	123.5	7.47 dd (7.9, 5.0)	123.9	7.42 dd (7.9, 5.0)	123.6
6'	8.36 d (4.9)	154.1	8.82 dd (5.0, 1.2)	154.0	8.80 d (3.8)	153.8

^aspectra recorded in C₆D₆; ^bspectra recorded in CDCl₃; *overlapped signals; [†]interchangeable signals

A careful analysis of 2D NMR experiments (COSY, HMQC and HMBC) corroborated this assumption by building the connections of the suggested tetracyclic skeleton. In this way, the key ^1H - ^1H COSY correlations (Figure 5.1) indicated two main fragments (A) and (B). These spin systems were then connected through long range HMBC correlations of C-6 with H-4/H-5/H-7/H-8. C-9 was assigned through the HMBC signals of C-8 and C-10 with H-9. In fact no $J_{8,9}$ was observed, evidencing an orthogonal relationship between these protons. Moreover, the HMBC cross-peaks of the quaternary carbon C-10 designated positions C-11, C-18 and C-19. The $^2J_{\text{C-H}}$ and $^3J_{\text{C-H}}$ HMBC correlations of C-6 and C-12 with H-17a/b established the location of C-17 between these two carbons. Finally, the ketone function was located at C-14 through its long range HMBC correlations with H-1a/H-1b/H-4/H-13/H-20. Fragment (A) was established as part of the pentacyclic ring through the correlations of C-15 with H-1a/H-1b/H-3/H-4 and correlations of C-1, C-2 and C-3 with H-16. The ester substitution pattern was also determined via HMBC through the couplings of the oxymethine protons and the corresponding carbonyl ester groups.

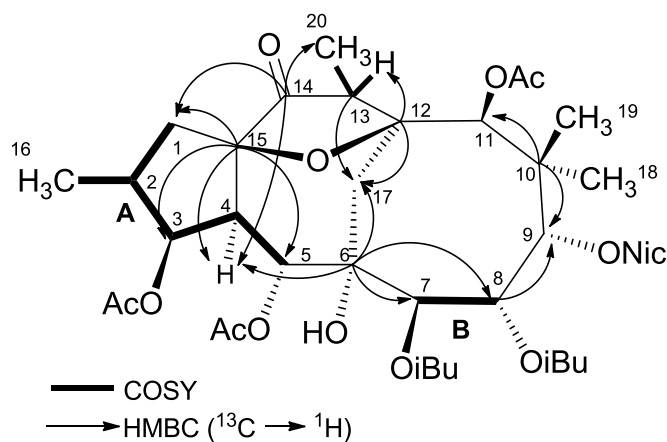


Figure 5.1. Key COSY and HMBC correlations for welwitschine (**19**). The spin systems A and B and their connection through the main heteronuclear $^2J_{\text{C-H}}$ and $^3J_{\text{C-H}}$ correlations.

Based on the molecular formula and the degree of unsaturation, one hydroxyl group at C-6 and an ether between C-12 and C-15 could be deduced. This 12,15-ether bridge is not common in macrocyclic jatrophanes; the only compounds that present such function were isolated exclusively from *E. helioscopia* (Kosemura *et al.*, 1985; Yamamura *et al.*, 1989; Tao *et al.*, 2008). Another rare structural feature of welwitschine

A (**1**) is the 5/8/8 fused ring system, which up to date was only found in salicifoline (Hohmann *et al.*, 2001).

The relative stereochemistry of welwitschine A (**19**) was determined by a NOESY experiment (Figure 5.2). The α -oriented H-4 was taken as a reference on a biogenetic basis (Liu and Tan, 2001; Tian *et al.*, 2011). Strong NOE interactions between H-4 and H-3/H-2/H-1a indicated α -orientation for these three protons. The stereochemistry at C-2 was further confirmed by comparing the coupling constant values $J_{2,3}$ and $J_{3,4}$ ($J_{2,3} = J_{3,4} = 4.7$ Hz) with literature data, which are in agreement with a β configuration for H-16 (H-16 α , $J_{2,3} \approx 2.0 - 3.5$ Hz and $J_{3,4} \approx 7.5$ Hz) (Tian *et al.*, 2011; Valente *et al.*, 2012). The nuclear Overhauser effect between H-5/H-8, H-8/H-9, H-8/H-19 and H-9/H-19 indicated these protons lay on the same side of the molecule. Whereas NOE cross-peaks between the H-18/H-11, H-11/H-7, H-11/H-17a and H-7/H-17a suggested an α -orientation for these protons. The relative configuration at C-13 was indicated by the NOE effects between H-20/H-11 and H-20/H-17a.

Crystal structure of **19**² was determined by X-ray crystallography (Figure 5.3 A), confirming all the assignments made by NMR. This compound crystallizes in $P2_1$ monoclinic space group, with two crystallographically independent molecules per asymmetric unit (Figure 5.3 B). Both molecules display similar relative configuration. Pairs of crystallographically independent molecules are formed via two O-H...O hydrogen bonds [2.855(7)Å, and 2.902(6)Å].

² Details for compound **19** (CCDC 1062514): C₈₀H₁₀₆N₂O₃₀, fw=1575.66, monoclinic, space group $P2_1$, $a=12.0328(4)$ Å, $b=21.7465(6)$ Å, $c=15.6177(4)$ Å, $\beta=95.277(1)^\circ$, $V=4069.4(2)$ Å³, $Z=2$, $T=150$ K, $\rho_{\text{calc}}=1.286$ mg.m⁻³, $\mu=0.098$ mm⁻¹; of 30469 reflections, 16390 were independent ($R_{\text{int}}=0.0495$); $R1(I > 2\sigma(I))=0.0674$, $wR2(I > 2\sigma(I))=0.1641$, GOF=1.018.

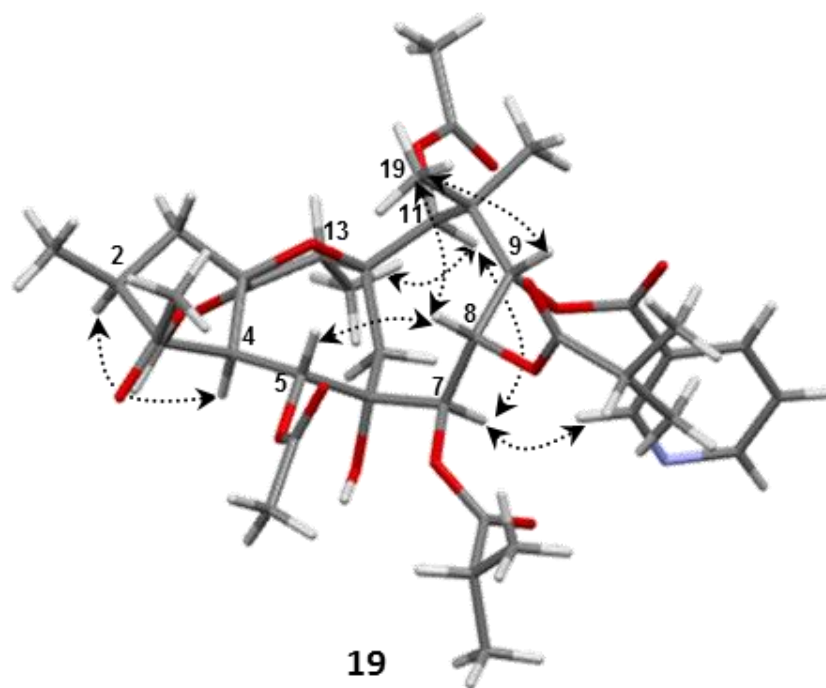


Figure 5.2. Key NOESY correlations of welwitschine A (**19**).

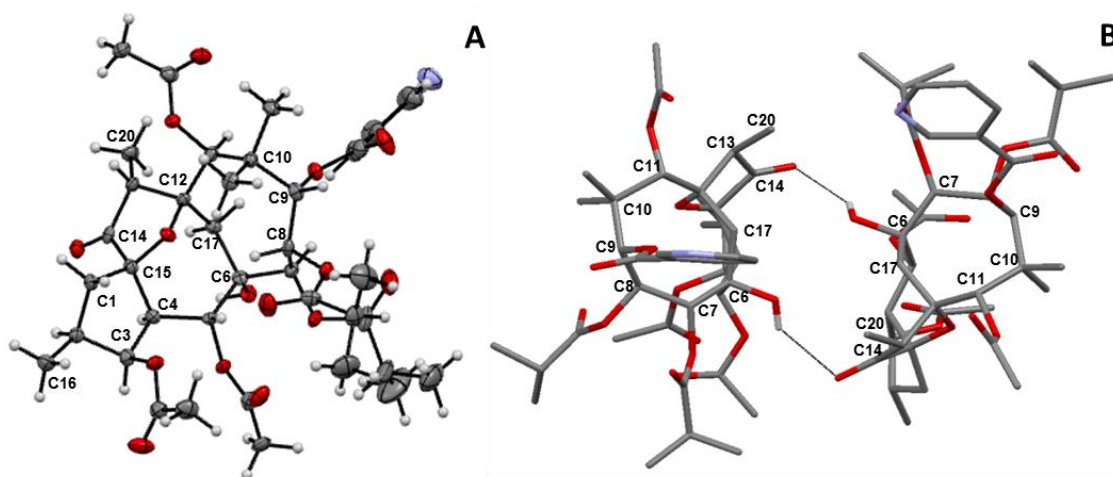
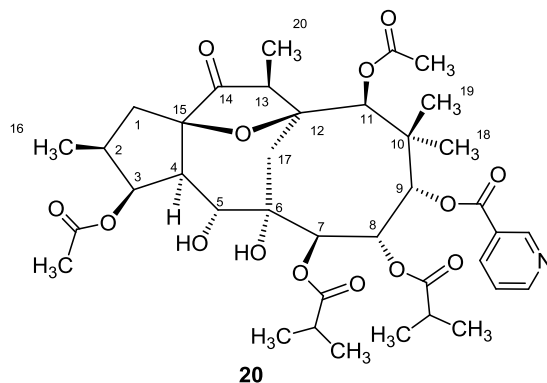


Figure 5.3. Crystallographic structure of **19**: (A) ORTEP diagram of welwitschine A (**19**); (B) Hydrogen bonds forming pairs of crystallographically independent molecules of **19** (hydrogen atoms were omitted for clarity).

5.1.1.2. Welwitschine B - 3 β ,11 β -diacetoxy-7 β ,8 α -diisobutyryloxy-9 α -nicotinoyloxy-12,15-epoxy-12,17-cyclojatropa-5 α ,6 α -diol-14-one (20)



Compound **20**, named welwitschine B, $[\alpha]_D^{24} -45.6$, was obtained as white crystals (m.p. 285-288 °C). Its molecular formula was established as $C_{38}H_{51}NO_{14}$, based on the pseudomolecular molecular ion peak at m/z 746.3377 $[M + H]^+$ on HRMS (calcd for $C_{38}H_{52}NO_{14}$, 746.3382). The NMR data (Table 5.1) indicated welwitschine B (**20**) as having the 5/8/8 diterpenic core and the same substitution pattern as **19**, with an exception at C-5. At this position, welwitschine B (**20**) bears a hydroxyl group (δ_{C5} 68.2; δ_{H5} 4.69 dd, $J = 10.5, 4.6$ Hz). The hydroxyl proton (δ_{OH} 3.62 d; $J_{5,OH} = 4.6$ Hz) shows an unusual coupling, suggesting its involvement in intramolecular hydrogen bonding. However, a detailed analysis of the ^{13}C NMR data (Table 5.1) revealed striking differences between diterpenes **20** and **19**. In fact, strong paramagnetic effects at C-4 ($\Delta\delta = +3.8$), C-7 ($\Delta\delta = +5.3$), C-8 ($\Delta\delta = +6.0$), C-11 ($\Delta\delta = +6.8$) and C-17 ($\Delta\delta = +11.8$) and a significant diamagnetic effect at C-9 ($\Delta\delta = -8.9$) were observed (Table 5.1). Moreover, opposite optical rotation signals were found for both compounds, indicating a different stereochemistry. When analyzing the NOESY spectrum, NOE correlations were found to be similar to those observed for **19**, at all tetrahedral centers except at C-13 (Figure 5.4A), despite similar constant values observed between H-20 and H-13 ($J_{20-13} = 7.1$ and 6.6 Hz, for compounds **20** and **19**, respectively). Conversely to compound **19**, no NOE effects were recorded for both H-20 and H-13.

The crystal structure of **20**³, determined by single crystal X-ray diffraction (Figure 5.4B), confirmed the NMR assignments, and showed C-13 configuration to be opposite

³ Details for compound **20** (CCDC 1406167): $C_{38}H_{50}NiO_{14}$, fw=744.79, orthorhombic, space group $P2_12_12_1$, $a=11.0875(10)$ Å, $b=14.3476(13)$ Å, $c=23.495(2)$ Å, $V=3737.5(6)$ Å³, $Z=4$, $T=150$ K, $\rho_{calc}=1.324$ mg.m⁻³, $\mu=0.101$ mm⁻¹; of 30303 reflections, 7703 were independent ($R_{int}=0.1236$); $R1(I > 2\sigma(I))=0.0661$, $wR2(I > 2\sigma(I))=0.1249$, GOF=0.995.

to compound **19**. Thus, it was established as *13S*. The analysis of the crystal structure of **20** further showed that in this case O-H \cdots N hydrogen bonds [2.930(6) Å] give rise to zigzag chains in a view along the c-axis (Figure 5.5).

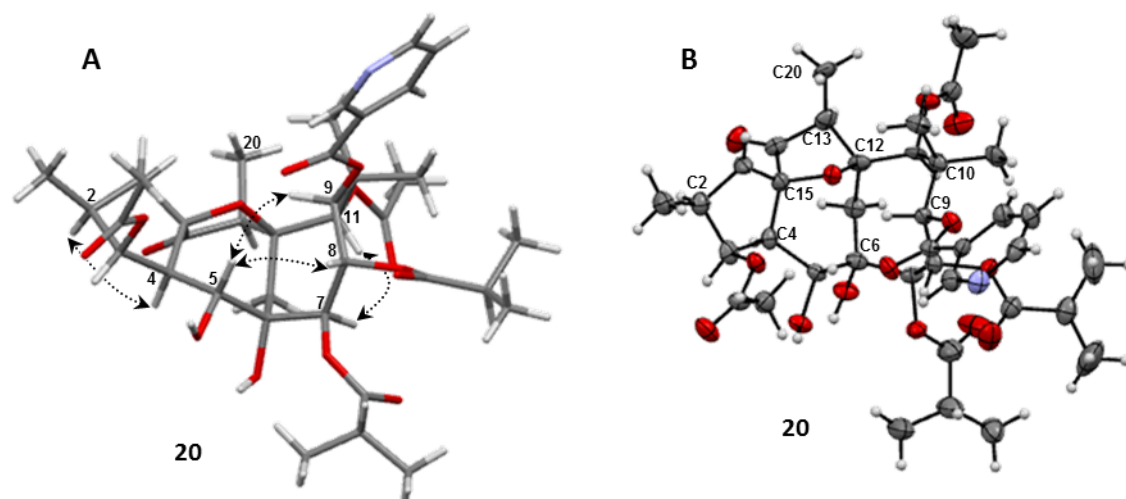


Figure 5.4 (A) Key NOESY correlations of welwitschine B. (B) ORTEP diagram of **20**.

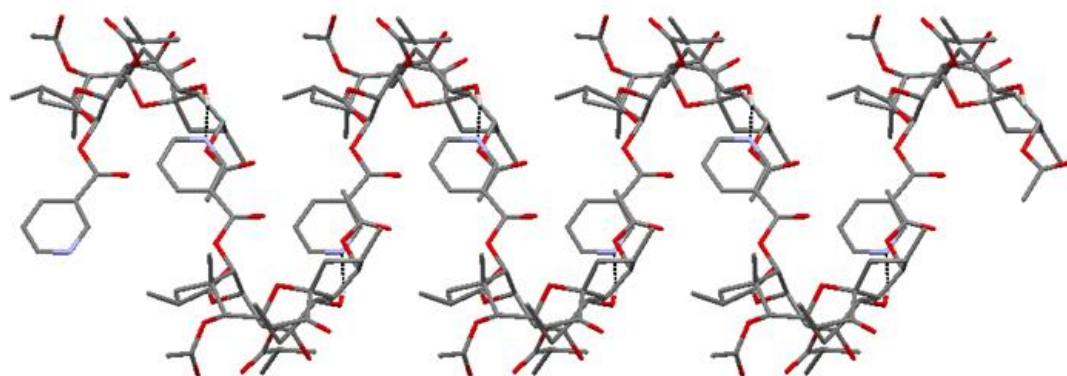
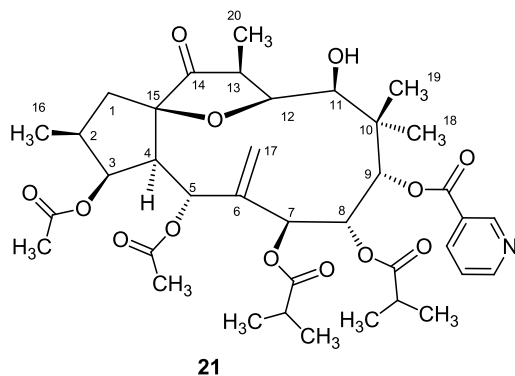


Figure 5.5. Hydrogen bonds in compound **20** giving rise to zigzag chains in a view along the c axis. Hydrogen atoms (except the ones involved in the hydrogen bonds in the respective images) were omitted for clarity.

Thus, comparison of the crystallographic structures of **19** and **20** revealed the compounds adopt two different conformations. The 5/8/8 diterpenic core of compound **20** is more bended than **19**. In this way, in compound **20**, a NOE signal between H-9/H-5 was recorded (Figure 5.4A), but the same was not found for **19**, which is in accordance to the distances measured between these protons [2.19367(16) and 4.60931(12-4.45480(8) Å, respectively]. This folded conformation made the nicotinoyloxyl moiety at C-9 to extend away, upwards from the diterpenic core, whereas, in **19**, with a less folded skeleton, this group adopted a conformation pointing downwards. The NOE interaction between the ortho proton at δ_H 9.27 and H-7 [distances of 2.58791(6) - 2.45380(6) Å] in compound **19** (Figure 5.2) and its absence in **20** supports this observation. Consequently, the strong paramagnetic and diamagnetic effects observed for welwitschine B (**20**), might be attributed to ring current effect of the nicotinoyl moiety.

4.1.1.3. Welwitschene - *3 β ,5 α ,-diacetoxy-7 β ,8 α -diisobutyryloxy-9 α -nicotinoyloxy-12,15-epoxy-jatroph-6(17)-en-11 β ol-14-one (21)*



Compound **21**, named welwitschene, $[\alpha]_D^{24} + 19.5$, has a molecular formula of $C_{38}H_{51}NO_{13}$, deduced from its ESI-TOF-HRMS spectrum that presented a pseudomolecular ion at m/z 730.3454 $[M + H]^+$ (calcd for $C_{38}H_{52}NO_{13}$, 730.3433), consistent with 14 degrees of unsaturation.

Through analysis of 1D and 2D NMR spectra, two acetoxy, two isobutyryloxy and one nicotinoyloxy ester residues were identified (Table 5.2). Moreover, the remaining signals indicated a $\Delta 6(17)$ jatrophane-type scaffold. The exomethylene double bond was evidenced by the presence of two broad singlets at δ_H 5.57 and 5.30 (Table 5.2).

Detailed structure information was obtained from 2D NMR data, which allowed the clear assignment of all the carbons and protons and the location of the functional groups (Figure 5.6). The presence of the 12,15-ether bridge was evidenced through the low-field resonances of C-15 (δ_C 87.8) and C-12 (δ_C 83.4) comparable to those found for compound **19** (δ_{C15} 85.5 and δ_{C12} 84.8, data recorded in $CDCl_3$). The broad singlet at δ 2.77, without correlation in the HMQC spectrum, but with a HMBC correlation with C-12, confirmed the existence of a hydroxyl group at C-11.

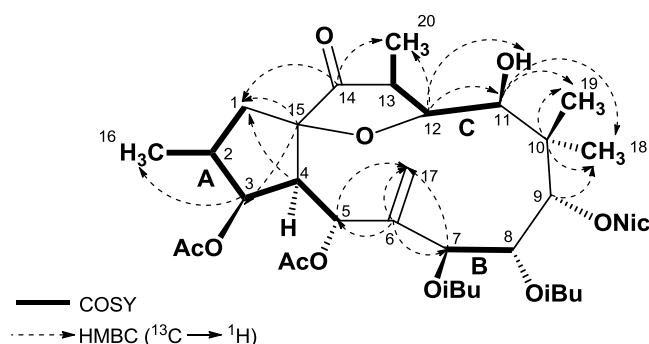


Figure 5.6. Key COSY and HMBC correlations for welwitschene (**21**). Spin systems A, B and C and their connection through the main heteronuclear $^2J_{C-H}$ and $^3J_{C-H}$ correlations.

The relative stereochemistry of welwitschene (**21**) was determined using the same approach as described above and all stereocenters presented the same configuration as compound **20** (Figure 5.7 A). Therefore, strong NOE interactions between H-4 α /H-2/H-3 and NOE cross-peaks between, H-13/H-11, H-13/H-7, H-7/H-11 and H-7/H-18 pointed out to the α -orientation of these protons. The β -configuration of the other protons was indicated by the NOESY correlations between H-19/H-9, H-19/H-8, H-9/H-8, H-9/H-5, H-8/H-5 and by the Overhauser effect between H-20/H-12, H-12/H-19.

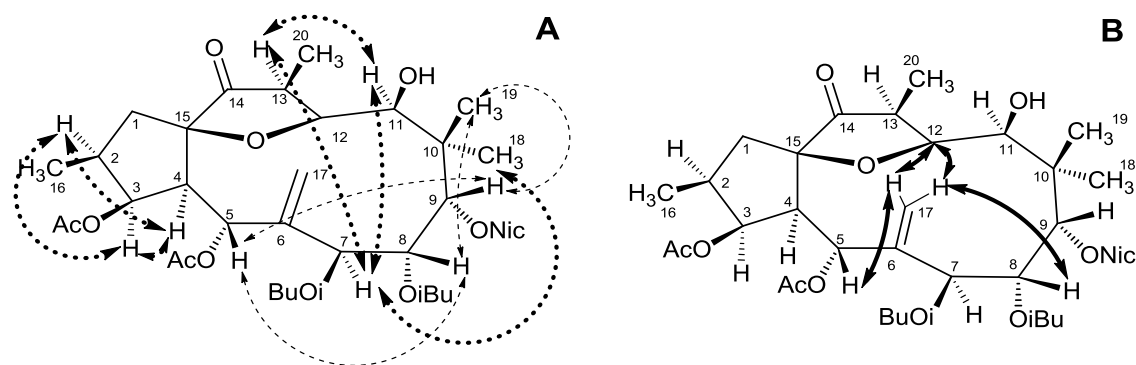


Figure 5.7. (A) Main NOESY correlations of welwitschene (**21**); dot bold: α -protons correlation and dash: β -protons correlation. (B) NOE signals that suggest a preferential *endo*-type conformation for welwitschene (**21**).

Through conformational analysis of $\Delta 6(17)$ -jatrophone derivatives, it was concluded that the macrocyclic ring could adopt two main conformations: *endo*- and *exo*-type, which can be diagnosed by the $J_{4,5}$ value and some NOESY correlations (Appendino *et al.*, 1998; Jakupovic *et al.*, 1998; Corea *et al.*, 2005). According to the *endo*-type conformation, the exomethylene is perpendicular to the main plane of the molecule and H-4/H-5 have anti-periplanar relationship, displayed as $J_{4,5} = 9\text{--}11$ Hz. The diagnostic NOEs for this kind of conformation are H-5/H-17a and H-17b/H-8. On the other hand, the *exo*-type conformation, with the exomethylene in the plane of the molecule, is characterized by a small $J_{4,5}$ coupling constant of 0-3 Hz, since H-4 and H-5 are almost orthogonal. Additionally, NOESY cross-peaks between H-4/H-7 and H-5/H-8 are also observed.

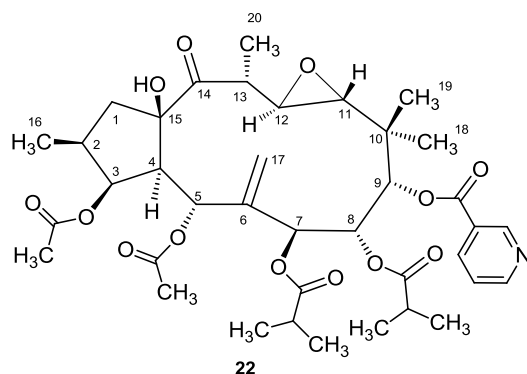
Therefore, according to the NOE interactions found between H-8/H-17b, H-5/H-17a (Figure 5.7B) and the anti-periplanar relationship of H-4 and H-5, evidenced by a large coupling constant value ($J_{4,5} = 10.1$ Hz), it was concluded that the macrocyclic ring of welwitschene (**21**) should adopt preferentially an *endo*-type conformation.

Table 5.2. ¹H and ¹³C NMR Data (δ) for compounds **21** (400 and 101 MHz) and **22** (300 and 101 MHz).

position	Welwitschene (21) ^a		Epoxiwelwitschene (22) ^a	
	δ H (J in Hz)	δ C	δ H (J in Hz)	δ C
1a	1.98 m		2.31 dd (13.9, 8.7)	
1b	1.81 m	45.6	1.58 dd (13.9, 11.2)	49.6
2	2.15 m	37.6	2.11 m*	37.2
3	5.49 bs	76.2	5.45 t (3.2)	78.4
4	3.10 bd (5.1)	54.2	3.43 dd (8.8, 3.2)	52.9
5	5.87 d (10.1)	66.4	5.62 d (8.8)	66.4
6	-	143.6	-	141.8
7	5.91 d (10.2)	75.2	5.76 d (2.3)	70.6
8	6.30 bd (8.3)	72.8	6.19 t (2.3)	69.5
9	6.55 bs	74.5	5.32 d (2.3)	79.4
10	-	44.3	-	38.6
11	3.91 bs*	76.2	3.12 d (1.8)	63.7
12	3.91 bs*	83.4	2.77 dd (8.8, 1.8)	58.8
13	2.38 m	46.7	3.23 m	43.7
14	-	221.6	-	214.7
15	-	87.8	-	87.0
16	0.91 d (7.2)*	13.3	0.89 d (7.0)	14.0
17 a	5.30 bs		5.39 bs	
17 b	5.57 bs	124.9	5.39 bs	122.9
18	1.34 s	21.6	1.11 s	26.5
19	1.02 s*	19.3	0.88 s	16.6
20	1.31 d (7.3)	17.2	1.27 d (6.7)	15.0
11-OH	2.77 bs	-	-	-
15-OH	-	-	3.57 s	-
3-OAc	-	172.0	-	170.3
	2.32 s	21.0	2.11 s	21.1 [†]
5-OAc	-	168.8	-	168.8
	1.88 s	20.8	1.90 s	21.2 [†]
7-OiBu	-	175.1	-	175.0
2'	2.45 m	34.0 [†]	2.11 m	33.9 [†]
3'	1.07 d (6.9)	18.4 [†]	0.70 d (7.0)	18.4 [†]
4'	1.03 d (6.9)*	18.5 [†]	0.86 d (7.0)	18.5 [†]
8- OiBu	-	175.6	-	176.0
2'	2.26 m	34.2 [†]	2.60 m	34.2 [†]
3'	0.97 d (6.8)	18.9 [†]	1.15 d (7.0)	18.8 [†]
4'	0.93 d (6.8)	19.1 [†]	1.18 d (7.0)	18.8 [†]
9-ONic	-	163.7	-	164.3
2'	9.10 s	150.7	9.27 d (1.6)	151.6
3'	-	126.4	-	125.2
4'	8.22 d (7.4)	137.4	8.38 dt (7.9, 1.9)	137.6
5'	7.37 dd (7.4, 4.0)	123.4	7.42 dd (7.9, 5.0)	123.5
6'	8.74 d (4.0)	153.3	8.78 dd (5.0, 1.6)	153.9

^aspectra recorded in CDCl₃; *overlapped signals; [†]interchangeable signals

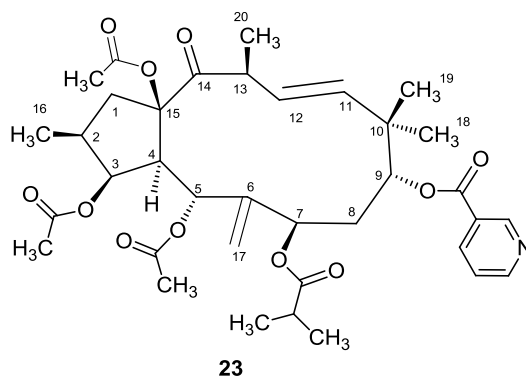
5.1.1.3. Epoxiwelwitschene - 3 β ,5 α ,-diacetoxy-7 β ,8 α -diisobutyryloxy-9 α -nicotinoyloxy-11,12-epoxy-jatroph-6(17)-en-15 β ol-14-one (**22**)



Compound **22**, $[\alpha]_D^{24} + 34.4$, was named as epoxiwelwitschene. Its molecular formula, $C_{38}H_{51}NO_{13}$, was deduced from HRMS-ESI-TOF that exhibited a pseudomolecular ion peak at m/z 730.3450 $[M + H]^+$ (calcd for $C_{38}H_{52}NO_{13}Na$, 730.3433). The 1H and ^{13}C NMR spectra (Table 5.2) of epoxiwelwitschene (**22**) indicated it as a $\Delta 6(17)$ -jatrophane polyester, with the same acylation pattern as compound **21**. The exomethylene double bond was depicted by the presence of a broad singlet at δ_H 5.39, which integration accounted for two protons. The chemical shifts at positions 11 (δ_C 63.7 and δ_H 3.11 bs) and 12 (δ_C 58.8 and δ_H 2.75 bd, $J = 8.8$ Hz) were consistent with an 11,12-epoxide ring (Hohmann *et al.*, 2001; Pan *et al.*, 2004). In addition, the presence of a broad singlet at δ_H 3.57, without correlation in the HMQC spectrum, but with HMBC cross-peaks with C-14 and C-15 confirmed the location of the alcohol function at C-15. The remaining structural features were clearly assigned through the interpretation of the 2D NMR data in the same way as it was described earlier.

The relative configurations of the tetrahedral centers of epoxiwelwitschene (**22**) were established based on a NOESY experiment. The epoxy group could be established as *trans*, through the strong NOE interactions between H-4 α /H-2/H-3/H-7, H-7/H-18, H-18/H-12 and between H-5 β /H-8, H-8/H-11 and H-11/H-9. Similarly to compound **21**, the macrocyclic ring of epoxiwelwitschene (**22**) may adopt preferentially the *endo*-type conformation (Jakupovic *et al.*, 1998).

5.1.1.4. Esulatin M (23)



Compound **23**, $[\alpha]_D^{24} - 15.8$, was isolated as an amorphous white powder. Its ESIMS presented a pseudomolecular ion at m/z 670 $[M + H]^+$, consistent with the molecular formula, $C_{36}H_{47}NO_{11}$. The IR spectrum was similar to those of compounds described above.

Detailed analysis of the 1H and ^{13}C NMR spectra (Table 5.3) indicated that compound **23** belongs to the $\Delta 6(17), \Delta 11$ -jatrophone-type. The low field olefinic signals corresponding to the 11,12-endocyclic double bond resonated at δ_C 138.2, 131.5 and δ_H 6.14, 5.84. Moreover, the presence of two broad singlets at δ 5.42 and 5.29, with HMQC correlations with a carbon at δ 110.0, corroborated the presence of the exomethylene group. As regard to the preferred conformation of the macrocycle, this compound seems to adopt preferentially the *exo*-type, presenting the characteristic $J_{4,5} = 2.7$ Hz. Conjugation of COSY and HMBC spectra allowed the establishment of the diterpenic core and acylation pattern. The relative stereochemistry of compound **23** was investigated through a NOESY experiment. According to its full spectroscopic data, this compound was identified as esulatin M, firstly isolated from the methanol extract of *Euphorbia esula* (Vasas *et al.*, 2011).

Table 5.3. ¹H and ¹³C NMR Data (δ) for compound **23** (400 and 101 MHz).

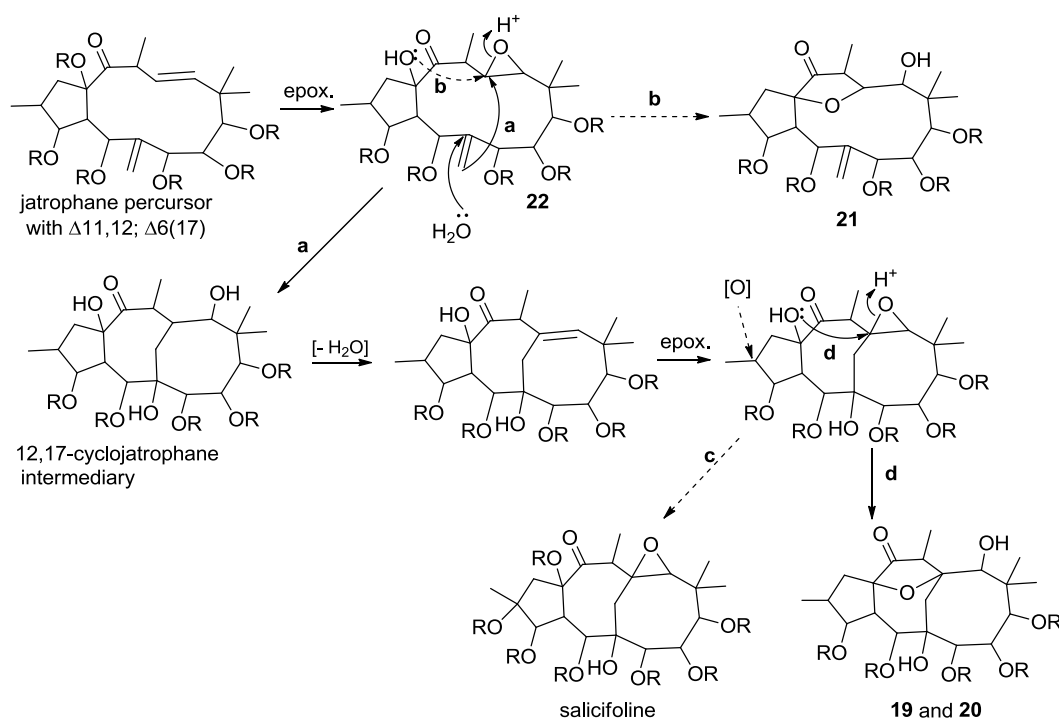
Position	Esulatin M(23) ^a	
	δH (J in Hz)	δC
1a	3.33 dd (13.9, 7.7)	46.7
1b	1.74 m	
2	2.40 m	38.7
3	5.76 bs	76.6
4	3.16 d (2.7)	53.6
5	6.12 bs	69.0
6	-	148.7
7	5.19 dd (6.5, 2.9)	69.0
8a	2.32 m	34.9
8b	2.29 m	
9	5.23 dd (7.3, 2.9)	75.9
10	-	49.7
11	6.14 d (16.0)	138.2
12	5.84 dd (16.0, 9.1)	131.5
13	3.73 m	43.9
14	-	212.7
15	-	93.4
16	0.67 d (6.9)	13.3
17a	5.42 bs	110.0
17b	5.29 bs	
18	0.91 s	
19	0.95 s	26.6
20	1.43 d (6.7)	23.6
3-OAc	-	169.3
	1.71 s	20.8
5-OAc	-	169.0
	1.75 s	21.0
15-OAc	-	170.1
	1.66 s	20.7
7-OiBu	-	176.1
2'	1.99 m	33.9
3'	0.81 d (7.0)	19.0
4'	0.64 d (7.0)	18.0
9-ONic		164.2
2'	9.59 s	151.6
3'		126.1
4'	8.11 d	136.6
5'	6.65 dd	123.5
6'	8.44 d	153.9

^aspectra recorded in C₆D₆

5.1.2. Biogenic interrelationships

A plausible biogenetic pathway for the rare 12,17-cyclojatrophanes is proposed (Scheme 5.1). As can be observed, jatrophanes **19-22** seem to be biogenetically interrelated. In this way, the 11,12-epoxidation of an appropriate $\Delta^6(17),\Delta^{11}$ -jatrophane precursor origins epoxiwelwitschene (**22**), whose epoxide can undergo a nucleophilic attack in two ways:

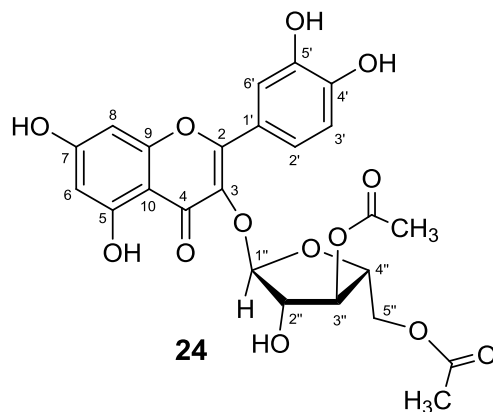
- 1) Ring-opening by the hydroxyl group at C-15 results in the formation of a tetrahydrofuran ring, and thus of welwitschene (**21**, Scheme 5.1b).
- 2) On the other hand, the attack by the 6(17)-exomethylene leads to the formation of a 12,17-transannular cyclization (Scheme 5.1a). This 12,17-cyclojatrophane intermediate would then subsequently suffer a dehydration at C-11. Epoxidation of the resulting double bond and oxidation at C-2 gives rise to salicifoline (Scheme 5.1c). Welwitschines A (**19**) and B (**20**) may be formed via epoxide ring-opening by the free hydroxyl at C-15 (Scheme 5.1d).



Scheme 5.1. Proposed biogenetic pathway for 12,17-cyclojatrophanes.

5.1.3. Structure elucidation of flavonoids

5.1.3.1 Quercetin 3-*O*- α -L-3'',5''-diacetyl-arabinofuranoside (**24**)



Compound **24**, $[\alpha]_D^{24}$ - 183.0, was isolated as yellow prismatic crystals (m.p. 141 – 145 °C). The ESIMS showed a pseudomolecular ion at m/z (negative mode) 517.0 $[M - H]^-$, consistent with the molecular formula $C_{24}H_{22}O_{13}$.

The 1H and ^{13}C NMR spectra were in accordance to quercetin bearing a glycoside moiety. The quercetin signals were similar to those described for compound **14** (Chapter 3). The sugar moiety was assumed to be an α -L-arabinofuranoside through the comparison of NMR data (Table 5.4) with the literature (Chin *et al.*, 2004; Chin and Kim, 2006; Moradi-Afrapoli *et al.*, 2012). Thus, the anomeric carbon was present at δ_C 105.9 (δ_H 5.61 bs), along with the other glycosidic signals at δ_C 81.4 (C-2''); δ_H 4.44 s), 81.2 (C-3''); δ_H 4.73 d, $J = 4.6$ Hz), 83.9 (C-4''); δ_H 3.67 dd, $J = 9.2, 5.0$ Hz) and 64.8 (C-5''); δ_H 4.11 dd, $J = 11.8, 5.0$ Hz and 3.93 dd, $J = 11.8, 6.3$ Hz). Additionally, the methyl protons of the acetyl groups were observed on the spectra as two singlets resonating at δ 2.12 and 1.93 and the corresponding carbons were assigned at δ_C 20.9 and 20.6, along with the ester carbonyls at δ_C 172.4 and 172.3. The HMBC long range correlations located these substituents at positions 3'' and 5'' of the pentose moiety, settling compound **24** as flavonol diacetylated glycoside.

Comparison with literature data enable to identify compound **24** as quercetin 3-*O*- α -L-3'',5''-diacetyl-arabinofuranoside. The isolation of this rare flavonoid, with a diacetylglucosyl moiety, has only two reports: from the aerial parts of *Rodgersia podophylla* (Saxifragaceae) (Chin and Kim, 2006) and from *Polygonum hyrcanicum*

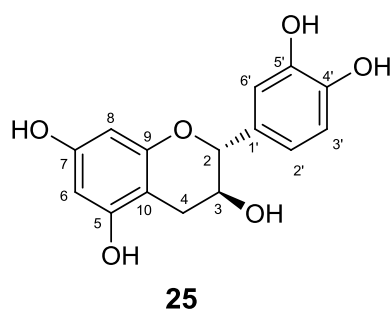
(Polygonaceae) (Moradi-Afrapoli *et al.*, 2012). The last study reported its *in vitro* activity as α -glucosidase inhibitor.

Table 5.4. ^1H and ^{13}C NMR data (δ) for flavonoids **24** (400 and 101 MHz, respectively) and **25** (300 and 75 MHz, respectively).

position	Quercetin 3- <i>O</i> - α -L-3'',5''-diacetyl-arabinofuranoside (24) ^a		Catechin (25) ^b	
	δ_{H} (J in Hz)	δ_{C}	δ_{H} (J in Hz)	δ_{C}
2	-	160.0	4.42 d (7.5)	81.0
3	-	134.9	3.76 m	66.3
4a	-	179.4	2.60 dd (16.0, 5.3)	27.9
4b	-		2.29 dd (16.0, 8.1)	
5	-	163.3	-	156.2
6	6.17 d (1.5)	99.9	5.83 d (2.3)	95.1
7	-	166.0	-	156.5
8	6.35 d (1.5)	94.8	5.63 d (2.3)	93.9
9	-	158.6	-	155.4
10	-	105.9	-	99.1
1'	-	123.1	-	130.6
2'	7.34 dd (8.3, 1.5)	122.9	6.53 dd (8.1, 1.9)	118.5
3'	6.85 d (8.3)	117.3	6.63 d (8.1)	115.1
4'	-	149.6	-	144.9
5'	-	146.4	-	144.9
6'	7.38 d (1.5)	116.3	6.66 d (1.9)	114.5
1''	5.61 s	105.9	-	-
2''	4.44 s	81.4	-	-
3''	4.73 d (4.6)	81.2	-	-
4''	3.67 dd (9.2, 5.0)	83.9	-	-
5''a	4.14 dd (11.8, 3.4)	64.8	-	-
5''b	3.93 dd (11.8, 6.3)		-	-
3''-OAc	-	172.4	-	-
	2.12 s	20.9	-	-
5''-OAc	-	172.3	-	-
	1.93 s	20.6	-	-

^aspectra recorded in MeOD; ^bspectra recorded in DMSO-d₆

5.1.3.2. Catechin (25)



Catechin (**25**), $[\alpha]_D^{24} + 18.0$, isolated from the most polar fractions of the methanolic extract of *E. welwitschii*, is a well-known flavonoid. Its structure identification was done mainly by one and two-dimension NMR experiments, along with comparison with literature data (Davis *et al.*, 1996; Zhang *et al.*, 2012). Similarly to the flavonoids **11-14** described on Chapter 3, the ^{13}C spectrum (Table 5.4) of compound **25** showed 15 resonances, with twelve typical flavonolic aromatic carbons (δ_{C} 115.1-156.5). Nevertheless, unlike compounds **11-14**, the downfield signal corresponding to a carbonyl was absent in this compound and instead a methylene at δ_{C} 27.9 was recorded. Therefore, it was concluded that compound **25** belongs to the flavonoids with the flavan-3-ol skeleton. The stereochemistry of compound **25** was confirmed by comparing the proton coupling constants $J_{(2,3)}$, $J_{(4a,3)}$ and $J_{(4b,3)}$, with the data reported for catechin and epicatechin (Table 5.5) (Davis *et al.*, 1996; Zhang *et al.*, 2012).

Table 5.5. Comparison of the proton coupling constants and ^{13}C shifts of compounds **25**, catechin and epicatechin, in different solvents.

Coupling constants J (Hz)	Compound 25	Catechin (2R , 3S)		Epicatechin (2R , 3R)
	DMSO-d6	DMSO-d6	Acetone-d6	Acetone-d6
$J_{(2,3)}$	7.5	7.8	7.8	1.6
$J_{(4a,3)}$	5.3	4.8	5.5	3.2
$J_{(4b,3)}$	8.1	7.3	8.8	4.6

5.2. Assessment of MDR reversal activity

The evaluation of compounds **19-24** as cancer MDR reversers followed a similar experimental design as previously described.

5.2.1. Modulation of P-gp efflux and ATPase activity

Compounds **19-24** were tested at 2 and 20 μM in the rhodamine-123 efflux assay. During the time of exposure, background signs of toxicity could be ruled out from this experiment, since no significant changes in the flow cytometry parameters FCS (forward scatter cell) and SSC (side scatter cell) were found (data not shown). The fluorescence activity ratio (FAR) values are presented in Table 5.6. Compound **24** was the only that did not show any P-gp modulation. On the other hand, compounds **19-23** showed to be able to revert the MDR phenotype, at 20 μM (Figure 5.7), being two-fold (**19**, **23**) and three-fold (**21**, **22**) more effective than the positive control verapamil (Table 5.6). At 2 μM , only compounds **21-23** maintained the strong modulator feature (FAR > 10). The results at 2 μM point to an interesting observation: the high conformational flexibility of the twelve-membered ring of jatrophanes **21-23** favors P-gp modulation, in contrast to the 5/8/8 fused ring system of welwitschines A and B (**19-20**). Similar observations were also found for rearranged polycyclic jatrophanes, based on segetane, paraliane and pepluane skeletons. These showed a lower P-gp modulatory efficiency when compared with molecules with the macrocyclic jatrophane-type scaffold (Corea *et al.*, 2009; Ferreira *et al.*, 2014a).

Table 5.6. Effect of compounds **21-24** on the P-gp mediated rhodamine-123 efflux, in *MDR1*-transfected L5178Y cells

Compound	Fluorescence Activity Ratio (FAR) ^a	
	2 μM	20 μM
Welwitschine A (19)	7.1	21.1
Welwitschine B (20)	5.4	13.2
Welwitschene (21)	17.1	26.8
Epoxiwelwitschene (22)	24.9	27.4
Esulatin M (23)	12.0	21.5
Compound 24	0.8	1.5
Verapamil	-	12.5

^aFAR = (L5178Y-MDR_{FL-1treated} / L5178Y-MDR_{FL-1control}) / (PAR_{FL-1treated} / PAR_{FL-1control}). FL-1: mean fluorescence intensity of the cells. DMSO (2%) FAR = 0.87

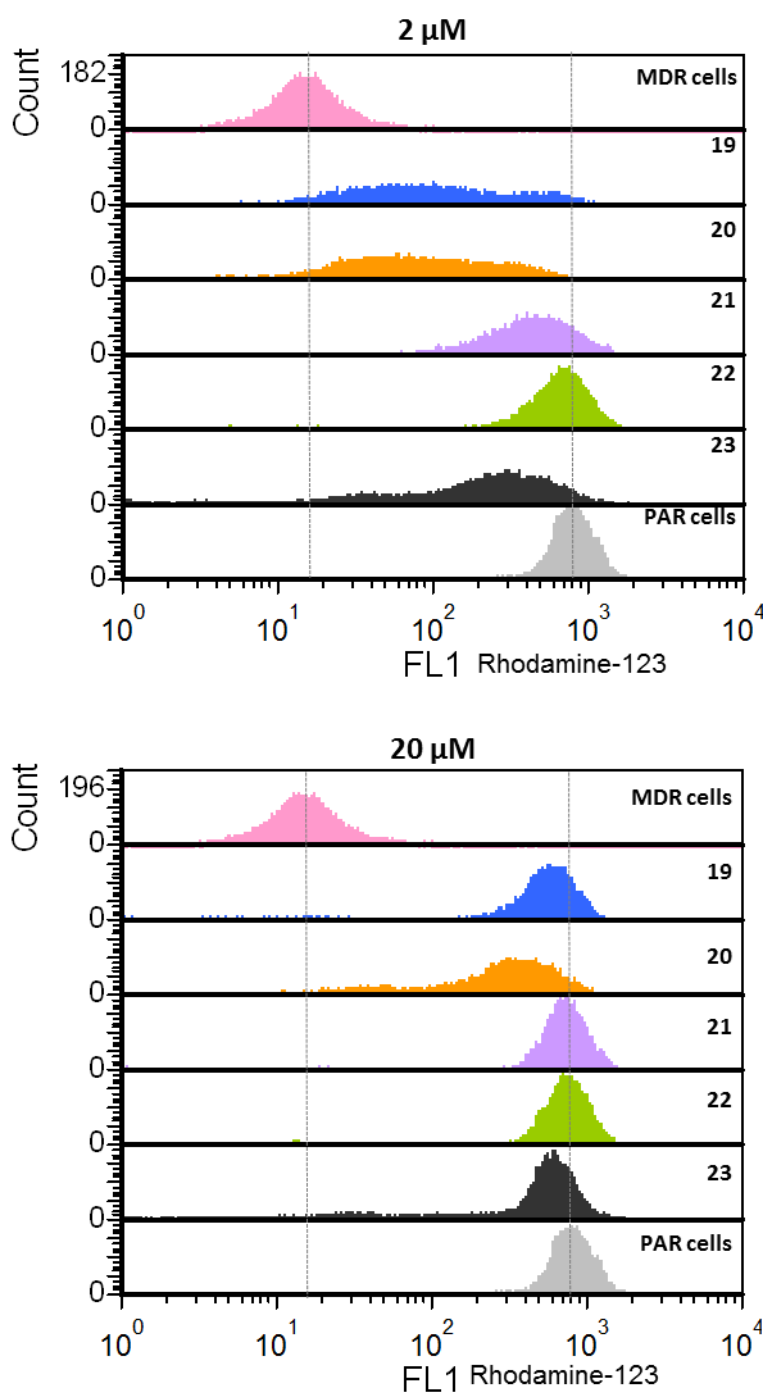


Figure 5.7. P-gp efflux modulation at 2 and 20 μM for compounds **19-23**. Flow cytometry histograms of rhodamine-123 accumulation showing MDR reversion in L5178Y-MDR cells.

As epoxiwelwitschene (**22**) was the strongest modulator of this set of molecules, was chosen to explore the possible P-gp modulatory mechanism by determining its effect on the ATPase activity. Thus, compound **22** was tested using a serial dilution of eight concentrations. The effects were presented as the relative ATPase activity, in which, the stimulated vanadate-sensitive ATPase activity is taken as 100% and the base line vanadate-sensitive ATPase activity as 0%. In this way, jatrophone **22** stimulated the P-gp ATPase activity 1.5 to 4 fold higher than verapamil, at all concentrations tested, being the effect more pronounced at lower concentrations (Figure 5.8, activation assay). Moreover, the inhibition assay indicated that epoxiwelwitschene (**22**) inhibited the verapamil-stimulated ATPase activity, with a 30% reduction being attained at higher concentrations and complete inhibition at 50 and 100 μM (Figure 5.8). Taking together these results, it can be concluded that epoxiwelwitschene (**22**) effectively interacts with P-gp, competing with verapamil for the same or overlapping binding sites.

In conclusion, combining the results from the rhodamine-123 and ATPase assays, it might be suggested that compound **22** acts as a competitive modulator.

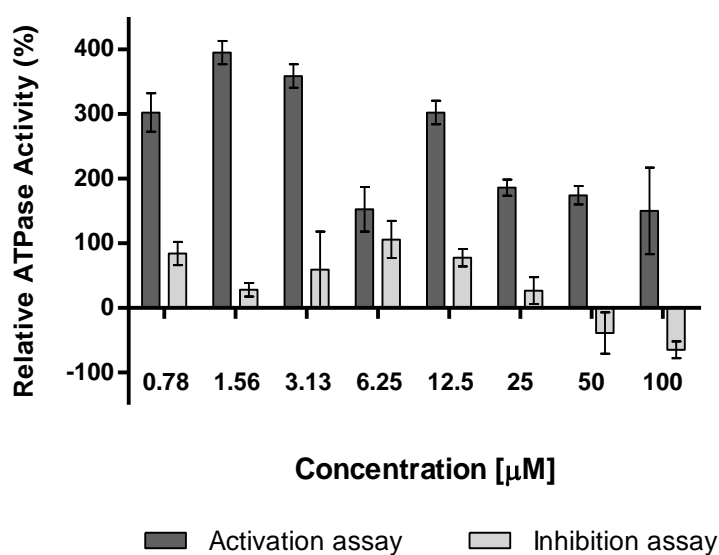


Figure 5.8. Effect of epoxiwelwitschene (**22**) on P-gp ATPase activity. Activation assay: to test the effect on the basal ATPase activity. Inhibition assay: to test the effect on drug-stimulated ATPase activity, measured in the presence of verapamil (40 μM). Results are expressed as the mean \pm SD from experiments performed in duplicate. The effects of compounds were presented as the relative ATPase activity, in which, the verapamil-stimulated vanadate-sensitive ATPase activity is taken as 100% and the baseline vanadate-sensitive ATPase activity as 0%.

5.2.2. Antiproliferative activity and chemosensitivity assays

The rhodamine-123 transport assay gives a quantitative evaluation on the P-gp efflux activity, but in the meantime, it is also significant to understand what will be the MDR reversal effects after long exposure.

Therefore, the antiproliferative activity of compounds **19-24** was evaluated in L5178Y mouse T lymphoma cell models by the MTT assay (Table 5.7). After 72 h incubation, the new 12,17-cyclojatrophanes **19** and **20** and the flavonol diacetylated glycoside **24** did not have antiproliferative effect. Conversely, jatrophanes **21-23** showed an interesting activity since they were more active in P-gp overexpressing cells than in the parental cell line, being welwitschene (**21**) the most potent presenting an $IC_{50} = 7.24 \pm 1.70 \mu\text{M}$ (SI = 0.26). This observation might support the evidence that these compounds are able to overcome the resistance caused by overexpression of P-gp.

Table 5.7. Antiproliferative activity of compounds **19-24** on L5178Y mouse T lymphoma cells and in *MDR1*-transfected cells.

Compound	L5178Y-parental IC_{50} ($\mu\text{M} \pm \text{SD}$)	L5178Y-MDR IC_{50} ($\mu\text{M} \pm \text{SD}$)	Selectivity index (SI)
Welwitschine A (19)	> 50	> 50	-
Welwitschine B (20)	> 50	> 50	-
Welwitschene (21)	27.86 ± 2.30	7.24 ± 1.70	0.26
Epoxiwelwitschene (22)	48.50 ± 2.28	32.49 ± 2.25	0.67
Esulatin M (23)	16.64 ± 5.91	14.13 ± 0.81	0.85
Compound 24	> 50	> 50	-
Doxorubicin	-	2.98 ± 1.01	

Values of IC_{50} are the mean \pm standard deviation of three independent experiments.

Selectivity index (SI) = IC_{50} MDR cells / IC_{50} PAR cells

Drug interaction studies were planned according to the Chou-Talalay method (Chou, 2006, 2010) and the compounds were tested in combination with doxorubicin. Combination indexes were evaluated at an inhibitory concentration of 50% (IC_{50}) at different ratios (compound:doxorubicin) (Figure 5.9). Welwitschene (**21**) showed an antagonistic nature at 400:1 ratio (CI = 1.6) and nearly additive at 200:1 ratio (CI = 0.93); except for these two, all the other tested ratios synergistically enhanced the cytotoxicity of doxorubicin (CI = 0.5 – 0.4). Furthermore, welwitschines A (**19**) and B (**20**),

epoxiwelwitschene (**22**) and esulatin M (**23**) synergistically enhanced the cytotoxicity of the drug (CI < 0.7) at all tested ratios. Interestingly, compound **19** exhibited the most significant effect, showing very strong synergism at the most of ratios tested.

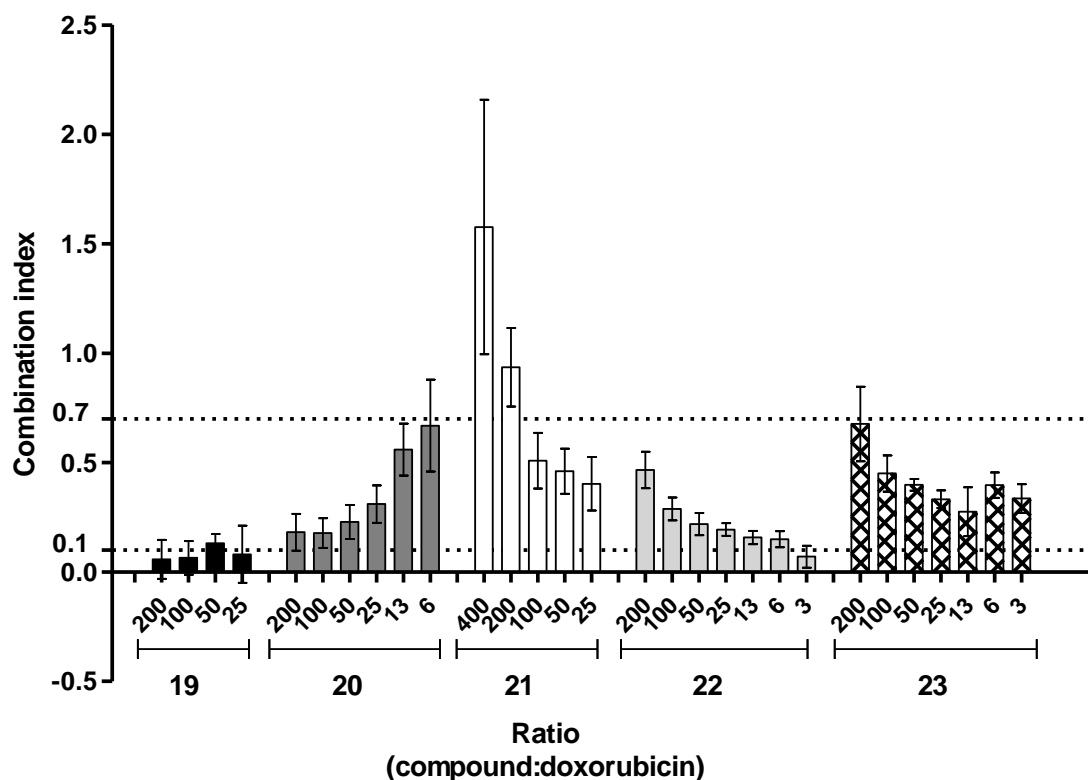


Figure 5.9. Effect of compounds **19-23** in combination with doxorubicin in L5178Y-MDR cells. Combination index (CI) values are mean \pm standard deviation for an inhibitory concentration of 50 % (IC_{50}). CI < 0.1: very strong synergism; 0.1 < CI < 0.3: strong synergism; 0.3 < CI < 0.7: synergism; 0.7 < CI < 0.9: moderate to slight synergism; 0.9 < CI < 1.1: nearly additive; 1.10 < CI < 1.45: moderate antagonism; 1.45 < CI < 3.30: antagonism (Chou, 2006, 2010).

Chapter 6

Resensitizing MDR phenotypes: collateral sensitivity
Results and Discussion

6.1 Antiproliferative activity and collateral sensitivity

Macrocyclic diterpenes and *ent*-abietane lactones, isolated from *Euphorbia* species, were identified as having a “collateral sensitivity” effect on MDR cell variants (Lage *et al.*, 2010). Some of which, presented additional activity as P-gp modulators and apoptosis inducers, on mouse T lymphoma cells (Duarte *et al.*, 2006, 2007).

Pursuing our research on MDR in cancer, the natural compounds **1-6**, **8**, **19-24** and the jolkinol D (**6.1-6.27**) derivatives were investigated for their potential collateral sensitivity effect, on the different cancer entities (Table 6.1), using a proliferation assay. The cancer cell lines derived from three different human tumor entities gastric (EPG85-257), pancreatic (EPP85-181), colon (HT-29) and their respective MDR counterparts have been well characterized for MDR and the main mechanisms associated to the drug resistant phenotypes are summarized in Table 6.1. They have been used in several studies aiming to find selective antiproliferative compounds (Drag *et al.*, 2009; Borska *et al.*, 2010; Coburger *et al.*, 2010; Duarte *et al.*, 2010; Hilgeroth *et al.*, 2013).

The relative resistance ratio ($RR = IC_{50(\text{resistant})}/IC_{50(\text{parental})}$) was used to explore if the compounds could confer a greater sensitivity in the drug-resistant sub-lines, than in the parental cell line. If this effect is observed, it is called as collateral sensitivity. In such cases, the RR value is lower than 0.5, meaning that there is high selectivity towards MDR phenotypes. However, other cases can be verified, for instance the development of resistance to a drug and simultaneous cross-resistance to various cytotoxic agents may result in loss of sensitivity, which is reflected by a RR value higher than 2 (Hall *et al.*, 2009a). And thus, this approach can lead to the selection of compounds that are highly effective against drug-resistant phenotypes. The cytotoxic agents etoposide and cisplatin were used as positive controls. The antiproliferative activity and collateral sensitivity effects of compounds **1-6**, **19-24** and jolkinol D (**6.1-6.27**) derivatives is presented in Tables 6.2-6.5.

Table 6.1. Characteristics of gastric, pancreatic and colon cancer cell lines and their drug selected sublines.

Origin	Gastric carcinoma			Pancreatic carcinoma			Colon carcinoma					
Cell line	EPG85-257P	EPG85-257RN	EPG85-257RDB	EPP85-181P	EPP85-181RN	EPP85-181RDB	HT-29P	HT-29RN	HT-29RDB			
Selection agent*	₄	Mitoxantrone (0.2 µg/ml) ¹	Daunorubicin (2.5 µg/ml) ¹	₅	Mitoxantrone (0.02 µg/ml) ²	Daunorubicin (2.5 µg/ml) ²	₃	Mitoxantrone (0.2 µg/ml) ⁶	Daunorubicin (0.25 µg/ml) ³			
	mRNA expressing level			Ref	mRNA expressing level			Ref	mRNA expressing level			Ref
MRP1	+	+	+	7	+	+	+	4	+	+	+	4
MRP2	+	+↑	+↑	4	+	+↑	+↑	4	+	+↑	+↑	4
MRP3	-	-	-	4	+↓	+↑	+↑	4	+	+↑	+	4
MRP4	+	+↑	+↑	4	+	+↑	+↑	4	+	+↑	+↑	4
MRP5	+	+↑	+↑	4	+	+↑	+↑	4	+	+↑	+↑	4
MRP6	-	-	-	4	+	-	-	4	+	-	+↑	4
MRP7	+	+	+	4	+	+	+	4	+	+	+	4
MRP8	+↓	-	-	4	-	-	-	4	-	-	-	4
MRP9	-	-	-	4	-	-	-	4	-	-	-	4
MDR1	-	-	+↑	4	-	-	+↑	2,4	-	-	-	4
BCRP	+↓	+↑	+↓	4,8	-	-	-	2,4	+↓	+↓	+↓	4
GPC3	+↓	+↑		9,10								
TAP	+	+↑	+	4								
TOPO II	+	+↓		11	+	+↓	+↓	12				

* To ensure the MDR phenotype the growth medium of each cell line is supplemented with a determined concentration of selection agent.

MRP = multidrug resistance protein; MDR1 = P-gp; BCRP = breast cancer resistance protein; GPC3 = gtypican-3; TAP = transporter associated protein; TOPO = DNA topoisomerase; + = mRNA expressed; +↓ = low levels of mRNA expressed; +↑ = high levels of mRNA expressed; - = no expression

⁴ (Dietel *et al.*, 1990)

⁵ (Lage *et al.*, 2000)

⁶ (Sinha *et al.*, 1999)

⁷ (Lage *et al.*, 2010)

⁸ (Ross *et al.*, 1999)

⁹ (Lage and Dietel, 1997)

¹⁰ (Wichert *et al.*, 2004)

¹¹ (Kellner *et al.*, 1997)

¹² (Lage and Dietel, 2002)

From the isolated compounds, welwitschene (**21**), epoxywelwitschene (**22**) and esulatin M (**23**) were the molecules that presented the strongest antiproliferative activity (Table 6.2). Collateral sensitivity was observed towards the resistant gastric cell line EPG85-257RDB for compounds **22** ($IC_{50} = 3.60 \pm 0.31 \mu\text{M}$, $RR = 0.14$) and **23** ($IC_{50} = 1.79 \pm 0.10 \mu\text{M}$, $RR = 0.17$). For the pancreatic cell lines, MDR selective antiproliferative effect was only observed for esulatin M (**23**) presenting $IC_{50} = 4.77 \pm 0.72 \mu\text{M}$, $RR = 0.37$ on EPG85-181RDB. As a result, compounds **23** and **24** were selected for apoptosis induction studies.

In respect to jolkinol D and derivatives (**6**, **6.1-6.27**), in order to search for significant collateral sensitivity effects, the non-parametric Kruskal-Wallis rank test was performed. The significant statistical differences were explored through comparison of antiproliferative activity on the pairs of parental and drug-resistant cell lines. In this way, statistical significance was only found between the parental cell line EPG85-257 and EPG85-257RDB (p value = 0.001) and between EPG85-257RDB and EPG85-257RN (p value = 0.017). This finding is mainly attributed to the lower IC_{50} values found on EPG85-257RDB cell line (Table 6.3). In fact, only compounds **6.4**, **6.19**, **6.24** and **6.25** presented an IC_{50} higher than $30 \mu\text{M}$. The other derivatives were highly effective towards this cell line, exhibiting an antiproliferative activity comparable to the positive controls cisplatin ($IC_{50} = 4.0 \pm 0.3 \mu\text{M}$; $RR = 1$) and etoposide ($IC_{50} = 6.2 \pm 0.3 \mu\text{M}$; $RR = 59$). These results and the RR values (Table 6.3) suggested that compounds **6** and derivatives exhibited a collateral sensitivity effect on EPG85-257RDB cells, which are characterized by P-gp overexpression. In respect to the other gastric MDR counterpart (EPG85-257RN), the best results were obtained for compounds **6.8**, **6.10**, **6.11**, **6.13**, **6.16**, **6.20-6.22** and **6.26** ($IC_{50} < 10 \mu\text{M}$; Table 6.3), but only compounds **6.10**, **6.11**, **6.16** and **6.26** showed a collateral sensitivity effect ($RR < 0.5$). Despite these promising results, no structure-activity relationships could be inferred for these cell lines. On the basis of their IC_{50} and RR values, jolkinolate L (**6.11**) and jolkinofornate B (**6.22**) were selected to study the possible mechanisms of collateral sensitivity.

Concerning pancreatic cancer cell lines, no significant statistical differences were detected between their IC_{50} (p values > 0.05). This was verified because the compounds presented a similar antiproliferative profile for both parental and resistant lines, independently from their MDR phenotype, and naturally this was reflected on the RR

values (Table 6.4). Jolkinoates L (**6.11**) and U (**6.20**) were chosen for further studies due to their activity: 17.76 ± 5.65 and 8.61 ± 0.58 μM (**6.11** and **6.20**, respectively for EPP85-181P); 10.11 ± 6.65 and 6.63 ± 0.95 μM (**6.11** and **6.20**, respectively for EPP85-181RN); 11.34 ± 4.07 and 5.86 ± 0.07 μM (**6.11** and **6.20**, respectively for EPP85-181RDB).

As for colon cancer cell lines, likewise, no significant statistical differences could be found (p values > 0.05). However, in this case, collateral sensitivity effect seemed to be towards the MDR phenotype, characterized by an altered topoisomerase II expression (HT-29RN), since the majority of the compounds presented $\text{RR} < 0.5$ (Table 6.5). Nevertheless, in overall the antiproliferative activity of the compounds in these cell lines was considered to be weak to moderate (Table 6.5). Once more, jolkinoate L (**6.11**) stands out from this set, as it showed to have an effective antiproliferative activity on HT-29RN ($\text{IC}_{50} = 3.82 \pm 1.08$ μM ; $\text{RR} = 0.41$) and on HT-29RDB ($\text{IC}_{50} = 9.67 \pm 2.77$ μM ; $\text{RR} = 1.04$), comparable to the positive controls (Table 6.5).

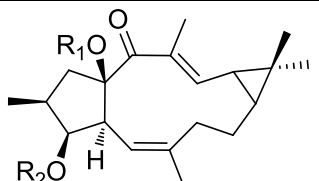
As it was mentioned for the gastric cells, direct structure-activity relationships between this set of lathyranes and antiproliferative activity on the other tumor entities was not clear, conversely to what was found for P-gp modulation (Chapter 4).

Table 6.2. Antiproliferative activity of compounds **1-5**, **8** and **19-24** on pancreatic carcinoma cells: EPP85-181P (parental), EPP85-181RN (MDR phenotype) and EPP85-181RDB (MDR phenotype) and on gastric carcinoma cells: EPG85-257P (parental), EPG85-257RN (MDR phenotype) and EPG85-257RDB (MDR phenotype).

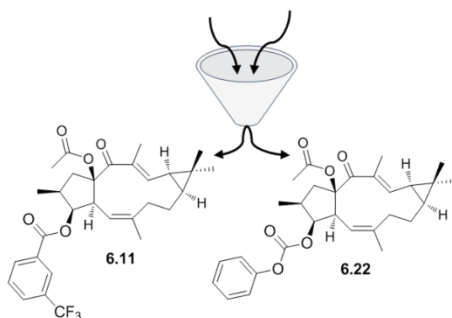
	EPP85-181P			EPP85-181RN			EPP85-181RDB			EPG85-257P			EPG85-257RN			EPG85-257RDB		
	IC ₅₀ (μM ± SD)	IC ₅₀ (μM ± SD)	RR	IC ₅₀ (μM ± SD)	RR	IC ₅₀ (μM ± SD)	RR	IC ₅₀ (μM ± SD)	RR	IC ₅₀ (μM ± SD)	RR	IC ₅₀ (μM ± SD)	RR	IC ₅₀ (μM ± SD)	RR	IC ₅₀ (μM ± SD)	RR	
Piscatolide (1)	84.65 ± 5.09	94.82 ± 5.18	1.12	>100	-	89.47 ± 7.65	83.09 ± 7.78	0.93	66.02 ± 7.10	0.74								
Piscatoric acid (2)	>100	>100	-	>100	-	>100	>100	-	>100	-								
Piscatoriol A (3)	>100	>100	-	>100	-	>100	>100	-	>100	-								
Piscatoriol B (4)	99.75 ± 0.35	>100	-	>100	-	99.85 ± 2.15	>100	1	39.51 ± 3.82	0.40								
Compound 5	>100	>100	-	>100	-	>100	>100	-	>100	-								
Compound 8	>100	>100	-	>100	-	>100	>100	-	>100	-								
Welwitschine A (19)	> 30	> 30	-	> 30	-	> 30	> 30	-	> 30	-								
Welwitschine B (20)	> 30	> 30	-	> 30	-	> 30	> 30	-	> 30	-								
Welwitschine (21)	> 30	> 30	-	> 30	-	28.26 ± 2.70	24.39 ± 1.50	0.86	17.19 ± 1.60	0.61								
Epoxiwelwitschine (22)	> 30	21.33 ± 2.53	0.71	18.21 ± 3.20	0.61	24.73 ± 3.42	21.24 ± 2.34	0.86	3.60 ± 0.31	0.14								
Esulatin M (23)	12.73 ± 2.21	11.24 ± 3.88	0.88	4.77 ± 0.72	0.37	10.67 ± 0.56	9.70 ± 0.13	0.91	1.79 ± 0.10	0.17								
Compound 24	>30	>30	-	>30	>30	>30	>30	-	>30	>30								
Cisplatin	0.08 ± 0.01	2.6 ± 0.2	34	0.09 ± 0.01	1.2	4.4 ± 0.4	2.6 ± 0.2	0.6	4.0 ± 0.3	1								
Etoposide	0.58 ± 0.03	4.5 ± 0.7	7.8	62.0 ± 4.2	106.9	0.105 ± 0.008	1.55 ± 0.09	14.8	6.2 ± 0.3	59								

IC₅₀ value indicates the mean ± SD of n = 3-4 independent experiments (each concentration was performed in triplicate per experiment)

Relative resistance (RR) = IC₅₀ (MDR cells) / IC₅₀ (parental cells).

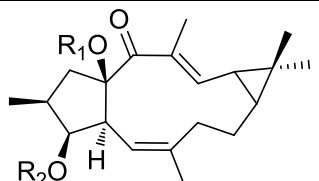
Table 6.3. Antiproliferative activity of jolkinol D (**6**) and derivatives on gastric carcinoma cells: EPG85-257P (parental), EPG85-257RN (MDR phenotype) and EPG85-257RDB (MDR phenotype).


Compound	R ₁	R ₂	EPG85-257P	EPG85-257RN	EPG85-257RDB
			IC ₅₀ ± SD	IC ₅₀ ± SD (RR)	IC ₅₀ ± SD
6	Ac	H	14.33 ± 1.14	14.77 ± 3.82 (1.03)	9.55 ± 6.31 (0.67)
6.1	Ac	Ac	27.31 ± 4.83	21.25 ± 3.14 (0.78)	4.18 ± 0.42 (0.15)
6.3	Ac	But	50.27 ± 5.94	25.65 ± 1.54 (0.51)	7.95 ± 0.09 (0.16)
6.4	Ac	Lauroyl	> 100	91.36 ± 12.22 (0.91)	47.71 ± 12.63 (0.48)
6.5	Ac	2-MetPent	16.94 ± 1.83	13.57 ± 3.43 (0.80)	4.50 ± 0.64 (0.27)
6.7	Ac	2-EtHex	20.60 ± 2.97	13.54 ± 0.86 (0.66)	5.47 ± 2.47 (0.27)
6.8	Ac	Bz	10.08 ± 3.38	5.40 ± 1.50 (0.54)	2.57 ± 0.24 (0.26)
6.9	Ac	4-MeBz	31.74 ± 2.22	19.32 ± 5.90 (0.61)	10.14 ± 1.52 (0.32)
6.10	Ac	4-OMeBz	22.32 ± 9.83	9.47 ± 3.04 (0.42)	4.06 ± 0.40 (0.18)
6.11	Ac	3-CF ₃ Bz	9.15 ± 2.44	3.58 ± 1.93 (0.39)	3.22 ± 0.70 (0.35)
6.12	Ac	SO ₂ Bz	19.83 ± 1.84	17.84 ± 0.61 (0.90)	3.65 ± 0.81 (0.18)
6.13	Ac	3-MeBz	4.82 ± 2.12	3.97 ± 1.80 (0.82)	4.80 ± 2.23 (0.99)
6.14	Ac	3-OMeBz	14.16 ± 3.20	10.50 ± 5.75 (0.74)	4.47 ± 0.92 (0.32)
6.15	Ac	2-OMeBz	19.86 ± 2.44	16.17 ± 3.21 (0.81)	4.05 ± 2.51 (0.20)
6.16	Ac	4-CF ₃ Bz	> 30	7.00 ± 0.62 (> 0.23)	10.77 ± 2.43 (0.36)
6.17	Ac	Cinnamoyl	> 30	> 30	8.14 ± 3.06 (> 0.15)
6.19	Ac	Biphenyl	94.77 ± 7.76	19.60 ± 3.13 (0.21)	51.41 ± 14.46 (0.54)
6.20	Ac	Adamantane	5.77 ± 0.28	4.45 ± 0.93 (0.77)	4.39 ± 1.01 (0.76)
6.21	Ac	Ethylformate	8.51 ± 1.85	7.04 ± 1.52 (0.83)	3.36 ± 0.77 (0.40)
6.22	Ac	Phenylformate	6.24 ± 1.08	5.55 ± 0.88 (0.89)	2.34 ± 0.67 (0.37)
6.23	H	H	57.95 ± 0.45	43.71 ± 1.29 (0.75)	13.39 ± 4.07 (0.23)
6.24	H	3-OMeBz	38.33 ± 4.08	21.87 ± 2.53 (0.57)	26.48 ± 22.65 (0.69)
6.25	H	4-CF ₃ Bz	> 30	> 30	> 30
6.26	H	Naphthoyl	18.72 ± 8.05	8.48 ± 1.69 (0.45)	5.86 ± 1.43 (0.31)
6.27	H	Biphenyl	> 30	16.89 ± 8.80 (> 0.56)	18.67 ± 6.24 (> 0.62)
Cisplatin			4.4 ± 0.4	2.6 ± 0.2 (0.6)	4.0 ± 0.3 (1)
Etoposide			0.105 ± 0.008	1.55 ± 0.09 (14.8)	6.2 ± 0.3 (59)

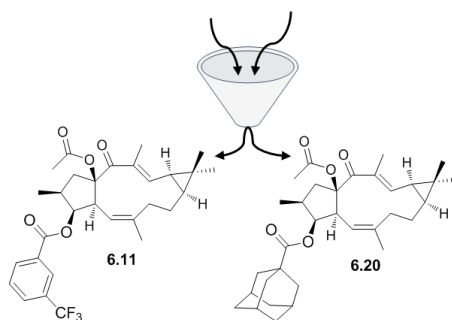


IC₅₀ value indicates the mean ± SD of n = 3-4 independent experiments (each concentration was performed in triplicate per experiment)

Relative resistance (RR) = IC₅₀ (MDR cells) / IC₅₀ (parental cells).

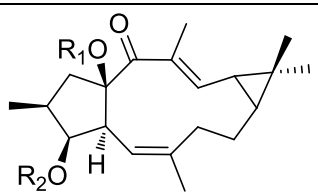
Table 6.4. Antiproliferative activity of jolkinol D (**6**) and derivatives on pancreatic carcinoma cells: EPP85-181P (parental), EPP85-181RN (MDR phenotype) and EPP85-181RDB (MDR phenotype).


Compound	R ₁	R ₂	EPP85-181P	EPP85-181RN	EPP85-181RDB
			IC ₅₀ ± SD	IC ₅₀ ± SD (RR)	IC ₅₀ ± SD (RR)
6	Ac	H	67.26 ± 24.17	29.45 ± 4.72 (0.44)	23.28 ± 0.4 (0.35)
6.1	Ac	Ac	47.08 ± 9.86	19.45 ± 8.63 (0.41)	21.15 ± 3.37 (0.45)
6.3	Ac	But	54.49 ± 6.19	45.19 ± 0.73 (0.83)	46.46 ± 0.54 (0.85)
6.4	Ac	Lauroyl	> 100	> 100 (1)	> 100 (1)
6.5	Ac	2-MetPent	22.71 ± 5.29	18.06 ± 5.61 (0.80)	29.26 ± 14.04 (1.29)
6.7	Ac	2-EtHex	28.04 ± 3.64	18.94 ± 4.03 (0.68)	20.37 ± 3.80 (0.73)
6.8	Ac	Bz	22.00 ± 16.11	13.53 ± 9.16 (0.62)	14.45 ± 11.26 (0.66)
6.9	Ac	4-MeBz	41.45 ± 2.33	36.29 ± 6.63 (0.88)	28.78 ± 1.27 (0.69)
6.10	Ac	4-OMeBz	27.72 ± 6.59	23.44 ± 1.86 (0.85)	17.28 ± 3.72 (0.62)
6.11	Ac	3-CF ₃ Bz	17.76 ± 5.65	10.11 ± 6.65 (0.57)	11.34 ± 4.07 (0.64)
6.12	Ac	SO ₂ Bz	30.27 ± 5.31	19.07 ± 11.72 (0.63)	18.69 ± 5.44 (0.62)
6.13	Ac	3-MeBz	21.73 ± 0.06	16.94 ± 3.89 (0.78)	15.83 ± 6.29 (0.73)
6.14	Ac	3-OMeBz	19.44 ± 1.44	21.67 ± 4.71 (1.11)	12.57 ± 4.73 (0.65)
6.15	Ac	2-OMeBz	24.83 ± 3.58	24.73 ± 7.36 (1.00)	23.43 ± 2.59 (0.94)
6.17	Ac	Cinnamoyl	> 100	98.61 ± 2.78 (0.99)	65.90 ± 38.92 (0.66)
6.19	Ac	4-Biphenyl	> 100	> 100	> 100
6.20	Ac	Adamantane	8.61 ± 0.58	6.63 ± 0.95 (0.77)	5.89 ± 0.07 (0.68)
6.21	Ac	Ethylformate	14.94 ± 3.66	11.11 ± 0.37 (0.74)	10.93 ± 1.35 (0.73)
6.22	Ac	Phenylformate	> 30	> 30	23.52 ± 1.44 (> 0.78)
6.23	H	H	97.46 ± 4.24	74.66 ± 16.23 (0.77)	69.09 ± 6.97 (0.71)
6.24	H	3-OMeBz	62.79 ± 7.61	51.77 ± 6.75 (0.82)	40.72 ± 1.17 (0.65)
6.25	H	4-CF ₃ Bz	96.35 ± 5.17	44.64 ± 20.97 (0.46)	33.27 ± 1.12 (0.35)
6.26	H	Naphthoyl	44.11 ± 24.77	30.14 ± 15.10 (0.68)	14.31 ± 3.90 (0.32)
6.27	H	4-Biphenyl	> 100	41.59 ± 19.86 (0.42)	37.52 ± 6.38 (0.38)
Cisplatin			0.08 ± 0.01	2.6 ± 0.2 (34)	0.09 ± 0.01 (1.2)
Etoposide			0.58 ± 0.03	4.5 ± 0.7 (7.8)	62.0 ± 4.2 (106.9)



IC₅₀ value indicates the mean ± SD of n = 3-4 independent experiments (each concentration was performed in triplicate per experiment)

Relative resistance (RR) = IC₅₀ (MDR cells) / IC₅₀ (parental cells).

Table 6.5. Antiproliferative activity of jolkinol D (**6**) and derivatives on colon carcinoma cells HT-29P (parental), HT-29RN (MDR phenotype) and HT-29RDB (MDR phenotype).


Compound	R ₁	R ₂	HT-29P	HT-29RN	HT29-RDB
			IC ₅₀ ± SD	IC ₅₀ ± SD (RR)	IC ₅₀ ± SD
6	Ac	H	19.95 ± 1.24	10.59 ± 1.05 (0.53)	8.13 ± 1.29 (0.41)
6.1	Ac	Ac	> 100	94.36 ± 4.78(0.94)	> 100
6.3	Ac	But	93.44 ± 8.28	43.81 ± 0.59 (0.47)	73.00 ± 11.92 (0.78)
6.4	Ac	Lauroyl	95.18 ± 6.82	91.44 ± 1.57 (0.96)	>100
6.5	Ac	2-MetPent	25.78 ± 2.87	11.82 ± 4.43 (0.46)	28.51 ± 4.53 (1.11)
6.7	Ac	2-EtHex	52.75 ± 1.08	19.60 ± 3.38 (0.37)	35.45 ± 0.24 (0.67)
6.8	Ac	Bz	65.77 ± 7.99	29.12 ± 5.24 (0.44)	34.28 ± 2.05 (0.52)
6.9	Ac	4-MeBz	> 100.00	93.25 (> 0.93)	> 100
6.10	Ac	4-OMeBz	70.92 ± 1.91	29.59 ± 4.61 (0.42)	52.94 ± 1.32 (0.75)
6.11	Ac	3-CF ₃ Bz	9.32 ± 2.33	3.82 ± 1.08 (0.41)	9.67 ± 2.77 (1.04)
6.12	Ac	SO ₂ Bz	77.61 ± 5.48	20.87 ± 3.77 (0.27)	27.80 ± 10.85 (0.36)
6.13	Ac	3-MeBz	48.05 ± 4.30	24.15 ± 1.33 (0.5)	27.92 ± 3.10 (0.58)
6.14	Ac	3-OMeBz	49.94 ± 4.57	26.30 ± 4.34 (0.53)	831.10 ± 1.91 (0.62)
6.15	Ac	2-OMeBz	> 100	> 100	> 100
6.16	Ac	4-CF ₃ Bz	> 100.00	81.49 (0.81)	93.09 (0.97)
6.17	Ac	Cinnamoyl	> 100	93.02 ± 5.15 (0.93)	99.05 ± 1.35 (0.99)
6.19	Ac	Biphenyl	> 100	> 100	> 100
6.23	H	H	97.75 ± 2.26	46.88 ± 3.82 (0.48)	49.92 ± 1.03 (0.51)
6.24	H	3-OMeBz	> 100	49.52 ± 6.03 (0.50)	64.32 ± 8.91 (0.64)
6.25	H	4-CF ₃ Bz	94.88 ± 7.25	23.26 ± 7.16 (0.25)	38.46 ± 5.21 (0.41)
6.26	H	Naphthoyl	>100	77.59 ± 16.84 (0.78)	93.87 ± 8.66 (0.94)
6.27	H	Biphenyl	> 100	> 100	> 100
Cisplatin			3.8 ± 0.1	3.8 ± 0.1 (1)	2.7 ± 0.1 (0.7)
Etoposide			2.3 ± 0.3	35.0 ± 2.6 (15.2)	26.0 ± 1.7 (11.3)

IC₅₀ value indicates the mean ± SD of n = 3-4 independent experiments (each concentration was performed in triplicate per experiment)

Relative resistance (RR) = IC₅₀ (MDR cells) / IC₅₀ (parental cells).

6.2. Apoptosis assays

Once the antiproliferative effects were determined, it was of interest, to assess whether the mechanism of cell death was apoptosis or necrosis. The membrane phospholipid phosphatidylserine and active caspase-3 were used as markers of apoptosis. In apoptotic cells, phosphatidylserine is translocated from the inner to the outer leaflet of the plasma membrane, being exposed to the external cellular environment. Therefore, can be detected using annexin V, a phospholipid-binding protein, conjugated to a fluorochrome (*e.g.* FITC). Since externalization of phosphatidylserine occurs in the earlier stages of apoptosis, annexin V staining can identify apoptosis at an earlier stage. This staining is used in conjunction with a vital dye, such as propidium iodide (PI), cells with intact membranes exclude PI, whereas membranes of dead and damaged cells are permeable to PI. Therefore, annexin V/PI staining allows the identification of early apoptotic cells (PI negative, Annexin V positive) and late apoptotic cells (PI positive, Annexin V positive), where membrane integrity is loss (Chen, 2009). Caspase-3 is one of the key effector molecules activated during the early stages of apoptosis. Active caspase-3 cleaves and activates other caspases, as well as other targets in the cytoplasm (*e.g.* Bcl-2), and in the nucleus (*e.g.* PARP) (Chen, 2009).

Therefore, compounds **22**, **23**, **6.11** and **6.22** were chosen for the apoptosis assays on gastric resistant cells and compounds **22**, **23**, **6.11** and **6.20** on pancreatic resistant cells.¹³ The ability to induce apoptosis was measured with the Annexin V/PI assay, for 72 h at 30 μ M.

EPG85-257RN cells, treated with the selected diterpenes, showed a 4-fold increase of total apoptosis, in comparison to the untreated control (Figure 6.1A). However differences between compounds were not found. On the other hand, EPG85-257RDB cells showed differentiation between treatments. Compound **6.11** showed about 6-fold increase in apoptotic cells, in comparison with the negative control. Also, compounds **22** and **23** showed a 2-fold increase on apoptosis. On the contrary, jolkinofornate B (**6.22**) did not show significant apoptosis induction.

¹³ Up to the submission of this work, only preliminary results for the parental cells were available, and thus, are not presented.

Concerning the pancreatic EPP85-181RN cells, epoxiwelwitschene (**22**) and esulatin M (**23**) induced apoptosis in 2-fold, while jolkinoates L (**6.11**) and U (**6.20**) induced in about 5-fold, in comparison with the untreated control (Figure 6.1B). Furthermore, on EPP85-181RDB, 2 to 4-fold apoptosis induction was observed for compounds **22**, **23** and **6.11**, though, compound **6.20** showed a remarkably high ability as apoptosis inducer, with about 16-fold apoptosis induction.

To investigate whether this induced apoptosis was caspase dependent, the activation of caspase-3, after 72 h exposure, was evaluated by a flow cytometry. However, only preliminary results were obtained upon the submission of this work, and thus, are not presented. But, for instance, results for compound **6.20** point to caspase-dependent pathway.

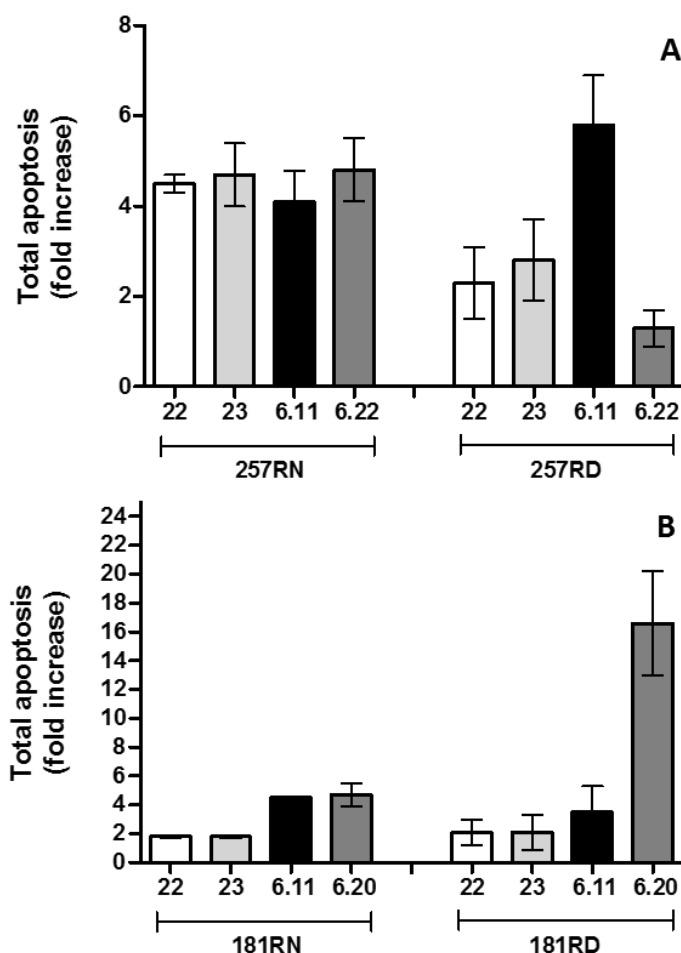


Figure 6.1. Induction of apoptosis on gastric (A) and pancreatic (B) cell lines. Total apoptosis (cells on the annexin V+/PI- quadrant, plus annexin V+/PI+ quadrant). Fold increase (treated sample/untreated sample).

Chapter 7

Conclusions

7. Conclusions

The main goal of this study was to search for bioactive diterpenes, as well as optimize their structures, in order to purpose new leads for cancer MDR modulation.

In this way, the methanol extracts of *Euphorbia piscatoria* and *Euphorbia welwitschii* were studied yielding twenty five terpenic and phenolic compounds. A small library of twenty seven diterpenic derivatives was also prepared. The chemical structures were deduced from their physical and spectroscopic data (IR, MS, ^1H and ^{13}C NMR and 2D NMR - COSY, HMQC, HMBC and NOESY experiments) and in some cases X-ray crystallography was used. The potential MDR reversal activity was assessed by two approaches: as P-glycoprotein efflux modulators and by exploring the collateral sensitivity effect.

The phytochemical study of *E. piscatoria* (aerial parts) yielded four new diterpenes: two *ent*-abietanes, piscatolide (**1**) and piscatoric acid (**2**), and two lathyrane-type macrocyclic diterpenes, piscatoriols A (**3**) and B (**4**) (Figure 7.1) The following known macrocyclic and polycyclic diterpenes were also isolated: 15-acetoxy-5,6-epoxylathyr-12-en-3-ol-14-one (**5**), jolkinol D (**6**), helioscopinolide E (**7**), *ent*-13[*R*]-hydroxy-3,14-dioxo-16-atiseene (**8**) and portlanquinol (**9**)

Piscatoric acid (**2**), with an unusual structure, was proposed as intermediate in the biogenesis of *ent*-abietane α,β -unsaturated lactones, like helioscopinolide (**7**). Due to structural similarities, biogenic relationships among the lathyranes **3-6** could also be proposed.

Regarding MDR reversal activity, compounds **3-5** were able to enhance, synergistically, the antiproliferative activity of doxorubicin (combination indexes < 0.5). Nevertheless, these compounds did not show P-gp modulatory ability.

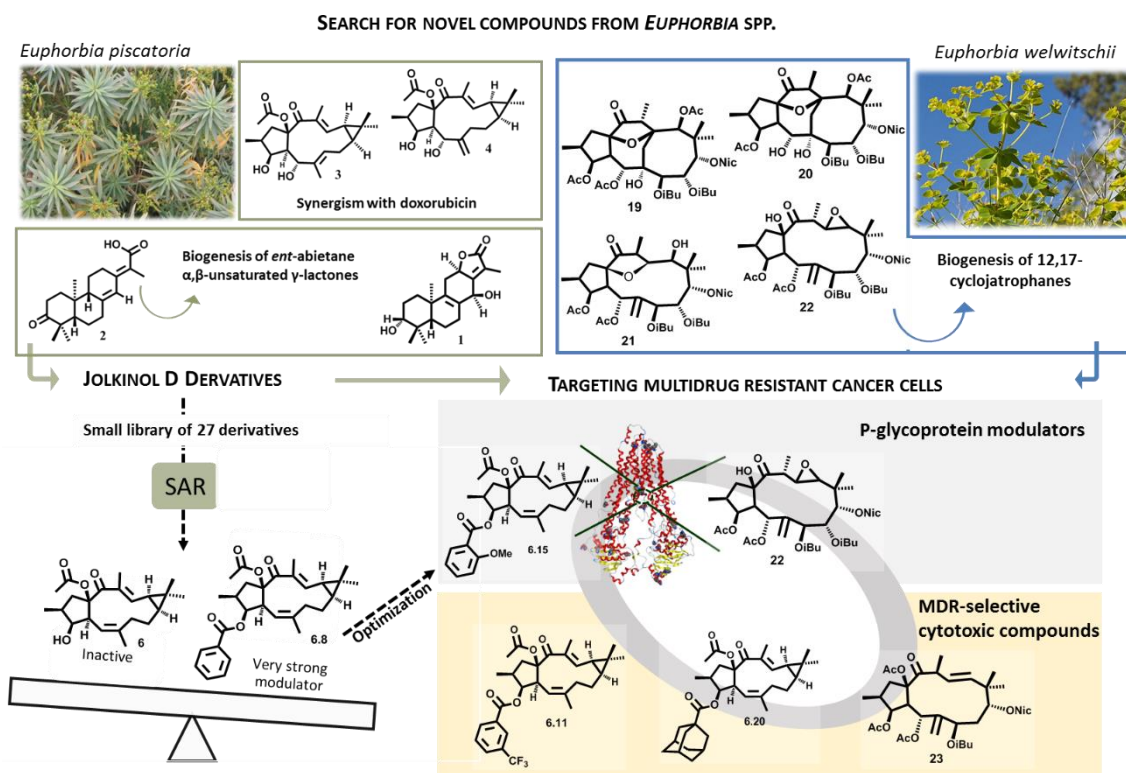


Figure 7.1. Summary of the main achievements obtained in this work.

Jolkinol D (6), isolated in large amount from *E. piscatoria*, was used as building block for the development of a small library of 27 acylated derivatives (6.1-6.27). The common scaffold of these compounds, and the limited variation achieved through the derivatization of the free hydroxyl at C-3, provided a good model for structure-activity relationships. Modulation of P-gp efflux was assayed using the rhodamine-123 transport assay in a *MDR1*-transfected mouse T lymphoma L5178Y cell model.

Structure-activity relationships of the first set of compounds (6, 6.1-6.12, 6.23) identified strong correlations between modulatory activity and $\log P$, molecular weight or accessible solvent area. Lipophilicity remains a critical factor among P-gp modulators. The data acquired in this study provided an insight on how the acylation of a single hydroxyl group could affect the modulation ability of P-gp efflux, highlighting the importance of the aroyl moiety. The following optimization steps (6.13-6.22, 6.24-6.27) showed that addition of electron donating groups to the aromatic moiety, namely methoxyl (6.10, 6.14, 6.15), favored P-gp modulation (Figure 7.1). In conclusion, this SAR study corroborated the importance of the aromatic ring for binding inside the drug-binding pocket, namely through electronic and steric effects.

The mechanism of P-gp modulation was investigated through the effects on the ATPase activity. The results of an inactive molecule (**6**) were compared with the strongest modulator (**6.15**), and it was verified that the profiles of the hydrolysis of ATP were different. Jolkinol D (**6**) showed to have a profile of a transported substrate that does not compete with verapamil for the same binding sites. While, jolkinoate P (**6.15**) showed to have profile more similar to an inhibitor: lower activation of the basal ATPase activity and inhibition of the verapamil transport, at some concentrations. These results suggest and reinforce the hypothesis of multifactorial inhibition mechanisms of P-gp, mainly due to the polyspecificity of this transporter.

In addition, combination between most of the jolkinol D derivatives and doxorubicin revealed a synergistic nature, through increase of its cytotoxicity, supporting once again the potential anti-MDR effect of these compounds.

The study of *E. welwitschii* (aerial parts) afforded four new jatrophanes (**19-22**) and esulatin M (**23**), a known $\Delta^6(17),\Delta^{11}$ -jatropane (Figure 7.1). Welwitschines A (**19**) and B (**20**) belong to the rare class of 12,17-cyclojatrophanes. Moreover, they present a unique combination of structural features: a 5/8/8 fused-ring system and an 12,15-ether bridge. Insights into to biogenetic pathway of 12,17-cyclojatrophanes were proposed, taking welwitschene (**21**) and epoxiwelwitschene (**22**) as precursors of welwitschines A (**19**) and B (**20**).

The jatrophanes **19-23** evidenced promising results concerning P-gp efflux modulation. For this kind of molecules, conformational flexibility was highlighted as an interesting feature. In this way, welwitschines **19** and **20**, presenting a more constrained tetracyclic scaffold, showed to be less active than jatrophanes **21-23** that share a flexible twelve-membered ring. Epoxiwelwitschene (**22**), the strongest modulator of this set of compounds, might impair P-gp transport through a mechanism of competitive modulation. The drug combination experiments also corroborated the anti-MDR potential of these diterpenes due to their synergistic interaction with doxorubicin.

The potential collateral sensitivity effect of compounds **1-6**, **8**, **19-24** and jolkinol D derivatives (**6.1-6.27**) was evaluated against parental gastric (EPG85-257), pancreatic (EPP85-181) and colon (HT-29) human cancer cells and their drug-selected counterparts,

resistant to novantrone (RN) and to daunorubicin (RDB), using a proliferation assay. The best results were obtained for the MDR cell line EPG85-257RDB. In fact, these compounds were able to decrease the level of resistance in 65 to 85%, in comparison with the parental cell line EPG85-257P. The most promising collateral sensitivity effect, in EPG85-257RDB cells, was obtained for compounds **22**, **23**, **6.11** and **6.22**, showing an IC_{50} range of 1.79 - 3.60 μ M (RR = 0.17 - 0.37). In reference to the pancreatic cells, the best results were obtained with compounds **22**, **23**, **6.11** and **6.20** in EPG85-181RDB cells (Figure 7.1). These compounds were able to reduce the levels of resistance in about 32 - 65%.

The cytotoxic drug-induced mechanisms of cell death were investigated using the annexin V/PI and active caspase-3 assays. The compounds were selected in regard to their selective antiproliferative effect ($IC_{50} < 10 \mu$ M and/or RR < 0.5). In this way, the selected compounds were: **22**, **23**, **6.11** and **6.20** for EPG85-181 cell lines and **22**, **23**, **6.11** and **6.22** for EPP85-257 cell lines. It was verified for both cases that cell death occurred through caspase-dependent apoptosis.

As a final remark, this work presents a contribution towards a more effective reversion of cancer MDR. The structural optimization of the compounds with the lathyrane scaffold and the isolation of jatrophanes from *E. welwitschii* provided the identification of some of the relevant structural requirements for P-gp efflux modulation, and identified compounds with significant collateral sensitivity effect. Thus, compounds **6.11**, **6.15**, **6.20**, **6.22**, **22** and **23** can be proposed as new lead candidates for the development of MDR reversal agents. Moreover, the phytochemical studies contributed to the knowledge of the chemical diversity of *Euphorbia* species, with new biogenetic pathways being explored for some of the isolated compounds.

Chapter 8

Materials and Methods

8.1. Chemistry

8.1.1. General experimental procedures

Melting points were determined on a Köpffler apparatus and are uncorrected. Optical rotations were obtained using a Perkin Elmer 241 polarimeter, with quartz cells of 10 cm path length; the samples were solubilized in CHCl_3 or MeOH.

The infrared spectra (IR) were collected on an Affinity-1 (Shimadzu) FTIR spectrophotometer and the UV spectra were recorded on a spectrophotometer Shimadzu UV-Visible 1603, using quartz or glass cuvettes with an internal width of 1 cm.

Low resolution mass spectrometry was taken on a Triple Quadrupole mass spectrometer (Micromass Quattro Micro API, Waters) and high resolution mass spectra were recorded on a FTICR-MS Apex Ultra (Bruker Daltonics) 7 T instrument.

NMR spectra were recorded on a Bruker 400 Ultra-Shield instrument (^1H 400 MHz, ^{13}C 101 MHz) and on a Bruker 300 Avance spectrometer (^1H 300 MHz, ^{13}C 75 MHz). ^1H and ^{13}C chemical shifts are expressed in δ (ppm), referenced to the solvent used, and the proton coupling constants J in hertz (Hz). Spectra were assigned using appropriate COSY, DEPT, HMQC, and HMBC sequences.

Column chromatography was performed on silica gel (Merck 9385) or Combiflash system (Teledyne-Isco) using SiO_2 or C-18 prepacked columns. TLCs were performed on pre-coated SiO_2 or RP-18 F_{254} plates (Merck Millipore 105554 and 105560, respectively), with visualization under UV light (λ 254 and 366 nm) and by spraying with sulfuric acid/methanol (1:1), followed by heating.

HPLC was performed on a Merck-Hitachi HPLC system, with UV detection. Analytical HPLC: Merck LiChrospher 100 RP-18; 5 μm , 125 \times 4 mm column. Semipreparative HPLC: Merck LiChrospher 100 RP-18; 10 μm , 250 \times 10 mm) column. Mixtures of MeOH/ H_2O and MeCN/ H_2O were used as mobile phase.

8.1.2. Phytochemical study of *Euphorbia piscatoria*

8.1.2.1. Plant Material

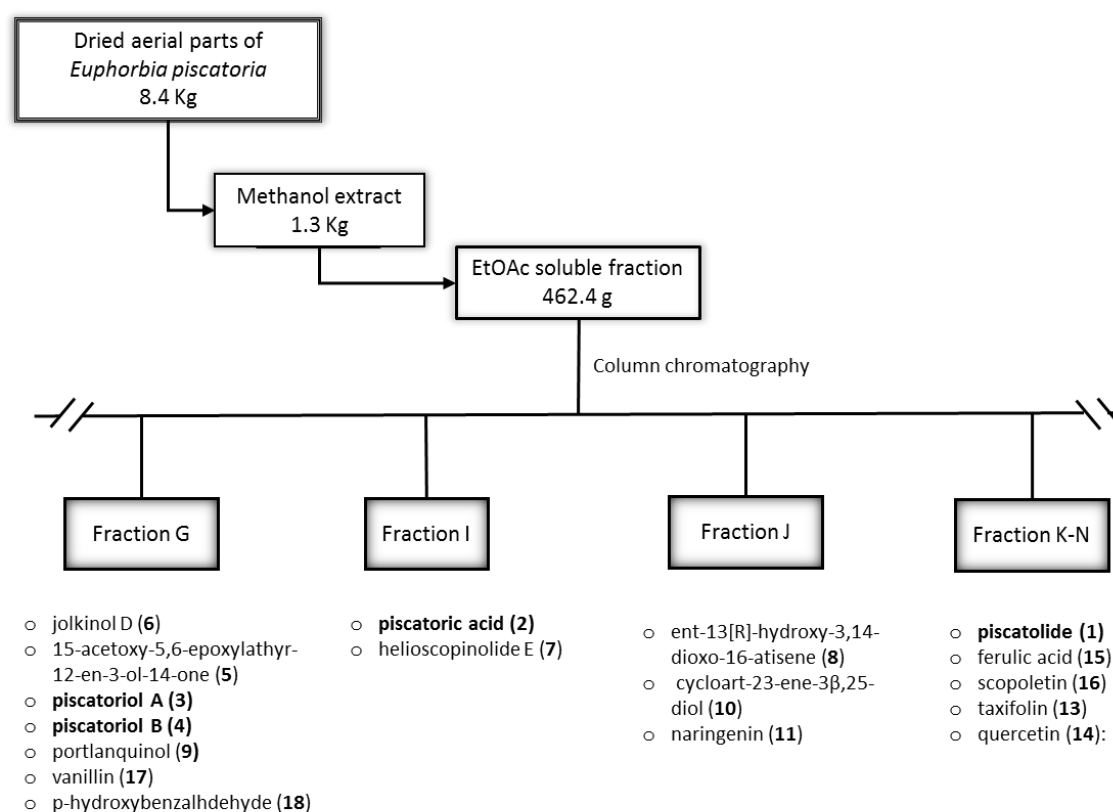
Euphorbia piscatoria Ait. was collected in the Garcia de Orta garden, Lisbon, Portugal (April 2011), and was identified by Dr. Teresa Vasconcelos (plant taxonomist) of Instituto Superior de Agronomia, University of Lisbon, Portugal. A voucher specimen (no. 276) has been deposited at the herbarium of Instituto Superior de Agronomia.

8.1.2.2. Extraction and Isolation.

The air-dried powdered aerial parts (8.4 kg) were exhaustively extracted with methanol (9×6 L) at room temperature (Figure 8.1). Evaporation of the solvent (under vacuum, 40 °C) from the crude extract yielded a residue of 1.3 kg. This residue was resuspended in MeOH/H₂O solution (1:2, 4 L) and extracted with EtOAc (8×3 L). The ethyl acetate soluble fraction was dried (Na₂SO₄) and evaporated under vacuum, yielding a residue (462.4 g) that was chromatographed over SiO₂ (2 kg), using mixtures of *n*-hexane-EtOAc (1:0 to 0:1) and EtOAc-MeOH (9:1 to 3:7) in increasing gradients of 5% of 2 L each eluent, except for *n*-hexane-EtOAc 7:3 gradient where 8 L were used. According to differences in composition as indicated by TLC, 14 crude fractions were obtained: fractions A-O (Table 8.1). *Euphorbia* diterpenes generally occur as polyesters, therefore, the typical oxymethine protons might be pinpointed at δ 6-4 ppm, in the ¹H NMR of the enriched crude fractions. In this way, ¹H NMR of these crude fractions was performed and fraction G was identified as the most diterpenic rich fraction. The other fractions studied (I, J, K-N) were also selected according to the ¹H NMR along with the TLC profile (Figure 8.1).

Table 8.1. Crude fractions of the EtOAc soluble fraction of the methanol extract of *E. piscatoria*.

Fraction	Amount (g)	Eluents (v/v)	
		<i>n</i> -hexane : EtOAc	EtOAc / MeOH
A	52.5	1:0 to 15:5	-
B	43.7	7:3	-
C	88.9	7:3	-
D	20.9	7:3	-
E	3.3	7:3	-
F	5.3	7:3 to 13:7	-
G	17.6	13:7 to 11:9	-
I	10.5	1:1 to 9:11	-
J	5.2	9:11	-
K-N	31.7	2:3 to 1:19	-
O	27.8	-	1:0 to 7:3

**Figure 8.1.** Study of *Euphorbia piscatoria*: extraction, fractionation procedures, and compounds isolated from Fractions G, I, J and K-N.

Study of fraction G

Jolkinol D (**6**) was obtained (2.9 g) through crystallization (EtOAc/*n*-hexane) from the crude fraction G (17.6 g). The mother liquid (14.7 g) of compound **1** was fractionated by column chromatography (4 x 90 cm, 500 g SiO₂) with *n*-hexane/EtOAc and EtOAc/MeOH (1:0 to 0:1 and 9:1 to 7:3, used in increasing gradients of 5%, 500 mL each eluent), originating five fractions (G₁-G₅). The fraction G₂ (4.2 g) was chromatographed (5 x 80 cm, 170 g SiO₂), with CH₂Cl₂/acetone (1:0 to 0:1, used in increasing gradients of 1%, 150 mL each eluent); subsequently, a sub-fraction (2.2 g) was fractionated using reverse-phase C-18 column (5 x 80 cm, 200 g C-18) chromatography (MeOH/H₂O, 1:1 to 1:0, used in increasing gradients of 5%, 200 mL each eluent), giving rise, after further purification by HPLC, to 15-acetoxy-5,6-epoxylathyr-12-en-3-ol-14-one (**5**; 10 mg), piscatoriol A (**3**; 5 mg; MeOH/H₂O, 11:9), piscatoriol B (**4**; 17 mg; MeOH/H₂O, 3:2) and portlanquinol (**9**; 17.3 mg; MeOH/H₂O, 7:3). The known phenolic compounds vanillin (**17**; 10 mg) and *p*-hydroxybenzaldehyde (**18**; 4 mg) were isolated from fraction G₁.

Jolkinol D, 15 β -acetoxy-3 β -hydroxylathyra-5E,12E-dien-14-one (**6**):

White prismatic crystals;

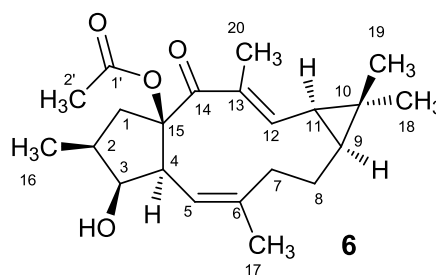
M.p. 186-188 ° (*n*-hexane/EtOAc);

$[\alpha]_D^{26} + 27.9$ (c 0.1, CHCl₃);

IR ν_{\max} 3446; 1740; 1639; 460 cm⁻¹;

ESIMS (negative mode) m/z (rel. int.): 383 [M + Na]⁺ (100);

¹H NMR (400 MHz, CDCl₃): δ 6.65 (1H, d, $J = 11.4$ Hz, H-12), 5.67 (1H, d, $J = 10.9$ Hz, H-5), 3.91 (1H, dd, $J = 8.2, 3.6$ Hz, H-3), 3.49 (1H, dd, $J = 14.0, 8.1$ Hz, H-1a), 2.57 (1H, d, $J = 13.3$ Hz, H-7a), 2.38 (1H, dd, $J = 10.9, 3.6$ Hz, H-4), 2.21 (1H, ddd, $J = 14.5, 6.8, 3.3$ Hz, H-8a), 2.04 (1H, m, H-2), 2.01 (3H, s, H-2'), 1.83 (3H, s, H-20), 1.77 (1H, td, $J = 13.1, 6.5$ Hz, H-7b), 1.57-1.48 (2H, m, H-1b, H-8b), 1.46 (3H, s, H-17), 1.40 (1H, dd, $J = 11.4, 8.2$ Hz, H-11), 1.17 (3H, s, H-18), 1.08 (3H, d, $J = 6.7$ Hz, H-16), 1.06 (1H, m, H-9), 1.04 (3H, s, H-19) ppm.



^{13}C NMR (101 MHz, CDCl_3): δ 195.5 (C-14), 170.0 (C-1'), 146.7 (C-12), 143.2 (C-6), 132.3 (C-13), 119.6 (C-5), 95.4 (C-15), 80.1 (C-3), 52.8 (C-4), 44.1 (C-1), 39.4 (C-2), 36.9 (C-7), 34.4 (C-9), 29.8 (C-11), 29.4 (C-18), 28.5 (C-8), 24.6 (C-10), 21.8 (C-2'), 21.1 (C-17), 16.6 (C-19), 13.9 (C-16), 12.5 (C-20) ppm.

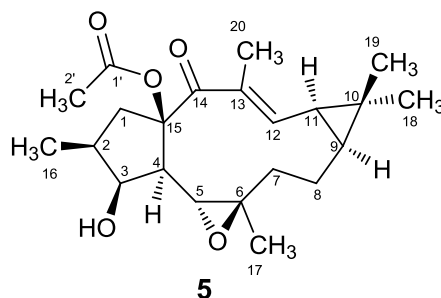
15-acetoxy-5,6-epoxylathyr-12-en-3-ol-14-one (5):

White powder;

$[\alpha]_D^{26}$ - 8.7 (c 0.1, CHCl_3); lit. $[\alpha]_D^{20}$ - 41.4 (c 0.15, MeOH);

IR (CH_2Cl_2) ν_{max} 3320, 1747, 1629, 1234, 1008 cm^{-1} ;

ESIMS (negative mode) m/z (rel. int.): 399 $[\text{M} + \text{Na}]^+$ (100);

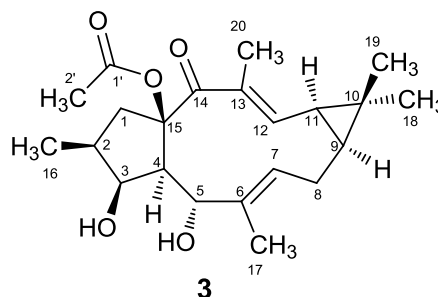


^1H NMR (400 MHz, CDCl_3): δ 6.92 (1H, dd, $J = 10.9, 1.0$ Hz, H-12), 4.07 (1H, bs, H-3), 3.51 (1H, d, $J = 9.4$ Hz, H-5), 3.45 (1H, dd, $J = 13.5, 7.4$ Hz, H-1a), 2.09 (1H, m, H-8a), 2.07 (3H, s, H-2'), 2.03 (1H, m, H-7a), 1.94 (1H, m, H-2), 1.86 (3H, d, $J = 1.0$ Hz, H-20), 1.61 (1H, m, H-1b), 1.54 (1H, m, H-7b), 1.51 (2H, m, H-8b and H-11), 1.49 (1H, dd, $J = 9.4, 3.6$ Hz, H-4), 1.20 (3H, s, H-18), 1.14 (1H, dd, $J = 8.0, 5.0$ Hz, H-9), 1.17 (3H, s, H-17), 1.07 (6H, m, H-16 and H-19) ppm.

^{13}C NMR (101 MHz, CDCl_3) δ 195.3 (C-14), 169.7 (C-1'), 143.9 (C-12), 134.5 (C-13), 92.0 (C-15), 78.7 (C-3), 63.9 (C-6), 58.1 (C-5), 53.6 (C-4), 45.0 (C-1), 38.8 (C-7), 38.4 (C-2), 33.8 (C-9), 29.9 (C-11), 29.2 (C-18), 26.3 (C-10), 23.3 (C-8), 21.6 (C-2'), 20.1 (C-17), 16.5 (C-19), 13.3 (C-16), 12.6 (C-20) ppm.

Piscatoriol A; 15 β -acetoxy-lathyra-6,12-diene-3 β ,5 α -diol-14-one (**3**):

White powder;

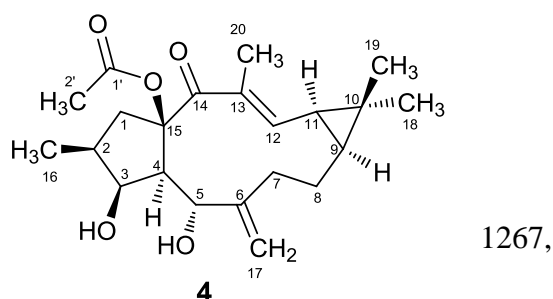
 $[\alpha]_D^{26} - 43.2$ (c 0.1, CHCl₃);UV (MeOH) λ_{\max} (log ϵ) 270 (3.50) nm;IR (CH₂Cl₂) ν_{\max} 3311, 1747, 1625, 1234, 1008 cm⁻¹;ESI-TOF-HRMS m/z : 399.2134 [M + Na]⁺ (calcd for C₂₂H₃₂O₅Na, 399.2142);

¹H NMR (400 MHz, CDCl₃): δ 6.44 (1H, dd, $J = 11.4, 1.0$ Hz, H-12), 5.37 (1H, d, $J = 6.3$ Hz, H-5), 5.25 (1H, dd, $J = 11.2, 4.9$ Hz, H-7), 4.34 (1H, t, $J = 3.6$ Hz, H-3) 3.33 (1H, dd, $J = 13.5, 7.6$ Hz, H-1a), 2.39 (1H, m, H-8b) 2.35 (1H, m, H-8a), 2.11 (1H, dd, $J = 6.3, 3.6$ Hz, H-4), 2.09 (3H, s, H-2'), 2.06 (1H, m, H-2), 1.75 (3H, d, $J = 1.0$, H-20), 1.69 (1H, m, H-1b), 1.65 (3H, s, H-17), 1.42 (1H, dd, $J = 11.4, 8.5$ Hz, H-11), 1.26 (1H, m, H-9), 1.23 (3H, s, H-18), 1.16 (3H, s, H-18) 1.07 (3H, d, $J = 6.8$ Hz, H-16) ppm.

¹³C NMR (101 MHz, CDCl₃): δ 197.9 (C-14), 170.1 (C-1'), 142.7 (C-12), 135.5 (C-6), 133.5 (C-13), 126.8 (C-7), 92.7 (C-15), 79.8 (C-3), 65.8 (C-5), 54.7 (C-4), 47.4 (C-1), 37.8 (C-2), 31.9 (C-9), 28.8 (C-19), 27.9 (C-11), 25.5 (C-10), 23.9 (C-8), 22.2 (C-2'), 17.8 (C-17), 17.0 (C-18), 13.5 (C-16), 12.2 (C-20) ppm.

Piscatoriol B; 15 β -acetoxy-lathyra-6(17),12-diene-3 β ,5 α -diol-14-one (**4**):

White powder;

 $[\alpha]_D^{26} - 103$ (c 0.1, CHCl₃);UV (MeOH) λ_{\max} (log ϵ) 273 (3.75) nm;IR (CH₂Cl₂) ν_{\max} 3444, 1741, 1622, 1371, 1244, 1037, 1012, 904, cm⁻¹;

ESIMS (positive mode) m/z (rel int.): 399 [M + Na]⁺ (100), 360 [M - CH₃]⁺ (75), 415 [M + K]⁺ (21);

ESI-TOF-HRMS m/z : 399.2134 $[M + Na]^+$ (calcd for $C_{22}H_{32}O_5Na$, 399.2142);

1H NMR (400 MHz, $CDCl_3$): δ 6.33 (1H, bd, $J = 11.2$ Hz, H-12), 4.95 (1H, bs, H-17a), 4.81 (1H, br, H-5), 4.75 (1H, bs, H-17b), 4.32 (1H, bs, H-3), 3.40 (1H, dd, $J = 13.7, 7.9$ Hz, H-1a), 2.72 (1H, dd, $J = 13.6, 5.5$ Hz, H-7a), 2.43 (1H, dd, $J = 8.6, 3.4$ Hz, H-4), 2.15 (1H, m, H-7b), 2.09 (1H, m, H-2), 2.06 (3H, s, H-2'), 2.01 (1H, m, H-8a), 1.90 (1H, m, H-1b), 1.70 (3H, s, H-20), 1.57 (1H, m, H-8b), 1.37 (1H, dd, $J = 11.2, 8.4$ Hz, H-11), 1.15 (3H, s, H-19), 1.12 (1H, m, H-9), 1.09 (3H, d, $J = 7.3$ Hz, H-16), 1.08 (3H, s, H-18) ppm.

^{13}C NMR (101 MHz, $CDCl_3$): δ 197.2 (C-14), 169.9 (C-1'), 148.2 (C-6), 145.5 (C-12), 133.7 (C-13), 113.6 (C-17), 92.8 (C-15), 79.6 (C-3), 66.8 (C-5), 54.2 (C-4), 47.3 (C-1), 37.5 (C-2), 35.4 (C-7), 34.6 (C-9), 29.1 (C-19), 28.4 (C-11), 24.8 (C-10), 22.1 (C-2'), 22.0 (C-8), 16.7 (C-18), 13.5 (C-16), 12.6 (C-20) ppm.

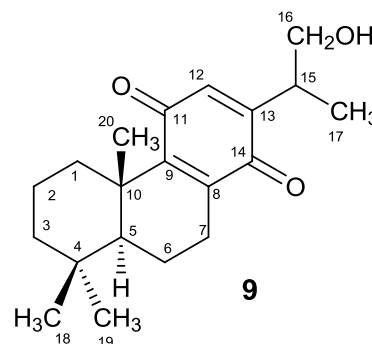
Portlanquinol, 16-hydroxy-abieta-8,12-diene-11,14-dione (**9**):

Yellow oil.

$[\alpha]_D^{26} + 30$ (c 0.1, $CHCl_3$);

IR (CH_2Cl_2) ν_{max} 3440, 1600, 1655, 918 cm^{-1} ;

ESIMS, m/z (rel. int.): 338 $[M + Na]^+$ (100);



1H NMR (400 MHz, $CDCl_3$): δ 6.39 (1H, s, H-12), 3.63 (2H, d, $J = 5.7$ Hz, H-16), 3.08 (1H, sextet, $J = 6.4$ Hz, H-15), 2.71 (1H, m, H-1b), 2.65 (1H, d, $J = 5.5$ Hz, H-7b), 2.29 (1H, m, H-7a), 1.86 (1H, m, H-6a), 1.71 (1H, m, H-2b), 1.52 (1H, m, H-2a), 1.44 (1H, m, H-3b), 1.42 (1H, m, H-6b), 1.27 (3H, s, H-20), 1.19 (1H, m, H-3a), 1.12 (3H, d, $J = 6.9$ Hz, H-17), 1.12 (1H, m, H-1a), 1.10 (1H, m, H-5), 0.92 (3H, s, H-18), 0.89 (3H, s, H-19) ppm.

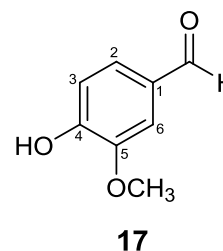
^{13}C NMR (101 MHz, $CDCl_3$): δ 188.7 (C-11), 187.8 (C-14), 151.4 (C-9), 148.7 (C-13), 142.9 (C-8), 134.2 (C-12), 66.8 (C-16), 51.7 (C-5), 41.5 (C-3), 38.7 (C-10), 36.5 (C-1), 34.6 (C-15), 33.7 (C-4), 33.6 (C-18), 26.2 (C-7), 21.9 (C-19), 20.3 (C-20), 19.1 (C-2), 17.5 (C-6), 15.5 (C-17) ppm.

Vanillin (17):

Yellow powder;

$^1\text{H NMR}$ (400 MHz, CDCl_3): δ 9.82 (1 H, s, 1-COH), 7.45 - 7.40 (2H, m, H-2/H-6), 7.05 (1 H, d, $J = 8.1$ Hz, H-3), 6.21 (1 H, s, OH), 3.96 (1 H, s, 5-OCH₃) ppm.

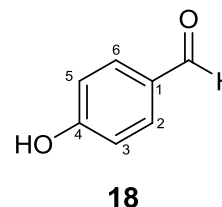
$^{13}\text{C NMR}$ (101 MHz, CDCl_3): δ 191.2 (1-CHO), 152.2 (C-4), 147.5 (C-5), 129.8 (C-1), 127.5 (C-2), 114.8 (C-3), 109.3 (C-6), 56.1 (OCH₃) ppm.

***p*-hydroxybenzaldehyde (18):**

White powder;

$^1\text{H NMR}$ (400 MHz, CDCl_3): δ 9.87 (1 H, s, CHO), 7.81 (2 H, d, $J = 8.4$ Hz, H-2 and H-6), 6.96 (2H, m, H-3 and H-5), 5.83 (1H, s, OH) ppm.

$^{13}\text{C NMR}$ (101 MHz, CDCl_3) δ 191.3 (CHO), 161.7 (C-4), 132.6 (C-2 and C-6), 129.9 (C-1), 116.1 (C-3 and C-5) ppm.

***Study of fraction I***

Fraction I (10.5 g), eluted with mixtures of *n*-hexane/EtOAc (1:1 to 9:11), was fractionated by reverse phase C-18 column chromatography (5 x 80 cm, 200 g C-18), using elution gradients of MeOH/H₂O (1:1 to 1:0, used in increasing gradients of 5%, 1 L each eluent), originating four fractions. The fraction I₁ (5.7 g) was chromatographed (5 x 80 cm, 200 g SiO₂) using *n*-hexane/EtOAc as eluents (1:0 to 1:1, used in increasing gradients of 5%, 500 mL each eluent), yielding four fractions. The fraction eluted with hexane/EtOAc (7:3 to 3:2) was chromatographed (5 x 80 cm, 120 g SiO₂) using *n*-hexane/EtOAc (1:0 to

0:1, used in increasing gradients of 5%, 250 mL each eluent) to obtain compound **2** (52 mg) and compound **7** (90 mg), after further purification by HPLC (MeOH/H₂O, 7:3).

Piscatoric acid; 3-oxo-ent-abieta-8(14),13(15)-dien-16-oic acid (**2**):

White powder;

$[\alpha]_D^{22} - 178.5^\circ$ (c 0.10, CHCl₃);

UV (MeOH) λ_{\max} (log ϵ) 263 (4.01) nm;

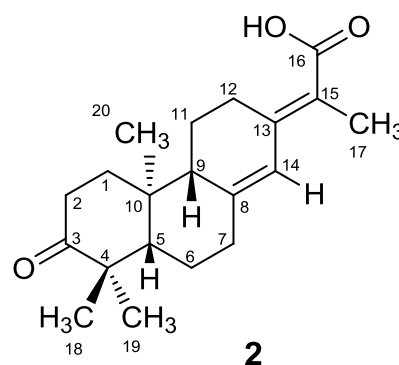
IR (CH₂Cl₂) ν_{\max} 3288-2500, 1705, 1665, 1284, 1263 cm⁻¹;

ESIMS (negative mode) m/z (rel. int.) 315 [M - H]⁻ (100);

ESI-TOF-HRMS m/z : 399.1924 [M + Na]⁺ (calcd for C₂₀H₂₈O₃Na, 339.1931);

¹H NMR (400 MHz, CDCl₃): δ 6.31 (1H, bs, H-14), 3.39 (1H, dt, $J = 15.3, 4.0$ Hz, H-12a), 2.66 (1H, td, $J = 15.0, 5.7$ Hz, H2a), 2.53 (1H, m, H-7a), 2.31 (1H, m, H-2b), 2.26 (1H, m, H-7b), 2.13 (1H, m, H-12b), 2.01 (1H, m, H-9), 2.00 (1H, m, H-1a), 1.97 (3H, d, $J = 1.1$ Hz, H-17), 1.81 (1H, m, H-11a), 1.64 (1H, m, H-6a), 1.55 (1H, m, H-5), 1.52 (1H, m, H-1b), 1.42 (1H, m, H-11b), 1.11 (3H, s, H-18), 1.08 (3H, s, H-19), 0.96 (3H, s, H-20) ppm.

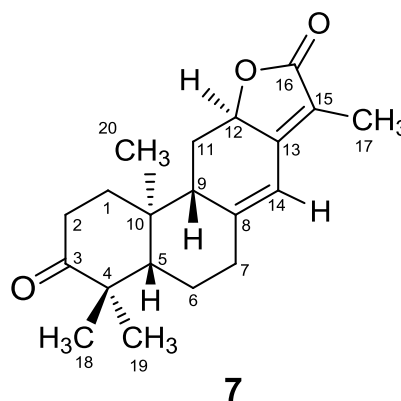
¹³C NMR (101 MHz, CDCl₃): δ 216.6 (C-3), 175.0 (C-16), 148.6 (C-8), 147.4 (C-13), 123.4 (C-14), 118.4 (C-15), 55.0 (C-5), 50.8 (C-9), 48.0 (C-4), 38.3 (C-10), 37.7 (C-1), 36.0 (C-7), 34.8 (C-2), 27.5 (C-12), 25.8 (C-18), 23.1 (C-6), 22.5 (C-19), 22.0 (C-11), 14.9 (C-10), 14.8 (C-17) ppm.



2

Helioscopinolide E (7):

White crystals;

M.p. . 180-183 °C (EtOAc/Hexane); $[\alpha]_D^{18} + 283.2^\circ$ (c 0.1, CHCl₃);**IR** (CH₂Cl₂) ν_{\max} 2941, 1745, 1699, 1666, 1454, 1086 cm⁻¹;**ESIMS** (positive mode) m/z (rel. int.): 337 [M + Na]⁺ (100);

¹H NMR (400 MHz, CDCl₃): δ 6.33 (1H, bs, H-14), 4.88 (1H, dd, $J = 13.2, 5.5$ Hz, H-12), 2.64 (1H, m, H-2a), 2.55 (2H, m, H-11a and H-7a), 2.46 (1H, ddd, $J = 15.7, 5.7, 3.6$ Hz, H-2b), 2.26 (1H, d, $J = 8.6$ Hz, H-9), 2.19 (2H, m, H-7b and H-1a), 1.84 (3H, d, $J = 1.3$ Hz, H-17), 1.80 (1H, m, H-6a), 1.64 (1H, m, H-5), 1.57 (2H, m, H-11b and H-1b) 1.13 (3H, s, H-18), 1.10 (3H, s, H-20), 1.06 (3H, s, H-19) ppm.

¹³C NMR (101 MHz, CDCl₃): δ 215.5 (C-3), 175.0 (C-16), 155.6 (C-13), 150.2 (C-8), 117.1 (C-15), 114.7 (C-14), 75.6 (C-12), 54.8 (C-5), 50.7 (C-9), 47.5 (C-4), 40.9 (C-10), 37.7 (C-1), 36.6 (C-7), 34.4 (C-2), 27.8 (C-11), 26.5 (C-18), 24.6 (C-6), 21.8 (C-19), 16.2 (C-10), 8.3 (C-17) ppm.

Study of fraction J

Fraction J (5.2 g), eluted with *n*-hexane/EtOAc (9:11 to 2:3), was chromatographed on SiO₂ (5 x 80 cm, 200 g) with mixtures of *n*-hexane/EtOAc and EtOAc/MeOH (1:0 to 0:1 and 1:0 to 7:3, used in increasing gradients of 5%, 300 mL each eluent), giving rise to thirteen fractions. Fraction *J*₆ (2.6 g) was fractionated on a Combiflash system (24 g SiO₂ flash column, RediSep®Rf, Teledyne Isco) with *n*-hexane/EtOAc and EtOAc/MeOH (1:0 to 0:1 and 9:1 to 7:3, used in increasing gradients of 5%, 5 mL/min), obtaining compounds **8** (35 mg), **10** (51 mg) **11** (576 mg).

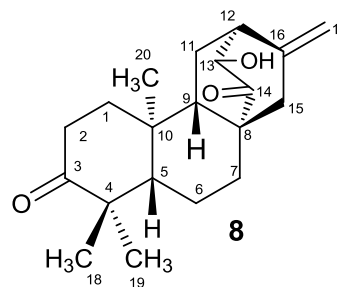
ent-13[R]-hydroxy-3,14-dioxo-16-atisene (8):

White crystals;

M.p. 174-177 °C; $[\alpha]_D^{26} + 38$ (c 0.1, CHCl₃);**IR** (CH₂Cl₂) ν_{\max} 3460, 1720, 1690, 900 cm⁻¹;**ESIMS** (positive mode) m/z (rel. int.): 317 [M + H]⁺ (100);

¹H NMR (400 MHz, CDCl₃): δ 5.02 (1H, s, H-17a), 4.86 (1H, s, H-17b), 3.88 (1H, d, $J = 2.7$ Hz, H-13), 2.81 (1H, dd, $J = 5.9, 2.7$ Hz, H-12), 2.55 (1H, ddd, $J = 15.8, 13.3, 6.4$ Hz, H-2a), 2.41 (1H, dt, $J = 13.5, 3.2$ Hz, H-7a), 2.36 (1H, dd, $J = 5.6, 3.2$ Hz, H-2b), 2.32 (2H, bs, H-15), 2.00 (1H, m, H-11b), 1.86 (1H, ddd, $J = 13.3, 6.4, 3.2$ Hz, H-1a), 1.75 (1H, ddd, $J = 14.0, 6.1, 2.7$ Hz, H-11a), 1.65 (1H, dd, $J = 11.5, 6.1$ Hz, H-9), 1.51 (1H, m, H-6a), 1.50 (1H, m, H-6b), 1.39 (1H, td, $J = 13.3, 5.6$ Hz, H-1b), 1.31 (1H, m, H-5), 1.08 (3H, s, H-18), 1.00 (3H, s, H-19), 0.94 (1H, m, H-7b), 0.84 (3H, s, H-20) ppm.

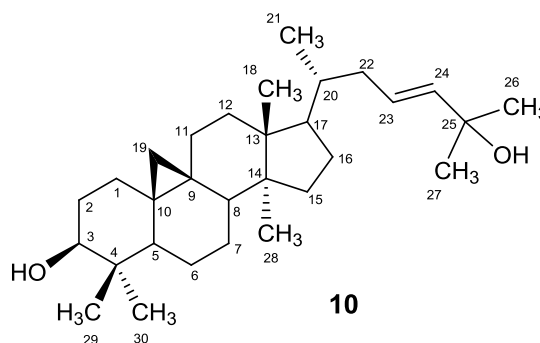
¹³C NMR (101 MHz, CDCl₃): δ 218.1 (C-14), 216.2 (C-3), 142.3 (C-16), 111.3 (C-17), 75.3 (C-13), 55.3 (C-5), 51.2 (C-9), 47.6 (C-4), 47.4 (C-8), 44.9 (C-12), 43.9 (C-15), 37.7 (C-10), 36.8 (C-1), 34.2 (C-2), 30.5 (C-7), 26.3 (C-18), 25.5 (C-11), 22.0 (C-19), 20.1 (C-6), 13.8 (C-20) ppm.

**Cycloart-23-ene-3 β ,25-diol (10):**

White crystals;

M. p. 212 – 215 °C; $[\alpha]_D^{18} + 42.8$ (c 0,1, CHCl₃);**IR** (CH₂Cl₂) ν_{\max} : 3352, 2907, 2362, 1470, 1372, 1047, 737 cm⁻¹;**¹H RMN (400 MHz, CDCl₃):** δ 5.59 (2H,

bs, H-23 and H-24), 3.28 (1H, dd, $J = 10.9, 4.3$ Hz, H-3), 1.31 (6H, s, H-26 and H-27), 0.96 (6H, s, H-18 and H-29), 0.88 (3H, s, H-28), 0.85 (3H, d, $J = 6.4$ Hz, H-21), 0.80 (3H, s, H-30), 0.55 (1H, d, $J = 4.0$ Hz, H-19a), 0.33 (1H, d, $J = 4.0$ Hz, H-19b) ppm.

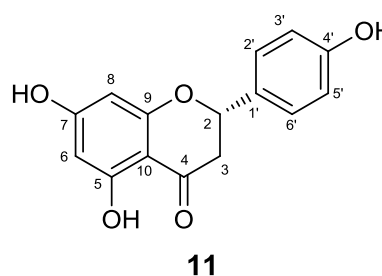


¹³C RMN (101 MHz, CDCl₃): δ 139.5 (C-24), 125.8 (C-23), 79.0 (C-3), 70.9 (C-25), 52.1 (C-17), 49.0 (C-14), 48.1 (C-8), 47.2 (C-5), 45.4 (C-13), 40.6 (C-4), 39.2 (C-22), 36.5 (C-20), 35.7 (C-12), 32.9 (C-15), 32.1 (C-1), 30.5 (C-19), 30.1 (C-27), 30.0 (C-16), 30.0 (C-26), 28.2 (C-7), 26.6 (C-2), 26.2 (C-10 and C-11), 25.6 (C-30), 21.3 (C-6), 20.1 (C-9), 19.4 (C-28), 18.4 (C-21), 18.2 (C-18), 14.2 (C-29) ppm.

Naringenin (11):

Yellow powder;

¹H RMN (400 MHz, MeOD): δ 5.29 (1H, dd $J = 13.0$, 2.9 Hz, H-2), 3.07 (1H, dd, $J = 17.1$; 13.0 Hz, H-3a), 2.65 (1H, dd $J = 17.1$, 2.9 Hz, H-3b), 5.85 (1H, d $J = 2.2$ Hz, H-6), 5.84 (1H, d, $J = 2.2$ Hz, H-8), 7.27 (1H, d, $J = 8.5$ Hz, H-2'), 6.78 (1H, d, $J = 8.5$ Hz, H-3'), 6.78 (1H, d, $J = 8.5$ Hz, H-5'), 7.27 (1H, d, $J = 8.5$ Hz, H-6') ppm.



¹³C NMR (101 MHz, MeOD): δ 197.7 (C-4), 168.3 (C-7), 163.7 (C-5), 164.8 (C-9), 159.0 (C-4'), 131.1 (C-1'), 129.0 (C-2'), 129.0 (C-6'), 116.3 (C-3'), 116.3 (C-5'), 103.3 (C-10), 97.0 (C-6), 96.1 (C-8), 80.4 (C-2), 44.0 (C-3) ppm.

Study of fraction K-N

Fractions K to N (*n*-hexane/EtOAc, 2:3 to 1:9) were pooled together (31.7 g) and submitted to column chromatography (4 x 90 cm, 400 g SiO₂), using *n*-hexane/EtOAc and EtOAc/MeOH (1:0 to 0:1 and 9:1 to 1:1, used in increasing gradients of 5%, 1 L each eluent), originating sixteen fractions. Aromadendrin (**12**) was isolated by precipitation of fractions KN₁₂ and KN₁₃ yielding 1.2 g. Compound **14** (131 mg) precipitated from sub-fraction KN₁₄ (6.9 g), that was subsequently separated by column chromatography (5 x 80 cm, 210 g) with CH₂Cl₂/acetone (1:0 to 1:1, used in increasing gradients of 1%, 250 mL each eluent). From this fractioning 19 mg of **16** and 441 mg of **13** were obtained. A fraction of this column (*n*-hexane/EtOAc; 3:7 to 1:4) was further purified on a Combiflash system

(12 g SiO₂ flash column, RediSep®Rf, Teledyne Isco) using *n*-hexane/CHCl₃ and CHCl₃/MeOH (1:1 to 0:1 and 0:1 to 7:3, used in increasing gradients of 1%, 5 mL/min) to obtain compound **1** that was additionally purified by preparative TLC (CH₂Cl₂/MeOH; 47:3), yielding 16 mg of pure compound. Purification of fraction KN₁₅ yielded compound **15** (4 mg).

Piscatolide; 3 α ,14 β -dihydroxy-ent-abieta-8,13(15)-dien-16,12-olide (**1**):

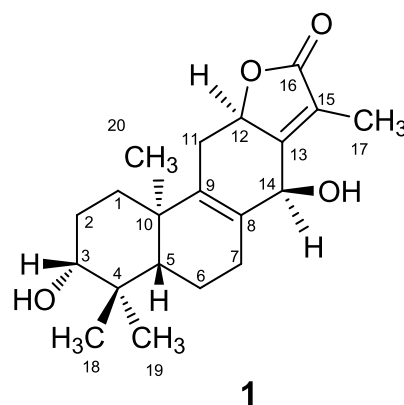
White powder;

$[\alpha]_D^{26} - 40$ (c 0.1, MeOH);

UV (MeOH) λ_{\max} (log ϵ) 218 (3.76) nm;

IR (CH₂Cl₂) ν_{\max} 3385, 1734, 1597, 1377 cm⁻¹;

ESIMS (negative mode) m/z (rel. int.) 331 [M - H]⁻ (100);



ESI-TOF-HRMS m/z : 355.1875 [M + Na]⁺ (calcd for C₂₀H₂₈O₄Na, 355.1885);

¹H RMN (400 MHz, CDCl₃/MeOD): δ 5.15 (1H, s, H-14), 4.92 (1H, t, $J = 8.2$ Hz, H-12), 3.34 (1H, m, H-3), 3.05 (1H, dd, $J = 15.3, 6.6$ Hz, H-11a), 2.65 (1H, m, H-7a), 2.25 (1H, m, H-7b), 2.19 (3H, s, H-17), 2.07 (1H, m, H-11b), 2.00 (1H, m, H-6a), 1.92 (1H, dt, $J = 12.6, 2.9$ Hz, H-1a), 1.85 (2H, m, H-2a and H-2b), 1.71 (1H, m, H-6b), 1.38 (1H, m, H-1b), 1.34 (1H, m, H-5), 1.22 (3H, s, H-20), 1.19 (3H, s, H-19), 1.00 (3H, s, H-18) ppm.

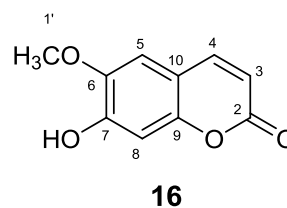
¹³C NMR (101 MHz, CDCl₃/MeOD): δ 176.9 (C-16), 162.7 (C-13), 137.8 (C-9), 130.4 (C-8), 121.6 (C-15), 78.7 (C-3), 79.1 (C-12), 70.1 (C-14), 51.4 (C-5), 38.6 (C-4), 34.6 (C-1), 39.2 (C-10), 27.4 (C-2), 29.2 (C-7), 32.9 (C-11), 18.6 (C-6), 28.3 (C-19), 19.1 (C-20), 16.0 (C-18), 9.0 (C-17) ppm.

Scopoletin (16):

White powder;

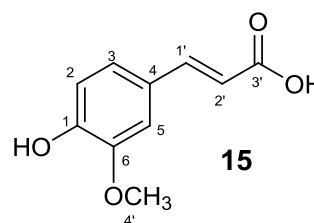
$^1\text{H NMR}$ (400 MHz, CDCl_3): δ 7.60 (1H, d, $J = 9.5$ Hz, H-4), 6.92 (1H, s, H-5), 6.84 (1H, s, H-8), 6.27 (1H, d, $J = 9.5$ Hz, H-3), 3.95 (3H, s, H-1') ppm.

$^{13}\text{C NMR}$ (101 MHz, CDCl_3): δ 161.6 (C-2), 150.2 (C7), 149.3 (C-9), 144.1 (C-6), 143.5 (C-4), 113.5 (C-3), 111.6 (C-10), 107.6 (C-8), 103.3 (C-5), 56.6 (C-1') ppm.

**Ferulic acid (15):**

White powder;

$^1\text{H NMR}$ (400 MHz, MeOD): δ 7.55 (1H, d, $J = 15.9$ Hz, H-1'), 7.14 (1H, s, H-6), 7.02 (1H, d, $J = 8.1$ Hz, H-4), 6.77 (1H, d, $J = 8.2$ Hz, H-3), 6.28 (1H, d, $J = 15.9$ Hz, H-2'), 3.85 (3H, s, H-4') ppm.

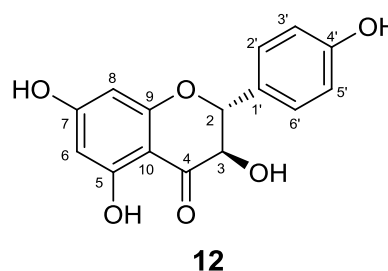


$^{13}\text{C NMR}$ (101 MHz, MeOD): δ 171.0 (C-3'), 150.4 (C-1), 149.3 (C-2), 146.7 (C-1'), 127.8 (C-5), 123.9 (C-4), 116.4 (C-2'), 116.2 (C-3), 111.6 (C-6), 56.40 (C-4') ppm.

Aromadendrin (12):

White powder;

$^1\text{H NMR}$ (400 MHz, MeOD): δ 7.32 (1H, d, $J = 8.6$ Hz, H-2'), 6.80 (2H, d, $J = 8.6$ Hz, H-3'/H-5'), 5.89 (1H, d, $J = 2.1$ Hz, H-6), 5.84 (1H, d, $J = 2.1$ Hz, H-8), 4.94 (1H, d, $J = 11.6$ Hz, H-2), 4.51 (1H, d, $J = 11.6$ Hz, H-3) ppm.

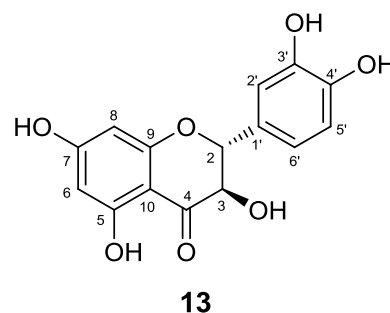


$^{13}\text{C NMR}$ (101 MHz, MeOD): δ 198.4 (C-4), 168.7 (C-7), 165.2 (C-5), 164.5 (C-9), 159.2 (C-4'), 130.3 (C-2'/C-6'), 129.3 (C-1'), 116.1 (C-3'/C-5'), 101.8 (C-10), 97.3 (C-6), 96.3 (C-8), 84.9 (C-2), 73.6 (C-3) ppm.

Taxifolin (13):

Yellow powder;

$^1\text{H NMR}$ (400 MHz, Acetone- d_6): δ 5.03 (1H, d, $J = 11.4$ Hz, H-2), 4.61 (1H, d, $J = 11.4$ Hz, H-3), 5.99 (1H, d, $J = 2.1$ Hz, H-6), 5.95 (1H, d, $J = 2.1$ Hz, H-8), 7.07 (1H, d, $J = 1.8$ Hz, H-2'), 6.86 (1H, d, $J = 8.1$ Hz, H-5'), 6.92 (1H, dd, $J = 8.1; 1.8$ Hz, H-6')

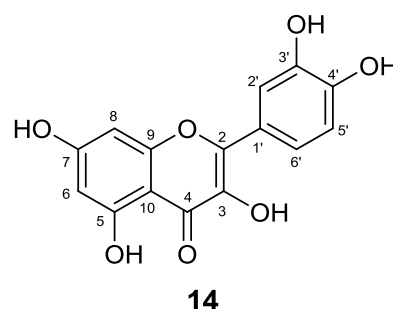


$^{13}\text{C NMR}$ (101 MHz, Acetone- d_6): δ 198.1 (C-4), 167.6 (C-7), 164.1 (C-5), 164.9 (C-9), 145.4 (C-3'), 144.6 (C-4'), 129.7 (C-1'), 120.8 (C-6'), 115.8 (C-2'), 115.6 (C-5'), 101.5 (C-10), 96.9 (C-6), 96.9 (C-8), 84.4 (C-2), 73.1 (C-3) ppm.

Quercetin (14):

White powder;

$^1\text{H NMR}$ (400 MHz, MeOD): δ 7.74 (1H, d, $J = 2.0$ Hz, H-2'), 7.64 (1H, dd, $J = 8.4, 2.0$ Hz, H-6'), 6.85 (1H, d, $J = 8.4$ Hz, H-5'), 6.39 (1H, d, $J = 2.0$ Hz, H-8), 6.19 (1H, d, $J = 2.0$ Hz, H-6) ppm.



$^{13}\text{C NMR}$ (101 MHz, MeOD): δ 177.2 (C-4), 165.5 (C-7), 162.4 (C-5), 158.1 (C-9), 147.9 (C-2), 148.6 (C-4'), 146.1 (C-3'), 137.2 (C-3), 124.1 (C-1'), 121.6 (C-6'), 115.9 (C-2'), 116.1 (C-5'), 104.4 (C-10), 99.1 (C-6), 94.3 (C-8) ppm.

8.1.3. Phytochemical study of *Euphorbia welwitschii*

8.1.3.1. Plant Material

Aerial parts of *Euphorbia welwitschii* Boiss. & Reut. were collected in the garden of Palácio da Pena, Sintra, Portugal (June 2010). The plant was identified by Dr. Teresa Vasconcelos (plant taxonomist) of Instituto Superior de Agronomia, Technical University of Lisbon, Portugal. A voucher specimen (no. 282/2010) has been deposited at the herbarium of Instituto Superior de Agronomia.

8.1.3.2. Extraction and Isolation

The air-dried powdered plant material (3.5 kg) was exhaustively extracted with methanol (10 × 5 L) at room temperature. Evaporation of the solvent (under vacuum, 40 °C) from the crude extract yielded a residue of 595 g. This residue was resuspended in MeOH/H₂O solution (1:2) and extracted with EtOAc (4 × 1 L). The ethyl acetate soluble fraction was dried (Na₂SO₄) and evaporated under vacuum, yielding a residue (225 g) that was chromatographed over SiO₂ (2 kg), using mixtures of *n*-hexane-EtOAc (1:0 to 0:1) and EtOAc-MeOH (9:1 to 3:7) in increasing gradients of 5%, of 2 L each eluent. According to differences in composition as indicated by TLC, nine crude fractions were obtained (Table 8.2). Due to the high content of chlorophylls, the ¹H NMR of the crude fractions was not useful. Therefore, the studied fractions G and I were selected according to the polarity and TLC profile.

Table 8.2. Crude fractions of the EtOAc soluble fraction of the methanol extract of *E. welwitschii*.

Fraction	Amount (g)	Eluents (v/v)	
		<i>n</i> -hexane : EtOAc	EtOAc / MeOH
A	23.0	1:0 to 9:1	-
B	8.2	9:1 to 4:1	-
C	4.8	4:1	-
D	5.6	15:5 to 7:3	-
E	2.5	7:3	-
F	5.3	7:3	-
G	21.3	7:3 to 13:7	-
H	4.0	3:2 to 0:1	1:0 to 19 :1
I	7.8	-	9:1-
J	12.2	-	7:3

Study of fraction G

Fraction G (21.3 g), eluted with *n*-hexane/EtOAc (7:3 to 13:7), was subjected to solid-phase extraction on polyamide (130 g; 1:6), for removal of chlorophylls, using mixtures of 3:2 MeOH/H₂O (2 L), 4:1 MeOH/H₂O (2 L) and MeOH (5 L). The fractions 3:1 and 4:1 MeOH/H₂O were pooled together (14 g) and were fractionated on a Combiflash system (120 g SiO₂ flash column, RediSep®Rf, Teledyne Isco) with *n*-hexane/EtOAc and EtOAc/MeOH (1:0 to 0:1 and 9:1 to 7:3, used in increasing gradients of 5%, 15 mL/min), giving rise to fractions G₁-G₅ (Figure 8.2).

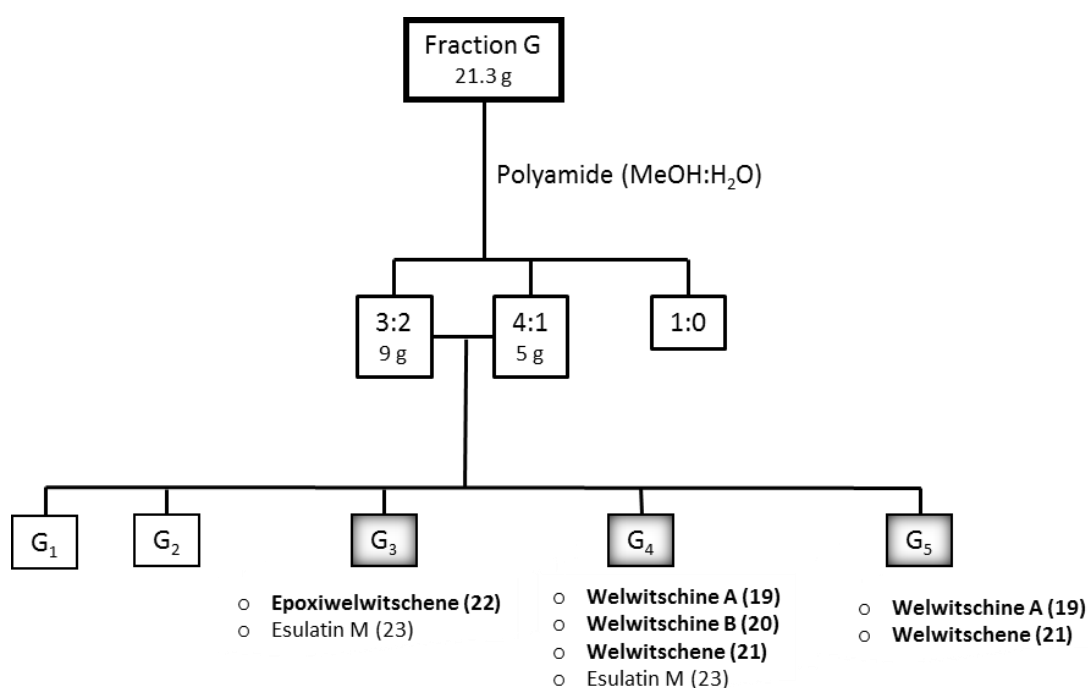


Figure 8.2. *Euphorbia. welwitschii*: study of fraction G and respective isolated compounds.

Fraction G₄ (4.2 g) was chromatographed using reverse-phase C-18 column (100 g C-18) chromatography (MeOH/H₂O, 1:1 to 1:0, used in increasing gradients of 5%, 300 mL each eluent), originating six fractions (G_{4A}-G_{4F}). Fraction G_{4C} (679 mg), eluted with 7:3 MeOH/H₂O, was subject to flash column chromatography (40 g SiO₂), using the following eluent system: CH₂Cl₂ (200 ml), 99:1 CH₂Cl₂/MeOH (400 ml) and 96:4 CH₂Cl₂/MeOH (400 ml). This separation yielded compounds **19** (326 mg) and **21** (86 mg).

Fraction G_{4D} (712 mg) was separated on a Combiflash system (12 g SiO₂ flash column, RediSep®Rf, Teledyne Isco) with *n*-hexane/EtOAc (1:0 to 0:1, used in increasing gradients of 5%, 5 mL/min), a sub-fraction (562 mg) was subsequently chromatographed over SiO₂ (40 g) with CH₂Cl₂/acetone as eluents (1:0 to 4:1, used in increasing gradients of 2.5%) and after further purification by HPLC this separation yielded compound **20** (13 mg; 16:9 acetonitrile/H₂O).

Fraction G₃ (3.2 g) was chromatographed using reverse-phase C-18 column (100 g C-18) chromatography (MeOH/H₂O, 1:1 to 1:0, used in increasing gradients of 5%, 300 mL each eluent), originating six fractions (G_{3A}-G_{3F}). A flash chromatography (CHCl₃ as eluent) of subfraction G_{3B} (549 mg) yielded 19 mg of compound **23**. Fraction G_{3C} (333 mg) was separated on a Combiflash system (12 g SiO₂ flash column, RediSep®Rf, Teledyne Isco) with *n*-hexane/EtOAc (1:0 to 0:1, used in increasing gradients of 5%, 5 mL/min). To obtain compound **22** a sub-fraction was further purified by preparative TLC (CH₂Cl₂/MeOH; 96:4), yielding 46 mg of pure compound.

Welwitschine A; 3β,5α,11β-triacetoxy-7β,8α-diisobutyryloxy-9α-nicotinoyloxy-12,15-epoxy-12,17-cyclojatroph-6α-ol-14-one (**19**):

White crystals;

M.p. 225-228 °C;

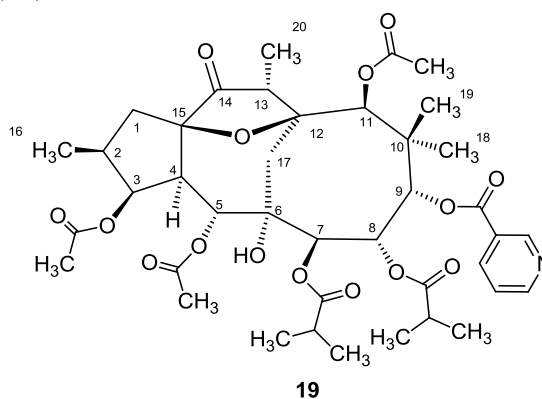
$[\alpha]_D^{24} + 2.9$ (c 0.1, CHCl₃);

IR (CH₂Cl₂) ν_{\max} 3447, 2957, 2916, 1738, 1641, 1375, 1232 cm⁻¹;

ESIMS (positive mode) m/z (rel. int.) 788 [M + H]⁺ (100);

ESI-TOF-HRMS m/z 788.3499 [M + H]⁺ (calcd for C₄₀H₅₄NO₁₅ 788.3488);

¹H NMR (400 MHz, CDCl₃): δ 9.27 (1H, s, 9-ONic-H-2'), 8.82 (1H, dd, $J = 5.0, 12$ Hz, 9-ONic-H-6'), 8.30 (1H, d, $J = 7.9$ Hz, 9-ONic-H-4'), 7.47 (1H, dd, $J = 7.9, 5.0$ Hz, 9-ONic-H-5'), 6.00 (1H, d, $J = 10.1$, H-8), 5.96 (1H, d, $J = 11.1$ Hz, H-5), 5.53 (1H, bs, H-9), 5.41 (1H, d, $J = 10.1$ Hz, H-7), 5.36 (1H, t, $J = 3.8$ Hz, H-3), 5.07 (1H, s, H-11), 2.96 (1H, s, 6-OH), 2.87 (1H, dd, $J = 11.1, 4.9$ Hz, H-4), 2.64 (1H, q, $J = 6.6$ Hz, H-13), 2.42



(1H, m, 7-OCOCH(CH₃)₂), 2.30 (1H, m, H-17b), 2.29 (1H, m, 7-OCOCH(CH₃)₂), 2.26 (1H, m, H-2), 2.15 (3H, s, 11-OCOCH₃), 2.09 (3H, s, 3-OCOCH₃), 2.01 (1H, m, H-1b), 2.01 (1H, m, H-17a), 1.98 (3H, s, 5-OCOCH₃), 1.86 (1H, m, H-1a), 1.63 (3H, s, H-19), 1.15 (3H, d, *J* = 7.0 Hz, 7-OCOCH(CH₃)₂), 1.13 (3H, d, *J* = 7.0 Hz, 7-OCOCH(CH₃)₂), 1.07 (3H, d, *J* = 7.0 Hz, 7-OCOCH(CH₃)₂), 1.03 (3H, d, *J* = 7.0 Hz, 7-OCOCH(CH₃)₂), 1.02 (3H, d, *J* = 6.6 Hz, H-20), 1.00 (3H, s, H-18), 0.90 (3H, d, *J* = 6.6 Hz, H-16) ppm.

¹³C NMR (101 MHz, CDCl₃): δ 218.7 (C-14), 175.4 (8-OCOCH(CH₃)₂), 175.3 (7-OCOCH(CH₃)₂), 171.3 (3-OCOCH₃), 170.1 (11-OCOCH₃), 168.7 (5-OCOCH₃), 164.2 (9-ONic), 154.0 (9-ONic-C-6'), 150.9 (9-ONic-C-1'), 137.3 (9-ONic-C-4'), 125.6 (9-ONic-C-2'), 123.9 (9-ONic-C-5'), 85.5 (C-15), 84.8 (C-12), 82.5 (C-9), 77.5 (C-3), 75.5 (C-7), 74.8 (C-11), 73.7 (C-6), 68.7 (C-5), 68.6 (C-8), 53.8 (C-13), 50.2 (C-4), 43.9 (C-10), 43.1 (C-1), 42.0 (C-17), 37.3 (C-2), 34.0 (7-OCOCH(CH₃)₂), 33.9 (8-OCOCH(CH₃)₂), 31.1 (C-18), 21.4 (5-OCOCH₃; 3-OCOCH₃), 21.0 (11-OCOCH₃), 20.7 (C-19), 19.5 (8-OCOCH(CH₃)₂), 19.0 (8-OCOCH(CH₃)₂), 18.8 (7-OCOCH(CH₃)₂), 18.5 (7-OCOCH(CH₃)₂), 13.1 (C-16), 7.7 (C-20) ppm.

Welwitschine B, 3β,11β-diacetoxy-7β,8α-diisobutyryloxy-9α-nicotinoyloxy-12,15-epoxy-12,17-cyclojatropa-5α,6α-diol-14-one (**20**):

White crystals;

M.p. 285-288 °C;

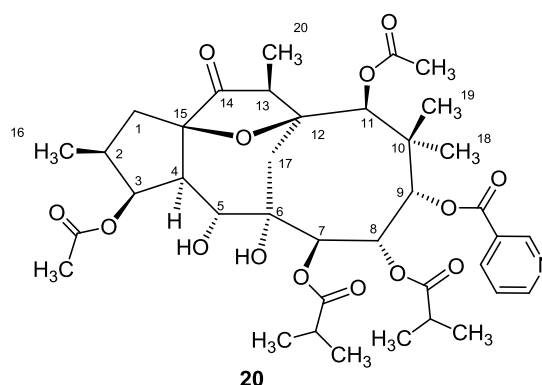
[α]_D²⁴ – 45.6 (c 0.1, CHCl₃);

IR (CH₂Cl₂) ν_{max} 3445, 2955, 2924, 1744, 1720, 1645 cm⁻¹;

ESIMS (positive mode) *m/z* 746 [M + H]⁺;

ESI-TOF-HRMS *m/z* 746.3377 [M + H]⁺ (calcd for C₃₈H₅₂NO₁₄, 746.3382);

¹H NMR (400 MHz, CDCl₃): δ 9.13 (1H, s, 9-ONic-H-2'), 8.80 (1H, d, *J* = 3.8 Hz, 9-ONic-H-6'), 8.21 (1H, d, *J* = 7.9 Hz, 9-ONic-H-4'), 7.42 (1H, dd, *J* = 7.9, 5.0 Hz, 9-ONic-H-5'), 6.77 (1H, d, *J* = 3.3 Hz, H-4), 5.83 (1H, dd, *J* = 8.0, 3.3 Hz, H-8), 5.51 (1H, d, *J* =



8.0 Hz, H-7), 5.42 (1H, bs, H-3), 5.27 (1H, s, H-11), 4.69 (1H, dd, $J = 10.5, 4.6$ Hz, H-5), 4.09 (1H, s, 6-OH), 3.62 (1H, d, $J = 4.6$ Hz, 5-OH), 2.84 (1H, d, $J = 16.3$ Hz, H-17a), 2.60 (1H, dd, $J = 10.5, 4.9$ Hz, H-4), 2.44 (2H, m, 7-OCOCH(CH₃)₂; 8-OCOCH(CH₃)₂), 2.42 (3H, s, 3-OCOCH₃), 2.36 (1H, m, H-13), 2.26 (1H, m, H-2), 2.18 (3H, s, 11-OCOCH₃), 2.07 (1H, m, H-1b), 1.87 (1H, m, H-1a), 1.87 (1H, m, H-17b), 1.30 (3H, s, H-18), 1.26 (3H, s, H-19), 1.23 (3H, d, $J = 7.1$ Hz, H-20), 1.08 (3H, d, $J = 7.0$ Hz, 8-OCOCH(CH₃)₂), 1.05 (3H, d, $J = 7.0$ Hz, 8-OCOCH(CH₃)₂), 1.04 (3H, d, $J = 7.0$ Hz, 7-OCOCH(CH₃)₂), 1.02 (3H, d, $J = 7.0$ Hz, 7-OCOCH(CH₃)₂), 0.98 (3H, d, $J = 6.6$ Hz, H-16) ppm.

¹³C NMR (101 MHz, CDCl₃): δ 220.2 (C-14), 176.4 (8-OCOCH(CH₃)₂), 175.5 (7-OCOCH(CH₃)₂), 172.7 (3-OCOCH₃), 170.1 (5-OCOCH₃), 164.6 (9-OCNic), 153.8 (9-ONic-C-6'), 150.8 (9-ONic-C-1'), 137.2 (9-ONic-C-4'), 125.9 (9-ONic-C-3'), 123.6 (9-ONic-C-5'), 85.6 (C-15), 84.9 (C-12), 81.3 (C-11), 80.8 (C-7), 77.9 (C-3), 74.6 (C-8), 74.2 (C-9), 72.7 (C-6), 68.2 (C-5), 54.7 (C-13), 54.0 (C-4), 53.8 (C-17), 43.0 (C-10 and C-1), 37.1 (C-2), 34.2 (8-OCOCH(CH₃)₂), 34.1 (7-OCOCH(CH₃)₂), 23.6 (C-18), 20.8 (5-OCOCH₃ and 3-OCOCH₃), 20.7 (C-19), 19.2 (8-OCOCH(CH₃)₂), 19.0 (8-OCOCH(CH₃)₂), 18.9 (7-OCOCH(CH₃)₂), 18.8 (7-OCOCH(CH₃)₂), 13.0 (C-16 and C-20) ppm.

Welwitschene; 3 β ,5 α ,-diacetoxy-7 β ,8 α -diisobutyryloxy-9 α -nicotinoyloxy-12,15-epoxy-jatroph-6(17)-en-11 β ol-14-one (**21**):

White powder;

$[\alpha]_D^{24} + 19.5$ (c 0.1, CHCl₃);

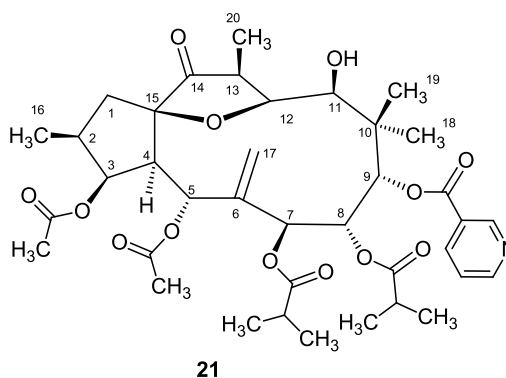
IR (CH₂Cl₂) ν_{\max} 3447, 1732, 1641, 1462, 1265, 1246, 740 cm⁻¹;

ESIMS (positive mode) m/z 748 [M + H]⁺;

ESI-TOF-HRMS m/z 730.3454 [M + H]⁺ (calcd for C₃₈H₅₂NO₁₃, 730.3433);

¹H NMR (400 MHz, CDCl₃): δ 9.10 (1H, s, 9-ONic-H-2'), 8.74 (1H, d, $J = 4.0$ Hz, 9-ONic-H-6'), 8.22 (1H, d, $J = 7.4$ Hz, 9-ONic-H-4'), 7.37 (1H, dd, $J = 7.4, 4.0$ Hz, 9-ONic-H-5'), 6.55 (1H, bs, H-9), 6.30 (1H, bd, $J = 8.3$ Hz, H-8), 5.91 (1H, d, $J = 10.2$ Hz, H-7), 5.87 (1H, d, $J = 10.1$ Hz, H-5), 5.57 (1H, bs, H-17b), 5.49 (1H, bs, H-3), 5.30 (1H, bs, H-17a), 3.91 (2H, bs, H-11 and H-12), 3.10 (1H, bd, $J = 5.1$ Hz, H-4), 2.77 (1H, bs, 11-OH), 2.45 (1H, m, 7-OCOCH(CH₃)₂), 2.38 (1H, m, H-13), 2.32 (3H, s, 3-OCOCH₃), 2.26 (1H, m, 8-OCOCH(CH₃)₂), 2.15 (1H, m, H-2), 1.98 (1H, m, H-1a), 1.88 (3H, s, 5-OCOCH₃), 1.81 (1H, m, H-1b), 1.34 (3H, s, H-18), 1.31 (3H, d, $J = 7.3$ Hz, H-20), 1.07 (3H, d, $J = 6.9$ Hz, 7-OCOCH(CH₃)₂), 1.03 (3H, d, $J = 6.9$ Hz, 7-OCOCH(CH₃)₂), 1.02 (3H, s, H-19), 0.97 (3H, d, $J = 6.8$ Hz, 8-OCOCH(CH₃)₂), 0.93 (3H, d, $J = 6.8$ Hz, 8-OCOCH(CH₃)₂), 0.91 (3H, d, $J = 7.2$ Hz, H-16) ppm.

¹³C NMR (101 MHz, CDCl₃): δ 221.6 (C-14), 175.6 (8-OCOCH(CH₃)₂), 175.1 (7-OCOCH(CH₃)₂), 172.0 (3-OCOCH₃), 168.8 (5-OCOCH₃), 163.7 (9-ONic), 153.3 (9-ONic-C-6'), 150.7 (9-ONic-C-1'), 143.6 (C-6), 137.4 (9-ONic-C-4'), 126.4 (9-ONic-C-2'), 124.9 (C-17), 123.4 (9-ONic-C-5'), 87.8 (C-15), 83.4 (C-12), 76.2 (C-11 and C-3), 75.2 (C-7), 74.5 (C-9), 72.8 (C-8), 66.4 (C-5), 54.2 (C-4), 46.7 (C-13), 45.6 (C-1), 44.3 (C-10), 37.6 (C-2), 34.2 (8-OCOCH(CH₃)₂), 34.0 (7-OCOCH(CH₃)₂), 21.6 (C-18), 21.0 (3-OCOCH₃), 20.8 (5-OCOCH₃), 19.3 (C-19), 19.1 (8-OCOCH(CH₃)₂), 18.9 (8-OCOCH(CH₃)₂), 18.5 (7-OCOCH(CH₃)₂), 18.4 (7-OCOCH(CH₃)₂), 17.2 (C-20), 13.3 (C-16) ppm.



21

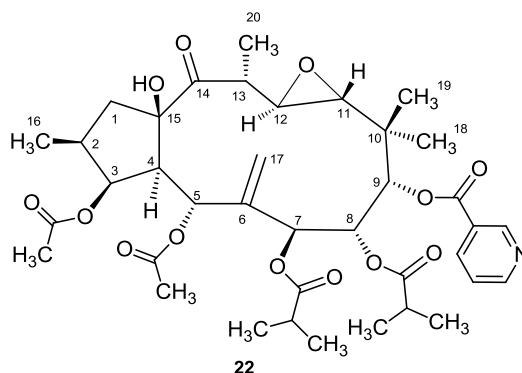
Epoxiwelwitschene; 3 β ,5 α ,-diacetoxy-7 β ,8 α -diisobutyryloxy-9 α -nicotinoyloxy-11,12-epoxy-jatroph-6(17)-en-15 β ol-14-one (**22**):

White powder;

$[\alpha]_D^{24} + 34.4$ (c 0.1, CHCl₃);

IR (CH₂Cl₂) ν_{\max} 3443, 2960, 1732, 1643 cm⁻¹;

ESIMS (positive mode) m/z 753 [M + Na]⁺;



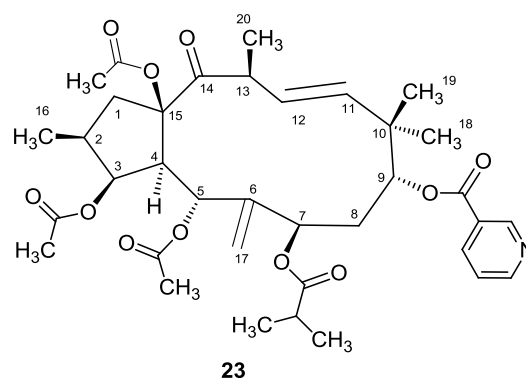
ESI-TOF-HRMS m/z 730.3450 [M + H]⁺ (calcd for C₃₈H₅₂NO₁₃, 730.3433);

¹H NMR (300 MHz, CDCl₃): δ 9.27 (1H, d, $J = 1.6$ Hz, 9-ONic-H-2'), 8.78 (1H, dd, $J = 5.0, 1.6$ Hz, 9-ONic-H-6'), 8.38 (1H, dt, $J = 7.9, 1.9$ Hz, 9-ONic-H-4'), 7.42 (1H, dd, $J = 7.9, 5.0$ Hz, 9-ONic-H-5'), 6.19 (1H, t, $J = 2.3$ Hz, H-8), 5.76 (1H, d, $J = 2.3$ Hz, H-7), 5.62 (1H, d, $J = 8.8$ Hz, H-5), 5.45 (1H, t, $J = 3.2$ Hz, H-3), 5.39 (2H, bs, H-17a and H-17b), 5.32 (1H, d, $J = 2.3$ Hz, H-9), 3.57 (1H, s, 15-OH), 3.43 (1H, dd, $J = 8.8, 3.2$ Hz, H-4), 3.23 (1H, m, H-13), 3.12 (1H, d, $J = 1.8$ Hz, H-11), 2.77 (1H, dd, $J = 8.8, 1.8$ Hz, H-12), 2.60 (1H, m, 8-OCOCH(CH₃)₂), 2.31 (1H, dd, $J = 13.9, 8.7$ Hz, H-1a), 2.11 (3H, s, 3-OCOCH₃), 2.11 (1H, m, H-2), 2.11 (1H, m, 7-OCOCH(CH₃)₂), 1.90 (3H, s, 5-OCOCH₃), 1.58 (1H, dd, $J = 13.9, 11.2$ Hz, H-1b), 1.27 (3H, d, $J = 6.7$ Hz, H-20), 1.18 (3H, d, $J = 7.0$ Hz, 8-OCOCH(CH₃)₂), 1.15 (3H, d, $J = 7.0$ Hz, 8-OCOCH(CH₃)₂), 1.11 (3H, s, H-18), 0.89 (3H, d, $J = 7.0$ Hz, H-16), 0.88 (1H, s, H-19), 0.86 (3H, d, $J = 7.0$ Hz, 7-OCOCH(CH₃)₂), 0.70 (3H, d, $J = 7.0$ Hz, 7-OCOCH(CH₃)₂) ppm.

¹³C NMR (101 MHz, CDCl₃): δ 214.7 (C-14), 176.0 (7-OCOCH(CH₃)₂), 175.0 (7-OCOCH(CH₃)₂), 170.3 (3-OCOCH₃), 168.8 (5-OCOCH₃), 164.3 (9-ONic), 153.9 (9-ONic-C-6'), 151.6 (9-ONic-C-1'), 141.8 (C-6), 137.6 (9-ONic-C-4'), 125.2 (9-ONic-C-2'), 123.5 (9-ONic-C-5'), 122.9 (C-17), 87.0 (C-15), 79.4 (C-9), 78.4 (C-3), 70.6 (C-7), 69.5 (C-8), 66.4 (C-5), 63.7 (C-11), 58.8 (C-12), 52.9 (C-4), 49.6 (C-1), 43.7 (C-13), 38.6 (C-10), 37.2 (C-2), 34.2 (8-OCOCH(CH₃)₂), 33.9 (7-OCOCH(CH₃)₂), 26.5 (C-18), 21.2 (5-OCOCH₃), 21.1 (3-OCOCH₃), 18.8 (8-OCOCH(CH₃)₂), 18.8 (8-OCOCH(CH₃)₂), 18.5 (7-OCOCH(CH₃)₂), 18.4 (7-OCOCH(CH₃)₂), 14.0 (C-16), 16.6 (C-19), 15.0 (C-20) ppm.

Esulatin M (23):

White powder;

 $[\alpha]_D^{24} - 15.4$ (c 0.1, CHCl₃);**IR** (CH₂Cl₂) ν_{\max} 3524, 2949, 1765, 1375, 1215 cm⁻¹;**ESIMS** (positive mode) m/z (rel. int.) 670[M + H]⁺; (100);

¹H NMR (400 MHz, C₆D₆): δ 9.59 (1H, s, 9-ONic-H-2'), 8.44 (1H, d, $J = 4.9$ Hz, 9-ONic-H-6'), 8.11 (1H, d, $J = 7.8$ Hz, 9-ONic-H-4'), 6.65 (1H, dd, $J = 7.8, 4.9$ Hz, 9-ONic-H-5'), 6.14 (1H, d, $J = 16.0$ Hz, H-11), 6.12 (1H, bs, H-5), 5.84 (1H, dd, $J = 16.0, 9.1$ Hz, H-12), 5.76 (1H, bs, H-3), 5.42 (1H, bs, H-17a), 5.29 (1H, bs, H-17b), 5.23 (1H, dd, $J = 7.3, 2.9$ Hz, H-9), 5.19 (1H, dd, $J = 6.5, 2.9$ Hz, H-7), 3.73 (1H, m, H-13), 3.33 (1H, dd, $J = 13.9, 7.7$ Hz, H-1a), 3.16 (1H, d, $J = 2.7$ Hz, H-4), 2.40 (1H, m, H-2), 2.32 (1H, m, H-8a), 2.29 (1H, m, H-8b), 1.99 (1H, m, 7-OCOCH(CH₃)₂), 1.75 (3H, s, 5-OCOCH₃), 1.74 (1H, m, H-1b), 1.71 (3H, s, 3-OCOCH₃), 1.66 (3H, s, 15-OCOCH₃), 1.43 (3H, d, $J = 6.7$ Hz, H-20), 0.95 (3H, s, H-19), 0.91 (3H, s, H-18), 0.81 (3H, d, $J = 7.0$ Hz, 7-OCOCH(CH₃)₂), 0.67 (3H, d, $J = 6.9$ Hz, H-16), 0.64 (3H, d, $J = 7.0$ Hz, 7-OCOCH(CH₃)₂) ppm.

¹³C NMR (101 MHz, C₆D₆): δ 212.7 (C-14), 176.1 (7-OCOCH(CH₃)₂), 170.1 (15-OCOCH₃), 169.3 (3-OCOCH₃), 169.0 (5-OCOCH₃), 164.2 (9-OCNic), 153.9 (9-ONic-C-6'), 151.6 (9-ONic-C-2'), 148.7 (C-6), 138.2 (C-11), 136.6 (9-ONic-C-4'), 131.5 (C-12), 126.1 (9-ONic-C-3'), 123.5 (9-ONic-C-5'), 110.0 (C-17), 93.4 (C-15), 76.6 (C-3), 75.9 (C-9), 69.0 (C-7), 69.0 (C-5), 53.6 (C-4), 49.7 (C-10), 46.7 (C-1), 43.9 (C-13), 38.7 (C-2), 34.9 (C-8), 33.9 (7-OCOCH(CH₃)₂), 26.6 (C-18), 23.6 (C-19), 21.0 (5-OCOCH₃), 20.8 (3-OCOCH₃), 20.7 (15-OCOCH₃), 19.0 (7-OCOCH(CH₃)₂), 18.0 (7-OCOCH(CH₃)₂), 13.3 (C-16) ppm.

Study of fraction I

Fraction I (7.8 g), eluted with EtOAc/MeOH (9:1), was fractionated on a Combiflash system (120 g SiO₂ flash column, RediSep®Rf, Teledyne Isco) with *n*-hexane/EtOAc and EtOAc/MeOH (1:1 to 0:1 and 9:1 to 4:1), used in increasing gradients of 5%, 10 mL/min). A subsequent fraction (700 mg) was subjected to Combiflash system (43 g C-18 column, RediSep®Rf, Teledyne Isco) with MeOH/H₂O (0:1 to 1:0, used in increasing gradients of 5%, 5 mL/min) as eluents. The two main fractions of this column afforded 171 mg of compound **25** and 484 mg of compound **24**.

Quercetin 3-*O*- α -L-3'',5''-diacetyl-arabinofuranoside (**24**):

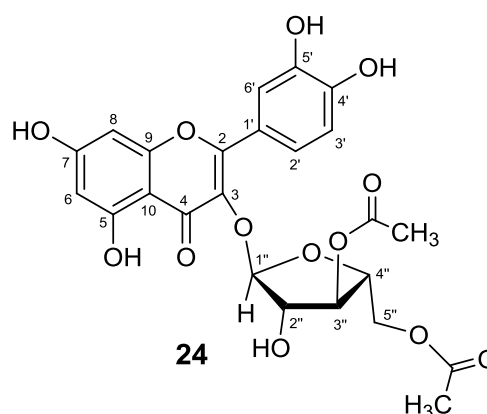
Yellow prismatic crystals;

M.p. 141-145 °C;

$[\alpha]_D^{24}$ – 183.0 (c 0.2, MeOH);

IR (KBr) ν_{\max} 3267, 1736, 1653, 1605, 1505, 1199 cm⁻¹;

ESIMS (negative mode) m/z (rel. int.) 517 [M – H]⁻ (100);



¹H NMR (400 MHz, MeOD): δ 7.38 (1H, d, J = 1.5 Hz, H-2'), 7.34 (1H, dd, J = 8.3, 1.5 Hz, H-6'), 6.85 (1H, d, J = 8.3 Hz, H-5'), 6.35 (1H, d, J = 1.5 Hz, H-8), 6.17 (1H, d, J = 1.5 Hz, H-6), 5.61 (1H, s, H-1''), 4.73 (1H, d, J = 4.6 Hz, H-3''), 4.44 (1H, s, H-2''), 4.14 (1H, dd, J = 11.8, 3.4 Hz, H-5a''), 3.93 (1H, dd, J = 11.8, 6.3 Hz, H-5b''), 3.67 (1H, dd, J = 9.2, 5.0 Hz, H-4''), 2.12 (3H, s, 3''-OCOCH₃), 1.93 (3H, s, 5''-OCOCH₃) ppm.

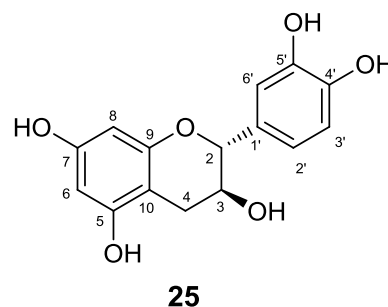
¹³C NMR (101 MHz, MeOD): δ 179.4 (C-4), 172.4 (3''-OCOCH₃), 172.3 (5''-OCOCH₃), 166.0 (C-7), 163.3 (C-5), 160.0 (C-2), 158.6 (C-9), 149.6 (C-4'), 146.4 (C-3'), 134.9 (C-3), 123.1 (C-1'), 122.9 (C-6'), 116.3 (C-2'), 117.3 (C-5'), 105.9 (C-1''), 105.9 (C-10), 99.9 (C-6), 94.8 (C-8), 83.9 (C-4''), 81.4 (C-2''), 81.2 (C-3''), 64.8 (C-5''), 20.9 (3''-OCOCH₃), 20.6 (5''-OCOCH₃) ppm.

Catechin (25):

Brown amorphous powder;

$[\alpha]_D^{24} + 18.0$ (c 0.1, MeOH);

¹H NMR (300 MHz, DMSO-*d*₆): δ 6.66 (1H, d, $J = 1.9$ Hz, H-6'), 6.63 (1H, d, $J = 8.1$ Hz, H-3'), 6.53 (1H, dd, $J = 8.1, 1.9$ Hz, H-2'), 5.83 (1H, d, $J = 2.3$ Hz, H-6), 5.63 (1H, d, $J = 2.3$ Hz, H-8), 4.42 (1H, d, $J = 7.5$ Hz, H-2), 3.81 – 3.69 (1H, m, H-3), 2.60 (1H, dd, $J = 16.0, 5.3$ Hz, H-4a), 2.29 (1H, dd, $J = 16.0, 8.1$ Hz, H-4b).



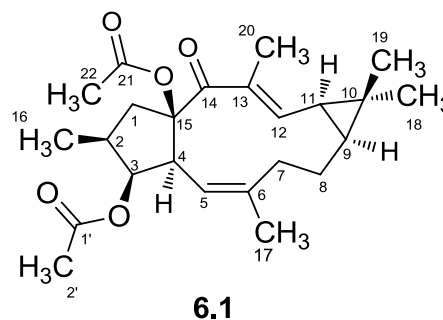
¹³C NMR (75 MHz, DMSO-*d*₆): δ 156.5 (C-7), 156.2 (C-5), 155.4 (C-9), 144.9 (C-4' and C-5'), 130.6 (C-1'), 118.5 (C-2'), 115.1 (C-3'), 114.5 (C-6'), 99.1 (C-10), 95.1 (C-6), 93.9 (C-8), 81.0 (C-2), 66.3 (C-3), 27.9 (C-4) ppm.

8.1.4. Preparation of a small library of macrocyclic lathyrane diterpenes

General preparation of Jolkinol D derivatives 6.1-6.12. A solution of compound **6** (14 mg, 0.039 mmol) in dry pyridine (2 ml) was stirred for 5 min at room temperature before addition of the suitable anhydride or chloride (2 eq.). The mixture was stirred for 48 h at room temperature. The reaction mixture was concentrated under vacuum at 40°C and the obtained residue was purified by flash column chromatography.

Jolkinolate A; 3 β ,15 β -diacetoxylathyra-5E,12E-dien-14-one (6.2):

Obtained from reaction with acetic anhydride (8 mg, 0.078 mmol). The residue was purified by flash column chromatography (silica gel, CH₂Cl₂/MeOH; 1:0 to 99:1) to afford 13 mg (0.032 mmol, 86% yield) of an amorphous white powder.



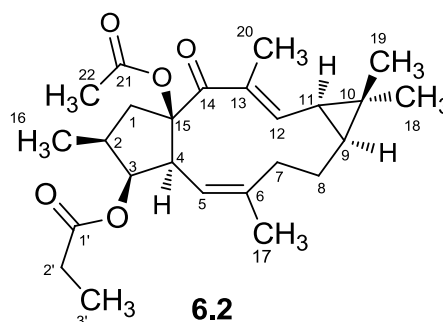
ESI-TOF-HRMS m/z 403.2550 [$M + H$]⁺ (calcd for C₂₄H₃₅O₅, 403.2450);

¹H NMR (400 MHz, CDCl₃): δ 6.66 (1H, *d*, *J* = 11.4, H-12), 5.34 (1H, *dt*, *J* = 10.7, 1.8 Hz, H-5), 5.23 (1H, *t*, *J* = 3.6 Hz, H-3), 3.50 (1H, *dd*, *J* = 13.9, 8.0 Hz, H-1 α), 2.50 (2H, *m*, H-4, H-7 α), 2.21–2.17 (2H, *m*, H-8 α , H-2), 2.13 (1H, *s*, H-2'), 2.01 (3H, *s*, H-22), 1.83 (3H, *s*, H-20), 1.75 (1H, *td*, *J* = 13.1, 2.6 Hz, H-7 β), 1.52, (1H, *dd*, *J* = 12.5, 2.8 Hz, H-8 β), 1.47 (1H, *dd*, *J* = 8.4, 4.9 Hz, H-1 β), 1.44 (3H, *d*, *J* = 1.3 Hz, H-17), 1.39 (1H, *dd*, *J* = 7.5, 3.9 Hz, H-11), 1.17 (3H, *s*, H-18), 1.06 (1H, *m*, H-9), 1.05 (3H, *s*, H-19), 0.95 (3H, *d*, *J* = 6.7 Hz, H-16) ppm.

¹³C NMR (101 MHz, CDCl₃): δ 195.4 (C-14), 170.8 (C-1'), 169.9 (C-21), 146.80 (C-12), 143.2 (C-6), 132.2 (C-13), 118.7 (C-5), 94.6 (C-15), 81.1 (C-3), 51.2 (C-4), 44.8 (C-1), 38.4 (C-2), 36.9 (C-7), 34.2 (C-9), 29.8 (C-11), 29.3 (C-18), 28.5 (C-8), 24.6 (C-10), 21.6 (C-22), 21.1 (C-2'), 21.0 (C-17), 16.4 (C-19), 13.9 (C-16), 12.4 (C-20) ppm.

Jolkinoate B; 15 β -acetoxy-3 β -propionatethylthra-5E,12E-dien-14-one (6.2):

Obtained from reaction with propionic anhydride (10 mg, 0.078 mmol). The residue was purified by flash column chromatography (silica gel, CH₂Cl₂/MeOH; 100:0 to 99:1) to afford 10 mg (0.023 mmol, 63% yield) of a yellow oil.



ESIMS (positive mode) *m/z* (rel. int.) 439 [M + Na]⁺ (100);

ESI-TOF-HRMS *m/z* 439.2458 [M + Na]⁺ (calcd for C₂₅H₃₆O₅Na, 439.2455);

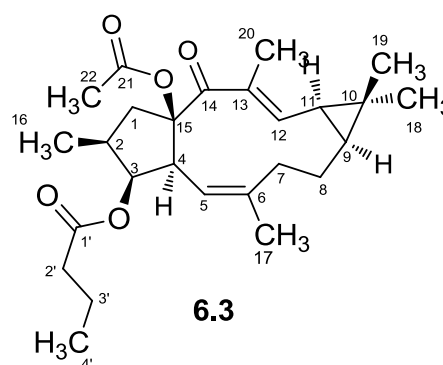
¹H NMR (400 MHz, CDCl₃): δ 6.65 (1H, *d*, *J* = 11.4 Hz, H-12), 5.33 (1H, *dt*, *J* = 10.7, 1.3 Hz, H-5), 5.24 (1H, *t*, *J* = 3.6 Hz, H-3), 3.52 (1H, *dd*, *J* = 13.9, 8.0 Hz, H-1 α), 2.50 (1H, *dd*, *J* = 10.7, 3.8 Hz, H-4), 2.44 (1H, *m*, H-7 α), 2.20–2.16 (2H, *m*, H-8 α , H-2), 2.01 (3H, *s*, H-22), 1.85 (3H, *d*, *J* = 1.0 Hz, H-20), 1.75 (1H, *td*, *J* = 13.1, 2.6 Hz, H-7 β), 1.50 (1H, *dd*, *J* = 14.4, 2.5 Hz, H-8 β), 1.45 (3H, *d*, *J* = 1.4 Hz, H-17), 1.41 (1H, *dd*, *J* = 7.9, 3.5 Hz, H-1 β), 1.38–1.32 (1H, *m*, H-11), 1.17 (3H, *s*, H-18), 1.06 (1H, *m*, H-9), 1.04 (3H, *s*, H-

19), 0.96 (3H, *d*, *J* = 6.7 Hz, H-16), 2.44 (2H, *q*, *J* = 15.1, 7.6, H-2'), 1.21 (3H, *t*, *J* = 7.6, H-3') ppm.

¹³C NMR (101 MHz, CDCl₃): δ 195.0 (C-14), 173.7 (C-1'), 169.5 (C-21), 146.5 (C-12), 142.8 (C-6), 131.9 (C-13), 118.6 (C-5), 94.3 (C-15), 80.6 (C-3), 50.9 (C-4), 44.4 (C-1), 38.1 (C-2), 36.7 (C-7), 33.5 (C-9), 29.0 (C-11), 28.9 (C-18), 28.3 (C-8), 27.6 (C-2'), 24.3 (C-10), 21.2 (C-22), 20.6 (C-17), 16.0 (C-19), 13.6 (C-16), 12.0 (C-20), 9.2 (C-3') ppm.

Jolkinoate C; 15β-acetoxy-3β-butanoatelathyra-5E,12E-dien-14-one (6.3):

Obtained from reaction with butanoic anhydride (12 mg, 0.078 mmol). The residue was purified by flash column chromatography (silica gel, *n*-hexane/EtOAc; 1:0 to 9:1) to afford 10 mg (0.024 mmol, yield 60%) of a yellow oil.



ESIMS (positive mode) *m/z* (rel. int.) 453 [M + Na]⁺ (100), 381 [M + Na - CH₃CH₂CH₂CO]⁺ (35);

ESI-TOF-HRMS *m/z* 453.2606 [M + Na]⁺ (calcd for C₂₆H₃₈O₅Na, 453.2617);

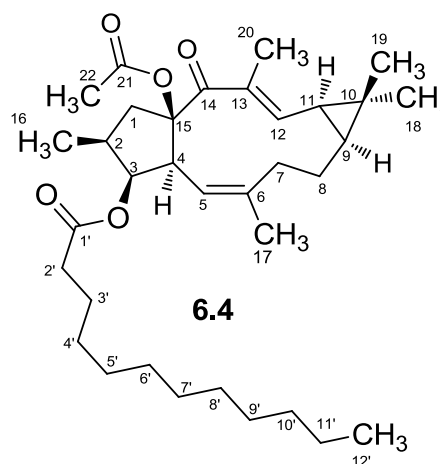
¹H NMR (400 MHz, CDCl₃): δ 6.65 (1H, *d*, *J* = 11.4 Hz, H-12), 5.33 (1H, *d*, *J* = 10.6 Hz, H-5), 5.24 (1H, *t*, *J* = 3.6 Hz, H-3), 3.52 (1H, *dd*, *J* = 13.9, 8.0 Hz, H-1α), 2.49 (1H, *dd*, *J* = 10.7, 3.8 Hz, H-4), 2.37 (1H, *td*, *J* = 7.3, 1.9 Hz, H-7α), 2.22–2.12 (2H, *m*, H-8α, H-2), 2.00 (3H, *s*, H-22), 1.82 (3H, *s*, H-20), 1.74 (1H, *td*, *J* = 13.1, 2.9 Hz, H-7β), 1.48 (1H, *dd*, *J* = 13.5, 2.5 Hz, H-11), 1.48–1.46 (1H, *m*, H-1β, H-8β), 1.45 (3H, *s*, H-17), 1.39 (1H, *dd*, *J* = 7.9, 3.5 Hz, H-1β), 1.16 (3H, *s*, H-18), 1.08–1.04 (1H, *m*, H-9), 1.04 (3H, *s*, H-19), 0.96 (3H, *d*, *J* = 7.4 Hz, H-16), 2.30 (2H, *t*, *J* = 7.4 Hz, H-2'), 1.65 (2H, *q*, *J* = 7.4 Hz, H-3'), 0.94 (3H, *t*, *J* = 3.4 Hz, H-4') ppm.

¹³C NMR (101 MHz, CDCl₃): δ 195.4 (C-14), 173.2 (C-1'), 169.8 (C-21), 146.8 (C-12), 143.0 (C-6), 132.2 (C-13), 118.8 (C-5), 94.6 (C-15), 80.4 (C-3), 50.9 (C-4), 44.5 (C-1),

38.2 (C-2), 35.6 (C-2'), 36.1 (C-7), 34.2 (C-9), 29.7 (C-11), 29.3 (C-18), 28.4 (C-8), 24.6 (C-10), 21.6 (C-22), 21.0 (C-17), 18.0 (C-3'), 16.0 (C-19), 13.8 (C-16), 13.5 (C-4'), 12.0 (C-20) ppm.

Jolkinoate D; *15β-acetoxy-3β-lauroyloxy-lathyr-5E,12E-dien-14-one (6.4)*:

Obtained from reaction with lauroyl chloride (17 mg, 0.078 mmol). The residue was purified by flash column chromatography (silica gel, n-hexane/EtOAc; 1:0 to 9:1) to afford 20 mg (0.036 mmol, yield 93%) of an amorphous dark yellow powder.



ESIMS (positive mode) m/z (rel. int.) 565 $[M + Na]^+$ (54), 381 $[M + Na - CH_3(CH_2)_{10}CO]^+$ (100);

ESI-TOF-HRMS m/z 565.3875 $[M + Na]^+$ (calcd for $C_{34}H_{54}O_5Na$, 565.3863);

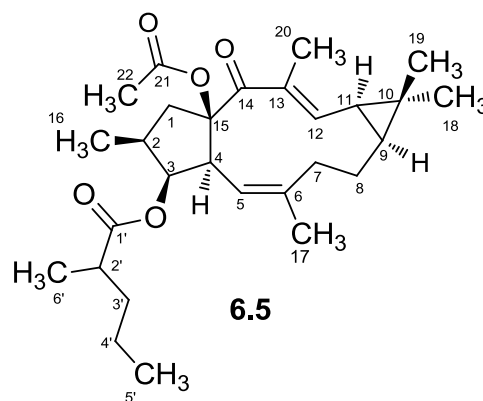
1H NMR (400 MHz, $CDCl_3$): δ 6.66 (1H, *d*, $J = 11.3$ Hz, H-12), 5.33 (1H, *d*, $J = 10.7$ Hz, H-5), 5.25 (1H, *t*, $J = 3.5$ Hz, H-3), 3.51 (1H, *dd*, $J = 13.8, 8.0$ Hz, H-1 α), 2.50 (1H, *dd*, $J = 10.6, 3.7$ Hz, H-4), 2.39 (1H, *td*, $J = 12.0, 2.4$ Hz, H-7 α), 2.21–2.17 (2H, *m*, H-8 α , H-2), 2.01 (3H, *s*, H-22), 1.83 (3H, *s*, H-20), 1.75 (1H, *td*, $J = 12.5, 3.0$ Hz, H-7 β), 1.47 (1H, *dd*, $J = 7.4, 4.3$ Hz, H-11), 1.46 (1H, *dd*, $J = 12.4, 2.9$ Hz, H-1 β), 1.44 (3H, *s*, H-17), 1.41 (1H, *dd*, $J = 7.3, 4.1$ Hz, H-8 β), 1.17 (3H, *s*, H-18), 1.08 (1H, *m*, H-9), 1.05 (3H, *s*, H-19), 0.94 (3H, *d*, $J = 6.7$ Hz, H-16), 2.34 (2H, *t*, $J = 7.5$ Hz, H-2'), 1.67 – 1.58 (18H, *m*, H-3' – H-11'), 0.87 (3H, *t*, $J = 6.8$ Hz, H-12') ppm.

^{13}C NMR (100 MHz, $CDCl_3$): δ 195.3 (C-14), 173.3 (C-1'), 169.7 (C-21), 146.7 (C-12), 142.9 (C-6), 132.1 (C-13), 118.7 (C-5), 94.5 (C-15), 80.7 (C-3), 51.2 (C-4), 44.8 (C-1), 38.3 (C-2), 36.8 (C-7), 34.6 (C-2'), 34.1 (C-9), 34.1 – 29.3 (C-3' – C-11'), 29.2 (C-11), 29.1 (C-18), 28.3 (C-8), 24.7 (C-10), 22.7 (C-22), 20.8 (C-17), 16.3 (C-19), 14.1 (C-16), 13.9 (C-12'), 12.3 (C-20) ppm.

Jolkinoate E; *15 β -acetoxy-3 β -(2-methylvaleroate)lathyra-5E,12E-dien-14-one*

(6.5):

Obtained from reaction with 2-methylvaleryl chloride (10 mg, 0.078 mmol). The residue was purified by column chromatography (silica gel, CH₂Cl₂) followed by a preparative TLC with *n*-hexane/EtOAc (3:2) to afford 16 mg (0.036 mmol, yield 94%) of a yellow oil.



ESIMS (positive mode) m/z (rel. int.) 481 [M + Na]⁺ (100), 430 [M - CH₂=CH₂]⁺ (18);

ESI-TOF-HRMS m/z 481.2933 [M + Na]⁺ (calcd for C₂₈H₄₂O₅Na, 481.2924);

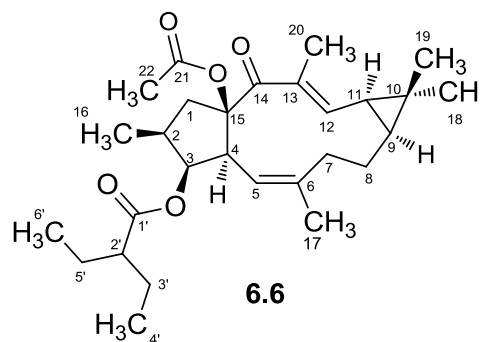
¹H NMR (400 MHz, CDCl₃): δ 6.66 (1H, d, J = 11.4 Hz, H-12), 5.34 (1H, d, J = 10.7 Hz, H-5), 5.24 (1H, t, J = 4.1 Hz, H-3), 3.53 (1H, dd, J = 13.9, 8.0 Hz, H-1 α), 2.55 (1H, dd, J = 13.7, 6.8 Hz, H-4), 2.50 (1H, ddd, J = 10.6, 3.7, 1.7 Hz, H-7 α), 2.21–2.18 (2H, m, H-8 α , H-2), 2.01 (3H, d, J = 2.5, H-22), 1.83 (3H, s, H-20), 1.75 (1H, td, J = 13.1, 2.5 Hz, H-7 β), 1.48 (1H, dd, J = 5.7, 2.8 Hz, H-8 β), 1.46 (1H, dd, J = 8.6, 2.3 Hz, H-1 β), 1.44 (3H, d, J = 1.3 Hz, H-17), 1.38 (1H, dd, J = 7.6, 3.6 Hz, H-11), 1.17 (3H, s, H-18), 1.09 (1H, m, H-9), 1.04 (3H, d, J = 1.2 Hz, H-19), 0.95 (3H, d, J = 6.6 Hz, H-16), 2.54 (1H, m, H-2'), 1.21 (2H, dd, J = 7.0, 2.9 Hz, H-3'), 1.12 (2H, m, H-4'), 0.95 (3H, t, J = 7.1 Hz, H-5'), 1.17 (3H, d, J = 6.7 Hz, H-6') ppm.

¹³C NMR (101 MHz, CDCl₃): δ 195.2 (C-14), 175.9 (C-1'), 169.6 (C-21), 146.7 (C-12), 142.8 (C-6), 132.1 (C-13), 118.8 (C-5), 94.6 (C-15), 80.5 (C-3), 51.3 (C-4), 44.8 (C-1), 39.8 (C-2'), 38.3 (C-2), 36.07 (C-7), 34.12 (C-9), 29.59 (C-11), 29.39 (C-3'), 29.15 (C-18), 28.88 (C-4'), 28.22 (C-8), 24.49 (C-10), 21.39 (C-22), 20.8 (C-17), 20.31 (C-5'), 16.6 (C-6'), 16.3 (C-19), 13.8 (C-16), 12.3 (C-20) ppm.

Jolkinoate F; *15β-acetoxy-3β-(2-ethylbutyrate)lathyra-5E,12E-dien-14-one*

(**6.6**):

Obtained from reaction with 2-ethylbutyryl chloride (9 mg, 0.078 mmol). The residue was purified by column chromatography (silica gel, CH₂Cl₂) followed by a preparative TLC with n-hexane/EtOAc (9:1) to afford 15 mg (0.033 mmol, yield 84%) of a yellow oil.



ESIMS (positive mode) m/z (rel. int.) 481 [M + Na]⁺ (100), 399 [M - CH₃CO₂]⁺ (12);

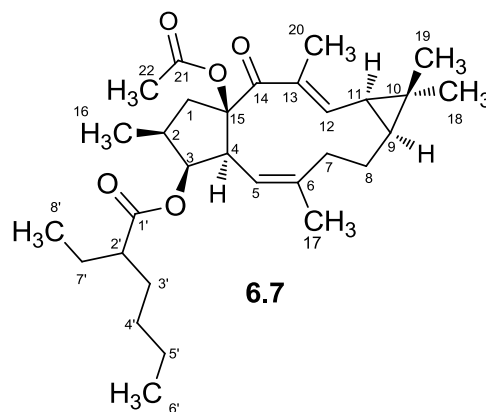
ESI-TOF-HRMS m/z 481.2934 [M + Na]⁺ (calcd for C₂₈H₄₂O₅Na, 481.2924);

¹H NMR (400 MHz, CDCl₃): δ 6.65 (1H, dd, J = 11.4, 0.9 Hz, H-12), 5.36 (1H, d, J = 10.7 Hz, H-5), 5.26 (1H, t, J = 3.5 Hz, H-3), 3.53 (1H, dd, J = 13.9, 8.0 Hz, H-1α), 2.50 (1H, dd, J = 10.7, 3.7 Hz, H-4), 2.44 (1H, dd, J = 13.2, 3.9 Hz, H-7α), 2.20–2.16 (2H, m, H-8α, H-2), 2.00 (3H, s, H-22), 1.83 (3H, d, J = 0.9 Hz, H-20), 1.74 (1H, td, J = 12.0, 2.4 Hz, H-7β), 1.49 (1H, dd, J = 7.2, 1.5 Hz, H-8β), 1.44 (1H, dd, J = 12.8, 7.3 Hz, H-1β), 1.44 (3H, d, J = 1.2 Hz, H-17), 1.39 (1H, dd, J = 11.5, 8.1 Hz, H-11), 1.16 (3H, s, H-18), 1.06 (1H, m, H-9), 1.04 (3H, s, H-19), 0.89 (3H, d, J = 6.9 Hz, H-16), 2.28 (1H, m, H-2'), 1.68 – 1.58 (4H, m, H-3', H-5'), 0.93 (6H, t, J = 7.5 Hz, H-4', H-6') ppm.

¹³C NMR (101 MHz, CDCl₃): δ 195.6 (C-14), 175.7 (C-1'), 169.8 (C-21), 146.9 (C-12), 142.8 (C-6), 132.2 (C-13), 119.1 (C-5), 94.7 (C-15), 80.8 (C-3), 51.4 (C-4), 48.4 (C-2'), 44.9 (C-1), 38.4 (C-2), 36.8 (C-7), 34.2 (C-9), 29.6 (C-18), 29.3 (C-11), 28.3 (C-8), 24.6 (C-10), 22.7 (C-3'/C-5'), 21.5 (C-22), 21.0 (C-17), 16.4 (C-19), 14.0 (C-16), 12.4 (C-4'/C-6'), 12.1 (C-20) ppm.

Jolkinoate G; *15β-acetoxy-3β-(2-ethylhexanoate)lathyra-5E,12E-dien-14-one*
(**6.7**):

Obtained from reaction with 2-ethylhexanoyl chloride (13 mg, 0.078 mmol). The residue was purified by flash column chromatography (silica gel CH₂Cl₂/MeOH 99:1) to afford 18 mg (0.038 mmol, yield 97%) of a yellow oil.



ESIMS (positive mode) m/z (rel. int.) 509 [$M + Na$]⁺ (100), 427 [$M - CH_3CO_2$]⁺ (12);

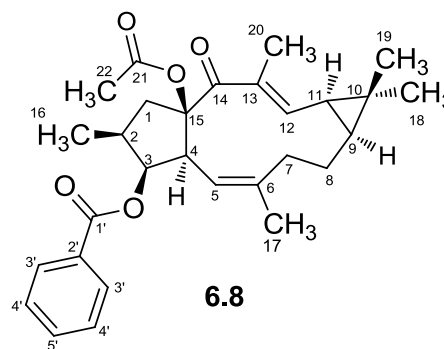
ESI-TOF-HRMS m/z 509.3256 [$M + Na$]⁺ (calcd for C₃₀H₄₆O₅Na, 509.3237);

¹H NMR (400 MHz, CDCl₃): δ 6.67 (1H, d, $J = 11.4$ Hz, H-12), 5.39 (1H, d, $J = 10.7$ Hz, H-5), 5.28 (1H, t, $J = 3.5$ Hz, H-3), 3.55 (1H, dd, $J = 13.9, 8.0$ Hz, H-1α), 2.55 (1H, dd, $J = 10.7, 3.7$ Hz, H-4), 2.44 (1H, d, $J = 13.4$, H-7α), 2.30 – 2.20 (2H, m, H-8α, H-2), 2.00 (3H, s, H-22), 1.83 (3H, s, H-20), 1.76 (1H, td, $J = 12.8, 2.7$ Hz, H-7β), 1.66–1.56 (8H, m, H-1β, H-8β), 1.44 (3H, d, $J = 1.0$ Hz, H-17), 1.39 (1H, dd, $J = 11.5, 8.3$ Hz, H-11), 1.16 (3H, s, H-18), 1.06 (1H, m, H-9), 1.04 (3H, s, H-19), 0.92 (3H, d, $J = 7.4$ Hz, H-16), 2.26 (1H, m, H-2'), 1.66 – 1.56 (8H, m, H-3', H-4', H-5', H-7'), 0.96 (3H, t, $J = 7.3$ Hz, H-8'), 0.95 (3H, t, $J = 8.8$ Hz, H-6') ppm.

¹³C NMR (101 MHz, CDCl₃): δ 195.3 (C-14), 175.5 (C-1'), 169.8 (C-21), 146.9 (C-12), 142.8 (C-6), 132.2 (C-13), 119.1 (C-5), 94.6 (C-15), 80.74 (C-3), 51.4 (C-4), 49.8 (C-2'), 44.9 (C-1), 38.5 (C-2), 36.9 (C-7), 34.26 (C-9), 29.7 (C-11), 29.3 (C-18), 28.3 (C-8), 25.3 – 25.0 (C-3'/C-4'/C-5'/C-7'), 24.6 (C-10), 21.5 (C-22), 20.9 (C-17), 16.4 (C-19), 14.1 (C-16), 12.4 – 12.2 (C-6'/C-8'), 12.1 (C-20) ppm.

Jolkinoate I; 15 β -acetoxy-3 β -benzoyloxylathyra-5E,12E-dien-14-one (6.8):

Obtained from reaction with benzoyl chloride (14 mg, 0.10 mmol, 2.5 eq). The residue was purified by two sequential flash column chromatography (silica gel, CH₂Cl₂ and silica gel, CH₂Cl₂/MeOH; 99:1) to afford 17 mg (0.037 mmol, yield 96%) of an amorphous white powder.



ESIMS (positive mode) m/z (rel. int.) 487 [M + Na]⁺ (100), 381 [M + Na - C₆H₅CO]⁺ (9), 405 [M - CH₃CO₂]⁺ (7);

ESI-TOF-HRMS m/z 487.2453 [M + Na]⁺ (calcd for C₂₉H₃₆O₅Na, 487.2455);

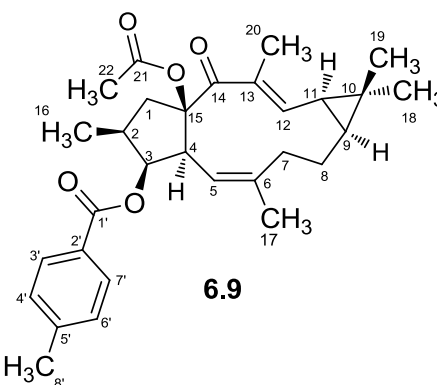
¹H NMR (400 MHz, CDCl₃): δ 8.11 (2H, t, J = 7.1 Hz, H-3'), 7.62 (1H, t, J = 7.4 Hz, H-5'), 7.48 (2H, t, J = 7.7 Hz, H-4'), 6.69 (1H, d, J = 11.4 Hz, H-12), 5.51 (1H, t, J = 3.4 Hz, H-3), 5.39 (1H, d, J = 10.6 Hz, H-5), 3.64 (1H, dd, J = 14.0, 8.1 Hz, H-1 α), 2.63 (1H, dd, J = 10.6, 3.6 Hz, H-4), 2.42 (1H, d, J = 13.4 Hz, H-7 α), 2.29 (1H, m, H-2), 2.14 (1H, m, H-8 α), 2.08 (3H, s, H-22), 1.86 (3H, s, H-20), 1.71 (1H, td, J = 13.2, 2.5 Hz, H-7 β), 1.64 (1H, dd, J = 13.9, 12.4, H-11), 1.47 (3H, d, J = 1.2 Hz, H-17), 1.45–1.41 (2H, m, H-1 β , H-8 β), 1.17 (3H, s, H-18), 1.06 (1H, m, H-9), 1.04 (3H, s, H-19), 1.00 (3H, d, J = 6.7 Hz, H-16) ppm.

¹³C NMR (101 MHz, CDCl₃): δ 195.3 (C-14), 171.2 (C-1'), 169.8 (C-21), 147.0 (C-12), 143.4 (C-6), 133.8 (C-13), 133.2 (C-5'), 130.3 (C-2'), 129.8 (C-3'/C-7'), 128.6 (C-4'/C-6'), 118.7 (C-5), 94.9 (C-15), 81.9 (C-3), 51.7 (C-4), 45.2 (C-1), 38.9 (C-2), 36.7 (C-7), 34.3 (C-9), 29.8 (C-11), 29.3 (C-18), 28.5 (C-8), 24.7 (C-10), 21.6 (C-22), 21.1 (C-17), 16.5 (C-19), 14.2 (C-16), 12.4 (C-20) ppm.

Jolkinoate J; *15β-acetoxy-3β-(4-methylbenzoyloxy)lathyra-5E,12E-dien-14-one*

(6.9):

Obtained from reaction with 4-methylbenzoyl chloride (17 mg, 0.11 mmol, 2.8 eq). The residue was purified by two sequential flash column chromatography (silica gel, *n*-hexane/CH₂Cl₂ 2:1 and silica gel, CH₂Cl₂/MeOH 99:1) to afford 10 mg (0.021 mmol, yield 55%) of an amorphous white powder.



ESIMS (positive mode) m/z (rel. int.) 501 [M + Na]⁺ (100), 419 [M - CH₃CO₂]⁺ (7), 318 [M - CH₃CO₂ - CH₃C₆H₄CO]⁺ (6);

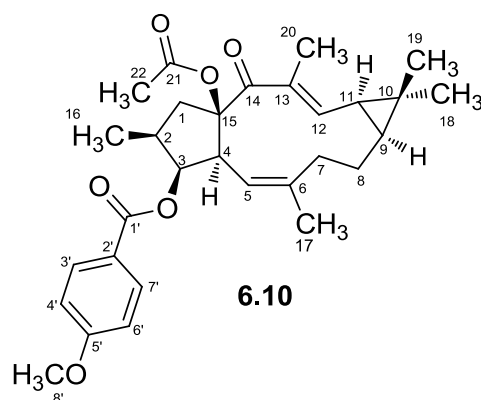
ESI-TOF-HRMS m/z 501.2610 [M + Na]⁺ (calcd for C₃₀H₃₈O₅Na, 501.2611);

¹H NMR (400 MHz, CDCl₃): δ 8.01 (2H, dd, J = 18.1, 8.2 Hz, H-3'/H-7'), 7.30 (2H, dd, J = 12.1, 8.0 Hz, H-4'/H-6'), 6.69 (1H, dd, J = 11.4, 0.9, H-12), 5.49 (1H, t, J = 3.3, H-3), 5.38 (1H, d, J = 10.6 Hz, H-5), 3.63 (1H, dd, J = 14.0, 8.1 Hz, H-1α), 2.62 (1H, dd, J = 10.6, 3.5 Hz, H-4), 2.45 (3H, s, H-8'), 2.42 (1H, m, H-7α), 2.27 (1H, m, H-2), 2.13 (1H, m, H-8α), 2.08 (3H, s, H-22), 1.86 (3H, d, J = 0.9 Hz, H-20), 1.70 (1H, td, J = 13.1, 2.5 Hz, H-7β), 1.60 (1H, dd, J = 13.9, 12.4 Hz, H-11), 1.46 (3H, d, J = 1.4 Hz, H-17), 1.45 (1H, dd, J = 11.3, 8.0 Hz, H-8β), 1.26 (1H, dd, J = 7.6, 6.7 Hz, H-1β), 1.16 (3H, s, H-18), 1.06 (1H, m, H-9), 1.03 (3H, s, H-19), 1.00 (3H, d, J = 6.7 Hz, H-16) ppm.

¹³C NMR (101 MHz, CDCl₃): δ 195.3 (C-14), 169.8 (C-21), 166.1 (C-1'), 147.0 (C-12), 143.9 (C-6), 132.3 (C-13), 130.8 (C-5'), 129.8 (C-4'/C-6'), 129.3 (C-3'/C-7'), 127.7 (C-2'), 118.82 (C-5), 94.9 (C-15), 81.6 (C-3), 51.7 (C-4), 45.2 (C-1), 38.9 (C-2), 36.7 (C-7), 34.3 (C-9), 29.8 (C-11), 29.3 (C-18), 28.5 (C-8), 24.7 (C-10), 22.0 (C-8'), 21.6 (C-22), 21.1 (C-17), 16.4 (C-19), 14.1 (C-16), 12.4 (C-20) ppm.

Jolkinoate K; *15β-acetoxy-3β-(4-methoxybenzoyloxy)lathyra-5E,12E-dien-14-one* (**6.10**):

Obtained from reaction with 4-methoxybenzoyl chloride (13 mg, 0.078 mmol). The residue was purified by two sequential flash column chromatography (silica gel, CH₂Cl₂ and silica gel, CH₂Cl₂/MeOH; 99:1) to afford 14 mg (0.028 mmol, yield 73%) of an amorphous white powder.



ESIMS (positive mode) m/z (rel. int.) 517 [M + Na]⁺ (100), 435 [M - CH₃CO₂]⁺ (9);

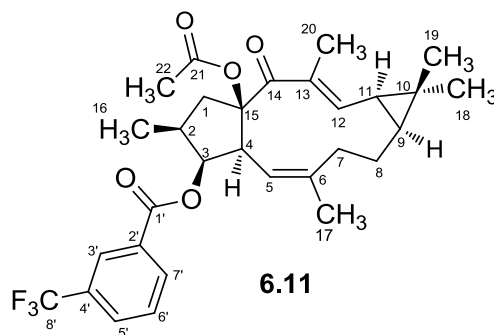
ESI-TOF-HRMS m/z 517.2565 [M + Na]⁺ (calcd for C₃₀H₃₈O₆Na, 517.2560);

¹H NMR (400 MHz, CDCl₃): δ 8.05 (2H, d, J = 8.9 Hz, H-3'/H-7'), 6.96 (2H, d, J = 8.9 Hz, H-4'/H-6'), 6.69 (1H, d, J = 11.4 Hz, H-12), 5.47 (1H, t, J = 3.3 Hz, H-3), 5.38 (1H, d, J = 10.6 Hz, H-5), 3.89 (3H, s, H-6'), 3.63 (1H, dd, J = 14.0, 8.1 Hz, H-1α), 2.61 (1H, dd, J = 10.7, 3.6 Hz, H-4), 2.42 (1H, d, J = 13.6 Hz, H-7α), 2.27 (1H, m, H-2), 2.14 (1H, m, H-8α), 2.08 (3H, s, H-22), 1.86 (3H, d, J = 0.9 Hz, H-20), 1.70 (1H, td, J = 13.0, 2.4 Hz, H-7β), 1.59 (1H, dd, J = 14.9, 11.2 Hz, H-11), 1.46 (3H, d, J = 1.4 Hz, Me-17), 1.40 (1H, m, H-8β), 1.25 (1H, m, H-1β), 1.17 (3H, s, H-18), 1.06 (1H, m, H-9), 1.04 (3H, s, H-19), 0.99 (3H, d, J = 6.7 Hz, H-16) ppm.

¹³C NMR (101 MHz, CDCl₃): δ 195.3 (C-14), 169.8 (C-21), 163.6 (C-1'), 146.9 (C-12), 143.3 (C-6), 133.3 (C-13), 132.3 (C-5'), 131.8 (C-3'/C-7'), 122.8 (C-2'), 118.9 (C-5), 113.8 (C-4'/C-6'), 94.9 (C-15), 81.7 (C-3), 55.7 (C-8'), 51.7 (C-4), 45.3 (C-1), 38.9 (C-2), 36.7 (C-7), 34.3 (C-9), 29.8 (C-11), 29.3 (C-18), 28.5 (C-8), 24.7 (C-10), 21.6 (C-22), 21.1 (C-17), 16.5 (C-19), 14.1 (C-16), 12.4 (C-20) ppm.

Jolkinoate L; *15β-acetoxy-3β-(3-trifluoromethylbenzoyloxy)lathyra-5E,12E-dien-14-one (6.11)*:

Obtained from reaction with 3-trifluoromethylbenzoyl chloride (16 mg, 0.078 mmol). The residue was purified by column chromatography (silica gel, CH₂Cl₂/acetone 19:1) and preparative TLC (2 runs) with *n*-hexane/acetone (9:1) to afford 13 mg (0.024 mmol, yield 62%) of an amorphous white powder.



ESIMS (positive mode) *m/z* (rel. int.) 555 [M + Na]⁺ (100), 318 [M - CH₃CO₂⁻ - F₃CC₆H₄CO]⁺ (13);

ESI-TOF-HRMS *m/z* 555.2331 [M + Na]⁺ (calcd for C₃₀H₃₅F₃O₅Na, 555.2334);

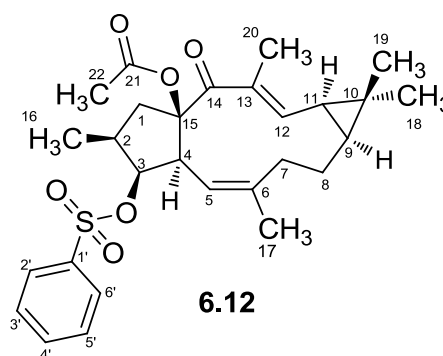
¹H NMR (400 MHz, CDCl₃): δ 8.34 (1H, *s*, H-3'), 8.29 (1H, *d*, *J* = 7.8, H-5'), 7.87 (1H, *d*, *J* = 7.8, H-7'), 7.65 (1H, *t*, *J* = 7.8, H-6'), 6.70 (1H, *d*, *J* = 12.4, H-12), 5.53 (1H, *t*, *J* = 3.4, H-3), 5.37 (1H, *d*, *J* = 10.6, H-5), 3.66 (1H, *dd*, *J* = 14.1, 8.1, H-1α), 2.65 (1H, *dd*, *J* = 10.6, 3.6, H-4), 2.42 (1H, *d*, *J* = 13.3, H-7α), 2.31 (1H, *m*, H-2), 2.14 (1H, *m*, H-8α), 2.08 (3H, *s*, H-22), 1.86 (3H, *d*, *J* = 1.0, H-20), 1.72 (1H, *td*, *J* = 13.1, 2.5, H-7β), 1.59 (1H, *dd*, *J* = 14.0, 12.3, H-11), 1.47 (3H, *d*, *J* = 1.4, H-17), 1.45–1.41 (2H, *m*, H-1β, H-8β), 1.17 (3H, *s*, H-18), 1.06 (1H, *m*, H-9), 1.04 (3H, *s*, H-19), 1.00 (3H, *d*, *J* = 6.7, H-16) ppm.

¹³C NMR (101 MHz, CDCl₃): δ 195.5 (C-14), 170.2 (C-1'), 164.9 (C-21), 147.3 (C-12), 144.2 (C-6), 133.5 (C-13), 132.6 (C-7'), 131.7 (C-4'), 131.6 (C-2'), 130.1 (C-5'), 129.7 (C-6'), 126.7 (C-3'), 125.5 (C-8'), 118.7 (C-5), 95.1 (C-15), 83.0 (C-3), 51.9 (C-4), 45.6 (C-1), 39.2 (C-2), 37.0 (C-7), 34.7 (C-9), 30.1 (C-11), 29.6 (C-18), 28.8 (C-8), 25.1 (C-10), 21.6 (C-22), 21.4 (C-17), 16.74 (C-19), 14.5 (C-16), 12.7 (C-20) ppm.

Jolkinoate M; *15β-acetoxy-3β-benzenesulfoxylathyra-5E,12E-dien-14-one (6.12):*

Obtained from reaction with benzenesulfonyl chloride (14 mg, 0.078 mmol). The residue was purified by column chromatography (silica gel, CH₂Cl₂/acetone (19:1) and preparative TLC with *n*-hexane/acetone (9:1)

to afford 13 mg (0.024 mmol, yield 68%) of an amorphous white powder.



ESIMS (positive mode) m/z (rel. int.) 523 [M + Na]⁺ (100), 381 [M + Na - C₆H₅O₃S]⁺;

ESI-TOF-HRMS m/z 523.2127 [M + Na]⁺ (calcd for C₂₈H₃₆O₆SNa, 523.2125);

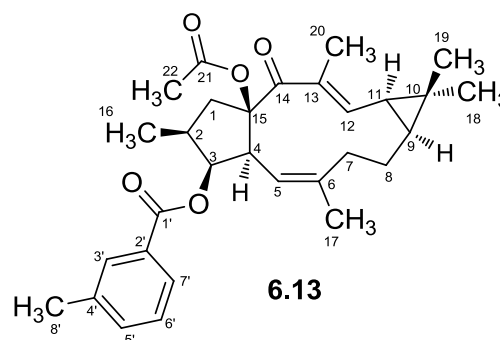
¹H NMR (400 MHz, CDCl₃): δ 7.91 (2H, *d*, J = 8.6 Hz, H-2'/H-6'), 7.63 (1H, *t*, J = 7.4 Hz, H-4'), 7.54 (2H, *t*, J = 7.6 Hz, H-3'/H-5'), 6.57 (1H, *d*, J = 11.8 Hz, H-12), 5.14 (1H, *d*, J = 10.5 Hz, H-5), 4.90 (1H, *t*, J = 3.4 Hz, H-3), 3.47 (1H, *dd*, J = 14.0, 8.0 Hz, H-1α), 2.45 (1H, *dd*, J = 10.5, 3.6 Hz, H-4), 2.19–2.06 (3H, *m*, H-7α, H-8α, H-2), 1.98 (3H, *s*, H-22), 1.79 (3H, *d*, J = 0.5 Hz, H-20), 1.60 (1H, *td*, J = 12.9, 2.2 Hz, H-7β), 1.45 (1H, *dd*, J = 13.5, 13.0 Hz, H-11), 1.36 (3H, *d*, J = 1.2 Hz, H-17), 1.35–1.25 (2H, *m*, H-1β, H-8β), 1.15 (3H, *s*, H-18), 1.05 (1H, *m*, H-9), 1.00 (3H, *s*, H-19), 0.91 (3H, *d*, J = 6.7 Hz, H-16) ppm.

¹³C NMR (101 MHz, CDCl₃): δ 194.91 (C-14), 169.7 (C-21), 147.0 (C-12), 143.2 (C-6), 137.6 (C-1'), 133.5 (C-13), 131.9 (C-2'/C-6'), 129.0 (C-4'), 127.8 (C-3'/C-5'), 118.6 (C-5), 93.7 (C-15), 91.4 (C-3), 51.5 (C-4), 44.1 (C-1), 38.7 (C-2), 36.5 (C-7), 34.2 (C-9), 29.6 (C-11), 29.1 (C-18), 28.1 (C-8), 24.6 (C-10), 21.4 (C-22), 20.7 (C-17), 16.3 (C-19), 14.0 (C-16), 12.2 (C-20) ppm.

General preparation of derivatives 6.13-6.19. A solution of compound **6** (20 mg, 0.056 mmol), dry TEA (2.2 eq), DMAP (catalytic amount) in CH₂Cl₂ (2 ml) was stirred for 5 min at room temperature before addition of the suitable chloride. This mixture was then stirred at reflux temperature for 48 to 72 h. The reaction crude was concentrated under vacuum at 40 °C and the obtained residue was purified by flash column chromatography.

Jolkinoate N; *15β-acetoxy-3β-(3-methylbenzoyloxy)lathyra-5E,12E-dien-14-one (6.13):*

Obtained from reaction with 3-methylbenzoyl chloride (Sigma-Aldrich Chemie GmbH, Riedstr D-8955, Steinhelm,



Germany - 28 mg, 0.18 mmol, 3.3 eq). The residue was purified by Combiflash system (4 g SiO₂ flash column, RediSep®Rf, Teledyne Isco) with *n*-hexane/EtOAc (1:0 to 3:1, 5 mL/min) and preparative TLC with CH₂Cl₂/MeOH (99:1) to afford 8 mg (0.017 mmol, 30% yield) of an amorphous white powder.

ESIMS (positive mode) *m/z* (rel. int.) 479 [M + H]⁺ (100);

ESI-TOF-HRMS *m/z* 517.2567 [M + Na]⁺ (calcd for C₃₀H₃₈O₅Na, 517.2561);

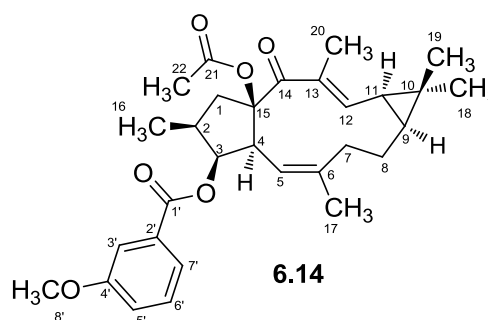
¹H NMR (400 MHz, CDCl₃): δ 7.90-7.87 (2H, m, H-3'/H-7'), 7.44-7.34 (2H, m, H-4'/H-5'), 6.69 (1H, d, *J* = 11.4 Hz, H-12) 5.50 (1H, bs, H-3), 5.39 (1H, d, *J* = 10.7 Hz, H-5), 3.63 (1H, dd, *J* = 14.0, 8.1 Hz, H-1a), 2.62 (1H, dd, *J* = 10.6, 3.2 Hz, H-4), 2.42 (3H, s, H-8'), 2.41 (1H, m, H-7a), 2.27 (1H, m, H-2), 2.13 (1H, m, H-8a), 2.06 (3H, s, H-22), 1.86 (3H, s, H-18), 1.70 (1H, m, H-7b), 1.61 (1H, m, H-1b), 1.46 (3H, s, H-17), 1.41 (1H, m, H-8b), 1.37 (1H, m, H-11), 1.16 (3H, s, H-19), 1.07 (1H, m, H-9), 1.03 (3H, s, H-18), 0.99 (3H, d, *J* = 6.7 Hz, H-16) ppm.

¹³C NMR (101 MHz, CDCl₃): δ 195.3 (C-14), 169.7 (C-22), 166.1 (C-1'), 147.0 (C-12), 143.4 (C-6), 138.4 (C-4'), 133.9 (C-5'), 132.3 (C-13), 130.4 (C-3'), 130.3 (C-2'), 128.5 (C-6'), 126.9 (C-7'), 118.8 (C-5), 94.9 (C-15), 81.7 (C-3), 51.7 (C-4), 45.2 (C-1), 38.9 (C-2),

36.7 (C-7), 34.3 (C-11), 29.8 (C-11), 29.3 (C-19), 28.5 (C-8), 24.7 (C-10), 21.6 (C-22/C-8'), 21.0 (C-17), 16.4 (C-18), 14.1 (C-16), 12.4 (C-20) ppm.

Jolkinoate O; *15 β -acetoxy-3 β -(3-methoxybenzoyloxy)lathyra-5E,12E-dien-14-one (6.14):*

Obtained from reaction with 3-methoxybenzoyl chloride (47 mg, 0.275 mmol, 5 eq). The residue was purified by Combiflash system (4 g SiO₂ flash column, RediSep®Rf, Teledyne Isco) with *n*-hexane/EtOAc (1:0 to 3:1, 5 mL/min) and two subsequent preparative TLC with CH₂Cl₂/MeOH (99:1) and *n*-hexane/EtOAc (3:1) to afford 6 mg (0.012 mmol, 30% yield) as a yellow oil.



ESIMS (positive mode) m/z (rel. int.) 495 [M + H]⁺ (100);

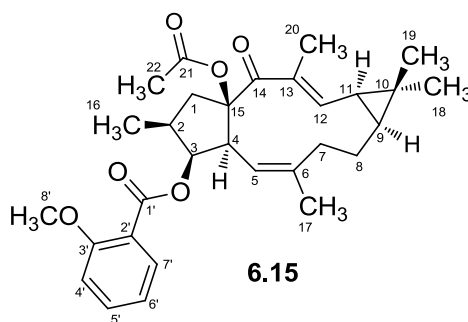
ESI-TOF-HRMS m/z 517.2568 [M + Na]⁺ (calcd for C₃₀H₃₈O₆Na, 517.2561);

¹H NMR (400 MHz, CDCl₃): δ 7.70 – 7.67 (1H, m, H-7'), 7.64 (1H, dd, J = 2.5, 1.4 Hz, H-3'), 7.39 (1H, t, J = 8.0 Hz, H-6'), 7.14 (1H, ddd, J = 8.2, 2.6, 0.8 Hz, H-5'), 6.69 (1H, dd, J = 11.4, 0.9 Hz, H-12), 5.49 (1H, t, J = 3.4 Hz, H-3), 5.39 (1H, d, J = 10.7 Hz, H-5), 3.86 (3H, s, H-8'), 3.63 (1H, dd, J = 14.1, 8.1 Hz, H-1a), 2.63 (1H, dd, J = 10.6, 3.6 Hz, H-4), 2.42 (1H, m, H-7a), 2.28 (1H, m, H-2), 2.13 (1H, m, H-8a), 2.09 (3H, s, H-22), 1.86 (3H, d, J = 0.8 Hz, H-20), 1.71 (1H, m, H-7b), 1.64 – 1.55 (1H, m, H-1b), 1.46 (3H, d, J = 1.4 Hz, H-17), 1.44 – 1.36 (2H, m, H-8b/H-11), 1.17 (3H, s, H-19), 1.04 (4H, s, H-9/H-18), 1.00 (3H, d, J = 6.8 Hz, H-16) ppm.

¹³C NMR (101 MHz, CDCl₃): δ 195.3 (C-14), 169.8 (C-22), 165.8 (C-1'), 159.0 (C-4'), 146.9 (C-12), 143.4 (C-6), 129.6 (C-6'), 122.8 (C-2'), 121.9 (C-7'), 118.8 (C-5'), 118.8 (C-5), 115.2 (C-3'), 95.9 (C-15), 82.0 (C-3), 55.6 (C-8'), 51.7 (C-4), 45.2 (C-1), 38.9 (C-2), 36.7 (C-7), 34.3 (C-9), 29.8 (C-11), 29.3 (C-19), 28.5 (C-8), 24.7 (C-10), 21.6 (C-22), 21.1 (C-17), 16.5 (C-18), 14.2 (C-16), 12.4 (C-20) ppm.

Jolkinoate P; *15 β -acetoxy-3 β -(2-methoxybenzoyloxy)lathyra-5E,12E-dien-14-one*
(**6.15**):

Obtained from reaction with 2-methoxybenzoyl chloride (47 mg, 0.275 mmol, 5 eq). The residue was purified by Combiflash system (4 g SiO₂ flash column, RediSep®Rf, Teledyne Isco) with *n*-hexane/EtOAc (1:0 to 3:1, 5 mL/min) and preparative TLC with CH₂Cl₂/MeOH (99:1) to afford 26 mg (0.012 mmol, 96% yield) as a yellow oil.



ESIMS (positive mode) m/z (rel. int.) 495 [M + H]⁺ (100);

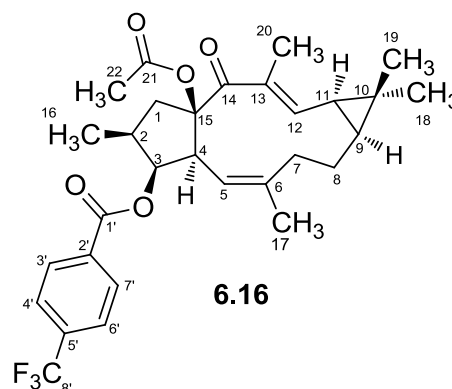
ESI-TOF-HRMS m/z 517.2567 [M + Na]⁺ (calcd for C₃₀H₃₈O₆Na, 517.2561);

¹H NMR (400 MHz, CDCl₃): δ 7.93 (1H, dd, J = 7.7, 1.8 Hz, H-7'), 7.55 – 7.48 (1H, m, H-5'), 7.05 – 6.96 (2H, m, H-6'/H-4'), 6.68 (1H, dd, J = 11.4, 0.8 Hz, H-12), 5.50 (1H, t, J = 3.4 Hz, H-3), 5.44 (1H, d, J = 10.7 Hz, H-5), 3.92 (3H, s, C-8'), 3.58 (1H, dd, J = 13.9, 8.0 Hz, H-1a), 2.60 (1H, dd, J = 10.6, 3.7 Hz, H-4), 2.44 (1H, d, J = 13.3 Hz, H-7a), 2.29 – 2.19 (1H, m, H-2), 2.18 – 2.10 (1H, m, H-8a), 1.85 (3H, d, J = 0.7 Hz, H-20), 1.71 (1H, td, J = 13.0, 2.5 Hz, H-7b), 1.57 (1H, dd, J = 13.7, 12.5 Hz, H-1b), 1.45 (3H, d, J = 1.3 Hz, H-17), 1.42 – 1.36 (2H, m, H-8b/H-11), 1.16 (3H, s, H-18), 1.06 (1H, dd, J = 8.4, 3.6 Hz, H-9), 1.02 (6H, m, H-16/H-19) ppm.

¹³C NMR (101 MHz, CDCl₃): δ 195.4 (C-14), 169.8 (C-22), 165.2 (C-1'), 159.9 (C-3'), 146.9 (C-12), 143.0 (C-6), 133.9 (C-5'), 132.3 (C-13), 131.8 (C-7'), 120.1 (C-4'/C6'), 120.0 (C-2'), 119.1 (C-5), 112.3 (C-4'/C-6'), 94.8 (C-15), 81.3 (C-3), 56.0 (C-8'), 51.6 (C-4), 45.1 (C-1), 38.9 (C-2), 36.8 (C-7), 34.3 (C-9), 29.8 (C-11), 29.3 (C-18), 28.5 (C-8), 24.6 (C-10), 21.5 (C-22), 21.0 (C-17), 16.4 (C-19), 14.1 (C-16), 12.4 (C-20) ppm.

Jolkinoate Q; *15β-acetoxy-3β-(4-trifluoromethylbenzoyloxy)lathyra-5E,12E-dien-14-one* (6.16):

Obtained from reaction with 4-trifluoromethylbenzoyl chloride (57 mg, 0.275 mmol, 5 eq). The residue was purified by Combiflash system (4 g SiO₂ flash column, RediSep®Rf, Teledyne Isco) with *n*-hexane/EtOAc (1:0 to 3:1, 5 mL/min) and preparative TLC with CH₂Cl₂/MeOH (99:1) to afford 19 mg (0.012 mmol, 63% yield) as an amorphous white powder.



ESIMS (positive mode) m/z (rel. int.) 533 [M + H]⁺ (90), 555 [M + Na]⁺ (60);

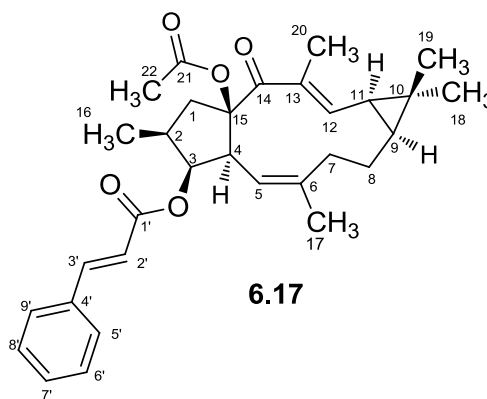
ESI-TOF-HRMS m/z 555.2332 [M + Na]⁺ (calcd for C₃₀H₃₅F₃O₅Na, 555.2329);

¹H NMR (400 MHz, CDCl₃): δ 8.10 (2H, d, J = 8.1 Hz, H-2'/H-6'), 7.65 (2H, d, J = 8.2 Hz, H-3'/H-5'), 6.58 (1H, d, J = 11.4 Hz, H-12), 5.41 (1H, t, J = 3.3 Hz, H-3), 5.25 (1H, d, J = 10.6 Hz, H-5), 3.55 (1H, dd, J = 14.1, 8.1 Hz, H-1a), 2.55 (1H, dd, J = 10.6, 3.5 Hz, H-4), 2.31 (1H, d, J = 13.4 Hz, H-7a), 2.25 – 2.15 (1H, m, H-2), 2.04 – 2.01 (1H, m, H-8a), 1.98 (3H, s, H-22), 1.76 (3H, s, H-20), 1.61 (1H, m, H-7b), 1.47 (1H, m, H-1b), 1.37 (3H, s, H-17), 1.34 – 1.26 (2H, m, H-8b/C-11), 1.07 (3H, s, H-19), 0.96 (1H, m, H-9), 0.94 (3H, s, H-18), 0.90 (3H, d, J = 6.7 Hz, H-16) ppm.

¹³C NMR (101 MHz, CDCl₃): δ 195.1 (C-15), 169.6 (C-21), 164.7 (C-1'), 145.0 (C-12), 143.8 (C-6), 134.6 (C-13), 133.6 (C-4'), 132.3 (C-2'), 130.1 (C-2'/C-6'), 125.7 (C-3'/C-5'), 125.0 (C-8'), 118.4 (C-5), 94.8 (C-15), 82.6 (C-3), 51.6 (C-4), 45.2 (C-1), 38.8 (C-2), 36.7 (C-7), 34.3 (9), 29.8 (C-11), 29.3 (C-19), 28.5 (C-8), 24.7 (C-10), 21.6 (C-22), 21.1 (C-17), 16.4 (C-18), 14.1 (C-16), 12.4 (C-20) ppm.

Jolkinoate Q; *15 β -acetoxy-3 β -(cinnamoyloxy)lathyra-5E,12E-dien-14-one*
(**6.17**):

Obtained from reaction with cinnamoyl chloride (46 mg, 0.275 mmol, 5 eq). The residue was purified by Combiflash system (4 g SiO₂ flash column, RediSep®Rf, Teledyne Isco) with *n*-hexane/EtOAc (1:0 to 3:1, 5 mL/min) and preparative TLC with CH₂Cl₂/MeOH (99:1) to afford 23 mg (0.047 mmol, 85% yield) as an amorphous white powder.



ESIMS (positive mode) m/z (rel. int.) 491 [M + H]⁺ (100);

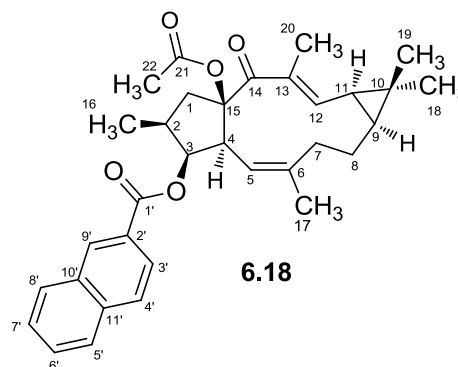
ESI-TOF-HRMS m/z 513.2616 [M + Na]⁺ (calcd for C₃₁H₃₈O₅Na, 513.2612);

¹H NMR (400 MHz, CDCl₃): δ 7.72 (1H, d, J = 16.0 Hz, H-3'), 7.57 – 7.52 (2H, m, J = 6.6, 2.8 Hz, H-5'/H-9'), 7.43 – 7.38 (3H, m, J = 6.4, 3.8 Hz, H-6'/H-7'/H-8'), 6.69 (1H, dd, J = 11.4, 0.8 Hz, H-12), 6.49 (1H, d, J = 16.0 Hz, H-2'), 5.40 (1H, m, H-6), 5.39 (1H, m, H-5), 3.58 (1H, dd, J = 14.0, 8.0 Hz, H-1a), 2.57 (1H, dd, J = 10.7, 3.8 Hz, H-4), 2.48 (1H, d, J = 13.2 Hz, H-7a), 2.16 (1H, m, H-8a), 2.08 (3H, s, H-22), 1.85 (3H, d, J = 0.7 Hz, H-20), 1.73 (1H, td, J = 13.0, 2.5 Hz, H-7b), 1.54 (1H, dd, J = 10.3, 9.1 Hz, H-1b), 1.46 (3H, d, J = 1.3 Hz, H-17), 1.40 (1H, dd, J = 11.4, 8.1 Hz, H-8b), 1.17 (3H, s, H-18), 1.05 (4H, s, H-9/H-19), 0.99 (3H, d, J = 6.7 Hz, H-16) ppm.

¹³C NMR (101 MHz, CDCl₃): δ 195.4 (C-14), 169.8 (C-21), 166.6 (C-1'), 146.9 (C-12), 145.0 (C-3'), 143.2 (C-6), 134.5 (C-4'), 132.3 (C-13), 130.6 (C-7'), 129.1 (C-6'/C-8'), 128.2 (C-5'/C-9'), 118.8 (C-2'), 118.3 (C-5), 94.8 (C-15), 81.3 (C-3), 51.5 (C-4), 45.1 (C-1), 38.7 (C-2), 36.8 (C-7), 34.3 (C-9), 29.8 (C-18), 29.3 (C-11), 28.5 (C-8), 24.7 (C-10), 21.7 (C-22), 21.0 (C-17), 16.5 (C-19), 14.0 (C-16), 12.4 (C-20) ppm.

Jolkinoate S; 15 β -acetoxy-3 β -(naphthoyloxy)lathyra-5E,12E-dien-14-one (6.18):

Obtained from reaction with naphthoyl chloride (60 mg, 0.275 mmol, 5 eq). The residue was purified by Combiflash system (4 g SiO₂ flash column, RediSep®Rf, Teledyne Isco) with *n*-hexane/EtOAc (1:0 to 3:1, 5 mL/min) and preparative TLC with CH₂Cl₂/MeOH (99:1) to afford 26.5 mg (0.016 mmol, 28% yield) as an amorphous white powder.



ESIMS (positive mode) m/z (rel. int.) 515 [$M + H$]⁺ (100);

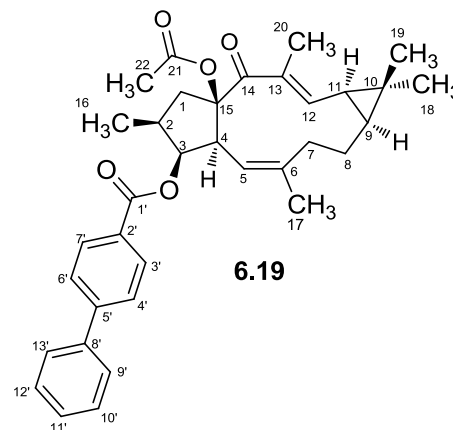
ESI-TOF-HRMS m/z 515.2797 [$M + H$]⁺ (calcd for C₃₃H₃₉O₅, 515.2792);

¹H NMR (400 MHz, CDCl₃): δ 8.65 (1H, s, H-9'), 8.12 (1H, dd, $J = 8.6, 1.5$ Hz, H-3'), 7.96 – 7.88 (3H, m, H-4'/H-5'/H-8'), 7.67 – 7.53 (2H, m, H-6'/H-7'), 6.71 (1H, d, $J = 11.4$ Hz, H-12), 5.58 (1H, t, $J = 3.4$ Hz, H-3), 5.43 (1H, d, $J = 10.6$ Hz, H-5), 3.68 (1H, dd, $J = 14.1, 8.1$ Hz, H-1a), 2.67 (1H, dd, $J = 0.6, 3.5$ Hz, H-4), 2.41 (1H, d, $J = 13.2$ Hz, H-7a), 2.32 (1H, m, H-2), 2.16 (3H, s, H-22), 2.15 – 2.07 (1H, m, H-8a), 1.87 (3H, d, $J = 0.7$ Hz, H-20), 1.74 – 1.69 (1H, m, H-7b), 1.69 – 1.63 (1H, m, H-1b), 1.48 (3H, d, $J = 1.3$ Hz, H-17), 1.41 (2H, m, H-8b/H-11), 1.16 (3H, s, H-18), 1.07 – 1.01 (7H, m, H-11/H-16/H-19) ppm.

¹³C NMR (101 MHz, CDCl₃): δ 195.3 (C-14), 169.7 (C-21), 166.1 (C-1'), 146.9 (C-12), 143.4 (C-6), 135.7 (C-11'), 132.7 (C-10'), 132.4 (C-13), 131.2 (C-9'), 129.3 (C-8'), 128.5 (C-6'), 128.4 (C-4'), 128.0 (C-5'), 127.8 (C-2'), 127.0 (C-7'), 125.4 (C-3'), 118.8 (C-5), 95.0 (C-15), 82.0 (C-3), 51.8 (C-4), 45.3 (C-1), 38.9 (C-2), 36.7 (C-7), 34.4 (C-9), 29.8 (C-18), 29.3 (C-11), 28.5 (C-8), 24.8 (C-10), 21.7 (C-22), 21.0 (C-17), 16.5 (C-19), 14.2 (C-16), 12.4 (C-20) ppm.

Jolkinoate **Q**; *15 β -acetoxy-3 β -(biphenyloxy)lathyra-5E,12E-dien-14-one* (**6.19**):

Obtained from reaction with biphenyl-4-carbonyl chloride (52 mg, 0.275 mmol, 5 eq). The residue was purified by Combiflash system (4 g SiO₂ flash column, RediSep®Rf, Teledyne Isco) with *n*-hexane/EtOAc (1:0 to 3:1, 5 mL/min) and preparative TLC with CH₂Cl₂/MeOH (99:1) to afford 27 mg (0.050 mmol, 90% yield) as an amorphous white powder.



ESI-TOF-HRMS m/z 563.2772 [$M + Na$]⁺ (calcd for C₃₅H₄₀O₅Na, 563.2768);

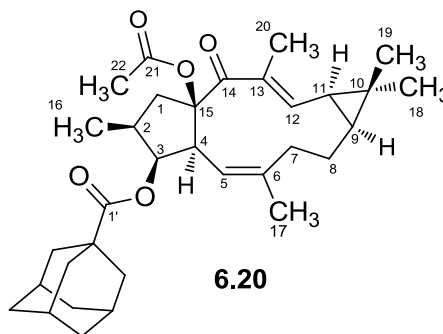
¹H NMR (400 MHz, CDCl₃): δ 8.17 (2H, d, $J = 8.4$ Hz, H-3'/H-7'), 7.71 (2H, d, $J = 8.4$ Hz, H-4'/H-6'), 7.67 – 7.62 (2H, m, H-9'/H-13'), 7.49 (2H, dd, $J = 10.1, 4.7$ Hz, H-10'/H-12'), 7.44 – 7.38 (1H, m, H-11'), 6.71 (1H, dd, $J = 11.4, 0.8$ Hz, H-12), 5.53 (1H, t, $J = 3.4$ Hz, H-3), 5.42 (1H, d, $J = 10.6$ Hz, H-5), 3.66 (1H, dd, $J = 14.0, 8.1$ Hz, H-1a), 2.65 (1H, dd, $J = 10.6, 3.6$ Hz, H-4), 2.44 (1H, d, $J = 13.3$ Hz, H-7a), 2.37 – 2.22 (1H, m, H-2), 2.18 – 2.12 (1H, m, H-8a), 2.11 (3H, s, H-22), 1.87 (3H, d, $J = 0.6$ Hz, H-20), 1.72 (1H, ddd, $J = 12.9, 10.3, 2.4$ Hz, H-7b), 1.62 (1H, dt, $J = 24.0, 12.0$ Hz, H-1b), 1.48 (3H, d, $J = 1.3$ Hz, H-17), 1.46 – 1.38 (2H, m, H-8b/H-11), 1.17 (3Hs, H-18), 1.07 (1H, dd, $J = 8.8, 3.7$ Hz, H-9), 1.04 (3H, s, H-19), 1.03 (3H, d, $J = 6.7$ Hz, H-16) ppm.

¹³C NMR (101 MHz, CDCl₃): δ 195.1 (C-14), 169.6 (C-21), 165.7 (C-1'), 146.8 (C-12), 145.9 (C-5'), 143.2 (C-6), 139.9 (C-8'), 132.2 (C-13), 130.1 (C-3'/C-7'), 129.1 (C-2'), 129.0 (C-10'/C-12'), 128.3 (C-11'), 127.3 (C-4'/C-6'), 127.2 (C-9'/C-13'), 118.7 (C-5), 94.8 (C-15), 81.8 (C-3), 51.6 (C-4), 45.1 (C-1), 38.8 (C-2), 36.6 (C-7), 34.2 (C-9), 29.7 (C-18), 29.1 (C-11), 28.4 (C-8), 24.5 (C-10), 21.5 (C-22), 20.9 (C-17), 16.3 (C-19), 14.0 (C-16), 12.3 (C-20) ppm.

General preparation of derivatives 6.20-6.22. A solution of compound **6** (20 mg, 0.056 mmol), AgOTf (1 mol%) in CH₂Cl₂ (2 ml) was heated to reflux temperature for 24 to 48 h. The reaction crude was concentrated under vacuum at 40 °C and the obtained residue was purified by flash column chromatography.

Jolkinoate **U**; *15β-acetoxy-3β-(adamantoxy)lathyra-5E,12E-dien-14-one (6.20)*:

Obtained from reaction with adamantane-1-carbonyl chloride (54 mg, 0.275 mmol, 5 eq). The residue was purified by Combiflash system (4 g SiO₂ flash column, RediSep®Rf, Teledyne Isco) with *n*-hexane/EtOAc (1:0 to 3:1, 5 mL/min) and preparative TLC with CH₂Cl₂/MeOH (99:1) to afford 18 mg (0.034 mmol, 62% yield) as an amorphous white powder.



ESIMS (positive mode) *m/z* (rel. int.) 523 [M + H]⁺ (100);

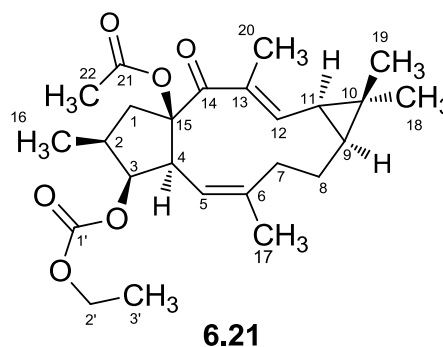
ESI-TOF-HRMS *m/z* 545.3244 [M + Na]⁺ (calcd for C₃₃H₄₆O₅Na, 545.3238);

¹H NMR (300 MHz, CDCl₃): δ 6.66 (1H, dd, *J* = 11.4, 1.1 Hz, H-12), 5.33 (1H, dd, *J* = 10.7 Hz, H-5), 5.22 (1H, t, *J* = 3.4 Hz, H-3), 3.55 (1H, dd, *J* = 13.8, 7.9 Hz, H-1a), 2.50 (1H, dd, *J* = 10.7, 3.6 Hz, H-4), 2.44 (1H, m, H-7a), 2.21 (2H, m, H-2/H-8a), 2.07 (3H, *J* = 4.4 Hz, adamantane), 2.01 (3H, s, H-22), 1.97 (6H, m, adamantane), 1.84 (3H, d, *J* = 1.1 Hz, H-20), 1.78 – 1.67 (8H, m, H-1b/H-7b/adamantane), 1.55 – 1.45 (2H, m, H-8b/H-11), 1.44 (3H, d, *J* = 1.5 Hz, H-17), 1.17 (3H, s, H-18), 1.05 (3H, s, H-19), 0.93 (3H, d, *J* = 6.7 Hz, H-16) ppm.

¹³C NMR (75 MHz, CDCl₃): δ 195.3 (C-14), 169.7 (C-1'/C-21), 146.8 (C-12), 142.9 (C-6), 132.3 (C-13), 119.0 (C-5), 94.8 (C-15), 80.3 (C-3), 51.5 (C-4), 45.0 (C-1), 39.4 (3CH₂, adamantane), 38.7 (C-2), 37.0 (C-7), 36.8 (3CH₂, adamantane), 34.3 (C-9), 29.8 (C-18/C-11), 28.2 (3CH, adamantane), 24.6 (C-10), 21.5 (C-22), 20.5 (C-17), 16.3 (C-19), 13.8 (C-16), 12.4 (C-20) ppm.

Jolkinofornate A; *15 β -acetoxy-3 β -(ethylformatoxy)lathyra-5E,12E-dien-14-one*
(**6.21**):

Obtained from reaction with ethyl chloroformate (18 mg, 0.167 mmol, 3 eq). The residue was purified by Combiflash system (4 g SiO₂ flash column, RediSep®Rf, Teledyne Isco) with *n*-hexane/EtOAc (1:0 to 3:1, 5 mL/min) and preparative TLC with CH₂Cl₂/MeOH (99:1) to afford 5 mg (0.012 mmol, 21% yield) as an amorphous white powder.



ESIMS (positive mode) m/z (rel. int.) 433 [M + H]⁺ (100), 455 [M + Na]⁺;

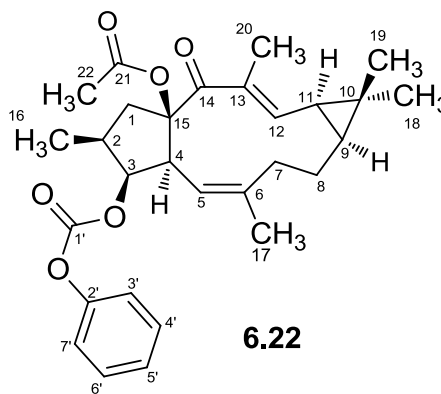
ESI-TOF-HRMS m/z 455.2539 [M + Na]⁺ (calcd for C₂₅H₃₆O₆Na, 455.2533);

¹H NMR (400 MHz, CDCl₃): δ 6.68 (1H, d, J = 11.3 Hz, H-12), 5.45 (1H, d, J = 10.9 Hz, H-5), 5.04 (1H, bs, H-5), 4.28 – 4.14 (2H, m, H-2'), 3.50 (1H, dd, J = 13.9, 8.1 Hz, H-1a), 2.51 (2H, dd, J = 10.6, 3.8 Hz, H-4/H-7a), 2.19 (1H, m, H-8a), 2.03 (3H, s, H-22), 1.83 (3H, s, H-20), 1.76 (1H, m, H-7b), 1.51 (1H, m, H-1b) 1.46 (3H, s, H-17), 1.39 (1H, dd, J = 11.2, 8.3 Hz, H-8b), 1.34 (3H, t, J = 7.1 Hz, H-3'), 1.17 (4H, s, H-18/H-11), 1.04 (4H, s, H-19/H-9), 1.01 (3H, d, J = 6.7 Hz, H-16) ppm.

¹³C NMR (101 MHz, CDCl₃): δ 195.4 (C-14), 170.0 (C-21), 155.4 (C-1'), 146.8 (C-12), 143.4 (C-6), 132.2 (C-13), 118.5 (C-5), 94.3 (C-15), 85.2 (C-3), 64.2 (C-2'), 51.4 (C-4), 44.5 (C-1), 38.6 (C-2), 36.9 (C-7), 34.2 (C-9), 29.8 (C-11), 29.3 (C-18), 28.5 (C-8), 24.7 (C-10), 21.7 (C-22), 20.9 (C-17), 16.5 (C-18), 14.5 (C-3'), 13.6 (C-16), 12.4 (C-20) ppm.

Jolkinofornate B; *15 β -acetoxy-3 β -(phenylformatoxy)lathyrin-5E,12E-dien-14-one*
(**6.22**):

Obtained from reaction with phenyl chloroformate (26 mg, 0.167 mmol, 3 eq). The residue was purified by Combiflash system (4 g SiO₂ flash column, RediSep®Rf, Teledyne Isco) with *n*-hexane/EtOAc (1:0 to 3:1, 5 mL/min) and preparative TLC with CH₂Cl₂/MeOH (99:1) to afford 22 mg (0.046 mmol, 81% yield) as an amorphous white powder.



ESIMS (positive mode) m/z (rel. int.) 481 [M + H]⁺ (100);

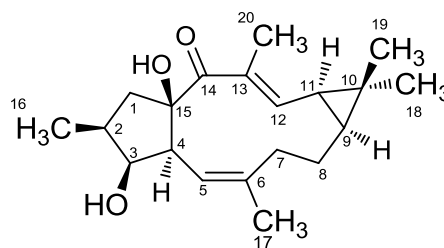
ESI-TOF-HRMS m/z 481.2591 [M + H]⁺ (calcd for C₂₉H₃₇O₆, 481.2584);

¹H NMR (300 MHz, CDCl₃): δ 7.45 – 7.35 (2H, m, H-3'/H-7'), 7.31 – 7.17 (3H, m, H-4'/H-5'/H-6'), 6.71 (1H, dd, J = 11.4, 1.1 Hz, H-12), 5.55 (1H, d, J = 10.7 Hz, H-5), 5.15 (1H, t, J = 3.7 Hz, H-3), 3.56 (1H, dd, J = 13.9, 8.0 Hz, H-1a), 2.58 (2H, dd, J = 10.6, 3.8 Hz, H-4/H-7a), 2.29 – 2.19 (2H, m, H-2/H-8a), 2.03 (3H, s, H-22), 1.86 (3H, d, J = 1.1 Hz, H-20), 1.83 – 1.76 (1H, m, H-7b), 1.62 – 1.53 (1H, m, H-1b), 1.50 (3H, d, J = 1.5 Hz, H-17), 1.40 (1H, m, H-8b/H-11), 1.20 (3H, s, H-18), 1.11 (4H, d, J = 6.8 Hz, H-16/H-9), 1.07 (3H, s, H-19) ppm.

¹³C NMR (75 MHz, CDCl₃): δ 195.3 (C-14), 170.0 (C-21), 153.7 (C-1'), 151.4 (C-2'), 146.9 (C-12), 143.8 (C-6), 132.2 (C-13), 129.6 (C-3'/C-7'), 126.1 (C-5'), 121.2 (C-4'/C-6'), 118.2 (C-5), 94.2 (C-15), 86.5 (C-3), 51.4 (C-1), 44.5 (C-1), 38.6 (C-2), 36.9 (C-7), 34.3 (C-9), 29.8 (C-18), 29.1 (C-11), 28.5 (C-8), 24.7 (C-10), 21.6 (C-22), 20.9 (C-17), 16.4 (C-19), 13.7 (C-16), 12.4 (C-20) ppm.

Jolkinodiol; $3\beta,15\beta$ -dihydroxylathyrane-5*E*,12*E*-dien-14-one (**6.23**):

Jolkinol D (100 mg, 0.277 mmol) in 10% KOH/MeOH solution was stirred for 72 h at room temperature. The residue was purified by column chromatography (silica gel, CH₂Cl₂/MeOH 99:1 to CH₂Cl₂/MeOH 3:1) to afford 71 mg (0.225 mmol, yield 81%) of an amorphous white powder.



6.23

HRMS-ESI-TOF: m/z 341.2095 [$M + Na$]⁺ (calcd. for C₂₀H₃₀O₃Na, 341.2087);

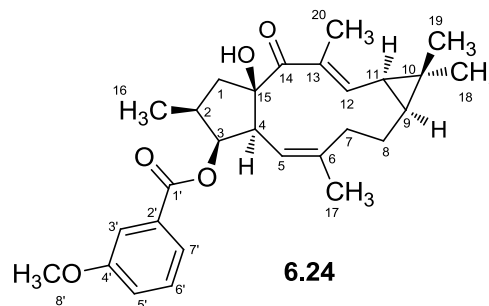
¹H NMR (400 MHz, CDCl₃): δ 7.44 (1H, *dd*, $J = 11.9, 0.8$ Hz, H-12), 5.66 (1H, *d*, $J = 10.7$ Hz, H-5), 3.96 (1H, *t*, $J = 3.0$ Hz, H-3), 3.43 (1H, *dd*, $J = 14.0, 9.3$ Hz, H-1 α), 2.54 (1H, *d*, $J = 13.2$ Hz, H-7 α), 2.28 (1H, *dd*, $J = 10.7, 3.1$ Hz, H-4), 2.17 (1H, *br d*, $J = 14.1$ Hz, H-8 α), 2.02 (1H, *m*, H-2), 1.82 (3H, *d*, $J = 0.9$ Hz, Me-20), 1.71 (1H, *td*, $J = 13.1, 2.0$ Hz, H-7 β), 1.56 (1H, *td*, $J = 14.3, 2.3$ Hz, H-11), 1.47–1.41 (2H, *m*, H-1 β , H-8 β), 1.41 (3H, *d*, $J = 1.2$ Hz, Me-17), 1.18 (3H, *s*, Me-18), 1.11 (3H, *d*, $J = 6.9$ Hz, Me-16), 1.08 (3H, *s*, Me-19), 1.05 (1H, *m*, H-9) ppm.

¹³C NMR (101 MHz, CDCl₃): δ 198.1 (C-14), 151.8 (C-12), 141.9 (C-6), 132.4 (C-13), 120.2 (C-5), 92.7 (C-15), 81.3 (C-3), 53.3 (C-4), 46.1 (C-1), 38.9 (C-2), 36.7 (C-7), 35.1 (C-9), 29.9 (C-11), 29.3 (C-18), 28.3 (C-8), 24.9 (C-10), 21.0 (C-17), 16.4 (C-19), 14.4 (C-16), 12.5 (C-20) ppm.

General preparation of derivatives 6.24-6.26. A solution of compound **6.23** (20 mg, 0.063 mmol), dry TEA (2.2 eq), DMAP (catalytic amount) in CH₂Cl₂ (2 ml) was stirred for 5 min at room temperature before addition of the suitable chloride. This mixture was then stirred at reflux temperature for 48 to 72 h. The reaction crude was concentrated under vacuum at 40 °C and the obtained residue was purified by flash column chromatography.

Jolkinolate A; *15β-hydroxy-3β-(3-methoxybenzoyloxy)lathyra-5E,12E-dien-14-one* (**6.24**):

Obtained from reaction with 3-methoxybenzoyl chloride (47 mg, 0.275 mmol, 4 eq). The residue was purified by Combiflash system (4 g SiO₂ flash column, RediSep®Rf, Teledyne Isco) with *n*-hexane/EtOAc (1:0 to 3:1, 5 mL/min) and preparative TLC with CH₂Cl₂/MeOH (99:1) and *n*-hexane/EtOAc (3:1) to afford 21 mg (0.046 mmol, 75% yield) as an amorphous white powder.



ESIMS (positive mode) m/z (rel. int.) 453 [M + H]⁺ (100);

ESI-TOF-HRMS m/z 475.2459 [M + Na]⁺ (calcd for C₂₈H₃₆O₅Na, 475.2455);

¹H NMR (400 MHz, CDCl₃): δ 7.64 (1H, d, J = 7.7 Hz, H-5'), 7.60 (1H, d, J = 2.3 Hz, H-3'), 7.43 – 7.36 (2H, H-12/H-6'), 7.14 (1H, dd, J = 8.3, 1.8 Hz, H-7'), 5.52 (1H, t, J = 3.3 Hz, H-3), 5.33 (1H, d, J = 10.6 Hz, H-5), 3.86 (3H, s, H-8'), 3.51 (1H, dd, J = 13.6, 8.5 Hz, H-1a), 2.52 (1H, dd, J = 10.7, 3.6 Hz, H-4), 2.41 (1H, d, J = 13.3 Hz, H-7a), 2.26 – 2.18 (1H, m, H-2), 2.10 (1H, d, J = 11.4 Hz, H-8a), 1.85 (3H, s, H-20), 1.69 (1H, td, J = 13.0, 2.1 Hz, H-7b), 1.56 – 1.48 (1H, m, H-1b), 1.47 (3H, d, J = 1.0 Hz, H-17), 1.42 (2H, dd, J = 11.7, 3.5 Hz, H-11/H-8b), 1.17 (3H, s, H-18), 1.05 (3H, s, H-19), 1.03 (4H, d, J = 6.8 Hz, H-16/H-9) ppm.

¹³C NMR (101 MHz, CDCl₃): δ 198.2 (C-14), 165.9 (C-1'), 159.8 (C-4'), 151.4 (C-12), 142.6 (C-6), 132.0 (C-2'/C-13), 131.6 (C-2'/C-13), 129.8 (C-6'), 121.9 (C-5'), 119.5 (C-7'), 118.8 (C-5), 114.3 (C-3'), 91.2 (C-15), 83.3 (C-3), 55.6 (C-8'), 52.1 (C-4), 47.2 (C-1), 38.6 (C-2), 36.9 (C-7), 34.8 (C-9), 30.0 (C-11), 29.3 (C-18), 28.5 (C-8), 25.0 (C-10), 21.0 (C-17), 16.4 (C-19), 14.5 (C-16), 12.6 (C-20) ppm.

Jolkinolate B; *15β-hydroxy-3β-(4-trifluoromethylbenzoyloxy)lathyra-5E,12E-dien-14-one (6.25):*

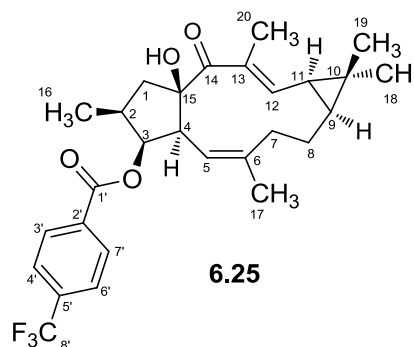
Obtained from reaction with 4-trifluoromethyl benzoyl chloride (57 mg, 0.314 mmol, 4 eq). The residue was purified by Combiflash system (4 g SiO₂ flash column,

RediSep®Rf, Teledyne Isco) with *n*-hexane/EtOAc (1:0 to 3:1, 5 mL/min) and preparative TLC with CH₂Cl₂/MeOH (99:1) to afford 17 mg (0.035 mmol, 55% yield) as an amorphous white powder.

ESIMS (positive mode) *m/z* (rel. int.) 491 [M + H]⁺ (100);

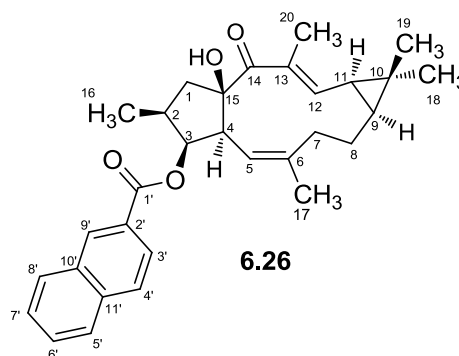
ESI-TOF-HRMS *m/z* 513.2262 [M + Na]⁺ (calcd for C₂₈H₃₃F₃O₄Na, 513.2223);

¹³C NMR (101 MHz, CDCl₃): δ 198.5 (C-14), 164.9 (C-1'), 151.4 (C-12), 142.7 (C-6), 131.9 (C-13), 130.2 (C-4'), 125.83, 125.80, 125.76, 125.73, 118.6 (C-5), 91.0 (C-15), 83.6 (C-3), 52.0 (C-4), 47.0 (C-1), 38.6 (C-2), 36.9 (C-7), 34.8 (C-9), 30.0 (C-11), 29.3 (C-18), 28.4 (C-8), 25.1 (C-10), 21.0 (C-17), 16.4 (C-19), 14.4 (C-16), 12.6 (C-20) ppm.



Jolkinolate C; *15β-hydroxy-3β-(naphthoyloxy)lathyra-5E,12E-dien-14-one (6.26):*

Obtained from reaction with naphthoyl chloride (60 mg, 0.275 mmol, 4 eq). The residue was purified by Combiflash system (4 g SiO₂ flash column, RediSep®Rf, Teledyne Isco) with *n*-hexane/EtOAc (1:0 to 3:1, 5 mL/min) and preparative TLC with CH₂Cl₂/MeOH (99:1) to afford 6 mg (0.013 mmol, 20% yield) as an amorphous white powder.



ESIMS (positive mode) *m/z* (rel. int.) 473 [M + H]⁺ (100);

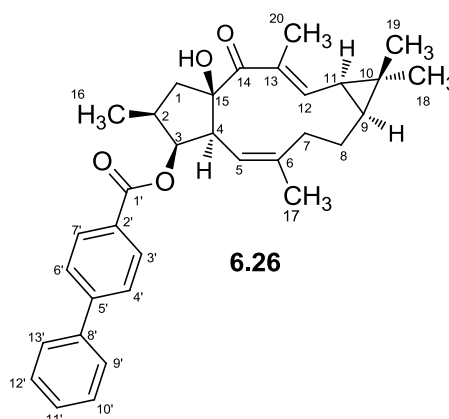
ESI-TOF-HRMS m/z 495.2509 $[M + Na]^+$ (calcd for $C_{31}H_{36}O_4Na$, 495.2506);

1H NMR (400 MHz, $CDCl_3$): δ 8.61 (1H, s, H-9'), 8.06 (1H, dd, $J = 8.6, 1.6$ Hz, H-3'), 7.99 (1H, d, $J = 8.0$ Hz, H-5'), 7.92 (2H, m, H-4'/H-8'), 7.60 (2H, m, H-6'/H-7'), 7.40 (1H, dd, $J = 11.8, 1.0$ Hz, H-12), 5.61 (1H, t, $J = 3.4$ Hz, H-3), 5.37 (1H, d, $J = 10.7$ Hz, H-5), 3.57 (1H, dd, $J = 13.7, 8.4$ Hz, H-1a), 2.57 (1H, dd, $J = 10.7, 3.6$ Hz, H-4), 2.40 (1H, d, $J = 13.3$ Hz, H-7a), 2.27 (1H, m, H-2), 2.11 – 1.98 (1H, m, H-8a), 1.87 (3H, d, $J = 0.9$ Hz, H-20), 1.69 (1H, m, H-7b), 1.61 (1H, m, H-1b), 1.49 (3H, d, $J = 1.3$ Hz, H-17), 1.44 (2H, m, H-8b/H-11), 1.17 (3H, s, H-18), 1.08 (3H, d, $J = 6.7$ Hz, H-16), 1.06 (4H, s, H-19/H-9) ppm.

^{13}C NMR (101 MHz, $CDCl_3$): δ 198.2 (C-14), 166.2 (C-1'), 151.4 (C-12), 142.6 (C-6), 135.7 (C-11'), 132.7 (C-13), 132.0 (C-10'), 131.2 (C-9'), 129.5 (C-5'), 128.6 (C-6'/C-7'), 128.5 (C-4'/C-8'), 127.95 (C-4'/C-8'), 127.6 (C-2'), 126.9 (C-6'/C-7'), 125.2 (C-3'), 118.9 (C-5), 91.5 (C-15), 83.3 (C-3), 52.2 (C-4), 47.3 (C-1), 38.7 (C-2), 36.9 (C-7), 34.9 (C-9), 30.1 (C-18), 29.3 (C-11), 28.5 (C-8), 25.1 (C-10), 21.0 (C-17), 16.4 (C-19), 14.5 (C-16), 12.6 (C-20) ppm.

Jolkinolate C; *15 β -hydroxy-3 β -(biphenyloxy)lathyra-5E,12E-dien-14-one (6.26):*

Obtained from reaction with biphenyl-4-carbonyl chloride (52 mg, 0.275 mmol, 4 eq). The residue was purified by Combiflash system (4 g SiO_2 flash column, RediSep®Rf, Teledyne Isco) with *n*-hexane/EtOAc (1:0 to 3:1, 5 mL/min) and preparative TLC with $CH_2Cl_2/MeOH$ (99:1) to afford 14 mg (0.028 mmol, 45% yield) as an amorphous white powder.



ESIMS (positive mode) m/z (rel. int.) 499 $[M + H]^+$ (100);

ESI-TOF-HRMS m/z 521.2664 $[M + Na]^+$ (calcd for $C_{33}H_{38}O_4Na$, 521.2662);

¹H NMR (400 MHz, CDCl₃): δ 8.14 (2H, d, $J = 8.4$ Hz, H-3'/H-7'), 7.71 (2H, dd, $J = 8.5$, 1.9 Hz, H-4'/H-6'), 7.66 – 7.62 (2H, m, H-9'/H-13'), 7.49 (2H, dd, $J = 10.1$, 4.7 Hz, H-10'/H-12'), 7.44 – 7.37 (2H, m, H11'/H-12), 5.57 (1H, t, $J = 3.4$ Hz, H-3), 5.37 (1H, d, $J = 10.6$ Hz, H-5), 3.54 (dd, $J = 13.6$, 8.4 Hz, H-1a), 2.55 (1H, dd, $J = 10.7$, 3.6 Hz, H-4), 2.43 (1H, d, $J = 13.3$ Hz, H-7a), 2.32 – 2.19 (1H, m, H-2), 2.14 – 2.07 (1H, m, H-8a), 1.87 (3H, s, H-20), 1.70 (td, $J = 13.0$, 2.3 Hz, H-7b), 1.57 (1H, dd, $J = 13.5$, 12.2 Hz, H-1b), 1.49 (3H, d, $J = 1.2$ Hz, H-17), 1.45 (2H, dd, $J = 11.8$, 8.3 Hz, H-8b/H-11), 1.18 (3H, s, H-18), 1.07 (4H, s, H-19/H-11), 1.06 (1H, d, $J = 6.5$ Hz, H-16) ppm

¹³C NMR (101 MHz, CDCl₃): δ 198.3 (C-14), 165.9 (C-1'), 151.3 (C-12), 146.1 (C-5'), 142.5 (C-6), 140.1 (C-8'), 132.0 (C-13), 130.2 (C-3'/C-7'), 129.1 (C-2'), 129.0 (C-10'/C-12'), 128.4 (C-11'), 127.4 (C-4'/C-6', C-9'/C-13'), 118.9 (C-5), 91.4 (C-15), 83.1 (C-3), 52.1 (C-4), 47.2 (C-1), 38.7 (C-2), 36.9 (C-7), 34.8 (C-9), 30.1 (C-18), 29.3 (C-11), 28.5 (C-8), 25.0 (C-10), 21.0 (C-17), 16.4 (C-19), 14.5 (C-16), 12.6 (C-20) ppm.

8.2. Biological Studies

8.2.1. Reversal of MDR mediated by P-glycoprotein

8.2.1.1. Cell lines and cultures

The L5178Y mouse T-lymphoma cells (ECACC cat. no. 87111908, U.S. FDA, Silver Spring, MD, USA) were transfected with the pHa *MDR1/A* retrovirus as described in literature (Pastan *et al.*, 1988). The *MDR1*-expressing cell line was selected by culturing the infected cells with colchicine (60 ng/ml), thus maintaining the MDR phenotype expression. L5178Y (parental, PAR) mouse T-cell lymphoma cells and the human *MDR1*-transfected sub-line (MDR) were cultured in McCoy's 5A supplemented with 10% heat-inactivated horse serum, 100 U/L of L-glutamine and 100 mg/L of a penicillin-streptomycin mixture, all obtained from Sigma-Aldrich (Sigma-Aldrich Kft, Budapest, Hungary). The cell lines were then incubated in a humidified atmosphere (5% CO₂, 95% air) at 37 °C.

8.2.1.2. Antiproliferative assay

The antiproliferative effects of the compounds were tested in a range of decreasing concentrations (2-fold dilutions) using PAR and MDR mouse T lymphoma cell lines as experimental model. The cells were distributed into 96-well flat bottom microtiter plates at a concentration of 1×10^5 /mL, for a final volume of 100 μ L of medium per well. The different concentrations of each compound were added into duplicate wells. The plates were initially incubated at 37 °C for 72 h and in the end of the incubation period, 15 μ L of MTT solution (thiazolyl blue tetrazolium bromide dissolved in PBS to a final concentration of 5 mg/ml) was added to each well and incubated for another 4 h. Then, 100 μ L of 10% SDS solution (sodium dodecyl sulphate) was added into each well and the plates further incubated overnight at 37 °C. Cell growth was determined by measuring the optical density (OD) at 550 nm (ref. 630 nm) with a Multiscan EX ELISA reader (Thermo Labsystems, Cheshire, WA, USA). The percentage of inhibition of cell growth was determined according to equation 1. All the experiments were performed in triplicate.

$$100 - \left[\frac{OD_{sample} - OD_{mediumcontrol}}{OD_{cellcontrol} - OD_{mediumcontrol}} \right] \times 100, \text{ Equation 1.}$$

8.2.1.3. Assay for rhodamine 123 accumulation

The cells were adjusted to a density of 2×10^6 /mL, resuspended in serum-free McCoy's 5A medium and distributed in 500 μ L aliquots. The test compounds were added at 2 and 20 μ M, verapamil (positive control, EGIS Pharmaceuticals PLC, Budapest, Hungary) at 22 μ M and DMSO at 2% as solvent control. The samples were incubated for 10 min at room temperature, after which 10 μ L (5.2 μ M final concentration) of rhodamine-123 was added to the samples. After 20 min incubation at 37 $^{\circ}$ C, the samples were washed twice, resuspended in 500 μ L phosphate-buffered saline (PBS) and analyzed by flow cytometry (Partec CyFlow[®] Space instrument, Partec GmbH, Münster, Germany). The resulting histograms were evaluated regarding mean fluorescence intensity (FL-1), standard deviation and peak channel of 20,000 individual cells belonging to the total and gated populations. The fluorescence activity ratio (FAR) was calculated on the basis of the quotient between FL-1 of treated/untreated resistant cell line (MDR mouse T lymphoma cells) over treated/untreated sensitive cell line (PAR mouse T lymphoma cells), according to equation 2. The evaluation of the stability of the esters, under these experimental conditions, is reported in the supplementary information.

$$FAR = \frac{FL-1 MDR_{treated} / FL-1 MDR_{untreated}}{FL-1 PAR_{treated} / FL-1 PAR_{untreated}}, \text{ Equation 2.}$$

8.2.1.4. Drug combination assay

The combination studies were designed as suggested in the CalcuSyn software manual (<http://www.biosoft.com>), using a fixed ratio of the drugs across a concentration gradient. The dilutions of doxorubicin (14.7–0.1 μ M) were made in a horizontal direction and the dilutions of resistance modifiers (at 2-fold of their IC_{50} 's) vertically in a microtiter plate to a final volume of 200 μ L of medium per well. The cells were distributed into plates at a concentration of 2×10^5 /mL per well and were incubated for 48 h, under the standard conditions. The cell growth rate was determined after MTT staining, as previously

described. Drug interactions were evaluated according to Chou using the software CalcuSyn Version 2 (Chou, 2010). Each dose–response curve (individual agents as well as combinations) was fit to a linear model using the median effect equation, in order to obtain the median effect value (corresponding to the IC_{50}) and slope (m). Goodness-of-fit was assessed using the linear correlation coefficient, r , and only data from analyses with $r > 0.90$ were presented. The extent of interaction between drugs was expressed using the combination index (CI) for mutually exclusive drugs. A CI close to 1 indicates additivity; $CI < 1$ defined as synergy; and $CI > 1$ as antagonism.

8.2.1.5. ATPase Activity Assay

P-gp ATPase activity was determined using the SB-MDR1 PREADEASY™ ATPase Kit (SOLVO Biotechnology, Szeged, Hungary) according to the manufacturer's instructions. Briefly, the purified Sf9 insect membrane vesicles (4 μ g protein/well), expressing high levels of human MDR1, were incubated in 50 μ L ATPase assay buffer, plus the assayed compounds and 2 mM MgATP for 10 min at 37 °C. Compounds were tested at 0.78, 1.56, 3.13, 6.25, 12.50, 25.00, 50.00 and 100.00 μ M. Final concentration of DMSO in experiment was 2%. ATPase reaction was stopped and the inorganic phosphate (Pi) produced was measured colorimetrically (optical density was read at 630 nm). The amount of Pi liberated by the transporter is proportional to its activity. Hence, ATPase activities were determined as the difference of the measured Pi liberation with and without the presence of 1.2 mM sodium orthovanadate (vanadate-sensitive ATPase activity). This ATPase kit includes two different tests: the activation and inhibition assays. The activation assay detects compounds that are transported by ABCB1 and thus stimulate baseline vanadate-sensitive ATPase activity, such as, verapamil (40 μ M) that was used as positive control. In the inhibition assay, the compounds were incubated in the presence of verapamil (40 μ M), and thus, inhibitors may reduce the verapamil-stimulated vanadate-sensitive ATPase activity. In some cases inhibitors may inhibit the baseline transporter ATPase activity as well, such as cyclosporine A (40 μ M), also used as positive control.

8.2.1.6. Curve fitting and data analysis.

All results were expressed as mean \pm SD unless otherwise noted. IC₅₀ values were obtained by best fitting the dose-dependent inhibition curves in GraphPadPrism5 program. K-means clustering was performed with Tanagra version 1.4.41 (<http://eric.univ-lyon2.fr/~ricco/tanagra/en/tanagra.html>) which subdivides the compounds (those with the nearest mean) into groups that exhibit high degree of similarity. FAR values were submitted to statistical analysis, evaluating the coefficient determination (r^2) between each evaluated property and the logarithm of 1/FAR.

8.2.2. Collateral sensitivity assays

8.2.2.1. Cell lines, cell culture and cell proliferation assay

The establishment and characterization of the Human carcinoma cell lines and drug-resistant sublines have been described previously (Table 6.1). The EPP85-181 (pancreatic) and EPG85-257 (gastric) were grown in Leibovitz L-15 medium (Biowhittaker, Walkersville, MD). HT-29 (colon) was grown in DMEM medium (Biowhittaker, Walkersville, MD). All were supplemented with 10 % fetal calf serum (FCS) (GIBCO/BRL, Grand Island, NY), 1 mM L-glutamine, 6.25 mg/L fetuin, 80 IE/L insulin, 2.5 mg/mL transferrin, 0.5 g/L glucose, 1.1 g/L NaHCO₃, 1 % minimal essential vitamins and 20,000 kIE/L trasylol. The cultures were maintained in a humidified atmosphere of 5 % CO₂ at 37 °C. Drug-resistant cell lines were established from parental cell lines by continuous exposure of the cells to step wise increasing concentrations of antineoplastic agents. For maintenance of drug-resistant phenotypes, the medium of drug-resistant sublines was supplemented respectively with the selection agent mitoxantrone and daunorubicin (Table 6.1).

The antiproliferative assay was based on sulforhodamine B (SRB) staining. All compounds were dissolved in DMSO. Briefly, 5 x 10³ /mL (EPG85-257P and EPP85-181P) and 7.5 x 10³ /ml (EPG85-257RN, EPG85-257RDB, EPP85-181RN, EPP85-181RDB, HT-29P, HT-29RN and HT-29RDB) were seeded in 96-well plates in triplicates. After 48 h attachment, a particular compound was added in dilution series for

5 days incubation. Cells were fixed with 10 % cold trichloroacetic acid for 1 h at 4 °C and were washed five times with tap water. Staining was performed with 0.4 1% SRB in 1% acetic acid for 10 min at room temperature. Then the plates were washed with 1 % acetic acid, dried overnight and resolubilized in 20 mM Tris-HCl (pH = 10) for one hour at room temperature. Cell growth was measured at 562 nm against the reference wavelength of 690 nm. Mean IC₅₀ values were obtained by best fitting the dose-dependent inhibition curves in GraphPadPrism5 program, from three to four independent experiments in triplicate for each cell line. Relative resistance (RR) values were determined as:

$$RR = \frac{IC_{50} \text{ MDR resistant cell line}}{IC_{50} \text{ parental cell line}}$$

8.2.2.2. Apoptosis assay using Annexin V/PI staining

For detection of cytotoxic drug-induced apoptosis a FITC Annexin V apoptosis detection kit (BD Pharmingen™, BD Biosciences) was used. Briefly, 6 x 10⁴ cell/ml of parental cell lines and 1 x 10⁵ cell/ml of resistant cell lines were seeded in six-well plates in complete medium and allowed to attach for 24 h. On the next day, the medium was discarded and new medium, with 30 μM of the tested compounds, was added to the gastric (EPG85-256) and pancreatic (EPP85-181) cancer cells. Cells were further incubated for 72 h, in 5 % CO₂ at 37 °C. After this incubation period, cells were trypsinized, washed in PBS and stained according to the manufacturer's instructions. Stained cells were analyzed using BD Accuri C6 flow cytometer (BD Pharmingen™, BD Biosciences) and analyzed with BD Accuri C6 software. The mean values and standard deviations were calculated from three independent experiments.

8.2.2.3. Statistical analysis

The non-parametric Kruskal-Wallis rank test (probability value p < 0.05 was considered statistically significant) was performed using SPSS 16.0 statistical package.

References

References

- Aller SG, Yu J, Ward A, Weng Y, Chittaboina S, Zhuo R, Harrell PM, Trinh YT, Zhang Q, Urbatsch IL, and Chang G (2009) Structure of P-glycoprotein reveals a molecular basis for poly-specific drug binding. *Science* **323**:1718–1722.
- Ambudkar S V, Dey S, Hrycyna C a, Ramachandra M, Pastan I, and Gottesman MM (1999) Biochemical, cellular, and pharmacological aspects of the multidrug transporter. *Annu Rev Pharmacol Toxicol* **39**:361–98.
- Ambudkar S V, Kimchi-Sarfaty C, Sauna ZE, and Gottesman MM (2003) P-glycoprotein: from genomics to mechanism. *Oncogene* **22**:7468–7485.
- Appendino G, Jakupovic S, Tron GC, Jakupovic J, Milon V, and Ballero M (1998) Macrocyclic diterpenoids from *Euphorbia semiperfoliata*. *J Nat Prod* **61**:749–756.
- Baguley BC (2010) Multiple drug resistance mechanisms in cancer. *Mol Biotechnol* **46**:308–16.
- Baird R (2003) Drug resistance reversal. *Eur J Cancer* **39**:2450–2461.
- Bech-Hansen NT, Till JE, and Ling V (1976) Pleiotropic phenotype of colchicine-resistant CHO cells: cross-resistance and collateral sensitivity. *J Cell Physiol* **88**:23–31.
- Boote DJ, Dennis IF, Twentyman PR, Osborne RJ, Laburte C, Hensel S, Smyth JF, Brampton MH, and Bleeheh NM (1996) Phase I study of etoposide with SDZ PSC 833 as a modulator of multidrug resistance in patients with cancer. *J Clin Oncol* **14**:610–618.
- Borghi D, Baumer L, Ballabio M, Arlandini E, Perellino NC, Minghetti A, and Vincieri FF (1991) Structure Elucidation of Helioscopinolides D and E from *Euphorbia calyptrata* Cell Cultures. *J Nat Prod* **54**:1503–1508.
- Borska S, Sopol M, Chmielewska M, Zabel M, and Dziegiel P (2010) Quercetin as a potential modulator of P-glycoprotein expression and function in cells of human pancreatic carcinoma line resistant to daunorubicin. *Molecules* **15**:857–70.
- Borst P, and Schinkel AH (1997) Genetic dissection of the function of mammalian P-glycoproteins. *Trends Genet* **13**:217–222.
- Calabrese EJ (2008) P-Glycoprotein Efflux Transporter Activity Often Displays Biphasic Dose-Response Relationships. *Crit Rev Toxicol* **38**:473–487.
- Callaghan R, Luk F, Bebawy M, Cuperus FJC, Claudel T, Gautherot J, Halilbasic E, and Trauner M (2014) Inhibition of the multidrug resistance P-glycoprotein: time for a change of strategy? *Drug Metab Dispos* **42**:623–31.
- Chang C, Bahadduri PM, Polli JE, Swaan PW, and Ekins S (2006) Rapid identification of P-glycoprotein substrates and inhibitors. *Drug Metab Dispos* **34**:1976–1984.
- Che C-T, Zhou T-X, Ma Q-G, Qin G-W, Williams ID, Wu H-M, and Shi Z-S (1999) Diterpenes and aromatic compounds from *Euphorbia fischeriana*. *Phytochemistry* **52**:117–121.

- Chen L, Li Y, Yu H, Zhang L, and Hou T (2012) Computational models for predicting substrates or inhibitors of P-glycoprotein. *Drug Discov Today* **17**:343–351.
- Chen T (2009) *A Practical Guide to Assay Development and High-Throughput Screening in Drug Discovery*, 291pp, CRC Press.
- Chin Y-W, and Kim J (2006) Three New Flavonol Glycosides from the Aerial Parts of *Rodgersia podophylla*. *Chem Pharm Bull (Tokyo)* **54**:234–236.
- Chin YW, Song WL, Young CK, Sang ZC, Kang RL, and Kim J (2004) Hepatoprotective flavonol glycosides from the aerial parts of *Rodgersia podophylla*. *Planta Med* **70**:576–577.
- Chou T-C (2010) Drug combination studies and their synergy quantification using the Chou-Talalay method. *Cancer Res* **70**:440–6.
- Chou T-C (2006) Theoretical basis, experimental design, and computerized simulation of synergism and antagonism in drug combination studies. *Pharmacol Rev* **58**:621–681.
- Chufan EE, Sim H, and Ambudkar S V (2015) Molecular Basis of the Polyspecificity of P-Glycoprotein (ABCB1): Recent Biochemical and Structural Studies, in *Adv Cancer Res* pp 71–96, Elsevier Inc.
- Coburger C, Lage H, Molnár J, Langner A, and Hilgeroth A (2010) Multidrug resistance reversal properties and cytotoxic evaluation of representatives of a novel class of HIV-1 protease inhibitors. *J Pharm Pharmacol* **62**:1704–10.
- Cojoc M, Mäbert K, Muders MH, and Dubrovskaya A (2014) A role for cancer stem cells in therapy resistance: Cellular and molecular mechanisms. *Seminars Cancer Biol* **31**:16–27.
- Conde J, de la Fuente JM, and Baptista P V (2013) Nanomaterials for reversion of multidrug resistance in cancer: a new hope for an old idea? *Front Pharmacol* **4**:1–5.
- Corea G, Di Pietro a., Dumontet C, Fattorusso E, and Lanzotti V (2009) Jatrophone diterpenes from *Euphorbia* spp. as modulators of multidrug resistance in cancer therapy. *Phytochem Rev* **8**:431–447.
- Corea G, Fattorusso C, Fattorusso E, and Lanzotti V (2005) Amygdaloidins A-L, twelve new 13 α -OH jatrophone diterpenes from *Euphorbia amygdaloides* L. *Tetrahedron* **61**:4485–4494.
- Cort A, and Ozben T (2015) Natural Product Modulators to Overcome Multidrug Resistance In Cancer. *Nutr Cancer* **0**:1–13.
- D'Auria JC (2006) Acyltransferases in plants: a good time to be BAHD. *Curr Opin Plant Biol* **9**:331–340.
- Dantzig AH, Law KL, Cao J, and Starling JJ (2001) Reversal of multidrug resistance by the P-glycoprotein modulator, LY335979, from the bench to the clinic. *Curr Med Chem* **8**:39–50.
- Das R, and Chakraborty D (2011) Silver Triflate Catalyzed Acetylation of Alcohols, Thiols, Phenols, and Amines. *Synthesis (Stuttg)* **2011**:1621–1625.
- Davis AL, Cai Y, Davies AP, and Lewis JR (1996) ^1H and ^{13}C NMR Assignments of Some Green Tea Polyphenols. *Magn Reson Chem* **34**:887–890.

- Dawson RJP, and Locher KP (2007) Structure of the multidrug ABC transporter Sav1866 from *Staphylococcus aureus* in complex with AMP-PNP. *FEBS Lett* **581**:935–938.
- De Pascual T, Urones JG, Marcos IS, Basabe P, Cuadrado MS, and Fernandez Moro R (1987) Triterpenes from *Euphorbia broteri*. *Phytochemistry* **26**:1767–1776.
- Dewick PM (2009a) The Mevalonate and Methylerythritol Phosphate Pathways: Terpenoids and Steroids, in *Medicinal Natural Products* pp 187–310, John Wiley & Sons, Ltd.
- Dewick PM (2009b) The Shikimate Pathway: Aromatic Amino Acids and Phenylpropanoids, in *Medicinal Natural Products* pp 137–186, John Wiley & Sons, Ltd.
- Didziapetris R, Japertas P, Avdeef A, and Petrauskas A (2003) Classification Analysis of P-Glycoprotein Substrate Specificity. *J Drug Target* **11**:391–406.
- Dietel M, Arps H, Lage H, and Niendorf A (1990) Membrane Vesicle Formation Due to Acquired Mitoxantrone Resistance in Human Gastric Carcinoma Cell Line EPG85-257. *Cancer Res* **50**:6100–6106.
- Dolghih E, Bryant C, Renslo AR, and Jacobson MP (2011) Predicting Binding to P-Glycoprotein by Flexible Receptor Docking. *PLoS Comput Biol* **7**:1–11.
- Dongping M (2007) Identify P-glycoprotein substrates and inhibitors with the rapid, HTS Pgp-glo™ assay system. *Promega Notes* 11–14.
- Drag M, Surowiak P, Drag-Zalesinska M, Dietel M, Lage H, and Oleksyszyn J (2009) Comparison of the cytotoxic effects of birch bark extract, betulin and betulinic acid towards human gastric carcinoma and pancreatic carcinoma drug-sensitive and drug-resistant cell lines. *Molecules* **14**:1639–51.
- Duarte N, Gyémánt N, Abreu PM, Molnár J, and Ferreira M-JU (2006) New Macrocyclic Lathyrane Diterpenes, from *Euphorbia lagascae*, as Inhibitors of Multidrug Resistance of Tumour Cells. *Planta Med* **72**:162–168.
- Duarte N, Lage H, Abrantes M, and Ferreira M-JU (2010) Phenolic compounds as selective antineoplastic agents against multidrug-resistant human cancer cells. *Planta Med* **76**:975–80.
- Duarte N, Varga A, Cherepnev G, Radics R, Molnár J, and Ferreira M-JU (2007) Apoptosis induction and modulation of P-glycoprotein mediated multidrug resistance by new macrocyclic lathyrane-type diterpenoids. *Bioorg Med Chem* **15**:546–554.
- Eid SY, El-Readi MZ, Fatani SH, Mohamed Nour Eldin EE, and Wink M (2015) Natural Products Modulate the Multifactorial Multidrug Resistance of Cancer. *Pharmacol Pharm* **06**:146–176.
- Ferlay J, Soerjomataram I, Dikshit R, Eser S, Mathers C, Rebelo M, Parkin DM, Forman D, and Bray F (2015) Cancer incidence and mortality worldwide : Sources , methods and major patterns in GLOBOCAN 2012. *Int J Cancer* **136**:E359–E386.
- Ferreira M-JU, Duarte N, Reis M, Madureira AM, and Molnár J (2014a) *Euphorbia* and *Momordica* metabolites for overcoming multidrug resistance. *Phytochem Rev* **13**:915–935.

- Ferreira RJ, dos Santos DJV a, Ferreira M-JU, and Guedes RC (2011) Toward a better pharmacophore description of P-glycoprotein modulators, based on macrocyclic diterpenes from *Euphorbia* species. *J Chem Inf Model* **51**:1315–24.
- Ferreira RJ, Ferreira MJU, and Dos Santos DJV a (2013) Molecular docking characterizes substrate-binding sites and efflux modulation mechanisms within P-glycoprotein. *J Chem Inf Model* **53**:1747–1760.
- Ferreira RJ, Ferreira MJU, and dos Santos DJV a (2014b) Reversing cancer multidrug resistance: Insights into the efflux by ABC transports from in silico studies. *Wiley Interdiscip Rev Comput Mol Sci* **5**:27–55.
- Genoux-Bastide E, Lorendeau D, Nicolle E, Yahiaoui S, Magnard S, DiPietro A, Baubichon-Cortay H, and Boumendjel A (2011) Identification of Xanthones as Selective Killers of Cancer Cells Overexpressing the ABC Transporter MRP1. *ChemMedChem* **6**:1478–1484.
- Ghanadian M, Saeidi H, Aghaei M, Rahiminejad MR, Ahmadi E, Ayatollahi SM, Choudhary MI, and Bahmani B (2015) New jatrophone diterpenes from *Euphorbia osyridea* with proapoptotic effects on ovarian cancer cells. *Phytochem Lett* **12**:302–307.
- Goodsell DS (2010) P-glycoprotein. *RCSB Protein Data Bank* **17**:403.
- Gottesman MM, Fojo T, and Bates SE (2002) Multidrug resistance in cancer: role of ATP-dependent transporters. *Nat Rev Cancer* **2**:48–58.
- Graham JG, Quinn ML, Fabricant DS, and Farnsworth NR (2000) Plants used against cancer - An extension of the work of Jonathan Hartwell. *J Ethnopharmacol* **73**:347–377.
- Gutmann D a P, Ward A, Urbatsch IL, Chang G, and van Veen HW (2010) Understanding polyspecificity of multidrug ABC transporters: closing in on the gaps in ABCB1. *Trends Biochem Sci* **35**:36–42.
- Hall MD, Brimacombe KR, Varonka MS, Pluchino KM, Monda JK, Li J, Walsh MJ, Boxer MB, Warren TH, Fales HM, and Gottesman MM (2011) Synthesis and Structure–Activity Evaluation of Isatin- β -thiosemicarbazones with Improved Selective Activity toward Multidrug-Resistant Cells Expressing P-Glycoprotein. *J Med Chem* **54**:5878–5889.
- Hall MD, Handley MD, and Gottesman MM (2009a) Is resistance useless? Multidrug resistance and collateral sensitivity. *Trends Pharmacol Sci* **30**:546–556.
- Hall MD, Marshall TS, Kwit ADT, Miller Jenkins LM, Dulcey AE, Madigan JP, Pluchino KM, Goldsborough AS, Brimacombe KR, Griffiths GL, and Gottesman MM (2014) Inhibition of Glutathione Peroxidase Mediates the Collateral Sensitivity of Multidrug-Resistant Cells to Tiopronin. *J Biol Chem* **0**–32.
- Hall MD, Salam NK, Hellowell JL, Fales HM, Kensler CB, Ludwig J a., Szakács G, Hibbs DE, and Gottesman MM (2009b) Synthesis, Activity, and Pharmacophore Development for Isatin- β -thiosemicarbazones with Selective Activity toward Multidrug-Resistant Cells. *J Med Chem* **52**:3191–3204.
- Hennessy M, and Spiers JP (2007) A primer on the mechanics of P-glycoprotein the multidrug transporter. *Pharmacol Res* **55**:1–15.

- Hilgeroth A, Baumert C, Coburger C, Seifert M, Krawczyk S, Hempel C, Neubauer F, Krug M, Molnár J, and Lage H (2013) Novel structurally varied N-alkyl 1,4-dihydropyridines as ABCB1 inhibitors: structure-activity relationships, biological activity and first bioanalytical evaluation. *Med Chem* **9**:487–93.
- Hohmann J, Evanics F, Dombi G, and Szabó P (2001) Salicifoline and salicinolide, new diterpene polyesters from *Euphorbia salicifolia*. *Tetrahedron Lett* **42**:6581–6584.
- Hohmann J, Molnár J, Rédei D, Evanics F, Forgo P, Kálmán A, Argay G, and Szabó P (2002) Discovery and Biological Evaluation of a New Family of Potent Modulators of Multidrug Resistance: Reversal of Multidrug Resistance of Mouse Lymphoma Cells by New Natural Jatrophone Diterpenoids Isolated from *Euphorbia* Species. *J Med Chem* **45**:2425–2431.
- Holohan C, Van Schaeybroeck S, Longley DB, and Johnston PG (2013) Cancer drug resistance: an evolving paradigm. *Nat Rev Cancer* **13**:714–26.
- Housman G, Byler S, Heerboth S, Lapinska K, Longacre M, Snyder N, and Sarkar S (2014) Drug resistance in cancer: an overview. *Cancers* **6**:1769–92.
- Jadranin M, Pešić M, Aljančić IS, Milosavljević SM, Todorović NM, Podolski-Renić A, Banković J, Tanić N, Marković I, Vajs VE, and Tešević V V. (2013) Jatrophone diterpenoids from the latex of *Euphorbia dendroides* and their anti-P-glycoprotein activity in human multi-drug resistant cancer cell lines. *Phytochemistry* **86**:208–217.
- Jakupovic J, Morgenstern T, Marco JA, and Berendsohn W (1998) Diterpenes from *Euphorbia paralias*. *Phytochemistry* **47**:1611–1619.
- Jassbi AR (2006) Chemistry and biological activity of secondary metabolites in *Euphorbia* from Iran. *Phytochemistry* **67**:1977–84.
- Jensen PB, Holm B, Sorensen M, Christensen IJ, and Sehested M (1997) In vitro cross-resistance and collateral sensitivity in seven resistant small-cell lung cancer cell lines: preclinical identification of suitable drug partners to taxotere, taxol, topotecan and gemcitabin. *Br J Cancer* **75**:869–77.
- Jiao W, Wan Z, Chen S, Lu R, Chen X, Fang D, Wang J, Pu S, Huang X, Gao H, and Shao H (2015) Lathyrol Diterpenes as Modulators of P-Glycoprotein Dependent Multidrug Resistance: Structure–Activity Relationship Studies on *Euphorbia* Factor L₃ Derivatives. *J Med Chem* **58**:3720–3738.
- Kartal-Yandim M, Adan-Gokbulut A, and Baran Y (2015) Molecular mechanisms of drug resistance and its reversal in cancer. *Crit Rev Biotechnol* **8551**:1–11.
- Kathawala RJ, Gupta P, Ashby CR, and Chen Z-S (2015) The modulation of ABC transporter-mediated multidrug resistance in cancer: A review of the past decade. *Drug Resist Updat* **18**:1–17.
- Kellner U, Hutchinson L, Seidel a, Lage H, Danks MK, Dietel M, and Kaufmann SH (1997) Decreased drug accumulation in a mitoxantrone-resistant gastric carcinoma cell line in the absence of P-glycoprotein. *Int J Cancer* **71**:817–24.

- King AJ, Brown GD, Gilday AD, Larson TR, and Graham IA (2014) Production of bioactive diterpenoids in the euphorbiaceae depends on evolutionarily conserved gene clusters. *Plant Cell* **26**:3286–98.
- Klepsch F, and Ecker GF (2010) Impact of the Recent Mouse P-Glycoprotein Structure for Structure-Based Ligand Design. *Mol Inform* **29**:276–286.
- Koehn FE, and Carter GT (2005) The evolving role of natural products in drug discovery. *Nat Rev Drug Discov* **4**:206–220.
- Kosemura S, Shizuri Y, and Yamamura S (1985) Isolation and structures of eupohelins, new toxic diterpenes from *Euphorbia helioscopia* L. *Bull Chem Soc Jpn* **58**:3112–3117.
- Kreso A, O'Brien C a, van Galen P, Gan OI, Notta F, Brown AMK, Ng K, Ma J, Wienholds E, Dunant C, Pollett A, Gallinger S, McPherson J, Mullighan CG, Shibata D, and Dick JE (2013) Variable clonal repopulation dynamics influence chemotherapy response in colorectal cancer. *Science* **339**:543–8.
- Krzyżanowski D, Bartosz G, and Grzelak A (2014) Collateral sensitivity: ABCG2-overexpressing cells are more vulnerable to oxidative stress. *Free Radic Biol Med* **76**:47–52.
- Laberge R, Ambadipudi R, and Georges E (2014) Biochemical and Biophysical Research Communications P-glycoprotein mediates the collateral sensitivity of multidrug resistant cells to steroid hormones. *Biochem Biophys Res Commun* **447**:574–579.
- Laberge R, Ambadipudi R, and Georges E (2009) P-glycoprotein (ABCB1) modulates collateral sensitivity of a multidrug resistant cell line to verapamil. *Arch Biochem Biophys* **491**:53–60.
- Laberge R-M, Karwatsky J, Lincoln MC, Leimanis ML, and Georges E (2007) Modulation of GSH levels in ABCC1 expressing tumor cells triggers apoptosis through oxidative stress. *Biochem Pharmacol* **73**:1727–1737.
- Lage H (2008) An overview of cancer multidrug resistance: a still unsolved problem. *Cell Mol Life Sci* **65**:3145–67.
- Lage H, and Dietel M (1997) Cloning and characterization of human cDNAs encoding a protein with high homology to rat intestinal development protein OCI-5. *Gene* **188**:151–6.
- Lage H, and Dietel M (2002) Multiple mechanisms confer different drug-resistant phenotypes in pancreatic carcinoma cells. *J Cancer Res Clin Oncol* **128**:349–57.
- Lage H, Duarte N, Coburger C, Hilgeroth a, and Ferreira MJU (2010) Antitumor activity of terpenoids against classical and atypical multidrug resistant cancer cells. *Phytomedicine* **17**:441–8.
- Lage H, Jordan a, Scholz R, and Dietel M (2000) Thermosensitivity of multidrug-resistant human gastric and pancreatic carcinoma cells. *Int J Hyperthermia* **16**:291–303.
- Lal AR, Cambie RC, Rutledge PS, and Woodgate PD (1990) Ent-atisane diterpenes from *Euphorbia fidjiana*☆. *Phytochemistry* **29**:1925–1935.
- Lal AR, Cambie RC, Rutledge PS, Woodgate PD, Rickard CEF, and Clark GR (1989) New oxidised ent-atisene diterpenes from *Euphorbia fidjiana*. *Tetrahedron Lett* **30**:3205–3208.

- Lanzotti V, Barile E, Scambia G, and Ferlini C (2015) Cyparissins A and B, jatrophone diterpenes from *Euphorbia cyparissias* as Pgp inhibitors and cytotoxic agents against ovarian cancer cell lines. *Fitoterapia* **104**:75–79.
- Larsen AK, and Skladanowski A (1998) Cellular resistance to topoisomerase-targeted drugs: From drug uptake to cell death. *Biochim Biophys Acta - Gene Struct Expr* **1400**:257–274.
- Lehnert M (1996) Clinical multidrug resistance in cancer: a multifactorial problem. *Eur J Cancer* **32A**:912–20.
- Liu C, Liao Z, Liu S, Qu Y, and Wang H (2014) Two new diterpene derivatives from *Euphorbia lunulata* Bge and their anti-proliferative activities. *Fitoterapia* **96**:33–38.
- Liu LG, and Tan RX (2001) New jatrophone diterpenoid esters from *Euphorbia turczaninowii*. *J Nat Prod* **64**:1064–1068.
- Longley DB, and Johnston PG (2005) Molecular mechanisms of drug resistance. *J Pathol* **205**:275–92.
- Loo TW, and Clarke DM (2005) Recent progress in understanding the mechanism of P-glycoprotein-mediated drug efflux. *J Membr Biol* **206**:173–85.
- Lorendeau D, Dury L, Genoux-Bastide E, Lecerf-Schmidt F, Simões-Pires C, Carrupt P-A, Terreux R, Magnard S, Di Pietro A, Boumendjel A, and Baubichon-Cortay H (2014) Collateral sensitivity of resistant MRP1-overexpressing cells to flavonoids and derivatives through GSH efflux. *Biochem Pharmacol* **90**:235–245.
- Lu D, Liu Y, and Aisa HA (2014) Jatrophone diterpenoid esters from *Euphorbia sororia* serving as multidrug resistance reversal agents. *Fitoterapia* **92**:244–251.
- Lu J, Li G, Huang J, Zhang C, Zhang L, Zhang K, Li P, Lin R, and Wang J (2014) Lathyrane-type diterpenoids from the seeds of *Euphorbia lathyris*. *Phytochemistry* **104**:79–88.
- Ludwig J a (2006) Selective Toxicity of NSC73306 in MDR1-Positive Cells as a New Strategy to Circumvent Multidrug Resistance in Cancer. *Cancer Res* **66**:4808–4815.
- MacMillan J, and Beale MH (1999) Diterpene Biosynthesis, in *Comprehensive Natural Products Chemistry* pp 217–243, Elsevier.
- Madureira AM, Molnár A, Abreu PM, Molnár J, and Ferreira M-JJU (2004) A new sesquiterpene-coumarin ether and a new abietane diterpene and their effects as inhibitors of P-glycoprotein. *Planta Med* **70**:828–833.
- Maki N, Hafkemeyer P, and Dey S (2003) Allosteric modulation of human P-glycoprotein. Inhibition of transport by preventing substrate translocation and dissociation. *J Biol Chem* **278**:18132–18139.
- Martin C, Berridge G, Higgins CF, Mistry P, Charlton P, and Callaghan R (2000) Communication between multiple drug binding sites on P-glycoprotein. *Mol Pharmacol* **58**:624–632.
- Matos AM, Reis M, Duarte N, Spengler G, Molnár J, and Ferreira M-JU (2015) Epoxylythryol Derivatives: Modulation of ABCB1-Mediated Multidrug Resistance in Human Colon Adenocarcinoma and Mouse T-Lymphoma Cells. *J Nat Prod* **78**:2215–2228.

- McDevitt CA, and Callaghan R (2007) How can we best use structural information on P-glycoprotein to design inhibitors? *Pharmacol Ther* **113**:429–441.
- McGarvey DJ, and Croteau R (1995) Terpenoid metabolism. *Plant Cell* **7**:1015–1026.
- Mishra BB, and Tiwari VK (2011) Natural products: An evolving role in future drug discovery. *Eur J Med Chem* **46**:4769–4807.
- Mistry P, Stewart AJ, Dangerfield W, Okiji S, Liddle C, Bootle D, Plumb J a, Templeton D, and Charlton P (2001) In Vitro and in Vivo Reversal of P-Glycoprotein-mediated Multidrug Resistance by a Novel Potent Modulator, XR9576. *Cancer Res* **61**:749–758.
- Mizutani M (2012) Impacts of Diversification of Cytochrome P450 on Plant Metabolism. *Biol Pharm Bull* **35**:824–832.
- Moradi-Afrapoli F, Asghari B, Saeidnia S, Ajani Y, Mirjani M, Malmir M, Dolatabadi Bazaz R, Hadjiakhoondi A, Salehi P, Hamburger M, and Yassa N (2012) In vitro α -glucosidase inhibitory activity of phenolic constituents from aerial parts of *Polygonum hyrcanicum*. *DARU J Pharm Sci* **20**:37.
- Murthy RSR, and Shah NM (2007) Strategies for Inhibition of P-Glycoproteins for Effective Treatment of Multidrug Resistance Tumors. *J Biomed Nanotechnol* **3**:1–17.
- Mwine TJ, and Van Damme P (2011) Why do Euphorbiaceae tick as medicinal plants?: a review of Euphorbiaceae family and its medicinal features. *J Med Plant Res* **5**:652–662.
- Newman DJ, and Cragg GM (2007) Natural products as sources of new drugs over the last 25 years. *J Nat Prod* **70**:461.
- Nobili S, Landini I, Mazzei T, and Mini E (2012) Overcoming tumor multidrug resistance using drugs able to evade P-glycoprotein or to exploit its expression. *Med Res Rev* **32**:1220–1262.
- Nobili S, Mini E, and Riganti C (2015) *Multidrug Resistance in Cancer: Pharmacological Strategies from Basic Research to Clinical Issues* (Nobili S, Mini E, and Riganti C eds), Frontiers Media SA.
- Nothias-Scaglia LF, Retailleau P, Paolini J, Pannecouque C, Neyts J, Dumontet V, Roussi F, Leyssen P, Costa J, and Litaudon M (2014) Jatrophone diterpenes as inhibitors of chikungunya virus replication: Structure-activity relationship and discovery of a potent lead. *J Nat Prod* **77**:1505–1512.
- O'Connor R, and Connor RO (2009) A review of mechanisms of circumvention and modulation of chemotherapeutic drug resistance. *Curr Cancer Drug Targets* **9**:273–80.
- Ohba S, Ito M, Saito Y, Shizuri Y, Kosemura S, and Yamamura S (1983) Structure of helioscopinolide A, C₂₀H₂₈O₃, a novel diterpene. *Acta Crystallogr Sect C Cryst Struct Commun* **39**:1139–1141.
- Overton WR (1988) Modified histogram subtraction technique for analysis of flow cytometry data. *Cytometry* **9**:619–26.
- Ozben T (2006) Mechanisms and strategies to overcome multiple drug resistance in cancer. *FEBS Lett* **580**:2903–2909.

- Özvegy C, Litman T, Szakács G, Nagy Z, Bates S, Váradi A, and Sarkadi B (2001) Functional Characterization of the Human Multidrug Transporter, ABCG2, Expressed in Insect Cells. *Biochem Biophys Res Commun* **285**:111–117.
- Pajeva IK, Globisch C, and Wiese M (2009) Combined Pharmacophore Modeling, Docking, and 3D QSAR Studies of ABCB1 and ABCC1 Transporter Inhibitors. *ChemMedChem* **4**:1883–1896.
- Pajeva IK, and Wiese M (2009) Structure–Activity Relationships of Tariquidar Analogs as Multidrug Resistance Modulators. *AAPS J* **11**:435–444.
- Palmeira A, Sousa E, H. Vasconcelos M, and M. Pinto M (2012) Three Decades of P-gp Inhibitors: Skimming Through Several Generations and Scaffolds. *Curr Med Chem* **19**:1946–2025.
- Pan Q, Ip FCF, Ip NY, Zhu HX, and Min ZD (2004) Activity of macrocyclic jatrophone diterpenes from *Euphorbia kansui* in a TrkA fibroblast survival assay. *J Nat Prod* **67**:1548–1551.
- Pastan I, Gottesman MM, Ueda K, Lovelace E, Rutherford a V, and Willingham MC (1988) A retrovirus carrying an MDR1 cDNA confers multidrug resistance and polarized expression of P-glycoprotein in MDCK cells. *Proc Natl Acad Sci U S A* **85**:4486–4490.
- Plaks V, Kong N, and Werb Z (2015) Perspective The Cancer Stem Cell Niche : How Essential Is the Niche in Regulating Stemness of Tumor Cells ? *Stem Cell* **16**:225–238.
- Pluchino KM, Hall MD, Goldsborough AS, Callaghan R, and Gottesman MM (2012) Collateral sensitivity as a strategy against cancer multidrug resistance. *Drug Resist Updat* **15**:98–105.
- Raub TJ (2006) P-glycoprotein recognition of substrates and circumvention through rational drug design. *Mol Pharm* **3**:3–25.
- Rawal MK, Shokoohinia Y, Chianese G, Zolfaghari B, Appendino G, Tagliatalata-Scafati O, Prasad R, and Di Pietro A (2014) Jatrophanes from *Euphorbia squamosa* as Potent Inhibitors of *Candida albicans* Multidrug Transporters. *J Nat Prod* **77**:2700–2706.
- Rédei D, Boros K, Forgo P, Molnár J, Kele Z, Pálinkó I, Pinke G, and Hohmann J (2015) Diterpene Constituents of *Euphorbia exigua* L. and Multidrug Resistance Reversing Activity of the Isolated Diterpenes. *Chem Biodivers* **12**:1214–1221.
- Reis M, J. Ferreira R, Serly J, Duarte N, M. Madureira A, J. V. A. Santos D, Molnar J, and U. Ferreira M-J (2012) Colon Adenocarcinoma Multidrug Resistance Reverted by Euphorbia Diterpenes: Structure-Activity Relationships and Pharmacophore Modeling. *Anticancer Agents Med Chem* **12**:1015–1024.
- Rinner U (2015) Progress in the Preparation of Jatrophone Diterpenes. *European J Org Chem* **2015**:3197–3219.
- Rivera D, and Obón C (1995) The ethnopharmacology of Madeira and Porto Santo Islands, a review. *J Ethnopharmacol* **46**:73–93.
- Robert J, and Jarry C (2003) Multidrug Resistance Reversal Agents. *J Med Chem* **46**:4805–4817.

- Ross DD, Yang W, Abruzzo L V, Dalton WS, Schneider E, Lage H, Dietel M, Greenberger L, Cole SPC, and Doyle LA (1999) Atypical Multidrug Resistance: Breast Cancer Resistance Protein Messenger RNA Expression in Mitoxantrone-Selected Cell Lines. *JNCI J Natl Cancer Inst* **91**:429–433.
- Saraswathy M, and Gong S (2013) Different strategies to overcome multidrug resistance in cancer. *Biotechnol Adv* **31**:1397–1407.
- Sarkadi ZS, Sarkadi B, Homolya L, Szakács G, Váradi A, and Sarkadi ZS (2006) Human multidrug resistance ABCB and ABCG transporters: participation in a chemoinnity defense system. *Physiol Rev* **86**:1179–236.
- Sauna ZE, and Ambudkar S V (2000) Evidence for a requirement for ATP hydrolysis at two distinct steps during a single turnover of the catalytic cycle of human P-glycoprotein. *Proc Natl Acad Sci* **97**:2515–2520.
- Sauna ZE, Kim I-W, and Ambudkar S V. (2007) Genomics and the mechanism of P-glycoprotein (ABCB1). *J Bioenerg Biomembr* **39**:481–487.
- Shadi S, Saeidi H, Ghanadian M, Rahimnejad MR, Aghaei M, Ayatollahi SM, and Iqbal Choudhary M (2015) New macrocyclic diterpenes from *Euphorbia connata* Boiss. with cytotoxic activities on human breast cancer cell lines. *Nat Prod Res* **29**:607–614.
- Sharom FJ (2014) Complex Interplay between the P-Glycoprotein Multidrug Efflux Pump and the Membrane: Its Role in Modulating Protein Function. *Front Oncol* **4**:1-19.
- Shi Q-W, Su X-H, and Kiyota H (2008) Chemical and pharmacological research of the plants in genus *Euphorbia*. *Chem Rev* **108**:4295–327.
- Shukla S, Ohnuma S, and Ambudkar S V (2011) Improving cancer chemotherapy with modulators of ABC drug transporters. *Curr Drug Targets* **12**:621–30.
- Silva R, Vilas-Boas V, Carmo H, Dinis-Oliveira RJ, Carvalho F, de Lourdes Bastos M, and Remião F (2014) Modulation of P-glycoprotein efflux pump: induction and activation as a therapeutic strategy. *Pharmacol Ther* **149**:1–123.
- Sinha P, Dietel M, Schadendorf D, and Lage H (1999) Search for novel proteins involved in the development of chemoresistance in colorectal cancer and fibrosarcoma cells in vitro using two-dimensional electrophoresis, mass spectrometry and microsequencing. *Electrophoresis* **20**:2961-2969.
- Slater LM, Sweet P, Stupecky M, and Gupta S (1986) Cyclosporin A reverses vincristine and daunorubicin resistance in acute lymphatic leukemia in vitro. *J Clin Invest* **77**:1405–1408.
- Sousa IJ, Ferreira M-JU, Molnár J, and Fernandes MX (2012) QSAR studies of macrocyclic diterpenes with P-glycoprotein inhibitory activity. *Eur J Pharm Sci* **48**:542–553.
- Stanković T, Dankó B, Martins A, Dragoj M, Stojković S, Isaković A, Wang H-C, Wu Y-C, Hunyadi A, and Pešić M (2015) Lower antioxidative capacity of multidrug-resistant cancer cells confers collateral sensitivity to protoflavone derivatives. *Cancer Chemother Pharmacol* **76**:555–565.

- Stouch TR, and Gudmundsson O (2002) Progress in understanding the structure–activity relationships of P-glycoprotein. *Adv Drug Deliv Rev* **54**:315–328.
- Swanton C (2012) Intratumor heterogeneity: Evolution through space and time. *Cancer Res* **72**:4875–4882.
- Szakács G, Hall MD, Gottesman MM, Boumendjel A, Kachadourian R, Day BJ, Baubichon-Cortay H, and Di Pietro A (2014) Targeting the Achilles Heel of Multidrug-Resistant Cancer by Exploiting the Fitness Cost of Resistance. *Chem Rev* **114**:5753–5774.
- Szakács G, Paterson JK, Ludwig J a, Booth-Genthe C, and Gottesman MM (2006) Targeting multidrug resistance in cancer. *Nat Rev Drug Discov* **5**:219–34.
- Tao HW, Hao XJ, Liu PP, and Zhu WM (2008) Cytotoxic macrocyclic diterpenoids from *Euphorbia helioscopia*. *Arch Pharm Res* **31**:1547–1551.
- Tarcsay A, and Keseru GM (2011) Homology modeling and binding site assessment of the human P-glycoprotein. *Future Med Chem* **3**:297–307.
- Tian Y, Xu W, Zhu C, Lin S, Li Y, Xiong L, Wang S, Wang L, Yang Y, Guo Y, Sun H, Wang X, and Shi J (2011) Lathyrane diterpenoids from the roots of *Euphorbia micractina* and their biological activities. *J Nat Prod* **74**:1221–1229.
- Tsuruo T, Lida H, Tsukagoshi S, and Sakurai Y (1981) Overcoming of vincristine resistance in P388 leukemia in vivo and in vitro through enhanced cytotoxicity of vincristine and vinblastine by verapamil. *Cancer Res* **41**:1967–1972.
- Tsuruo T, Naito M, Tomida A, Fujita N, Mashima T, Sakamoto H, and Haga N (2003) Molecular targeting therapy of cancer: drug resistance, apoptosis and survival signal. *Cancer Sci* **94**:15–21.
- Uemura D, Nobuhara K, Nakayama Y, Shizuri Y, and Hirata Y (1976) The structure of new lathyrane diterpenes, jolkinols A, B, C, and D, from *Euphorbia jolkini* Boiss. *Tetrahedron Lett* **17**:4593–4596.
- Valente C, Ferreira MJ, Abreu PM, Gyémánt N, Ugocsai K, Hohmann J, and Molnár J (2004) Pubescenes, jatrophone diterpenes, from *Euphorbia pubescens*, with multidrug resistance reversing activity on mouse lymphoma cells. *Planta Med* **70**:81–4.
- Valente I, Reis M, Duarte N, Serly J, Molnár J, and Ferreira MJU (2012) Jatrophone diterpenes from *euphorbia mellifera* and their activity as P-glycoprotein modulators on multidrug-resistant mouse lymphoma and human colon adenocarcinoma cells. *J Nat Prod* **75**:1915–1921.
- Vasas A, and Hohmann J (2014) *Euphorbia* Diterpenes: Isolation, Structure, Biological Activity, and Synthesis (2008–2012). *Chem Rev* **114**:8579–8612.
- Vasas A, Rédei D, Csupor D, Molnár J, and Hohmann J (2012) Diterpenes from European *Euphorbia* Species Serving as Prototypes for Natural-Product-Based Drug Discovery. *European J Org Chem* **2012**:5115–5130.

- Vasas A, Sulyok E, Rédei D, Forgo P, Szabó P, Zupkó I, Berényi Á, Molnár J, and Hohmann J (2011) Jatrophone diterpenes from *Euphorbia esula* as antiproliferative agents and potent chemosensitizers to overcome multidrug resistance. *J Nat Prod* **74**:1453–1461.
- Vieira C, Duarte N, Reis M a., Spengler G, Madureira AM, Molnár J, and Ferreira M-JU (2014) Improving the MDR reversal activity of 6,17-epoxylathyrane diterpenes. *Bioorg Med Chem* **22**:6392–6400.
- Vvarr JR, and Fergusson J (1988) Properties of Verapamil-hypersensitive Multidrug-resistant Chinese Hamster Ovary Cells. *Cancer Res* **48**:4477–4484.
- Wang H-B, Chen W, Zhang Y-Y, Wang X-Y, Liu L-P, Tong L-J, and Chen Y (2013) Four new diterpenoids from the roots of *Euphorbia fischeriana*. *Fitoterapia* **91**:211–6.
- Wang L, Ma Y, Sun Q, Li X, Yan Y, Yang J, Yang F, Liu F, Zang Z, Wu X, Huang S, and Zhao Y (2015) Structurally diversified diterpenoids from *Euphorbia dracunculoides*. *Tetrahedron* **71**:5484–5493.
- Wangpaichitr M, Wu C, You M, Maher JC, Dinh V, Feun LG, and Savaraj N (2009) N'1,N'3-Dimethyl-N'1,N'3-bis(phenylcarbonothioyl) Propanedihydrazide (Elesclomol) Selectively Kills Cisplatin Resistant Lung Cancer Cells through Reactive Oxygen Species (ROS). *Cancers* **1**:23–38.
- Warner E, Hedley D, Andrulis I, Myers R, Trudeau M, Warr D, Pritchard KI, Blackstein M, Goss PE, Franssen E, Roche K, Knight S, Webster S, Fraser RA, Oldfield S, Hill W, and Kates R (1998) Phase II study of dexverapamil plus anthracycline in patients with metastatic breast cancer who have progressed on the same anthracycline regimen. *Clin Cancer Res* **4**:1451–1457.
- Wichert A, Stege A, Midorikawa Y, Holm PS, and Lage H (2004) Glypican-3 is involved in cellular protection against mitoxantrone in gastric carcinoma cells. *Oncogene* **23**:945–55.
- Wiese M, and Pajeva IK (2001) Structure-activity relationships of multidrug resistance reversers. *Curr Med Chem* **8**:685–713.
- Wilting RH, and Dannenberg J-H (2012) Epigenetic mechanisms in tumorigenesis, tumor cell heterogeneity and drug resistance. *Drug Resist Updat* **15**:21–38.
- Wu C, Ohnuma S, and V. Ambudkar S (2011) Discovering Natural Product Modulators to Overcome Multidrug Resistance in Cancer Chemotherapy. *Curr Pharm Biotechnol* **12**:609–620.
- Wu Q, Yang Z, Nie Y, Shi Y, and Fan D (2014) Multi-drug resistance in cancer chemotherapeutics: Mechanisms and lab approaches. *Cancer Lett* **347**:159–166.
- Wu Q-C, Tang Y-P, Ding A-W, You F-Q, Zhang L, and Duan J-A (2009) ¹³C-NMR data of three important diterpenes isolated from *Euphorbia* species. *Molecules* **14**:4454–75.
- Xu C, and Wang J (2014) Delivery systems for siRNA drug development in cancer therapy. *Asian J Pharm Sci* **10**:1–12.
- Yamamura S, Shizuri Y, Kosemura S, Ohtsuka J, Tayama T, Ohba S, Ito M, Saito Y, and Terada Y (1989) Diterpenes from *Euphorbia helioscopia*. *Phytochemistry* **28**:3421–3436.

- Yang D-S, Peng W-B, Li Z-L, Wang X, Wei J-G, He Q-X, Yang Y-P, Liu K-C, and Li X-L (2014) Chemical constituents from *Euphorbia stracheyi* and their biological activities. *Fitoterapia* **97**:211–218.
- Yuan X-H, Li B-G, Zhang X-Y, Qi H-Y, Zhou M, and Zhang G-L (2004) Two Diterpenes and Three Diterpene Glucosides from *Phlogacanthus curviflorus*. *J Nat Prod* **68**:86–89.
- Zhang B, Jiang Q, Liao Z, Liu C, Liu S, Ji L, and Sun H-F (2013) Norlathyrane Diterpenes from the Root of *Euphorbia kansuensis*. *Chem Biodivers* **10**:1887–1893.
- Zhang S, Liu X, Zhang ZL, He L, Wang Z, and Wang GS (2012) Isolation and identification of the phenolic compounds from the roots of *Sanguisorba officinalis* L. and their antioxidant activities. *Molecules* **17**:13917–13922.
- Zhang X-D, Ni W, Yan H, Li G-T, Zhong H, Li Y, and Liu H (2014) Daphnane-Type Diterpenoid Glucosides and Further Constituents of *Euphorbia pilosa*. *Chem Biodivers* **11**:760–766.
- Zhang Z, Qi F, Li H, Dong L, Hai Y, Fan G, and Fei D (2014) A New Lathyrane Diterpenoid from the Whole Plant of *Euphorbia altotibetica*. *Bull Korean Chem Soc* **35**:641–643.
- Zhao J, Liu C, Qi W, Han M-L, Han Y, Wainberg MA, and Yue J (2014) Eurifoloids A–R, Structurally Diverse Diterpenoids from *Euphorbia neriiifolia*. *J Nat Prod* **77**:2224–2233.
- Zinzi L, Capparelli E, Cantore M, Contino M, Leopoldo M, and Colabufo NA (2014) Small and Innovative Molecules as New Strategy to Revert MDR. *Front Oncol* **4**:1–12.